DCT 223

In-Service Monitoring for Improved Maintenance and Management of DelDOT's Bridges

By

HARRY W. SHENTON, III
KEVIN S. CONNOR

Department of Civil and Environmental Engineering
University of Delaware

January 2012

Delaware Center for Transportation
University of Delaware
355 DuPont Hall
Newark, Delaware 19716
(302) 831-1446

The Delaware Center for Transportation is a university-wide multi-disciplinary research unit reporting to the Chair of the Department of Civil and Environmental Engineering, and is co-sponsored by the University of Delaware and the Delaware Department of Transportation.

DCT Staff

Ardeshir Faghri
Director

Jerome Lewis
Associate Director

Ellen Pletz
Assistant to the Director

Earl "Rusty" Lee
T^2 Program Coordinator

Matheu Carter
T^2 Engineer

Sandra Wolfe
Event Coordinator

DCT Policy Council

Natalie Barnhart, Co-Chair
Chief Engineer, Delaware Department of Transportation

Babatunde Ogunnaike, Co-Chair
Dean, College of Engineering

Delaware General Assembly Member
Chair, Senate Highways & Transportation Committee

Delaware General Assembly Member
Chair, House of Representatives Transportation/Land Use & Infrastructure Committee

Ajay Prasad
Professor, Department of Mechanical Engineering

Harry Shenton
Chair, Civil and Environmental Engineering

Michael Strange
Director of Planning, Delaware Department of Transportation

Ralph Reeb
Planning Division, Delaware Department of Transportation

Stephen Kingsberry
Executive Director, Delaware Transit Corporation

Shannon Marchman
Representative of the Director of the Delaware Development Office

James Johnson
Executive Director, Delaware River & Bay Authority

Holly Rybinski
Project Manager-Transportation, AECOM

Delaware Center for Transportation
University of Delaware
Newark, DE 19716
(302) 831-1446

FINAL REPORT:

IN-SERVICE MONITORING FOR IMPROVED MAINTENANCE AND MANAGEMENT OF DELDOT'S BRIDGES

by

Kevin S. Connor
Harry W. Shenton III, PH.D.

January, 2012

Task Number: 17-1490

Executive Summary

The results presented in the report document new results of a continuing effort to develop and implement a technology for monitoring the long-term performance of typical bridges in Delaware's bridge inventory. The objective of this investigation was to gather in-service strain data on a sample of typical bridges, some of which had been previously monitored, and to compare the new data with the historical data. Also, to develop methods for quantifying the differences between similar datasets, so that changes in behavior could be easily identified.

In this study researchers from the University of Delaware, in collaboration with personnel from DelDOT's bridge management group, deployed the In-Service Bridge Monitoring System (ISBMS) in 16 different monitoring trials, on 14 different bridges in Delaware (eleven of these bridges had been previously monitored in 2006 or 2007), between November of 2009 and March of 2011. Chapter 2 provides a brief description of the bridges, as well as where the strain sensor was placed on the bridge, and how access was gained to the bridges.

In a typical test setup a strain transducer is mounted to the bottom flange of a girder, at mid-span. The data acquisition system is then set to automatically trigger and collect strain data when the strain exceeds a user specified threshold. The maximum strain recorded from that "event" is date and time stamped and stored in memory. The system then re-arms itself and waits for the next trigger. In each trial, live load strains were recorded for approximately fourteen days on the bridge. Chapter 3 provides a summary of the data collected on each bridge, which includes a timeline plot and a histogram of the recorded strains. The number of events recorded ranged from a low of 807 to a high of 5,943. The maximum strain ranged from a low of 77$\mu\varepsilon$ to a high of 422$\mu\varepsilon$, corresponding to a maximum live-load stress of 2.2 ksi and 12.2 ksi, respectively.

A method for quantitatively comparing two different datasets from the same bridge is reported in Chapter 4. Normalized frequency distribution plots were first created so that histograms from difference monitoring trials could be compared on a single graph. Next, three different parameters were used to quantify the differences between the plots: area difference (AD), square-root-sum-of-squares difference (SRSS), and effective strain difference (ESD). Thresholds were developed for each of the parameters to indicate when two distributions are similar or different. To determine these threshold values, week-to-week variations from the same datasets that should be similar were calculated and an outlier determination technique was used to define the cut-off for each of the parameters. The thresholds were set at 230 for AD, 18.5 for SRSS, and 28.5 for ESD.

Of the 14 bridges that were monitored for this project, nine had previously been monitored in 2006-07; comparisons were made between the corresponding datasets. Using the thresholds defined, six of the nine indicated some significant difference between the datasets; the differences were confirmed by the visual comparison of the normalized histograms. Of the six that showed a difference, three of the differences could reasonably be attributed to changes in the traffic due to construction during the monitoring period or repairs that were made to the bridge between the monitoring periods, two could be possibly attributed to differences in the test setup (because of incomplete notes from the 2007-07 trial), and there was no obvious reason for the differences in the last case. The last case could be indicating a change in the bridge behavior between the monitoring periods because of damage or degradation of the bridge. The parameters indicated no change in the remaining three bridges that were compared; this was confirmed by visual comparison of the histograms.

Datasets were also available to assess if there is any type of seasonal variation in the data, i.e., datasets collected on the same bridge but at different times of the year. The analysis showed that none was evident, thus comparing datasets collected at different times of year should not be a concern. Note, however, this was based on a limited number of samples and should be confirmed with additional trials in the future. Finally, the results showed that the AD and SRRS parameters were more reliable and robust at detecting a change in the datasets than the ESD parameter.

In-service load ratings were developed for all of the bridges monitored during the project, using the collected in-service data. The procedure for load rating using the in-service data was developed in a previous investigation. It requires using the dataset to project what the maximum expected strain would be for the desired rating period (2-year, 50-year, 75-year). If the sensor was not in the location governing the theoretical load rating, the results of a BRASS model are then used to determine the equivalent "measured" strain at the governing location. Results show that for the HS20 truck, the 50-year rating based on the in-service data is higher than the theoretical rating determined using BRASS, in all but one case: in one case the BRASS rating was higher than the in-service rating. In many cases the theoretical ratings tend to be 2 to 3 times higher than the in-service rating. This illustrates the general trend that the theoretical ratings tend to be very conservative. For the governing vehicle rating, the in-service ratings were higher than the theoretical ratings, in 13 out of 16 cases.

This study demonstrated the benefit of gathering in-service strain data on typical highway bridges. The data can be used to determine if changes in the bridge behavior have occurred, which could be due to damage or deterioration of the structure. It also illustrated how the in-service data can be used to determine rating factors that more accurately reflect the true capacity of the structure. It is recommended that in-service monitoring of typical highway bridges be considered for incorporation as part of the normal inspection program of these types of bridges in Delaware.

TABLE OF CONTENTS

LIST OF TABLES

LIST OF FIGURES

Chapter 1

INTRODUCTION

1.1 Problem Description

As much of the transportation infrastructure in the United States begins to exceed its intended design life, it is imperative that the structural integrity of its components be routinely evaluated to ensure the safety of continued use. Currently, all bridges are required to undergo a complete inspection no less than once every two years. This entails at least a visual examination of all elements of the structure. Once inspected, load ratings are designated which indicate the "health" of the bridge. This method can be effective in catching major deteriorations in structures that may go unnoticed had the inspection not taken place. However, inspections are very qualitative and may be inconsistent from inspector to inspector due to the subjective nature of the examination and issues relating to the accessibility of structure elements. A more quantitative approach for evaluating bridges would provide an objective, consistent method regardless of the inspector. One such method is to instrument a bridge in order to collect strains caused by loads applied to the structure.

With the recent and continued advancement of sensor technology, placing gauges on bridges in order to collect existing, in-service data has become quite practical. New bridges, like the Indian River Inlet Bridge replacement in Delaware, are being instrumented during construction so that data can be collected permanently and continuously during their service lives. Existing bridges, like

Delaware's "Smart Bridge" (Bridge 1-821), have been extensively instrumented with permanent sensors as well. However this permanent, continual instrumentation is not practical for monitoring every bridge in the nation. Instead a temporary, easily deployable system is needed to collect data for a set period of time. With this in mind, the University of Delaware has developed the In-Service Bridge Monitoring System (ISBMS) (Shenton III, Connor, Chajes, Rakowski, & Brookes, 2009).

The ISBMS is small enough to be easily placed and removed, is capable of recording live load in-service data for a period up to three weeks and is easily communicated with using user interface software. At the end of the monitoring period, the data collected by the ISBMS can be used to determine a load rating for the bridge based on quantitative strain data, rather than limited, subjective visual observations. This method calculates load ratings based on the actual response of the bridge system that the current analytical method used in practice cannot completely analyze or predict. The collected data can also become part of an in-service data record. Data sets from different years can be compared to determine if any significant changes have occurred in the structure or traffic. Such variations could be investigated to determine if their cause is related to damage or deterioration of the bridge and whether rehabilitation is necessary.

It is the intent of this research to further investigate the usefulness of this method of acquiring in-service data on bridges and assist in its incorporation into the biennial inspection process. A successful system that is able to provide State Departments of Transportation with data that is unable to be produced using the current inspection system will be a substantial asset in the process of maintaining the national infrastructure in the years ahead.

1.2 Previous Work

Holloway developed the first generation of the ISBMS (Holloway, 1999). This prototype consisted of a modified "Snap Shock Plus M4" (SSPM4) data acquisition unit (manufactured by Instrumented Sensor Technology (IST)) and a full-bridge strain transducer, which were both battery powered. Using adjustable strain and integral triggers, peak live load strains could be recorded over a monitoring period on a bridge element. Work involved extensive laboratory testing followed by field testing on a bridge (Bridge 1-791.)

Under Howell, work on in-service monitoring continued and a second generation system was developed (Howell, 2003). This more versatile system was composed of completely different hardware that allowed for remote access and data retrieval. The system contained a single-board-computer and a cellular digital packet data modem and could be used with either a full-bridge or quarter-bridge strain transducer. Three modes of operation allowed for recording of peak strains, capturing dynamic waveforms of the strain and a rainflow program to investigate fatigue. The user interface for this system, however, was more complicated than the previous generation. Extensive testing was completed in the lab followed by field testing on a bridge (Bridge 1-704.)

Under Brookes, the original system developed by Holloway was upgraded and used to gather in-situ strain data (Brookes, 2007). Six bridges were monitored for a period of two weeks each. Load ratings for each bridge were calculated based on the maximum strain recorded during the monitoring period, in effect providing a load rating for a return period of two weeks.

Finally, under Rakowski, the same system used by Brookes collected strain data on another six bridges (Rakowski, 2008). The strain data recorded over the monitoring period was then used to project maximum strain values for a specified return period (e.g., 2-, 5-, 50-, 75- years). Rating factors were calculated based on the projected strains.

1.3 Contributions of this Research

During the course of this research, eleven of the bridges added to the ISBMS inventory under Brookes and Rakowski were monitored in a similar manner and using the same ISBMS. In addition, three bridges were added to the ISBMS inventory (Table 1.1). This was the first time that ISBMS data sets collected on the same bridges were compared.

Parameters were developed to determine whether data sets on common bridges are similar or dissimilar. Dissimilar data sets suggest that something about the bridge had changed between the original monitoring periods and those conducted during this research. While inevitably there is inherent variability between two data sets, differences due to structural changes or changes in traffic should be distinguishable when comparing the quantified parameters. In cases where parameters indicated a significant change, the bridge was further investigated for possible causes. In order to eliminate any differences resulting from temperature variations, data sets were collected during the same time of the year as in previous years. The effects of temperature variation were investigated on some of the bridges by monitoring them at different times of the year.

Again, recorded strain data was used to project maximums for a given return period and these projected strains were used to calculate rating factors. The resulting factors were compared to those calculated under Rakowski, in addition to rating factors calculated using conventional methods.

Details on the ISBMS and its operation, including communication, calibration, programming, deployment and data acquisition can be found in Appendix A. ISBM record forms were designed to facilitate future data comparisons and implementation and these can be found in Appendix C.

Table 1.1: ISBMS bridge inventory

Bridge Number	Facility Carried	Brookes	Rakowski	This Research
1-791	I-95 N	✓		✓
1-149	SR-41	✓		✓
1-826 N	I-495 N	✓		✓
1-234	SR-2	✓		
1-262 S	SR-7/SR-4 S	✓		✓
1-704	I-95 S	✓		✓
2-918 N	SR-1 N		✓	✓
1-911 S	SR-1 S		✓	✓
1-781	I-95 N		✓	✓
1-821 N	I-495 N		✓	✓
1-728	I-295 N (off-ramp)		✓	✓
1-394 S	US-13 S		✓	✓
1-826 S	I-495 S			✓
2-920 N	SR-1 N			✓
1-907 S	SR-1 S			✓

1.4 Report Outline

The remainder of this report will be organized as follows:

Chapter 2 – Bridge Descriptions provides general information about the bridges monitored during the course of this project. The location of the system during the monitoring period can be found in this section.

Chapter 3 – In-Service Data describes the data collected during the monitoring period. Timeline and histogram plots are included for each bridge.

Chapter 4 – Data Comparison describes the differences in data collected during different time periods. Normalized histograms are plotted and quantitative parameters are calculated in order to compare the data sets for bridges.

Chapter 5 – Strain Projection and Bridge Ratings uses collected in-service data to project future strains on each bridge. These extrapolated strains are then used to calculate and designate a load rating factor to the bridge. These are then compared to load rating factors assigned during inspection.

Chapter 6 – Conclusions provides conclusions from this report and recommendations for future work on this project.

Appendix includes supplemental ISBMS descriptions and materials. Appendix A describes the ISBMS and its calibration process. Appendix B supplements the Load Rating section. Appendix C includes ISBM Forms for all bridges monitored, which provide summaries of bridge information and data collected.

References lists the resources used throughout the project.

Chapter 2

BRIDGE DESCRIPTIONS

The ISBMS was deployed on fourteen bridges in Delaware for this project. In addition to descriptions, bridge plans and sections are provided in this chapter based on drawings supplied by the Delaware Department of Transportation (DelDOT.) Access to the bridges and gauge locations are also described. Operation of the ISBMS is described in Appendix A.

2.1 Selection

The selection of the bridges was based on certain criteria to narrow the amount of bridge options. The same criteria were used under Brookes and Rakowski. All bridges monitored are located in the state of Delaware. For convenience, most of the bridges are located in New Castle County so they are relatively close in proximity to Newark. The bridges do not include culverts or spans carrying or crossing railways. Ease of access was also a major consideration during bridge selection. All of the bridges are steel material since the system is mounted easier and is more reliable on steel wide-flange sections than on concrete. Finally, bridges along major truck traffic routes were picked to ensure a large amount of events during the monitoring period. While bridges were only monitored during inspection years in the past, this criterion was overlooked for scheduling practicality.

2.2 Monitoring

Attempts were made to place the ISBMS in the same location and monitor each bridge at the same time period as previous years to reduce data variability. Incomplete notes made insuring placement in the exact same location difficult (i.e. left or right side of flange). Time constraints made monitoring over the same time period impractical in some cases.

Unless otherwise noted all bridges are located in New Castle County, Delaware, and are composed of rolled, wide-flange steel members. Unless otherwise noted the strain transducer was placed longitudinally at mid-span on the girder specified on the bottom of the bottom flange. Spans being tested directly above live traffic or a body of water are noted.

Unless otherwise noted bridge elements are numbered according to designations in plan documents provided by DelDOT. If no designations are provided then the same system DelDOT uses for numbering bridge elements is utilized. The relevant methods are described in the Inspection Guidance section of the Elements Descriptions Chapter of the Pontis Element Data Collection Manual (DelDOT, p. 23). It states that if previous notes are not available numbering orientation for bridge elements (spans, girders, lanes, etc.) will be from west to east or south to north. If this method is used it will be noted that numbering is based on orientation.

2.3 Bridge Details

Of the fourteen bridges monitored for this project, eleven had been previously monitored in 2006 or 2007 under Brookes or Rakowski, respectively. Of those eleven, two were monitored twice during this project to provide data on the same bridge under different seasonal conditions. Three of the fourteen bridges had not been monitored previously and are new additions to the ISBMS inventory. A map of bridge locations (indicated by yellow pins) in northern Delaware is provided in Figure 2.1 and a map of bridges in southern New Castle and Kent counties is provided in Figure 2.2. A summary of bridge descriptions and monitoring locations is included in Table 2.1. Information in the table that relates to bridge numbers, locations, year built, ADT and percent trucks was provided using data from the 2009 National Bridge Inventory (NBI) (FHWA, 2009) while structure details were based on bridge drawings.

Bridge 1-234, which was monitored in 2006, was not monitored during this project. The decision not to monitor this bridge again was based on the low number of events recorded using a low trigger level of 15$\mu\varepsilon$. Events recorded using an even lower trigger may be picking up “noise” as opposed to truck traffic. Note that construction had been performed on the bridge since the monitoring period in 2006.

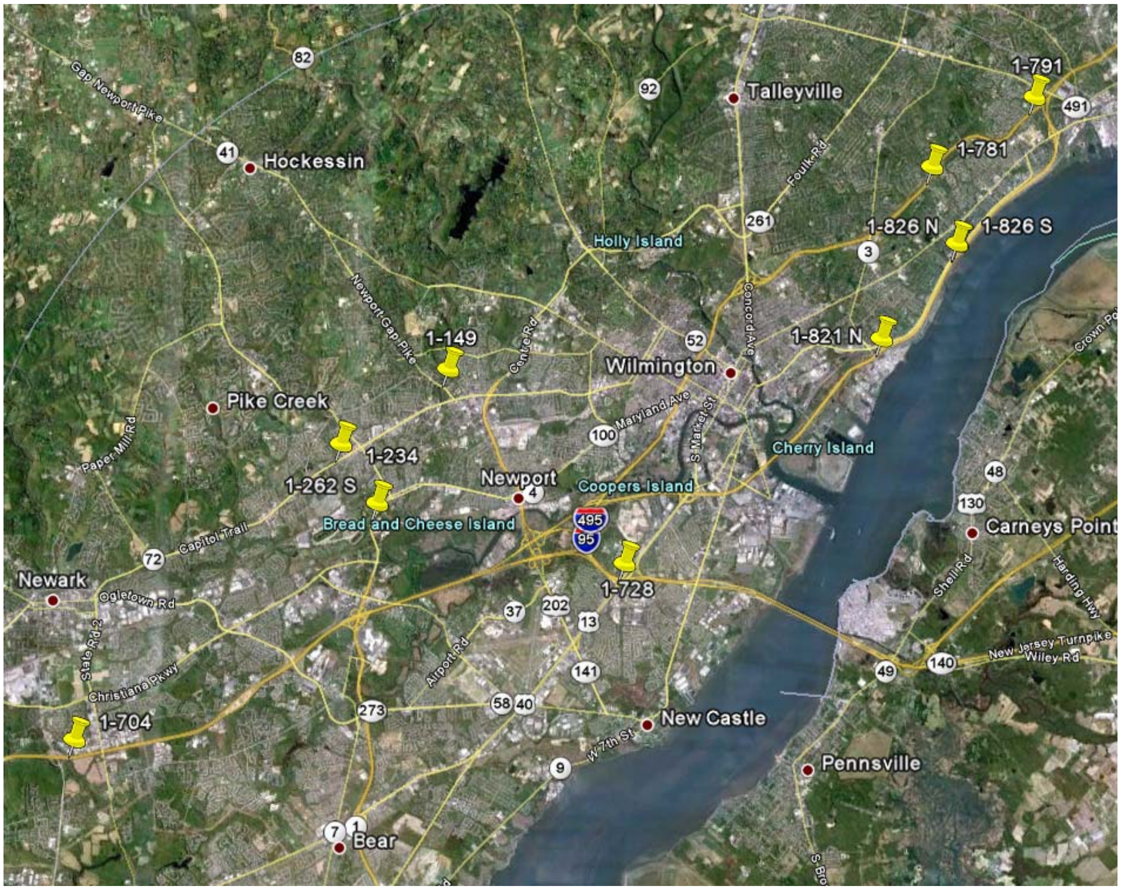

Figure 2.1: ISBMS bridge locations in northern Delaware

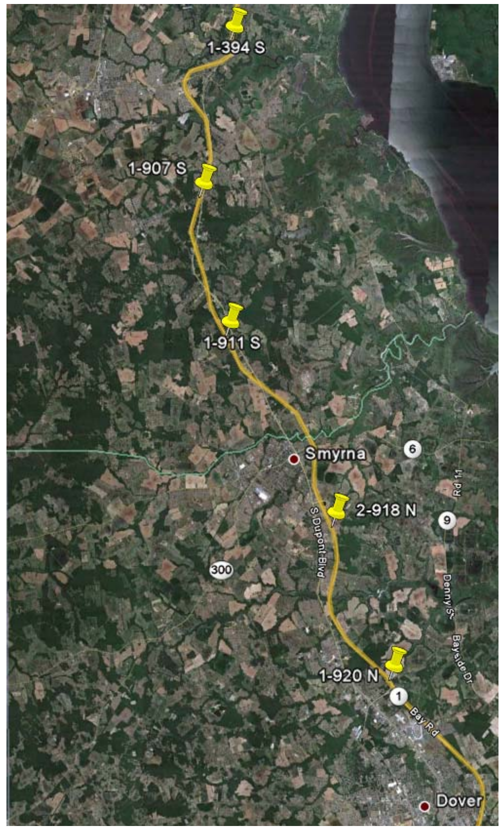

Figure 2.2: ISBMS bridge locations in southern New Castle and Kent counties, Delaware

Table 2.1: General bridge information and gauge locations

Bridge Number	Facility Carried	Facility Crossed	Year Built	ADT	Percent Trucks	Number of Spans	Number of Girders	Span Tested	Span Length	Girder Tested	Prev. Monitor
1-781	1-95 N	Silverside Rd	1967	25,420	12	3	6	1	32’-0”	10	✓
1-728	I-295 N	US-13 S	1958	3,670	12	3	5	1	35’-3”	3	✓
1-704	I-95 S	Christina Creek	1962	60,884	4	3	12	3	25’-1 ¾”	6	✓
1-826 S	I-495 S	Stoney Creek	1972	38,521	4	3	7	3	70’-0”	4	
1-262 S	SR-7/SR-4 S	White Clay Creek	1981	28,756	9	5	7	1	90’-0”	3	✓
1-826 N	I-495 N	Stoney Creek	1972	31,963	4	3	7	3	70’-0”	4	✓
1-911 S	SR-1 S	Black Diamond Rd	2003	19,190	12	1	6	1	65’-0”	3	✓
1-821 N	I-495 N	Edgemoor Rd	1975	39,148	12	4	9	3	76’-7 $^{5}/_{8}$”	5	✓
1-791	I-95 N	Darley Rd	1966	18,624	12	3	6	1	35’-0”	3	✓
2-918 N	SR-1 N	Big Oak Rd	1992	20,949	12	1	6	1	65’-0”	10	✓
2-920 N	SR-1 N	Dyke Branch Rd	1992	15,352	12	1	6	1	65’-0”	11	
1-907 S	SR-1 S	Pine Tree Rd	2003	2,528	7	1	5	1	81’-0”	3	
1-394 S	US-13 S	Drawyers Creek	1964	12,825	12	3	5	2	62’-0”	2	✓
1-149	SR-41	Red Clay Creek	1989	17,546	7	1	11	1	80’-0”	8	✓

2.3.1 Bridge 1-781

This bridge carries two northbound lanes of I-95 over Silverside Road and is located north of Wilmington. The structure consists of six girders over three simple spans (Figure 2.3). Girder 10 on Span 1 was instrumented under Lane 2. The gauge was placed on the bottom of a flange cover plate located on the bottom flange. The bridge had been previously monitored in 2007. Access to the bridge was by way of Silverside Road. The gauge was placed using a 16 foot ladder set on the mid-span diaphragm. The ISBMS was in “Active” mode at the time of retrieval.

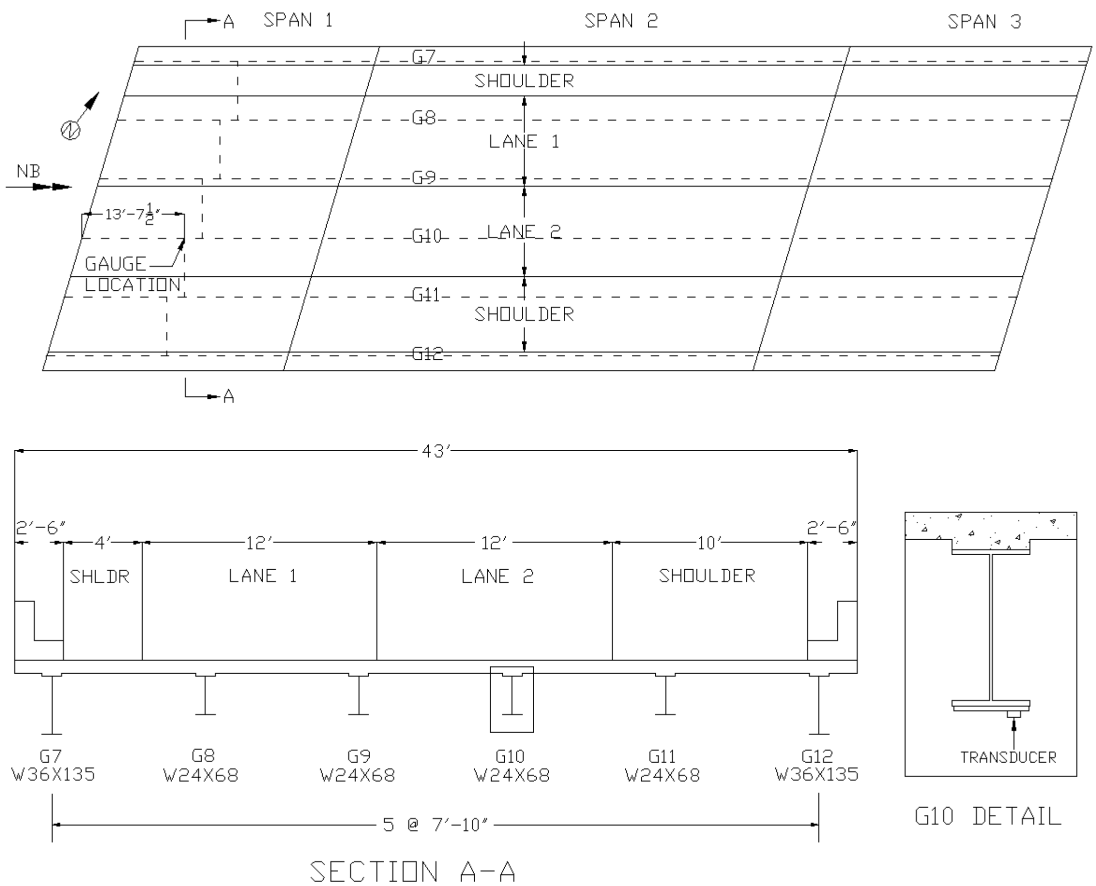

Figure 2.3: Bridge 1-781 plan, Span 1 cross-section and Girder 10 detail

2.3.2 Bridge 1-728

This bridge carries one lane of a northbound exit ramp of I-295 to US-13 N over the southbound lanes of US-13 and is located in the city of New Castle. The structure consists of five girders over three simple spans (Figure 2.4). Elements were numbered based on orientation. Girder 3 on Span 1 was instrumented under the roadway as shown in Section A-A. The bridge had been previously monitored in 2007. Access to the bridge was by way of US-13 S. The gauge was placed using a 24 foot ladder set on the mid-span diaphragm. The ISBMS was in “Standby” mode at the time of retrieval.

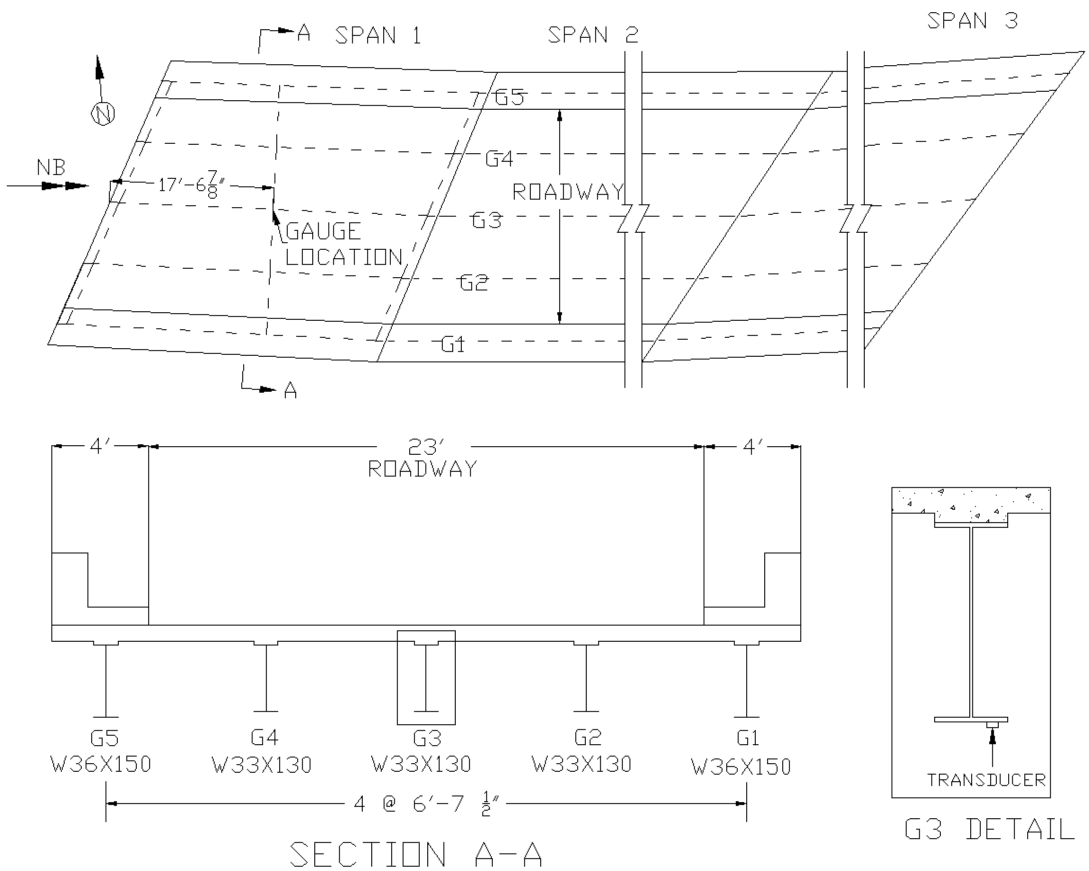

Figure 2.4: Bridge 1-728 plan, Span 1 cross-section and Girder 3 detail

2.3.3 Bridge 1-704

This bridge carries four southbound lanes in addition to an exit lane (Exit 1B) of I-95 over Christina Creek and is located just south of Newark. The structure consists of twelve girders over five simple spans (Figure 2.5). Elements were numbered based on orientation. Girder 6 on Span 3 was instrumented under Lane 3. The bridge had been previously monitored in 2006. Numbering of girder and span elements in 2006 and 2007 documentation was inverted relative to numbering based on orientation as shown in Figure 2.5. Access to the bridge was by way of Old

Cooches' Bridge Road. Note that Span 3 is above Christina Creek. The gauge was placed using a 16 foot ladder set from the bank of the river to the intermediate diaphragm. Since the diaphragm is not located exactly at mid-span the strain transducer was actually placed closer to the pier than the abutment. The ISBMS was in "Active" mode at the time of retrieval.

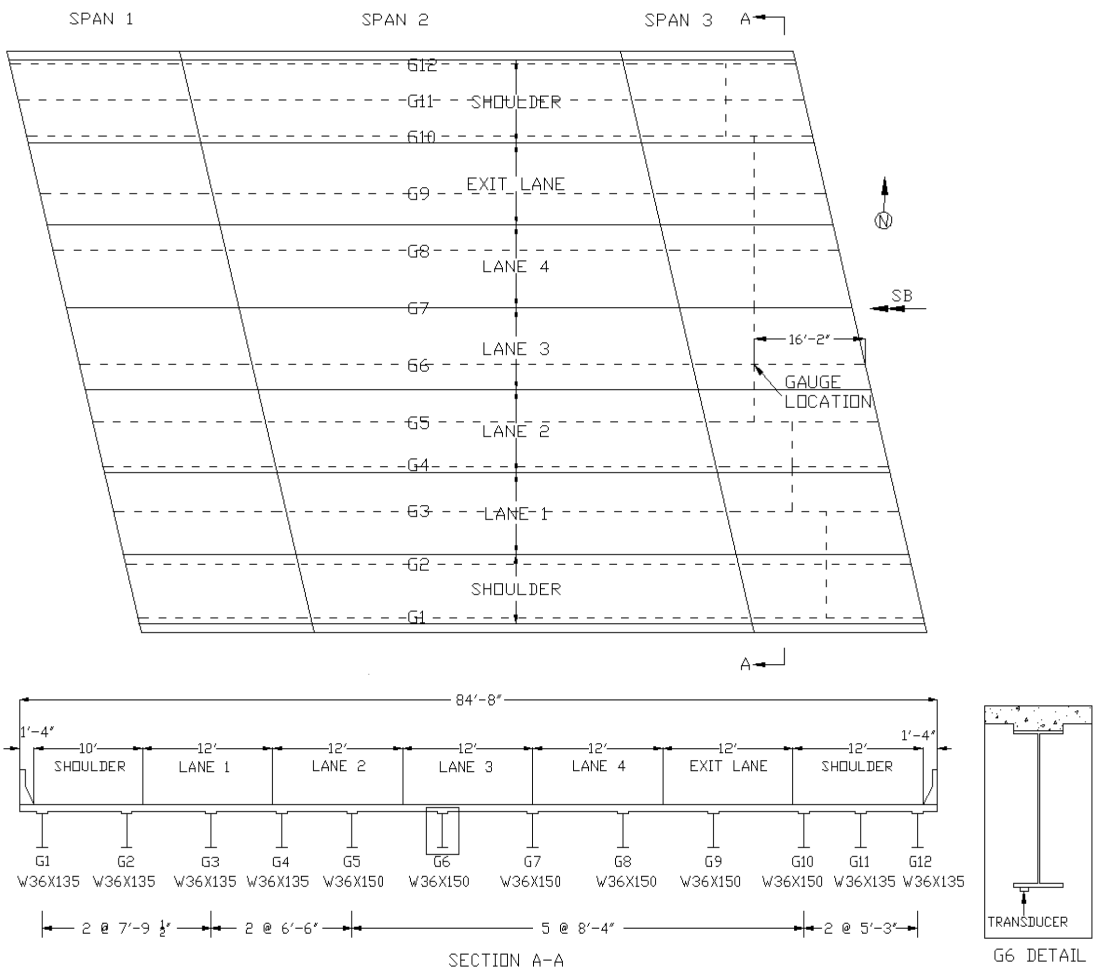

Figure 2.5: Bridge 1-704 plan, Span 3 cross-section and Girder 6 detail

2.3.4 Bridge 1-826 S

This bridge carries three southbound lanes of I-495 over Stoney Creek and is located north of I-495 N, Exit 4 in Wilmington. The structure consists of seven girders over three continuous spans (Figure 2.6). Girder 4 on Span 3 was instrumented under Lane 2. This bridge had not been monitored previously. Access to the bridge was by way of US-13 N (Governor Printz Boulevard.) The gauge was placed without any equipment. The ISBMS was in "Standby" mode at the time of retrieval.

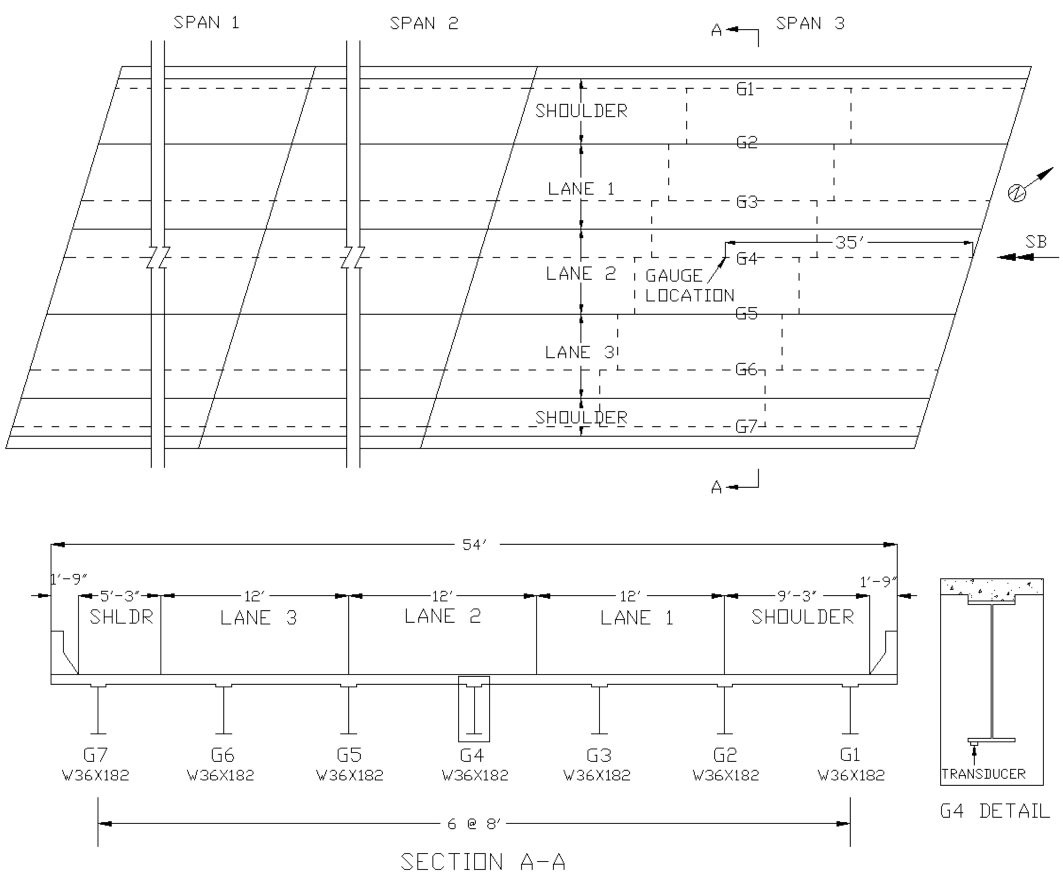

Figure 2.6: Bridge 1-826 S plan, Span 3 cross-section and Girder 4 detail

2.3.5 Bridge 1-262 S

This bridge carries three southbound lanes of SR-7/SR-4 (Stanton Christiana Road) over White Clay Creek and is located east of Delaware Park in Newark. The structure consists of seven built-up plate girders over five continuous spans (Figure 2.7). Girder 3 on Span 1 was instrumented under Lane 1. The bridge had been previously monitored in 2006. Note that the span monitored was numbered as Span 5 in 2006 and 2007 documentation. The trigger level was decreased from its 2006 level in order to collect more events in a two week period. Access to the bridge was by way of Old Route 7 near an industrial park. The gauge was placed using a 24 foot ladder set at mid-span of the girder. The ISBMS was in "Active" mode at the time of retrieval.

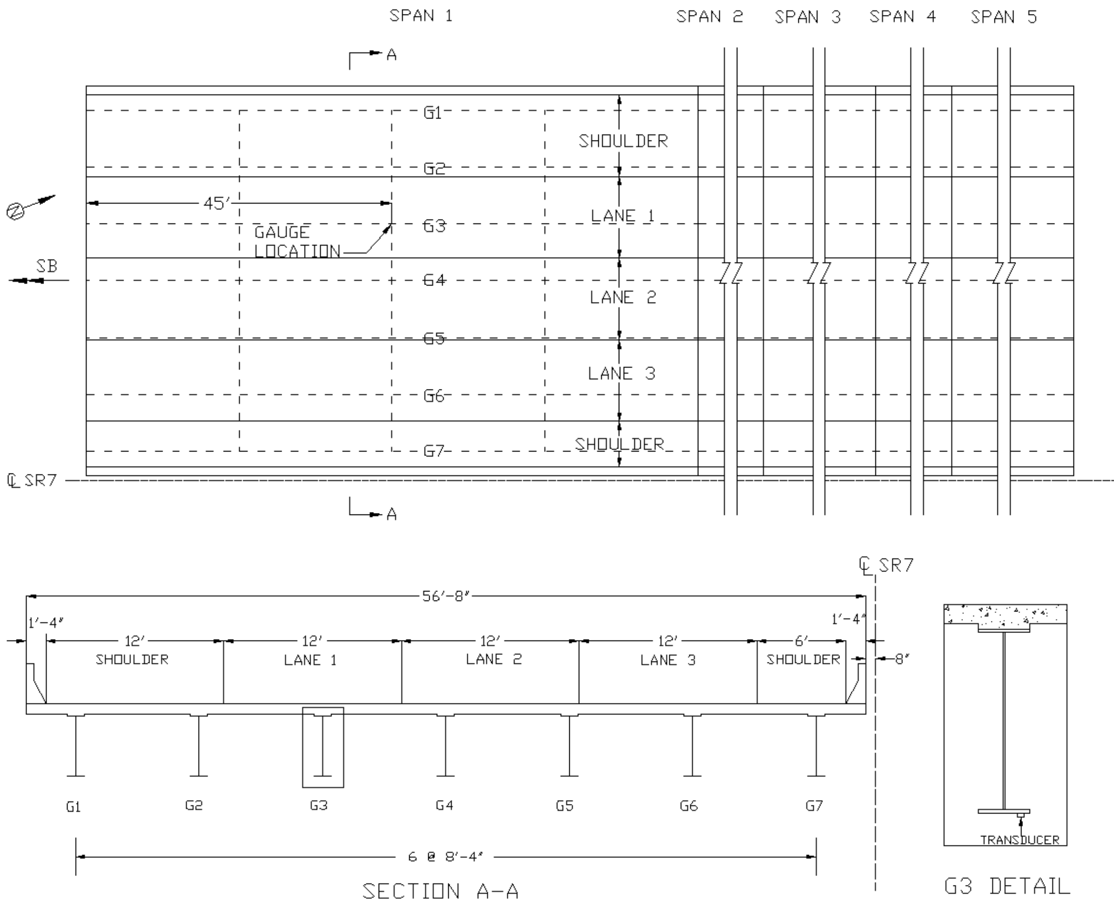

Figure 2.7: Bridge 1-262 S plan, Span 1 cross-section and Girder 3 detail

2.3.6 Bridge 1-826 N

This bridge carries three northbound lanes of I-495 over Stoney Creek and is located north of I-495, Exit 4 in Wilmington. The structure consists of seven girders over three continuous spans (Figure 2.8). Girder 4 on Span 3 was instrumented under Lane 2. The bridge had been previously monitored in 2006. Access to the bridge was by way of US-13 N (Governor Printz Boulevard.) The gauge was placed without any equipment. The location of the strain transducer was marked in permanent black marker. The ISBMS was in “Standby” mode at the time of retrieval.

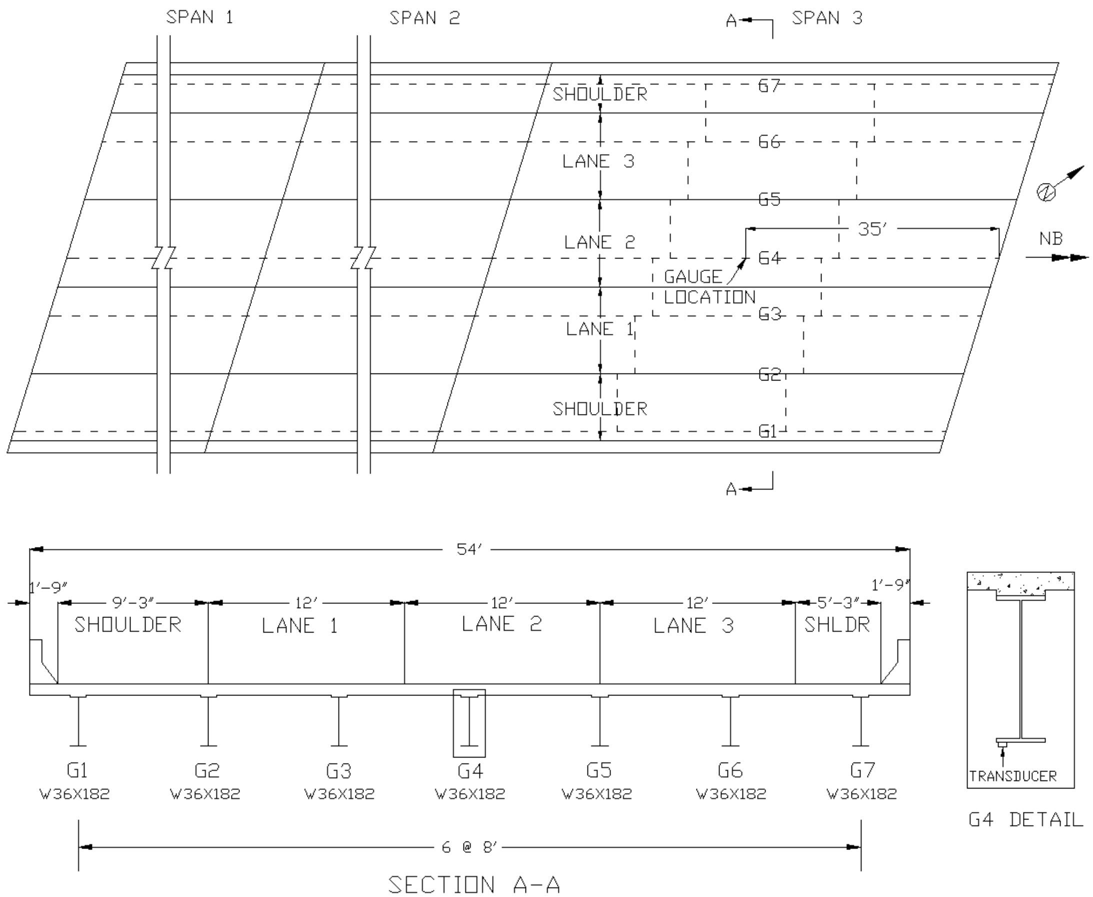

Figure 2.8: Bridge 1-826 N plan, Span 3 cross-section and Girder 4 detail

2.3.7 Bridge 1-911 S

This bridge carries two southbound lanes of SR-1 (Korean War Veteran Memorial Highway) over Black Diamond Road and is located between Odessa and Smyrna. The structure consists of six girders over a single simple span (Figure 2.9). Girder 3 was instrumented under Lane 1. The bridge had been previously monitored in 2007. Note the span is above live traffic. Access to the bridge was by way of Black Diamond Road. Traffic control was required and provided by DelDOT on the single-lane road. The gauge was placed using a bucket truck provided by DelDOT. The location of the strain transducer was marked in permanent black marker. The ISBMS was in “Standby” mode at the time of retrieval.

This bridge was monitored a second time for this project to study the effect of temperature. The ISBMS was in “Active” mode at the time of retrieval the second time.

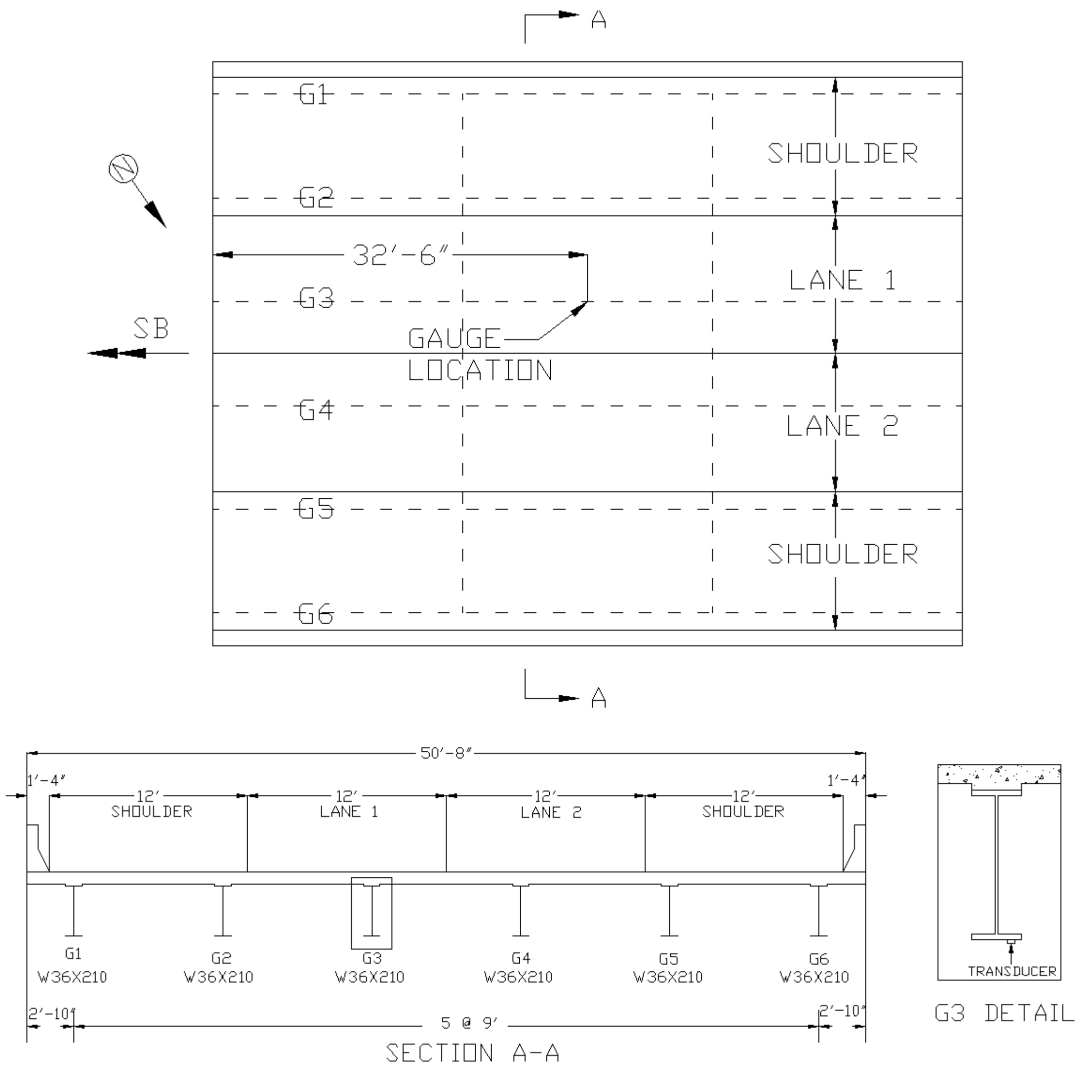

Figure 2.9: Bridge 1-911 S plan, cross-section and Girder 3 detail

2.3.8 Bridge 1-821 N

This bridge carries four northbound lanes of I-495 over Edgemoor Road and is located by I-495, Exit 4 in Wilmington. The structure consists of nine girders over four spans (Figure 2.10). Span 1 is simple, while Span 2, Span 3 and Span 4 are continuous. Girder 5 on Span 3 was instrumented under Lane 1. The bridge had been previously monitored in 2007. Numbering of bridge elements was inverted in

2007 documentation relative to numbering on bridge plans as shown in Figure 2.10. Access to the bridge was by way of an access road off of Edgemoor Road. The gauge was placed using a bucket truck provided by DelDOT. The ISBMS was in "Standby" mode at the time of retrieval.

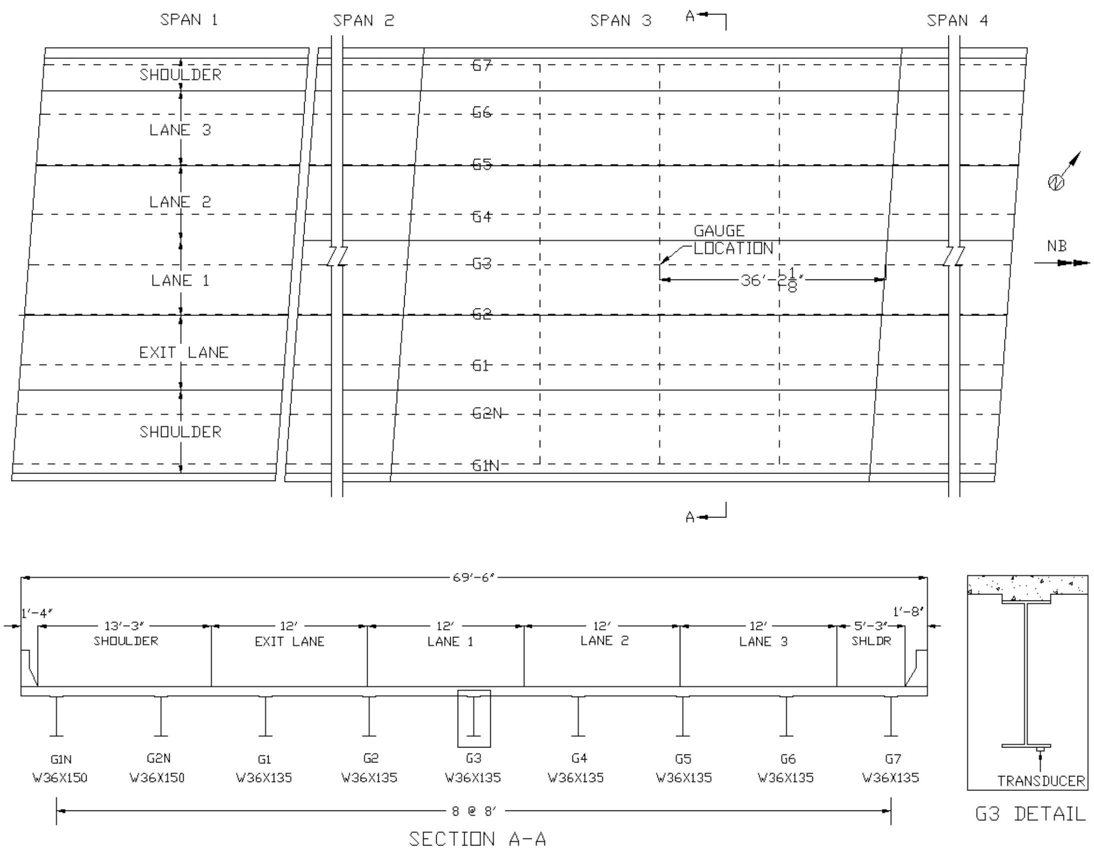

Figure 2.10: Bridge 1-821 N plan, Span 3 cross-section and Girder 3 detail

2.3.9 Bridge 1-791

This bridge carries two northbound lanes of I-95 over Darley Road and is located south of the Pennsylvania-Delaware border in Claymont. The structure consists of six girders over three continuous spans (Figure 2.11). Elements were numbered based on orientation. Girder 3 on Span 1 was instrumented under Lane 1. The bridge had been previously monitored in 2006. Access to the bridge was by way of Darley Road. A seven foot fence had to be scaled to gain access to the gauge location. The gauge was placed using a 16 foot ladder set on the mid-span diaphragm. The ISBMS was in "Active" mode at the time of retrieval.

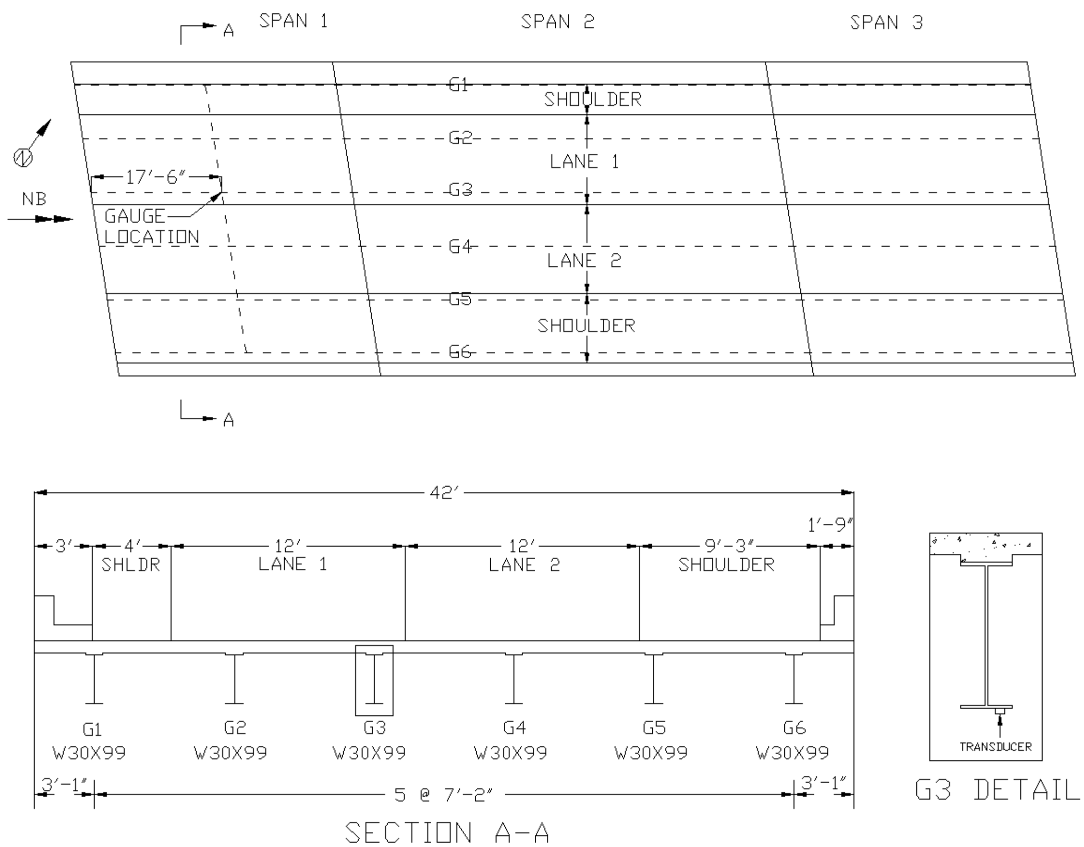

Figure 2.11: Bridge 1-791 plan, Span 1 cross-section and Girder 3 detail

2.3.10 Bridge 2-918 N

This bridge carries two northbound lanes of SR-1 (Korean War Veteran Memorial Highway) over Big Oak Road and is located south of Smyrna in Kent County. The structure consists of six girders over a single simple span (Figure 2.12). Girder 10 was instrumented under Lane 2. The bridge had been previously monitored in 2007. Note this span is above live traffic. Access to the bridge was by way of Big Oak Road. The gauge was placed using a bucket truck provided by DelDOT. The ISBMS was in "Active" mode at the time of retrieval.

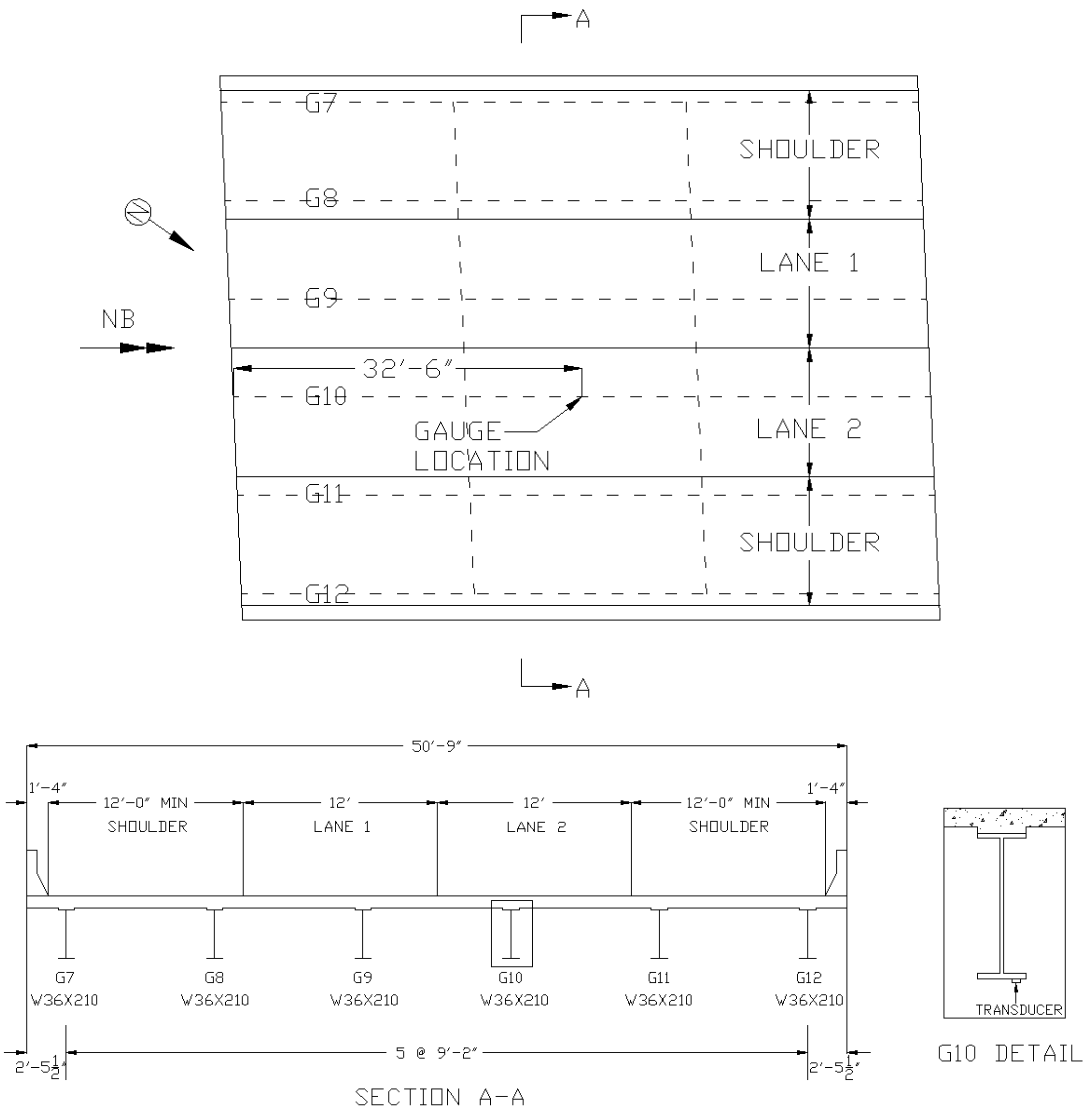

Figure 2.12: Bridge 2-918 N plan, cross-section and Girder 10 detail

2.3.11 Bridge 2-920 N

This bridge carries two northbound lanes of SR-1 (Korean War Veteran Memorial Highway) over Dyke Branch Road and is located north of Dover in Kent County. The structure consists of six girders over a single simple span (Figure 2.13). Girder 11 was instrumented under Lane 2. This bridge had not been monitored previously. Note this span is above live traffic. Access to the bridge was by way of Dyke Branch Road. The gauge was placed using a bucket truck provided by DelDOT. The location of the strain transducer was marked in permanent black marker. The ISBMS was in "Standby" mode at the time of retrieval.

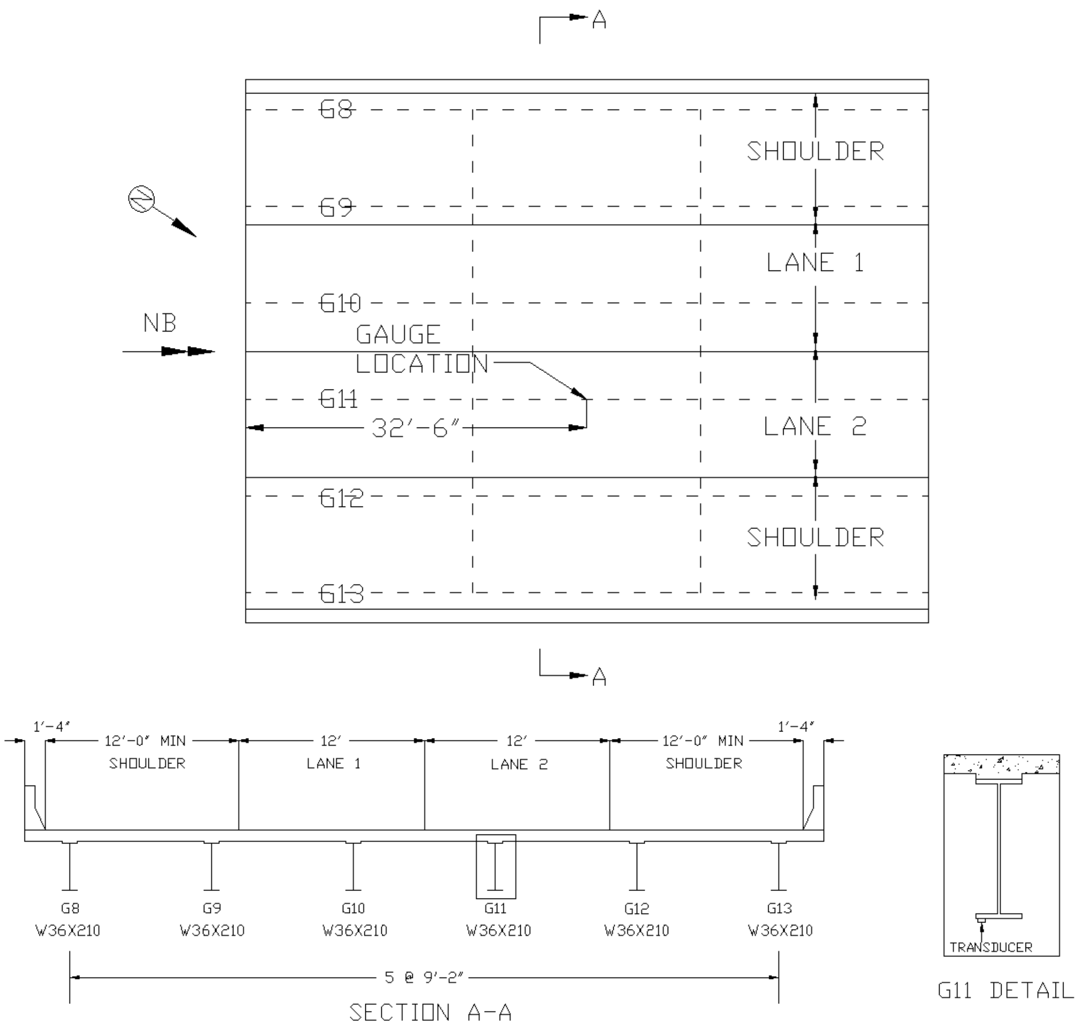

Figure 2.13: Bridge 2-920 N plan, cross-section and Girder 11 detail

2.3.12 Bridge 1-907 S

This bridge carries two southbound lanes of SR-1 (Korean War Veteran Memorial Highway) over Pine Tree Road and is located between Odessa and Smyrna. The structure consists of five built-up plate girders over a single simple span (Figure 2.14). Girder 3 was instrumented under Lane 1. This bridge had not been monitored previously. Note this bridge is above live traffic. Access to the bridge was by way of Pine Tree Road. Traffic control was required and provided by DelDOT. The gauge was placed using a bucket truck provided by DelDOT. The location of the strain transducer was marked in permanent black marker. The ISBMS was in “Active” mode at the time of retrieval.

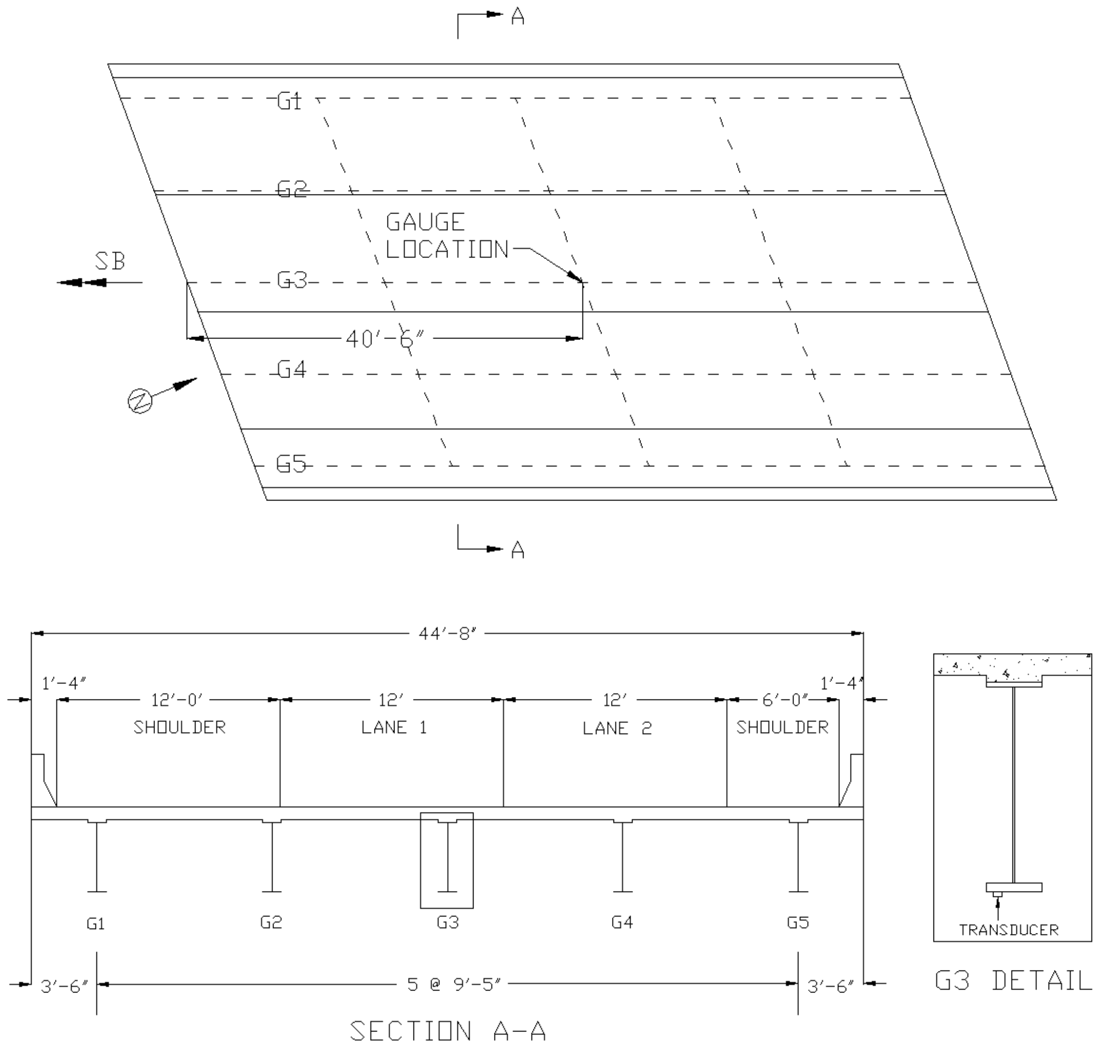

Figure 2.14: Bridge 1-907 S plan, cross-section and Girder 3 detail

2.3.13 Bridge 1-394 S

This bridge carries two southbound lanes of US-13 (S Dupont Highway) over Drawyers Creek and is located just north of Odessa. The structure consists of five girders over three continuous spans (Figure 2.15). Girder 2 on Span 2 was instrumented under Lane 1. This bridge had been previously monitored in 2007. Note Span 2 is above Drawyers Creek. Access to the bridge was made by way of a residential road adjacent to US-13 S. The gauge was placed using a row boat supplied by DelDOT. The ISBMS was in “Active” mode at the time of retrieval.

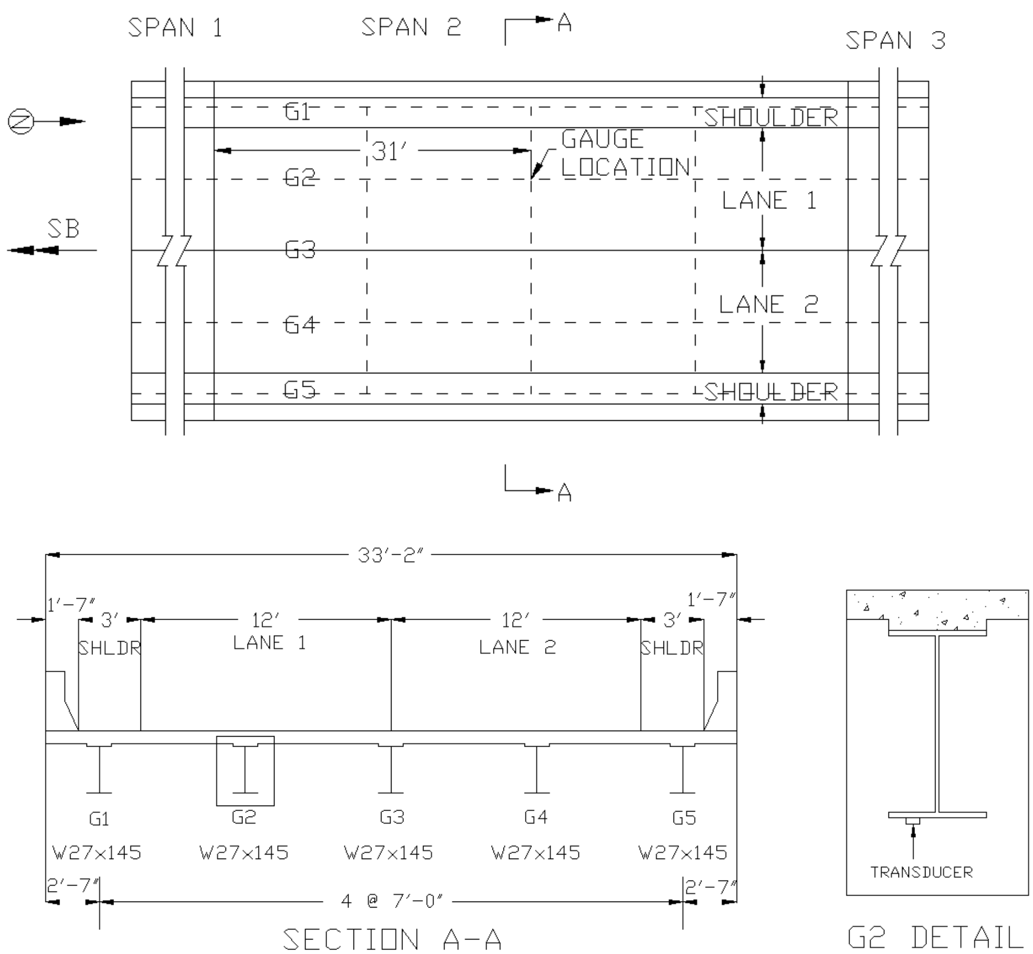

Figure 2.15: Bridge 1-394 S plan, cross-section and Girder 2 detail

2.3.14 Bridge 1-149

This bridge carries the northbound and southbound lanes of SR-41 (Newport Gap Pike) over Red Clay Creek and is located off of SR-2, between Newark and Wilmington. The structure consists of eleven girders over a single simple span (Figure 2.16). Girder 8 was instrumented under Lane 2. This bridge had been previously monitored in 2006. Numbering of girder and span elements in 2006 and 2007 documentation was inverted relative to numbering on bridge plans as shown in Figure 2.16. Note this span is above Red Clay Creek. Access to the bridge was made by way of the Wilmington and Western Railroad lot. The gauge was placed using a 16 foot articulating ladder and required waders to set up in several feet of water. The location of the strain transducer was marked in permanent black marker. The ISBMS was in "Standby" mode at the time of retrieval.

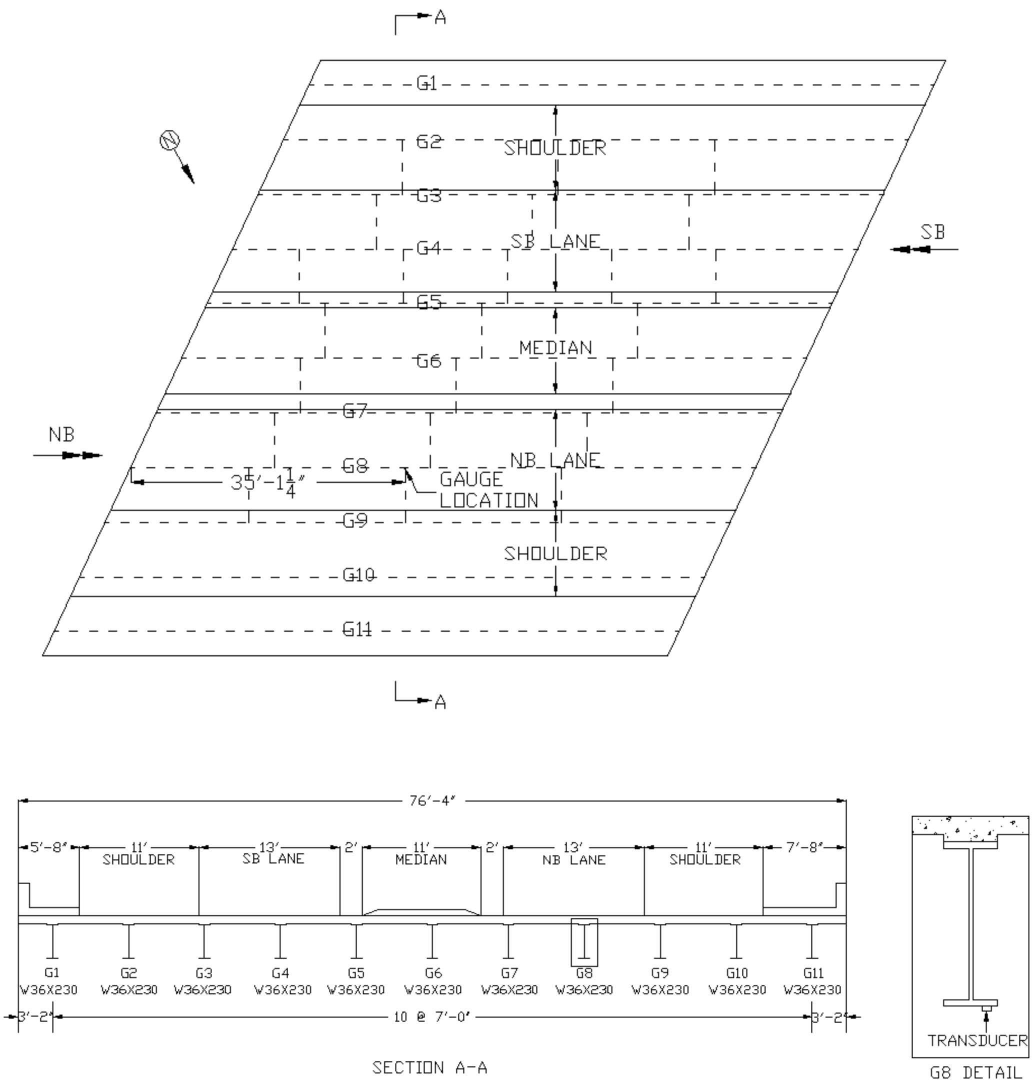

Figure 2.16: Bridge 1-149 plan, cross-section and Girder 8 detail

Chapter 3

IN-SERVICE BRIDGE DATA

The ISBMS collects bridge data as a series of peak strain magnitudes (events) along with the time each occurred. This chapter presents plots and a summary of the in-service data for each bridge as well as commentary on the effectiveness of the trigger level used and other monitoring issues. Descriptions of the bridges being monitored, including gauge locations, can be found in Section 2.3.

3.1 Data Presentation

The in-service data is presented in timeline and histogram plots. The timeline chronologically plots the peak strains that exceeded a specific trigger value. Ideally, triggers are set at values that will record the maximum number of events the system's memory can store (just over 5900) during the monitoring period (usually two weeks.) It is difficult to know what trigger level to use and is based on previous monitoring experience on each bridge. The trigger levels for this project were set between 25 με and 70 με. The histogram plots the number of events recorded for particular microstrain bins. The bins are set in increments of 5 με. For example, a bin of 60 με displays the number of events that were greater than 55 με and less than or equal to 60 με. The final bin in the histogram plots is always "More." Points in this bin are any events that exceeded the value of the bin prior to it. A summary of data collected for this report is provided in Table 3.1 and monitoring time periods for the course of the ISBMS project are provided in Table 3.2.

Table 3.1: Summary of collected in-service data (2009-2011)

Bridge Number	Date Activated	Date Deactivated	Number of Days	Threshold (με)	Number of Events	Maximum Event (με)
1-781	11/17/2009	12/08/2009	21	35	3,889	120.66
1-728	12/10/2009	12/19/2009	9	25	807	77.08
1-704	3/09/2010	03/23/2010	10	55	843	106.68
1-826 S	5/21/2010	5/26/2010	5	40	5,163	223.76
1-262 S	6/10/2010	6/24/2010	14	35	1,294	123.26
1-826 N	6/24/2010	6/29/2010	5	40	5,283	139.53
1-911 S	7/09/2010	7/15/2010	6	55	5,100	187.66
1-821 N	7/22/2010	7/27/2010	5	65	4,697	308.32
1-791	10/01/2010	10/15/2010	15	35	1,430	104.56
2-918 N	10/20/2010	11/03/2010	14	45	3,752	163.84
2-920 N	11/03/2010	11/16/2010	14	45	5,943	181.11
1-911 S	11/17/2010	12/02/2010	15	70	3,836	186.64
1-907 S	12/02/2010	12/16/2010	14	70	1,176	422.15
1-826 N	2/02/2011	2/10/2011	8	50	5,943	151.07
1-394 S	3/07/2011	3/31/2011	24	35	3,141	135.70
1-149	3/31/2011	4/13/2011	13	45	5,943	134.38

Table 3.2: Bridge monitoring periods (2006-2011)

Bridge Number	1st Monitor			2nd Monitor			3rd Monitor		
	Start Date	Days	Events	Start Date	Days	Events	Start Date	Days	Events
1-791	9/26/2006	14	2,889	10/1/2010	14.5	1,430			
1-149	3/21/2006	14	1,892	3/31/2011	13	5,943			
1-826 N	5/01/2006	15	4,204	5/21/2010	5	5,936	2/2/2011	8	5,943
1-234	8/16/2006	13	62						
1-262 S	6/06/2006	14	754	6/10/2010	14	2,983			
1-704	8/30/2006	13	1,543	3/9/2010	10	1,616			
2-918 N	10/24/2007	14	1,576	10/20/2010	14	3,752			
1-911 S	6/07/2007	5	5,937	7/9/2010	6	5,943	11/17/2010	15	3,836
1-781	9/17/2007	13	3,027	11/17/2009	21	5,328			
1-821 N	7/31/2007	6	5,937	7/22/2010	5	5,943			
1-728	12/04/2007	17	1,145	12/10/2009	9	1,059			
1-394 S	8/23/2007	20	1,275	3/7/2011	24	3,141			
1-826 S	6/24/2010	5	5,283						
2-920 N	11/03/2010	14	5,943						
1-907 S	12/02/2010	14	1,176						

3.2 In-service Data

Due to the modification of the calibration factor (see Calibration section in Appendix A) actual trigger values were set at non-integer values for some of the bridges monitored. For presentation purposes these were rounded up to the nearest five microstrain. Strains recorded below these values were then neglected. While only events at or above the rounded threshold values are presented in this section more events were actually recorded for the bridges shown in Table 3.3.

Table 3.3: Bridges with modified threshold values

Bridge Number	Trigger Value	Recorded Events	Presented Threshold	Presented Events
1-781	30.83	5,328	35	3,889
1-728	23.12	1,059	25	807
1-704	52.41	1,616	55	843
1-826 S	38.54	5,936	40	5,163
1-262 S	30.83	2,983	35	1,294
1-826 N	38.54	5,938	40	5,283
1-911 S (1)	53.96	5,943	55	5,100
1-821 N	61.66	5,943	65	4,697

Some bridges produced negative strain readings due to negative bending. The number of negative strain events exceeding the trigger level was low – always less than one percent of the events recorded. To simplify analysis all values recorded are assumed to be positive.

3.2.1 Bridge 1-781

This bridge was monitored for three weeks in November and December 2009, which included the Thanksgiving holiday traveling period. The timeline and histogram plots are presented in Figure 3.1 and Figure 3.2, respectively. The system actively collected data for the entire monitoring period. In the future, it is recommended that the trigger level be lowered to 30 με in order to collect more events.

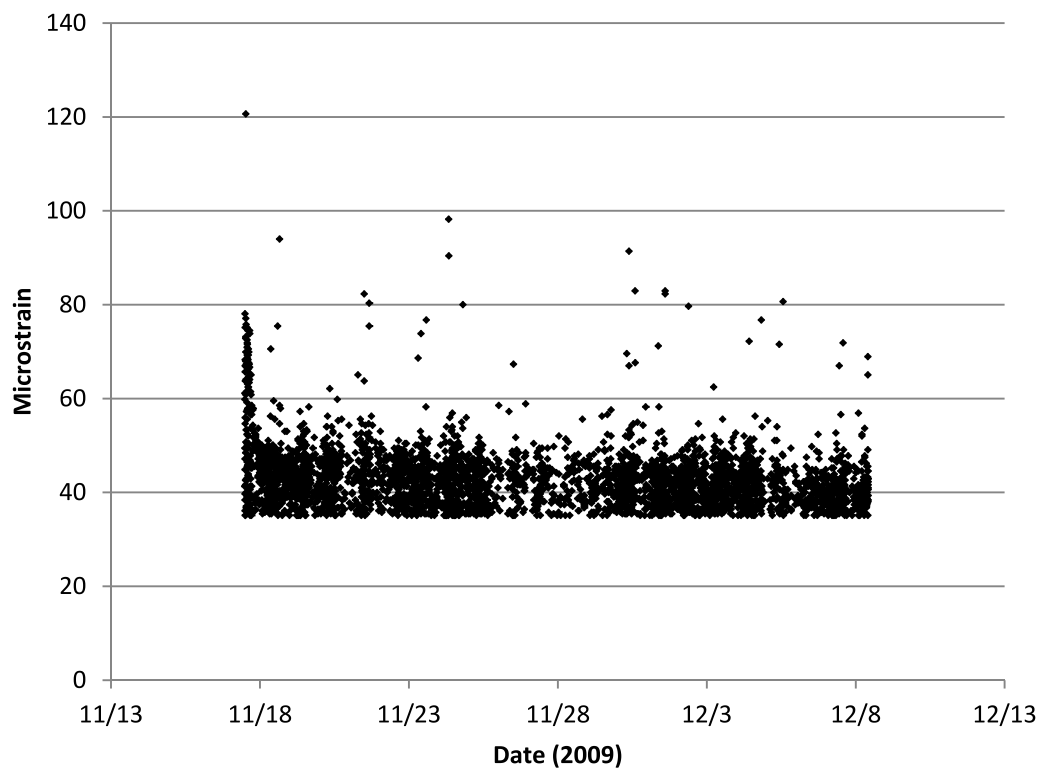

Figure 3.1: Bridge 1-728 timeline plot

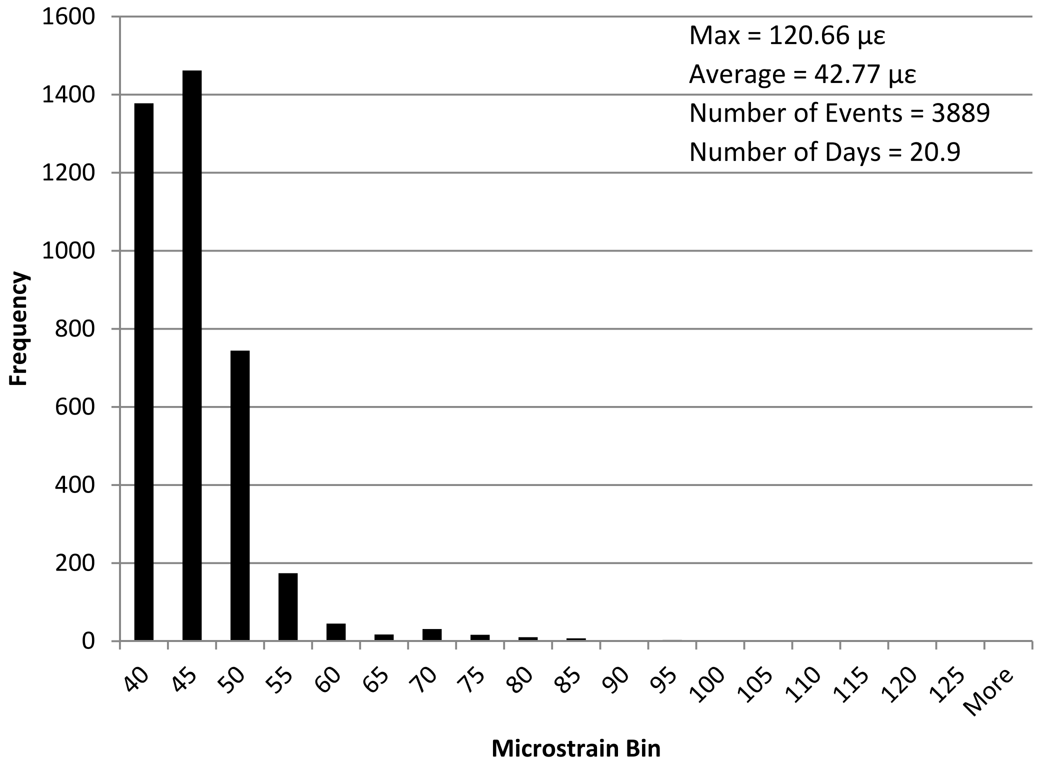

Figure 3.2: Bridge 1-781 histogram plot

3.2.2 Bridge 1-728

This bridge was monitored for nine days in December 2009. The timeline and histogram plots are presented in Figure 3.3 and Figure 3.4, respectively. The system deactivated during the morning of 12/19 and no data was collected after that point. This occurred during a snowstorm. In the future, it is recommended that the trigger level be lowered to 20 µε in order to collect more events.

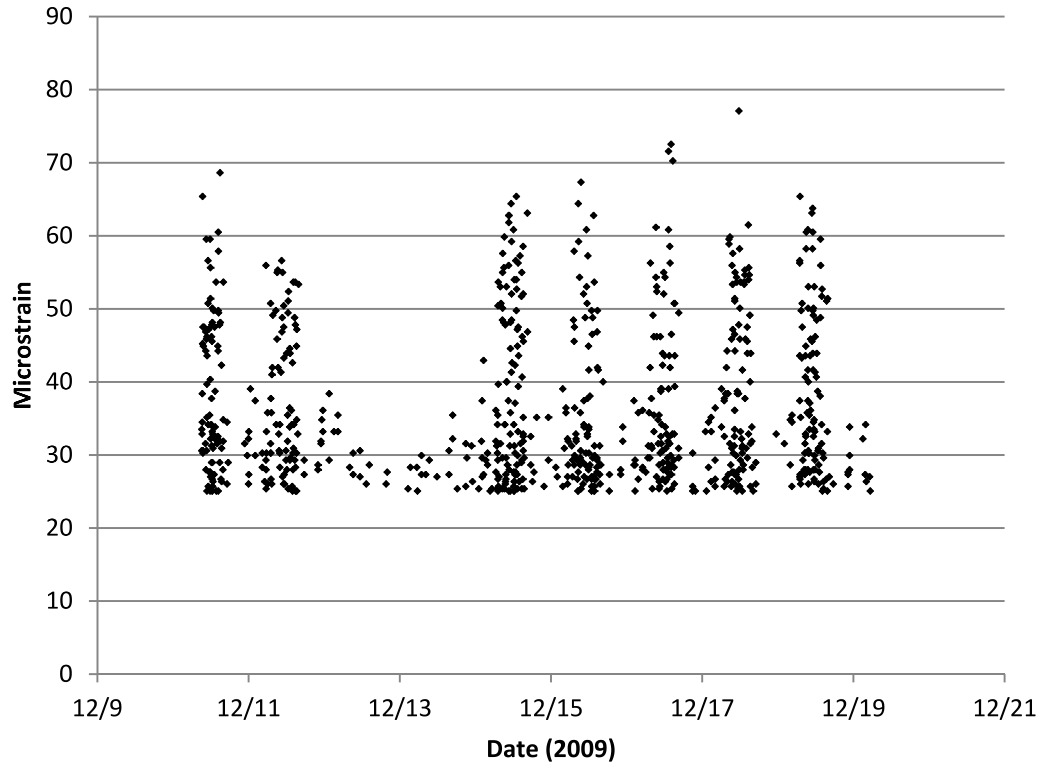

Figure 3.3: Bridge 1-728 timeline plot

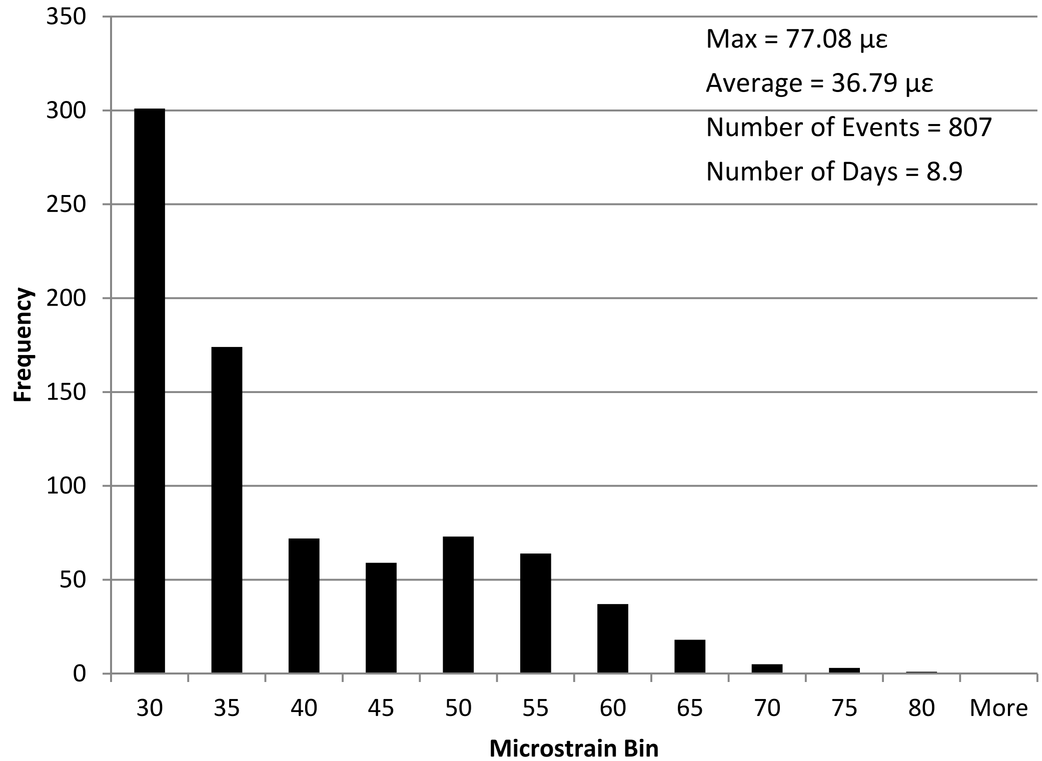

Figure 3.4: Bridge 1-728 histogram plot

3.2.3 Bridge 1-704

This bridge was monitored for two weeks in March 2010. The timeline and histogram plots are presented in Figure 3.5 and Figure 3.6, respectively. The system was still in “Active” mode at the time of retrieval on 3/23; however no events were recorded after 3/19. This may have been due to a low voltage in the 6-volt battery. In the future, it is recommended that the trigger level be lowered to 50 με in order to collect more events.

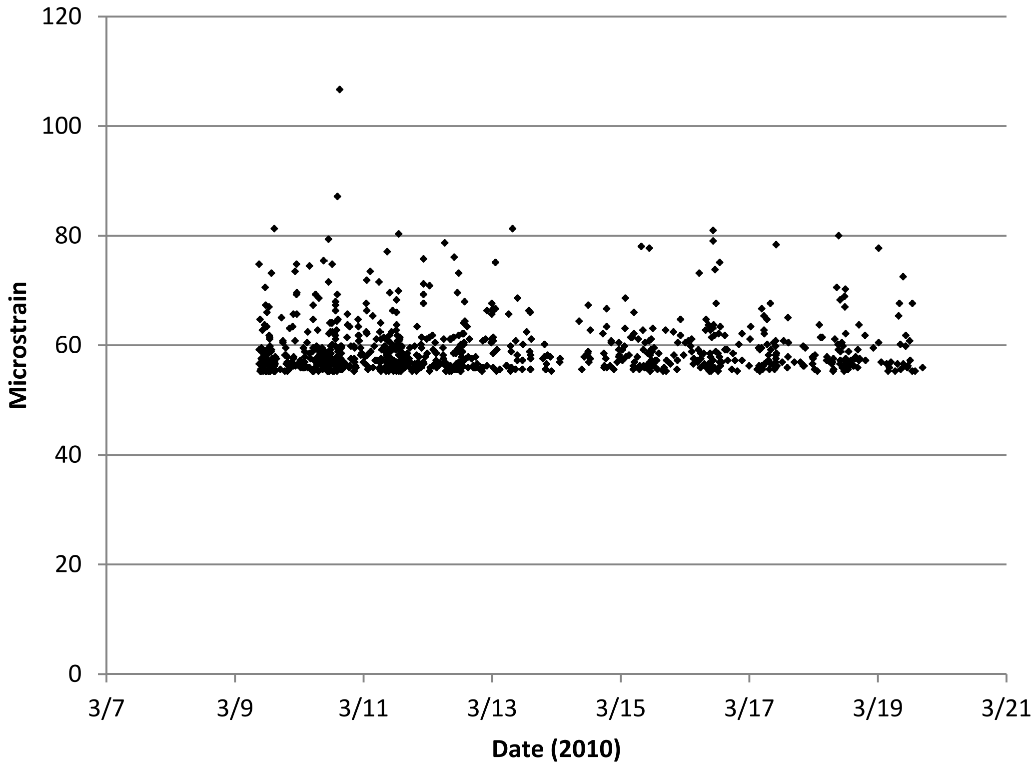

Figure 3.5: Bridge 1-704 timeline plot

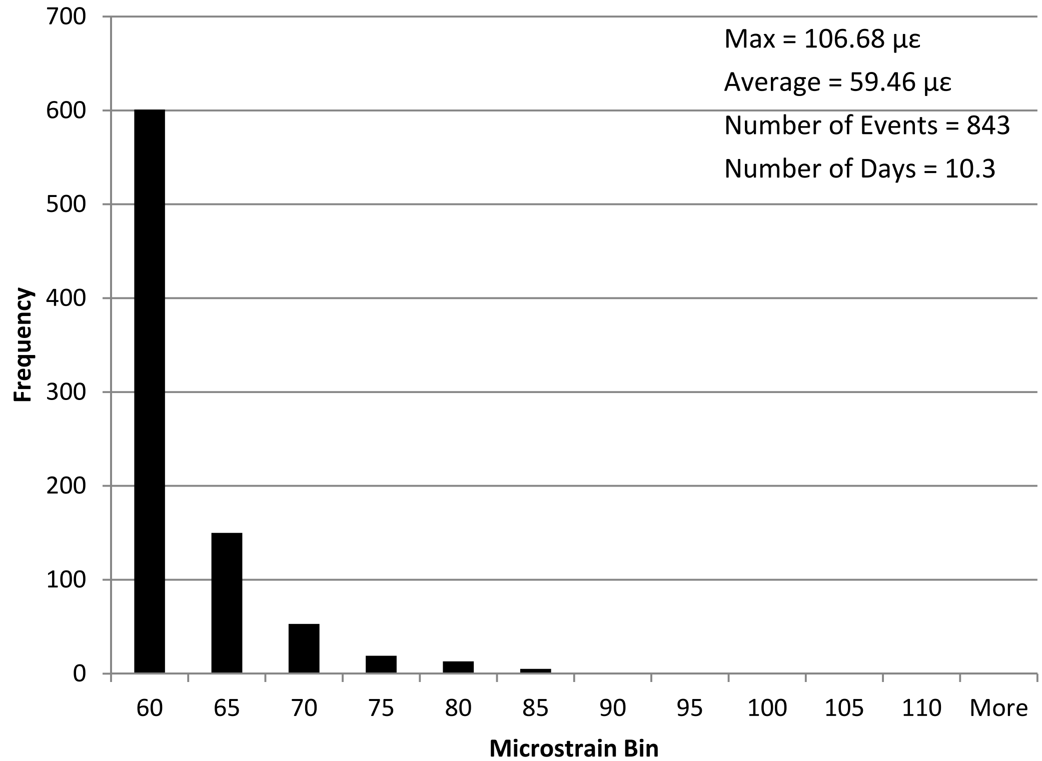

Figure 3.6: Bridge 1-704 histogram plot

3.2.4 Bridge 1-826 S

This bridge was monitored for five days in May 2010. The timeline and histogram plots are presented in Figure 3.7 and Figure 3.8, respectively. The trigger level was set too low causing the system to deactivate and cycle into "Standby" mode after its memory had filled on 5/26. In the future, it is recommended that the trigger level be raised to prevent the memory from filling up too soon.

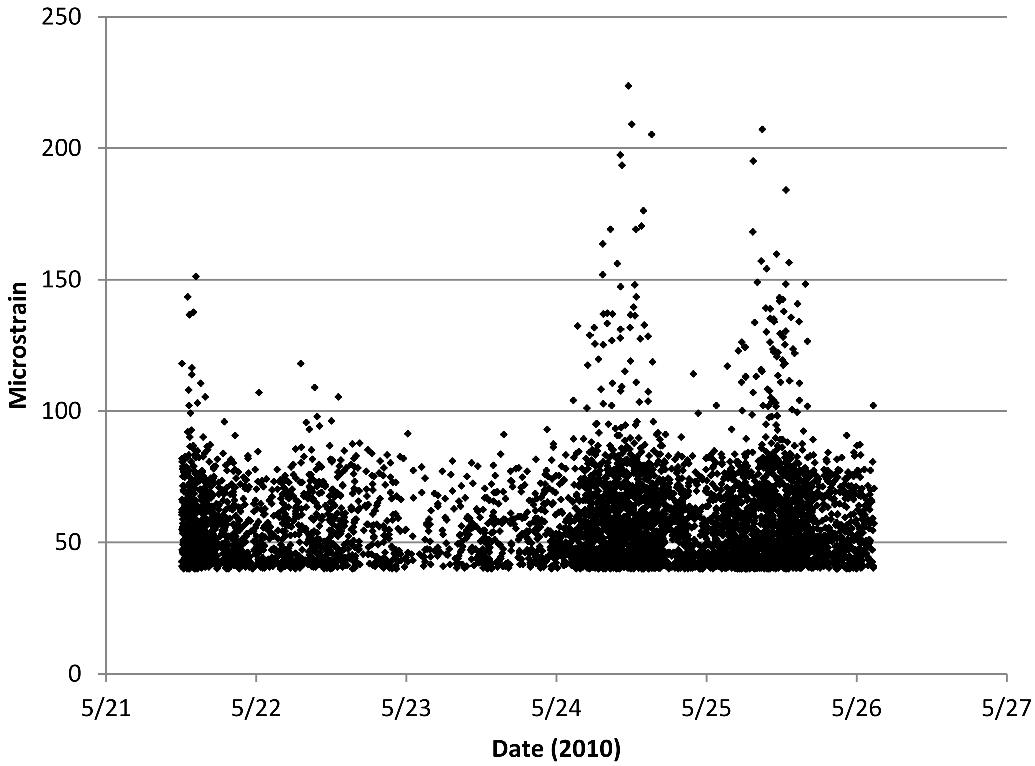

Figure 3.7: Bridge 1-826 S timeline plot

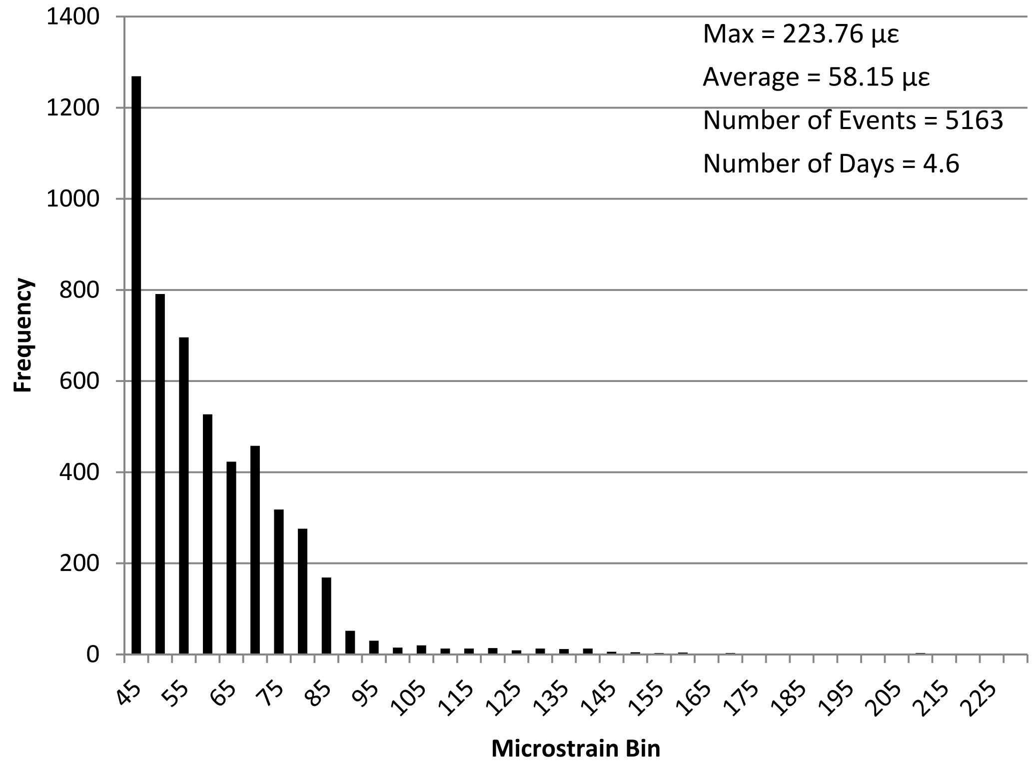

Figure 3.8: Bridge 1-826 S histogram plot

3.2.5 Bridge 1-262 S

This bridge was monitored for two weeks in June 2010. The timeline and histogram plots are presented in Figure 3.9 and Figure 3.10, respectively. The system actively collected data for the entire monitoring period. There is a distinct drop in the number of events collected during the second week of the monitoring period as shown in Figure 3.9. This may indicate a malfunction of the ISBMS or a shift in traffic patterns. However, the voltage levels for both the 9-volt and 6-volt batteries were above sufficient levels after ISBMS retrieval and no known variations in traffic were reported by DelDOT during monitoring. In the future, it is recommended that the trigger level be lowered to 30 με in order to collect more events.

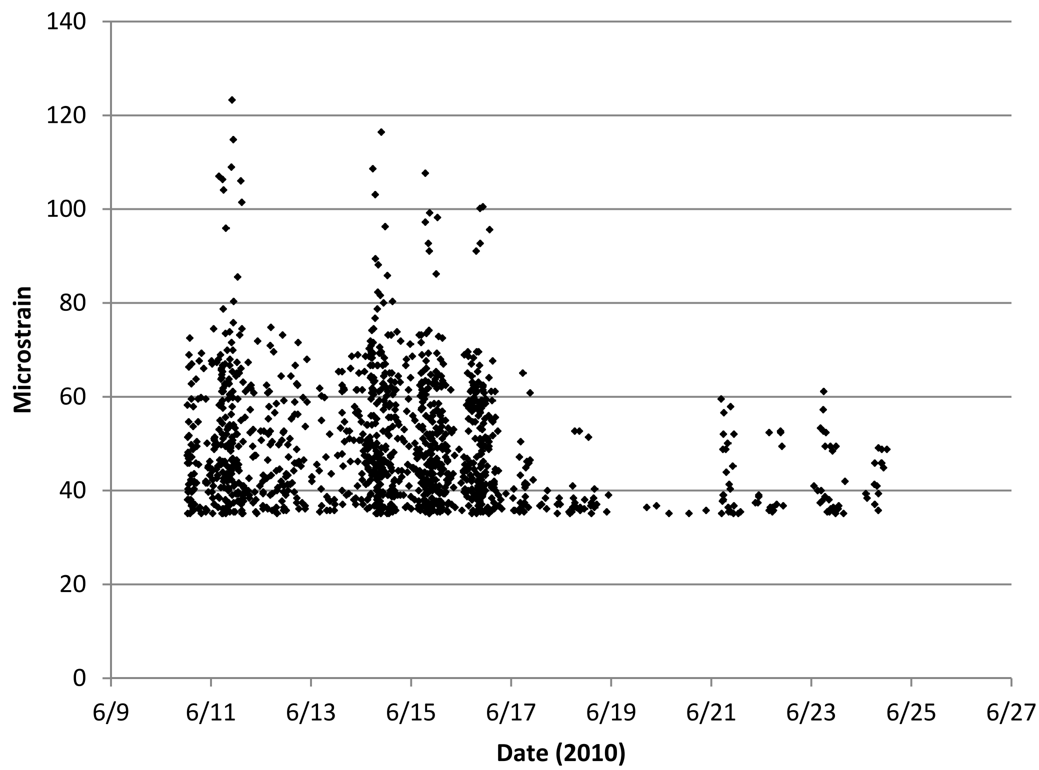

Figure 3.9: Bridge 1-262 S timeline plot

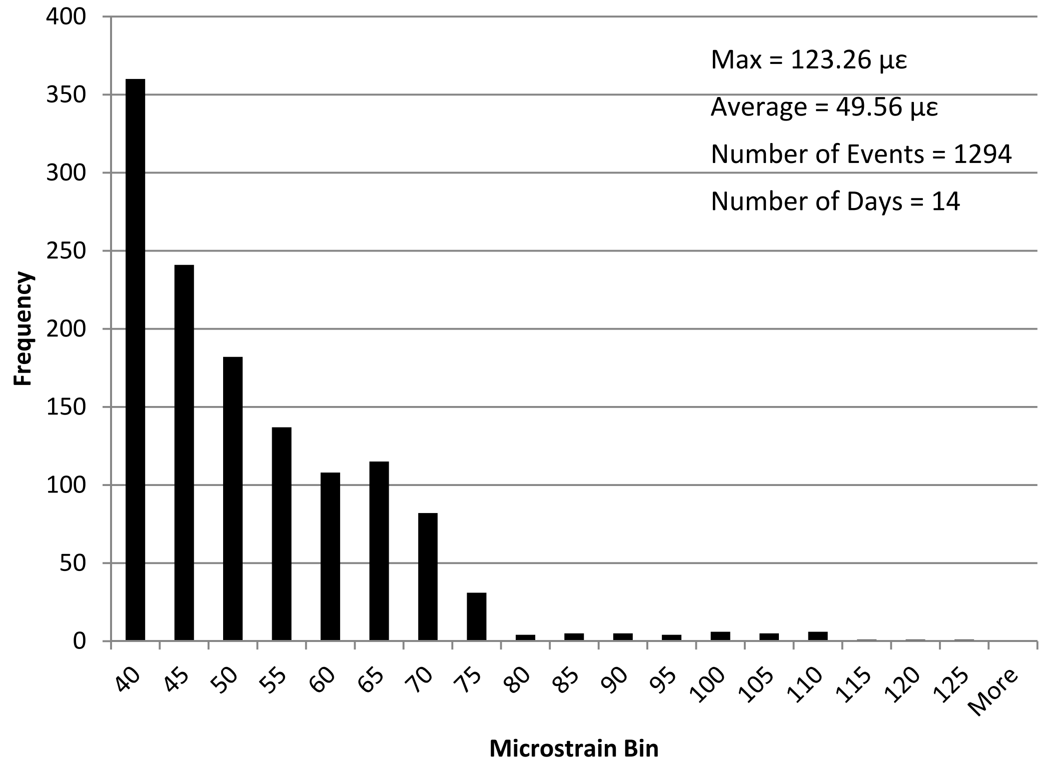

Figure 3.10: Bridge 1-262 S histogram plot

3.2.6 Bridge 1-826 N

This bridge was monitored for five days in June 2010 and for eight days in February 2011. The timeline and histogram plots for the June monitoring period are presented in Figure 3.11 and Figure 3.12, respectively. The timeline and histogram plots for the February monitoring period are presented in Figure 3.13 and Figure 3.14, respectively. During the first monitoring period, the trigger level was set too low causing the system to deactivate after its memory had filled on 6/29. The trigger level was raised for the second monitoring period but the system deactivated again after its memory had filled on 2/10. In the future, it is recommended that the trigger level be raised to prevent the memory from filling up too soon.

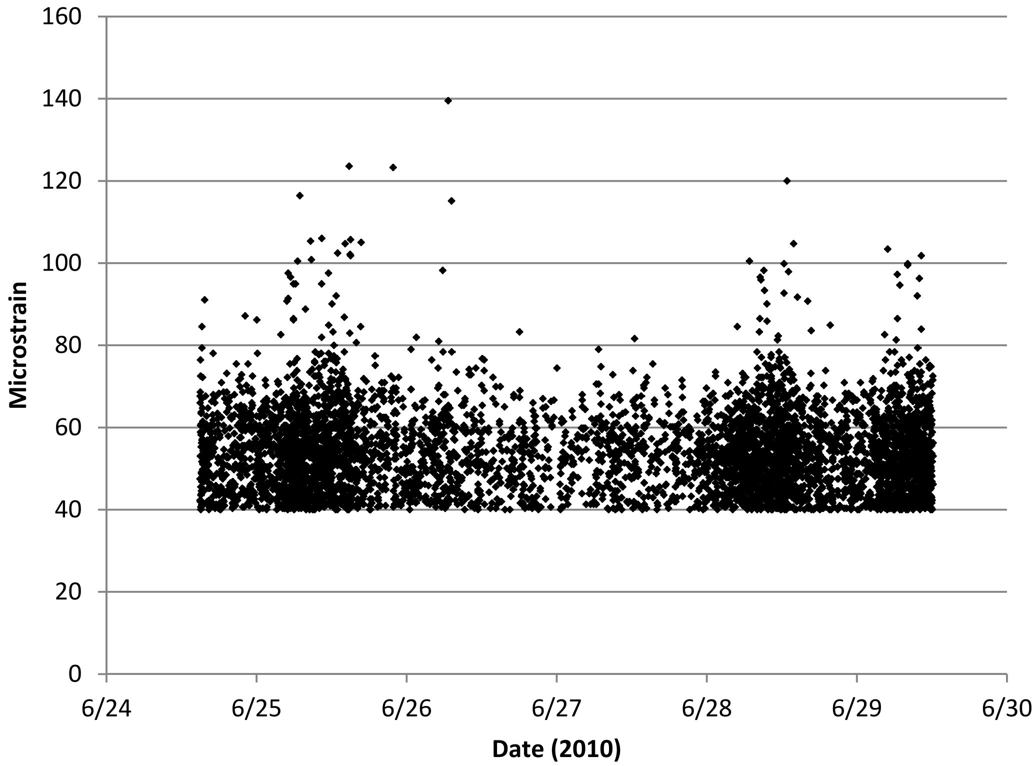

Figure 3.11: Bridge 1-826 N June 2010 timeline plot

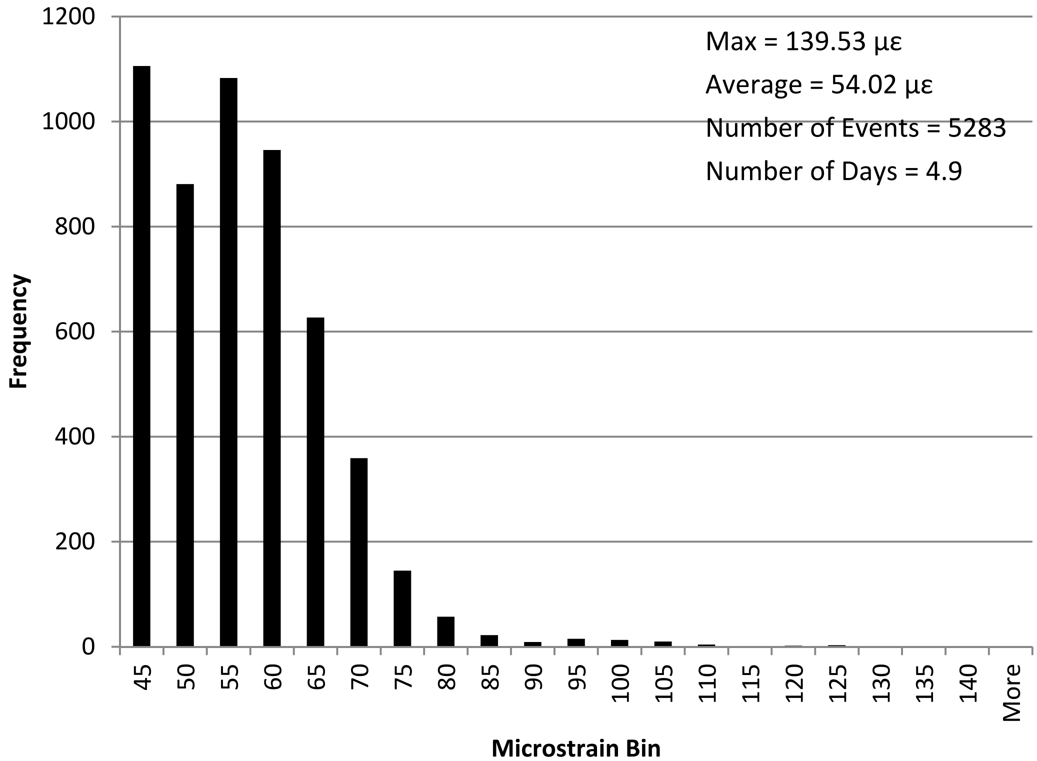

Figure 3.12: Bridge 1-826 N June 2010 histogram plot

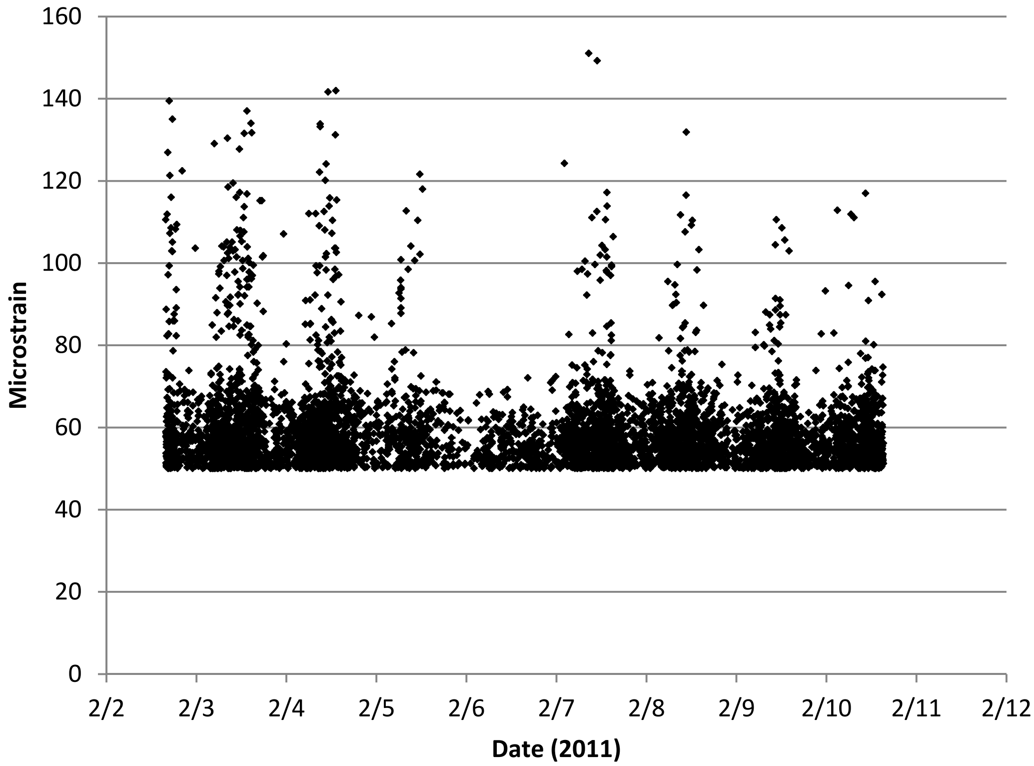

Figure 3.13: Bridge 1-826 N February 2011 timeline plot

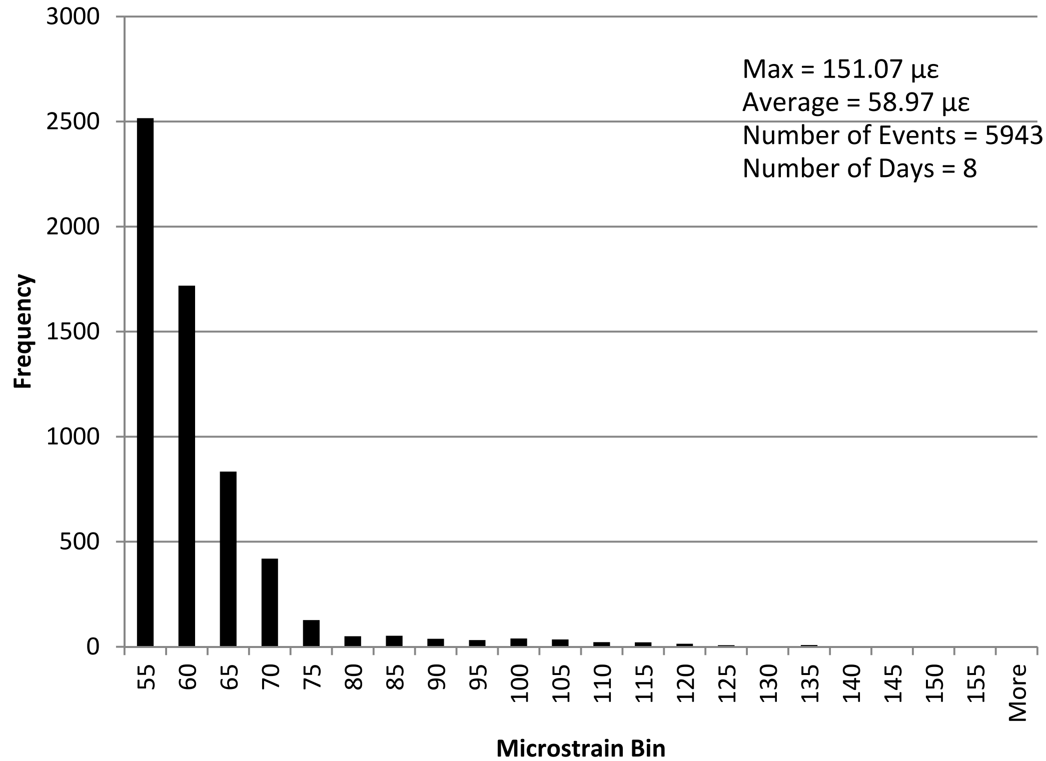

Figure 3.14: Bridge 1-826 N February 2011 histogram plot

3.2.7 Bridge 1-911 S

This bridge was monitored for six days in July 2010 and for fifteen days in November and early December 2010 which included the Thanksgiving holiday traveling period. The timeline and histogram plots for the July period are presented in Figure 3.15 and Figure 3.16, respectively. The timeline and histogram plots for the November period are presented in Figure 3.17 and Figure 3.18, respectively. During the first monitoring period, the trigger level was set too low causing the system to deactivate after its memory had filled on 7/15. The trigger level was raised significantly and the system actively collected data for the entire second monitoring period.

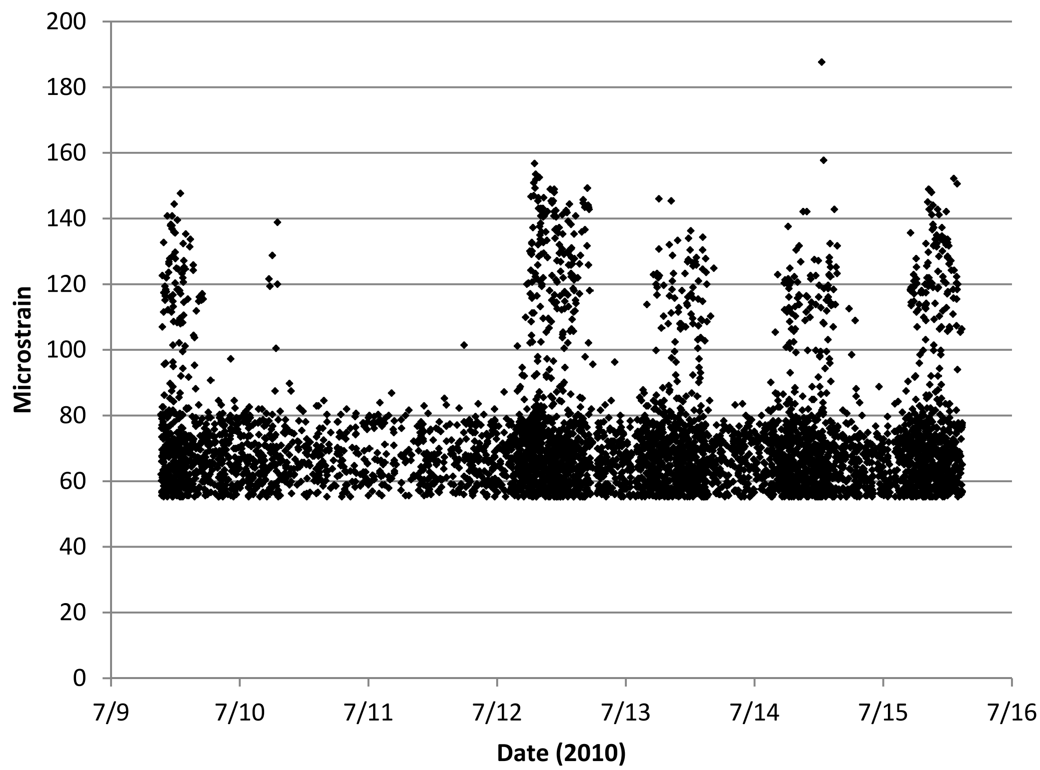

Figure 3.15: Bridge 1-911 S July timeline plot

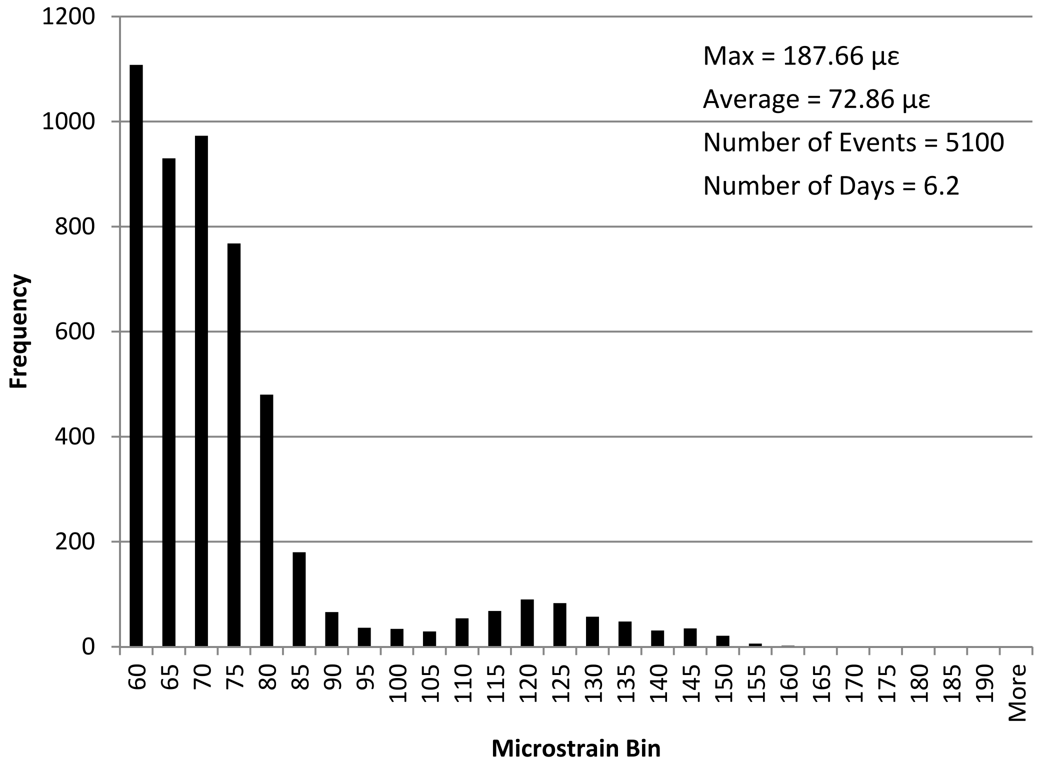

Figure 3.16: Bridge 1-911 S July histogram plot

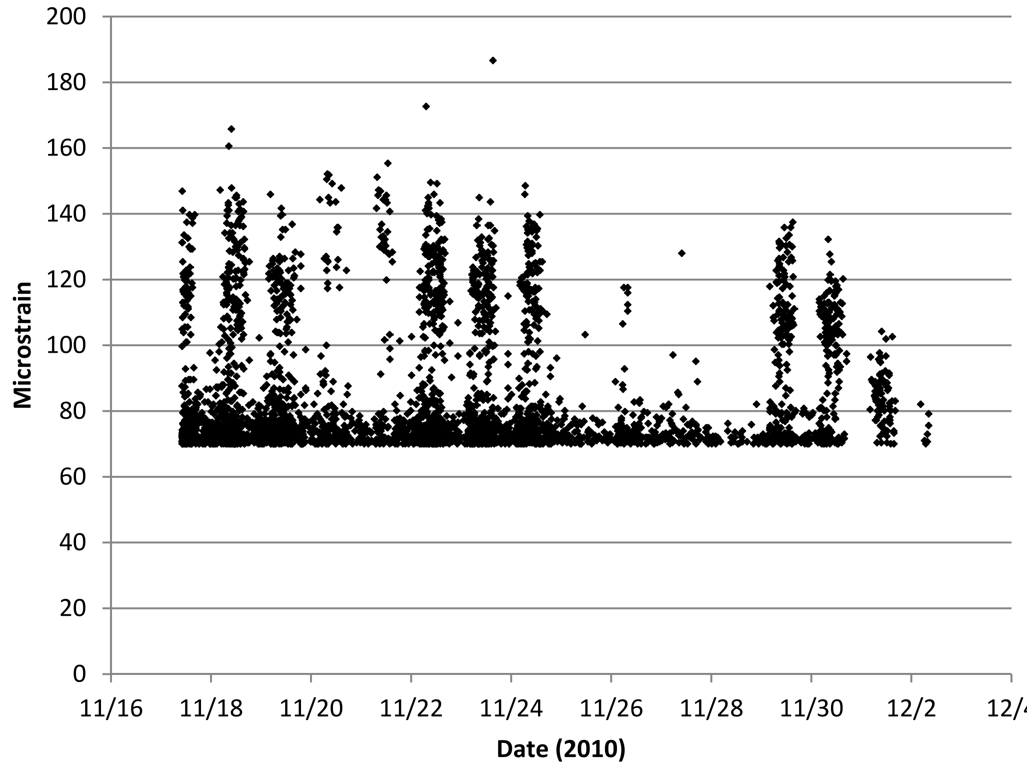

Figure 3.17: Bridge 1-911 S November timeline plot

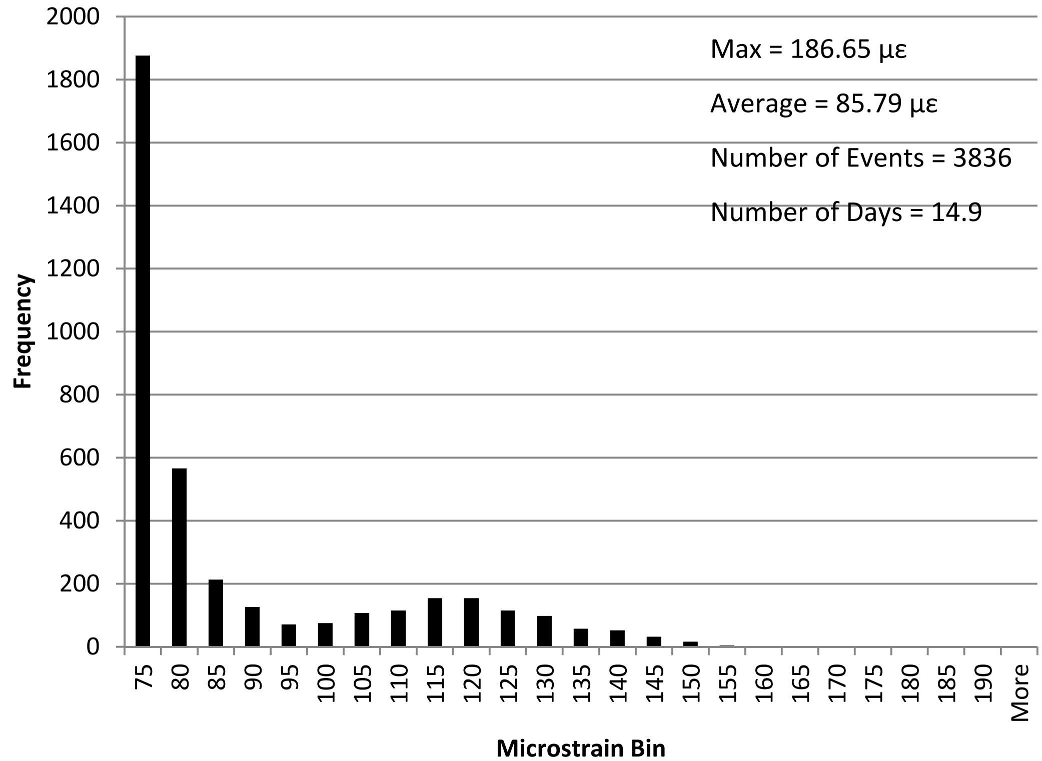

Figure 3.18: Bridge 1-911 S November histogram plot

3.2.8 Bridge 1-821 N

This bridge was monitored for five days in July 2010. The timeline and histogram plots are presented in Figure 3.19 and Figure 3.20, respectively. The trigger level was set too low causing the system to deactivate after its memory had filled on 7/27. In the future, it is recommended that the trigger level be raised to prevent the memory from filling up too soon.

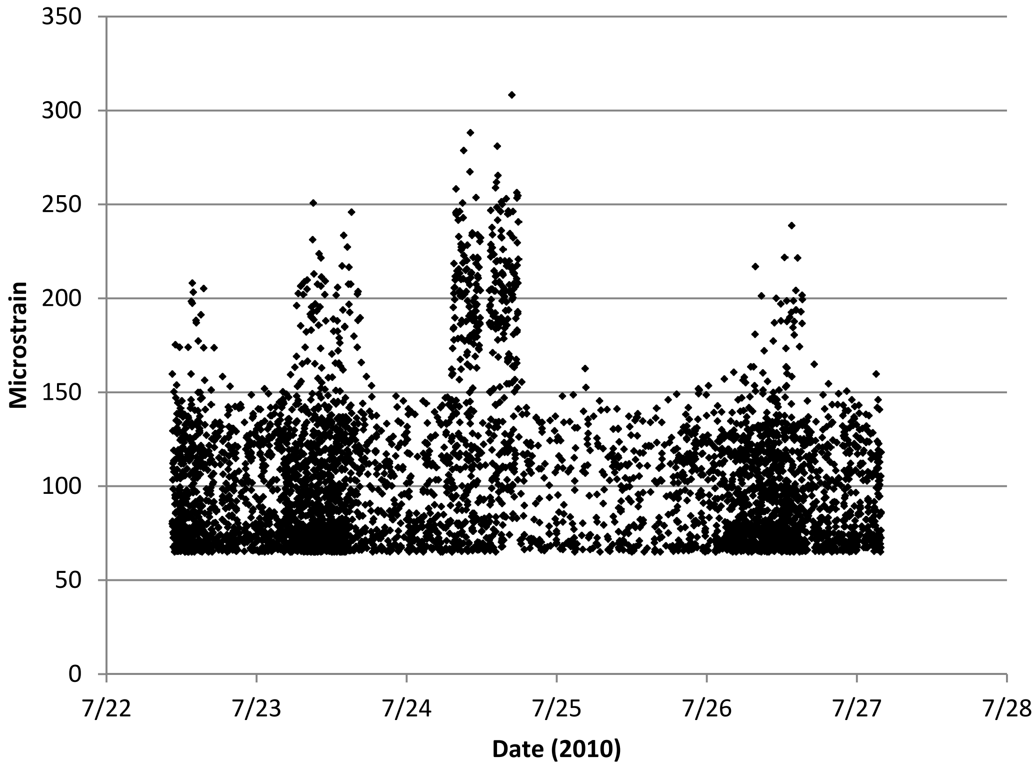

Figure 3.19: Bridge 1-821 N timeline plot

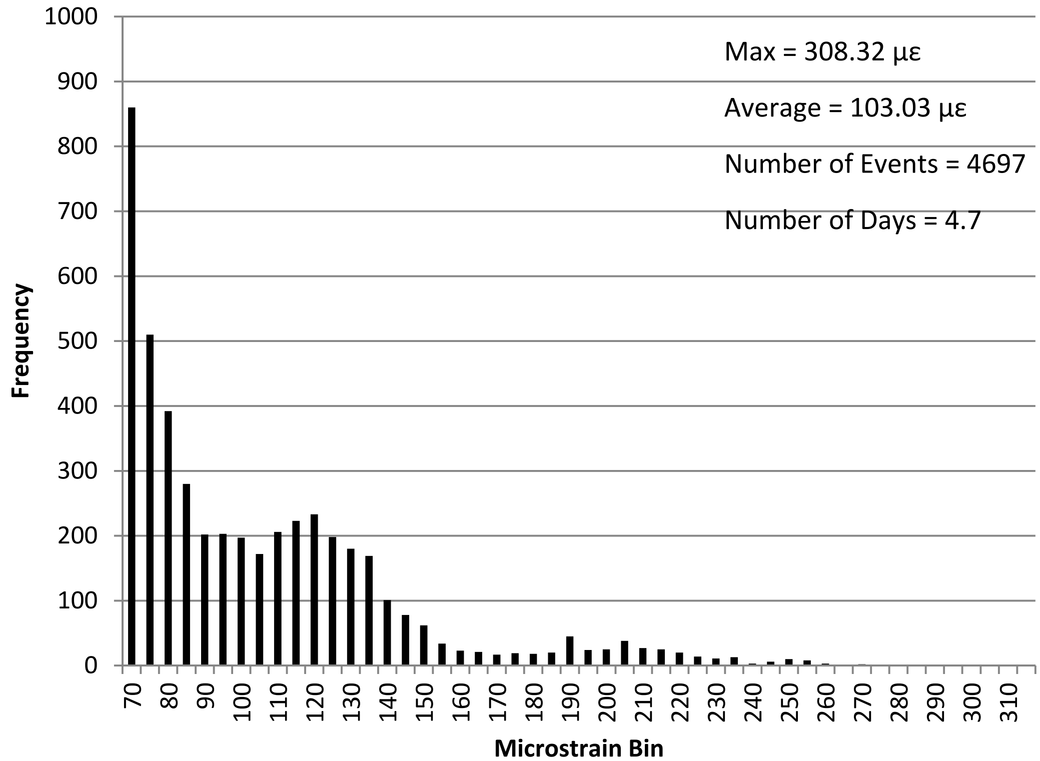

Figure 3.20: Bridge 1-821 N histogram plot

3.2.9 Bridge 1-791

This bridge was monitored for two weeks in October 2010. The timeline and histogram plots are presented in Figure 3.21 and Figure 3.22, respectively. The system actively collected data for the entire monitoring period.

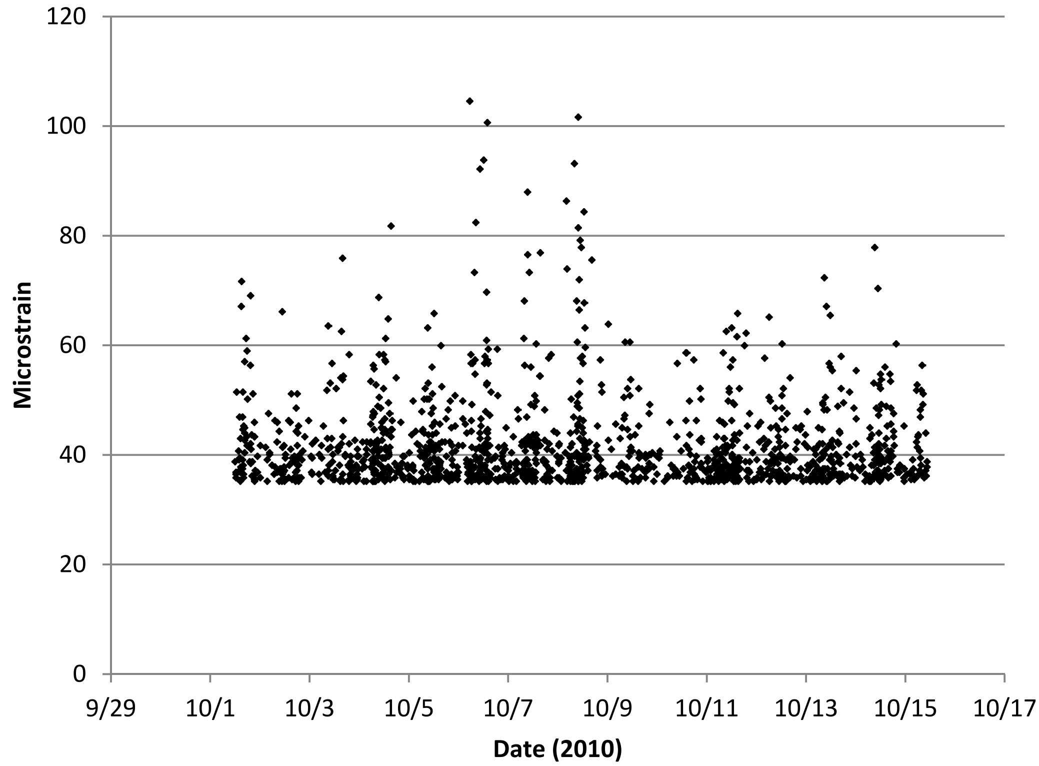

Figure 3.21: Bridge 1-791 timeline plot

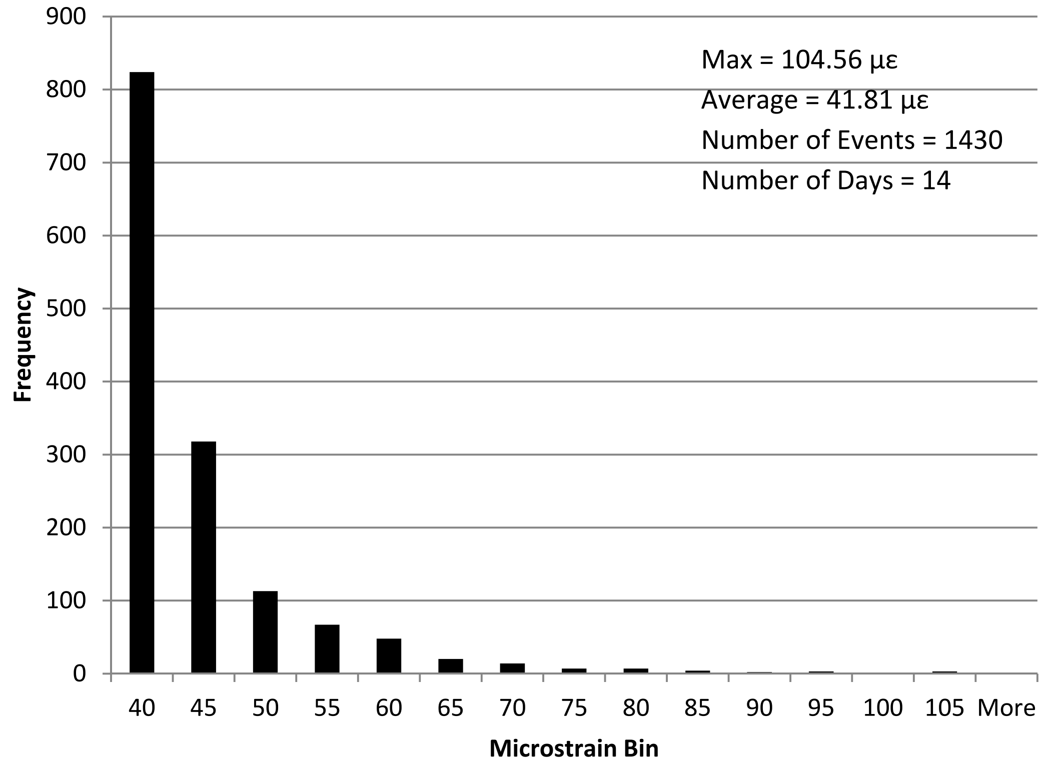

Figure 3.22: Bridge 1-791 histogram plot

3.2.10 Bridge 2-918 N

This bridge was monitored for two weeks in October and early November 2010. The timeline and histogram plots are presented in Figure 3.24 and Figure 3.25, respectively. The system actively collected data for the entire monitoring period.

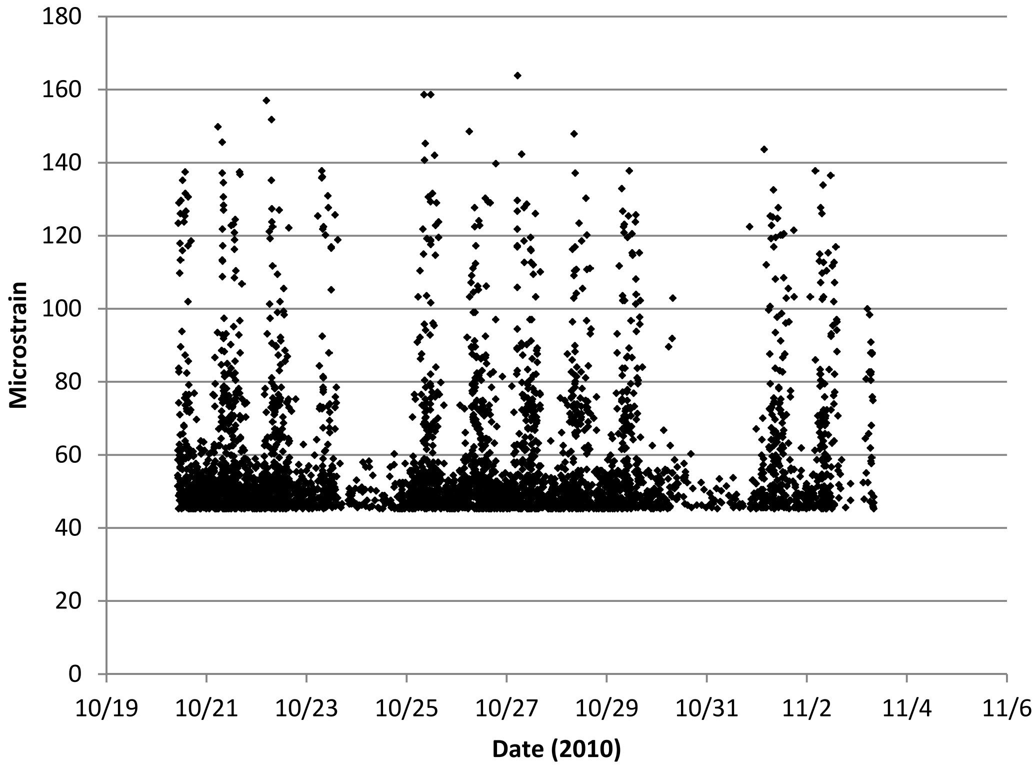

Figure 3.23: Bridge 2-918 N timeline plot

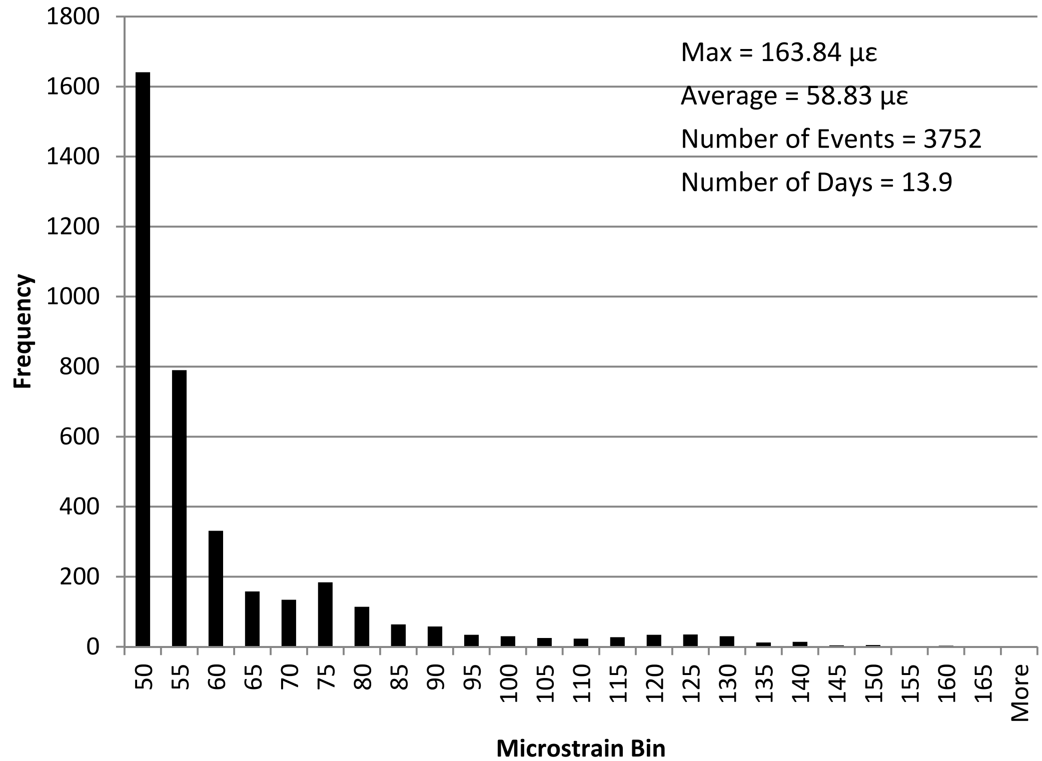

Figure 3.24: Bridge 2-918 N histogram plot

3.2.11 Bridge 2-920 N

This bridge was monitored for two weeks in November 2010. The timeline and histogram plots are presented in Figure 3.25 and Figure 3.26, respectively. The system actively collected data up until its memory was filled on 11/16 at which point it deactivated.

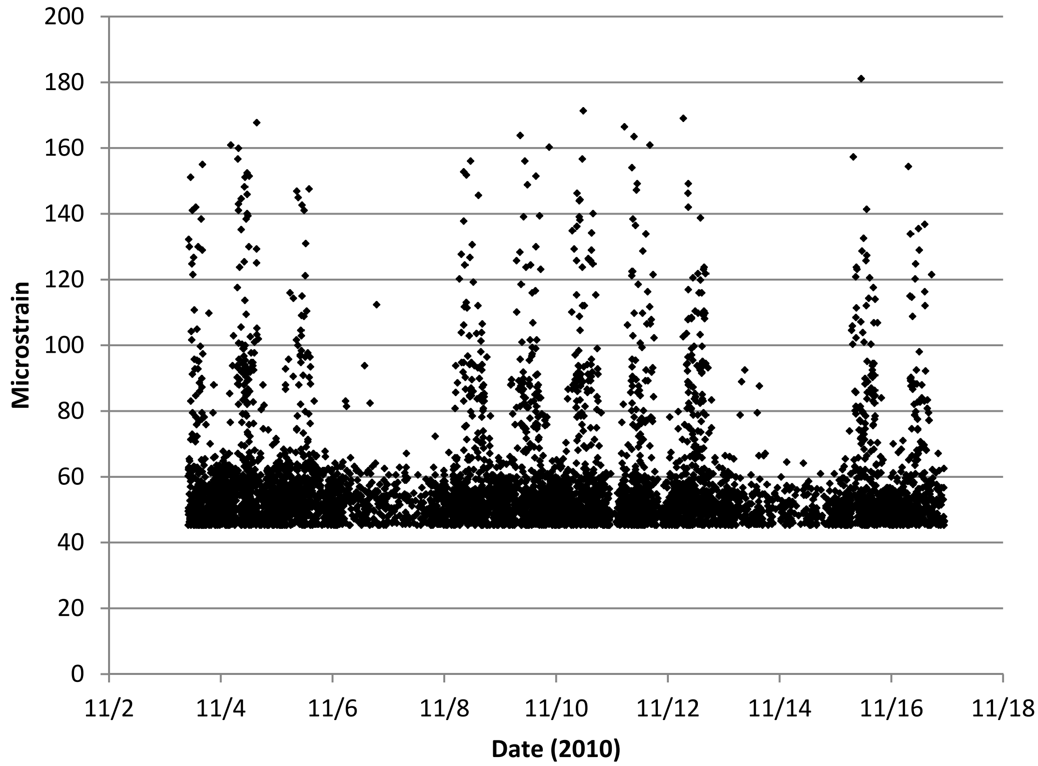

Figure 3.25: Bridge 2-920 N timeline plot

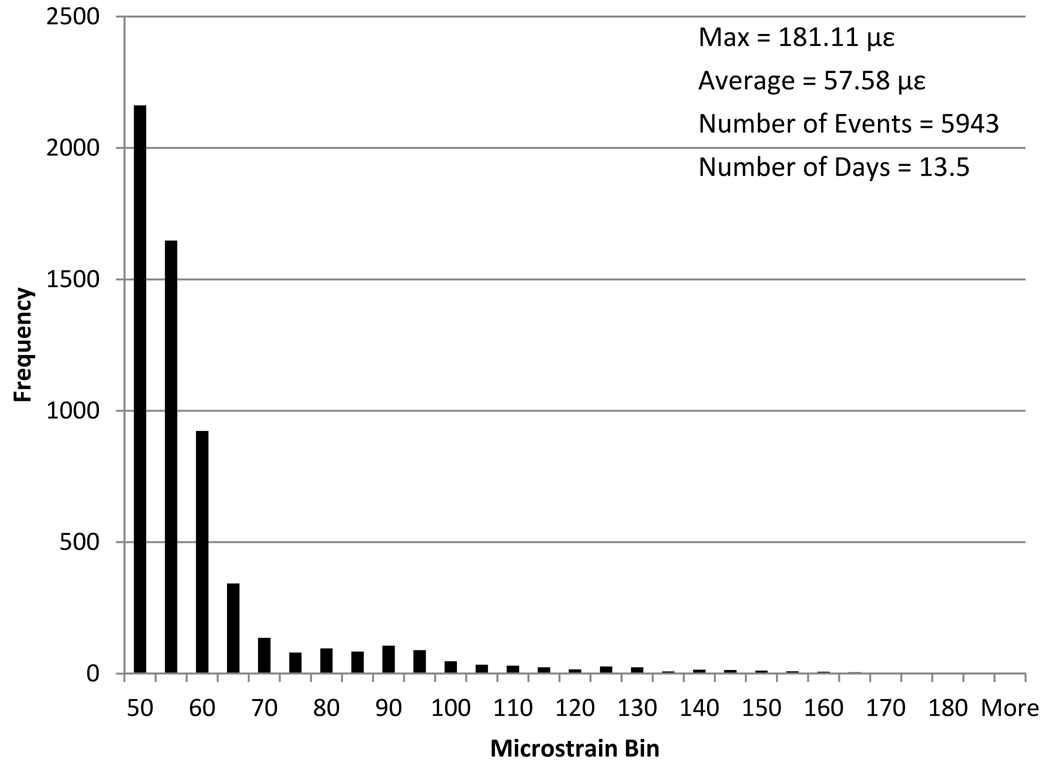

Figure 3.26: Bridge 2-920 N histogram plot

3.2.12 Bridge 1-907 S

This bridge was monitored for two weeks in December 2010. The timeline and histogram plots are presented in Figure 3.27 and Figure 3.28, respectively. The system actively collected data for the entire monitoring period. Note the unusual occurrence of one extreme event above 420 µε in the timeline.

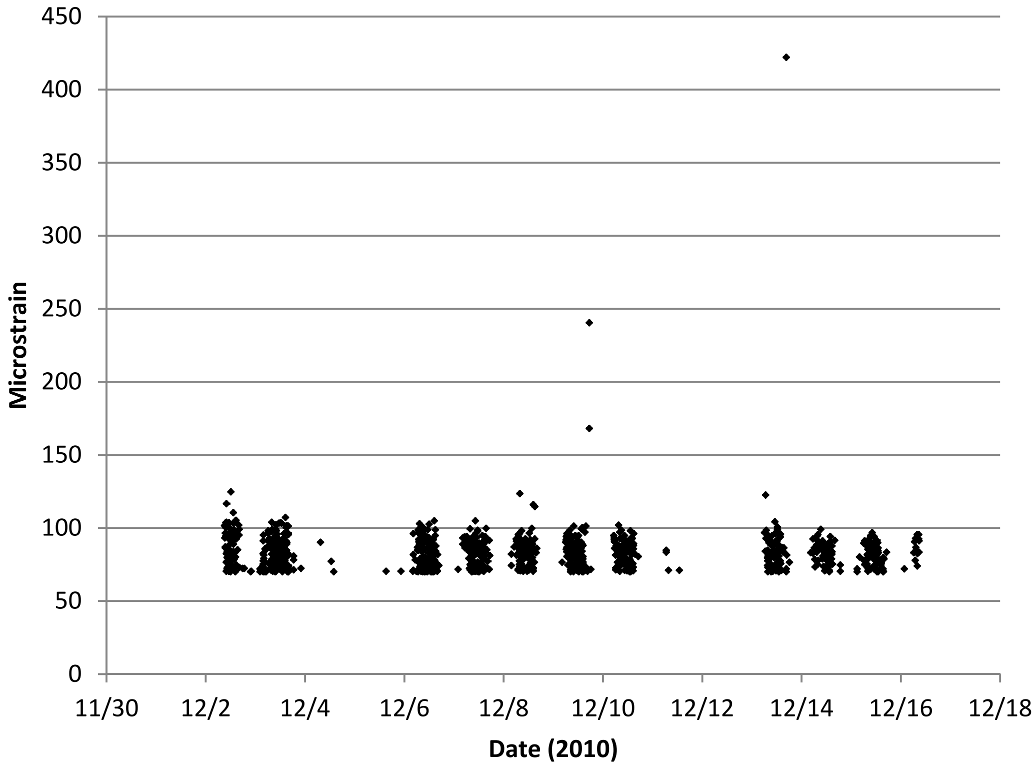

Figure 3.27: Bridge 1-907 S timeline plot

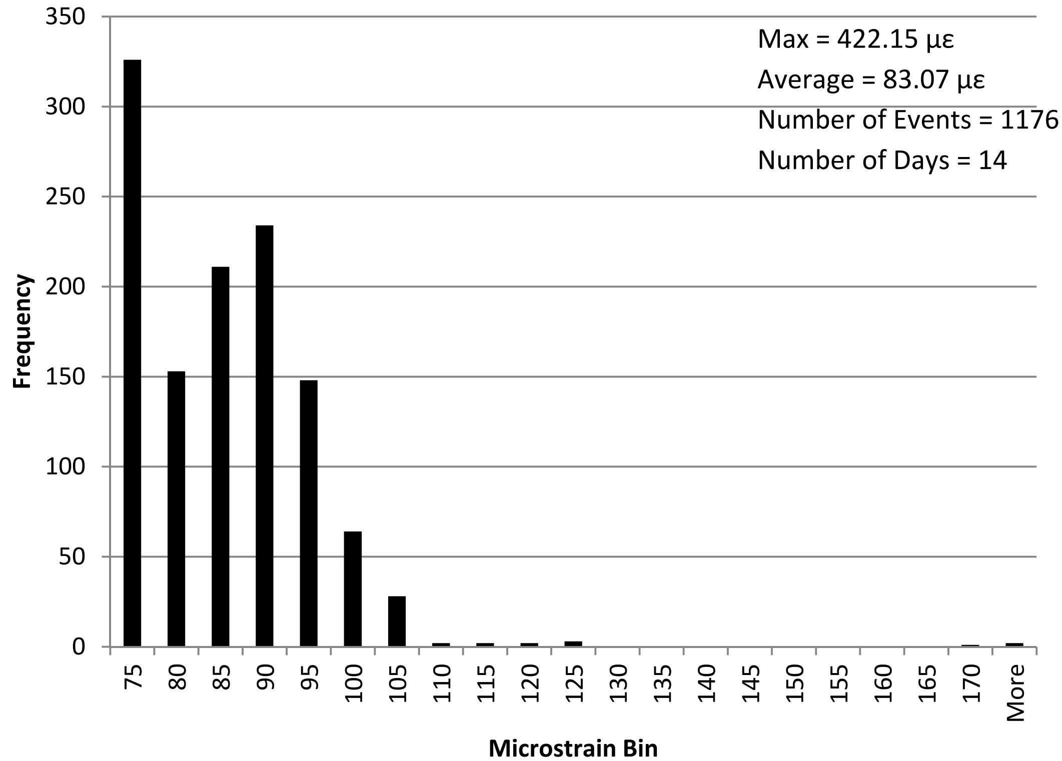

Figure 3.28: Bridge 1-907 S histogram plot

3.2.13 Bridge 1-394 S

This bridge was monitored for twenty-four days in March 2011. The timeline and histogram plots are presented in Figure 3.29 and Figure 3.30, respectively. While the system actively collected data for the entire monitoring period, there was a significant drop-off of the number of events collected after the first two weeks. This is clearly shown in the timeline plot.

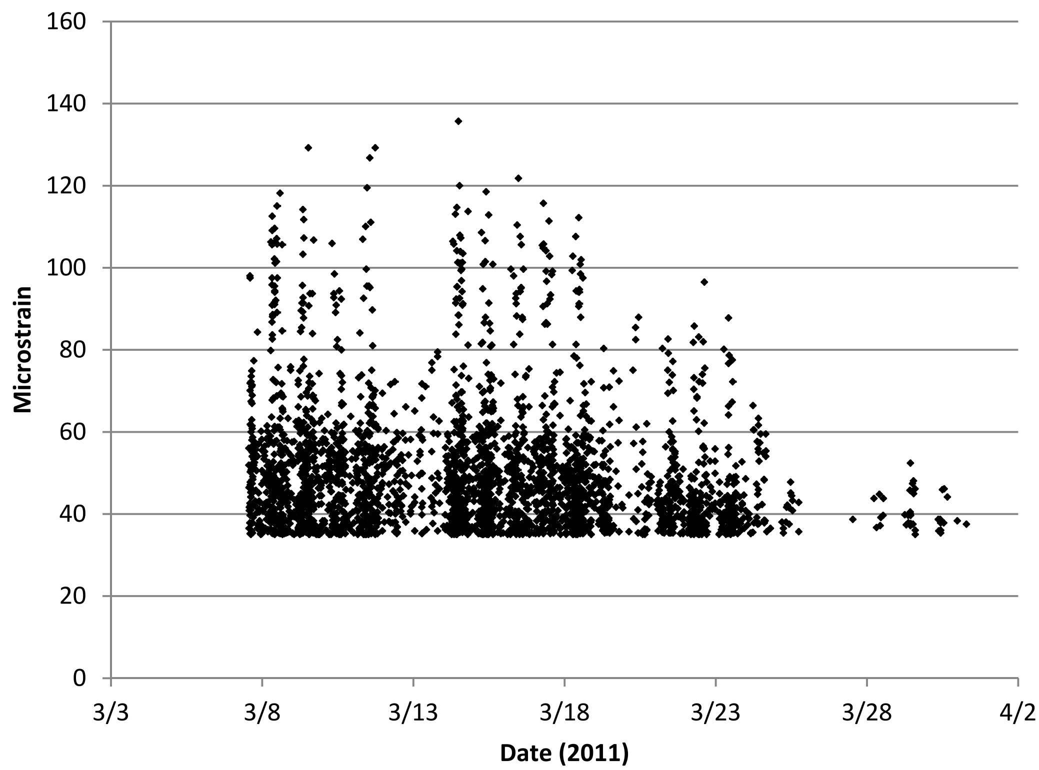

Figure 3.29: Bridge 1-394 S timeline plot

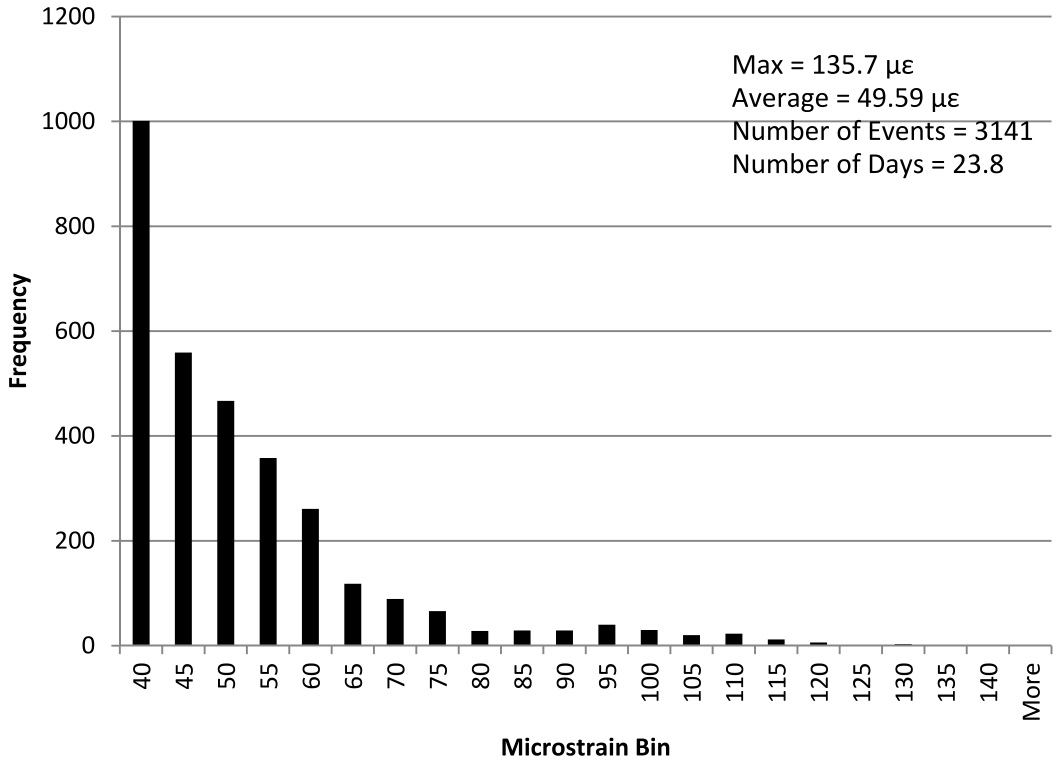

Figure 3.30: Bridge 1-394 S histogram plot

3.2.14 Bridge 1-149

This bridge was monitored for thirteen days in late March and April 2011. The timeline and histogram plots are presented in Figure 3.31 and Figure 3.32, respectively. The system actively collected data up until its memory was filled on 4/13 at which point it deactivated.

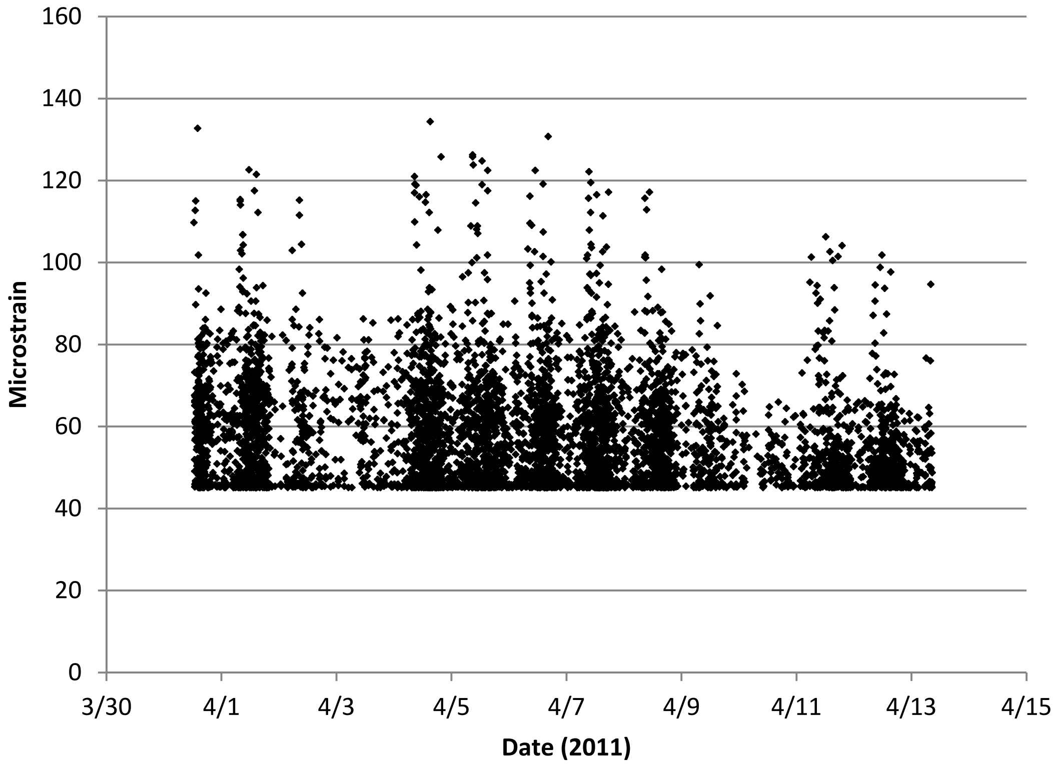

Figure 3.31: Bridge 1-149 timeline plot

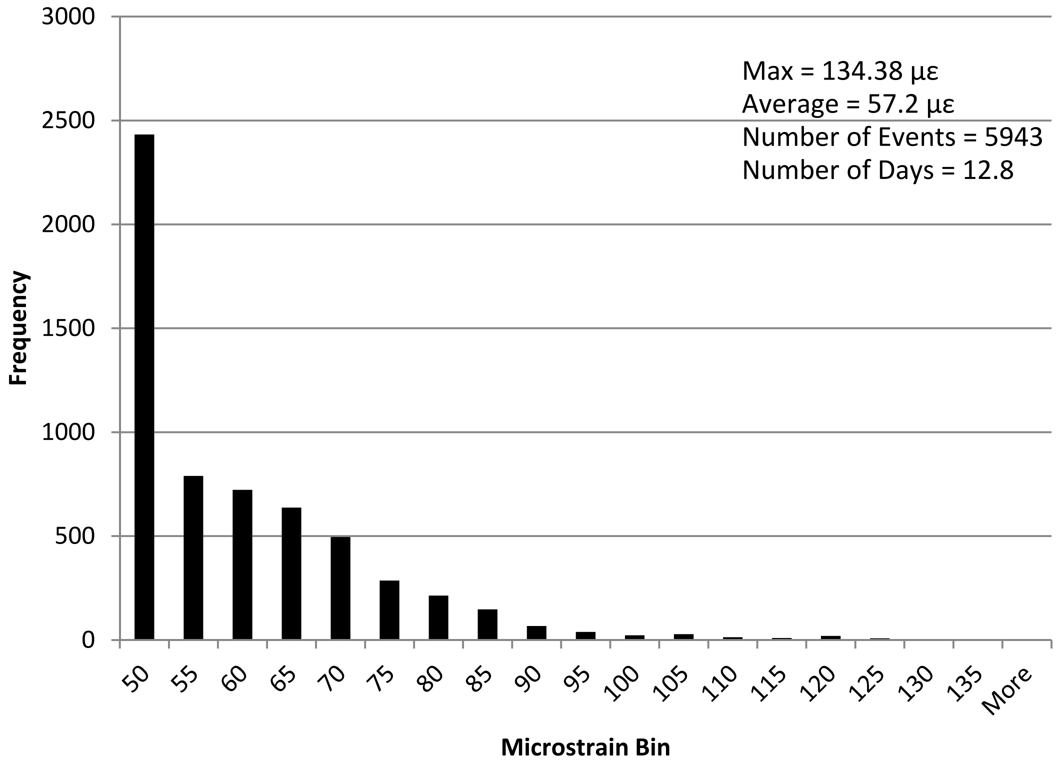

Figure 3.32: Bridge 1-149 histogram plot

Chapter 4

DATA COMPARISON

4.1 Introduction

In-service strain data collected on a bridge provides a quantitative "picture" of how the bridge is responding to the site specific traffic. Data sets that are collected at different times, whether they are a few weeks, months or years apart, can be compared. Two similar data sets would suggest that the condition of the bridge, as well as the traffic, has not changed. On the other hand, dissimilar data sets suggest that the bridge has changed in some way (i.e., has deteriorated or been damaged, or that traffic has changed.) However, no two data sets will be identical; there will be inherent variability in the data that shows up as a difference between the data sets. Two key questions must be answered: How can the differences between the data sets be quantified and when are the differences significant enough to suggest a change in the bridge condition or traffic?

Presented in this chapter are several proposed parameters for quantifying the difference in data sets. These include:

1. Area Difference (AD)
2. Square Root Sum of Squares of Differences (SRSSD)
3. Effective Strain Difference (ESD)

An example is presented to illustrate the different parameters. The parameters are then calculated for all bridges in the inventory and the results discussed. Descriptions of the bridges can be found in Section 2.3 and collected in-service data is presented in Section 3.2.

4.2 Comparison Parameters

Normalized histogram plots for the two different data sets are plotted together for this comparison. The data sets are normalized by dividing the frequency for a particular bin by the total number of events above a given threshold. This threshold is the lowest microstrain bin common in both data sets. The normalized frequency is reported as a percentage.

As an example, the frequencies for several microstrain bins are tabulated based on histogram data in Table 4.1. Data Set 1 has a threshold of 40 με, while Data Set 2 has a threshold of 45 με. It is these values that will be used to calculate sample comparison parameters. In Table 4.2 these frequencies are normalized relative to their respective total number of events.

Table 4.1: Raw histogram data for two data sets with dissimilar triggers

Microstrain Range	Number of Events Data Set 1	Number of Events Data Set 2
40 - 45	203	N/A
45 - 50	130	155
50 - 55	88	92
55 - 60	65	80
60 - 65	33	15
65 - 70	12	2
> 70	0	0
Total	531	344

Table 4.2: Frequencies and calculation of normalized frequencies for Table 4.1 data sets

Microstrain Bin	Frequency Data Set 1	Frequency Data Set 2	Norm. Freq. Data Set 1 (%)	Norm. Freq. Data Set 2 (%)
50	130	155	130/328·100 = 39.6	155/344·100 = 45.1
55	88	92	26.8	26.7
60	65	80	19.8	23.3
65	33	15	10.1	4.4
70	12	2	3.7	0.6
More	0	0	0.0	0.0
Total	328	344		

At this point the normalized histograms of each data set can be plotted on the same graph, as shown in Figure 4.1. A qualitative method of comparison is to analyze how similar the graphs appear to be. Do the graphs follow a similar distribution (i.e., normal distribution, exponential decay, etc.)? Does the difference of normalized frequency for a particular bin seem to be extreme? Visual comparison of the normalized histograms can indicate the level of similarity between data sets; however quantification is desired to express such a comparison and this is what the comparison parameters attempt to do.

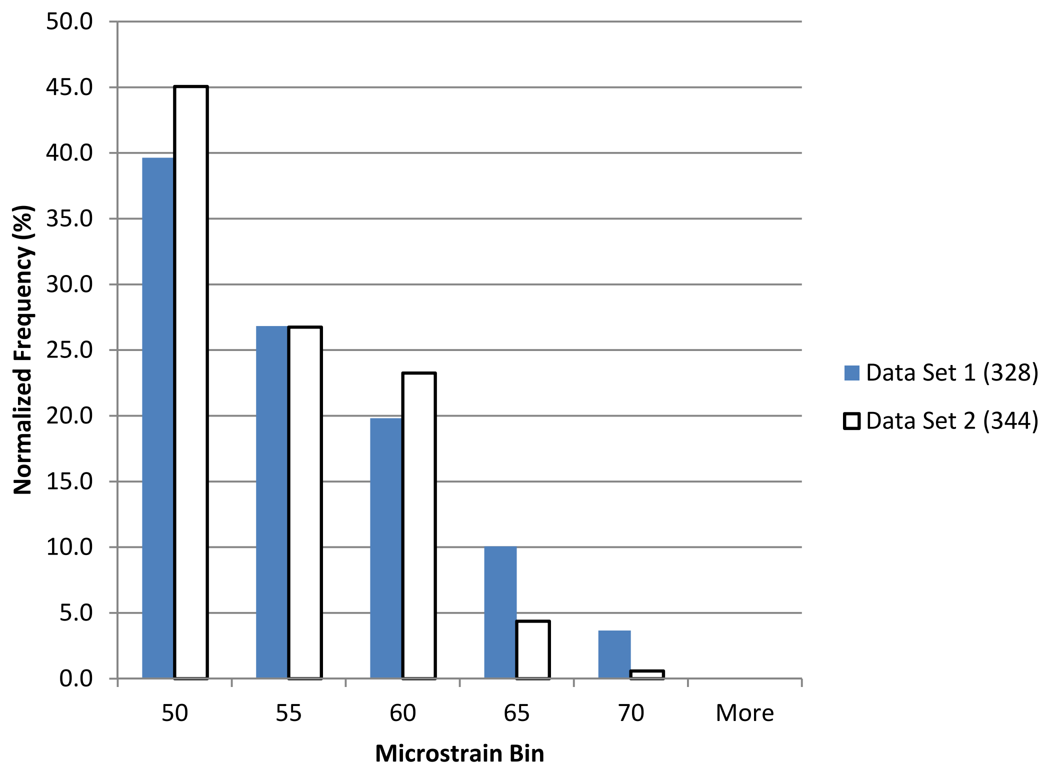

Figure 4.1: Normalized histogram comparison plot for Table 4.2 data sets

4.2.1 Area Difference (AD)

The Area Difference parameter is the difference of the areas under two normalized histogram plots. The difference is calculated between normalized frequencies for a microstrain bin multiplied by the bin size. This calculation is done for each microstrain bin and the results are summed. For the example, the absolute values of the differences of normalized frequencies multiplied by the bin size (5 με in this case) are calculated for each bin and summed in Table 4.3.

Table 4.3: Calculation of AD values for the data presented in Table 4.2

Microstrain Bin	AD
50	[45.1 – 39.6]·5 = 27.1
55	0.4
60	17.2
65	28.5
70	15.4
More	0.0
Sum	88.6

For this example the AD is **88.6**.

4.2.2 Square Root Sum of the Squares of Differences (SRSSD)

The SRSSD parameter is a multistep calculation. The difference of the normalized frequencies is squared. This is done for all microstrain bins and the results are summed. The square root of this sum is the SRSSD. The calculation can be simplified through the use of the Microsoft Excel function SUMXMY2(), taking the two normalized frequency vectors as inputs. The square root of the resulting value is then taken to yield this parameter. For the example, the differences of the normalized frequencies are squared for each bin and then summed in Table 4.4.

Table 4.4: Calculation of SRSSD values for the data presented in Table 4.2

Microstrain Bin	SRSSD
50	$(39.6 - 45.1)^2 = 29.4$
55	0.0
60	11.8
65	32.5
70	9.5
More	0.0
Sum	83.2

For this example the SRSSD is $\sqrt{83.2}$ = **9.1**.

4.2.3 Effective Strain Difference (ESD)

The Effective Strain Difference parameter uses an Effective Strain Equation (Equation 4.1) to yield a value for each data set. The absolute value of the difference is calculated for the ESD value. Inputs are the histogram frequencies, not the normalized frequencies. The equation used for Effective Strain is:

$$\sqrt[3]{\sum\left(\frac{n_i}{N} * {\varepsilon_i}^3\right)} \qquad \text{Equation 4.1}$$

where:

- $n_i \equiv$ number of events for a particular bin
- $N \equiv$ total number of events
- $\varepsilon_i \equiv$ microstrain bin

In this example N is equal to 328 for Data Set 1 and 344 for Data Set 2. Part of the calculation is completed in Table 4.5.

Table 4.5: Partial calculation ESD values for the data presented in Table 4.2

ε_i	n_i, DS1	n_i, DS2	$n_i/N\cdot\varepsilon_i$, DS1	$n_i/N\cdot\varepsilon_i$, DS2
50	130	155	$130/328*50^3 = 49543$	$155/344*50^3 = 56323$
55	88	92	44637	44496
60	65	80	42805	50233
65	33	15	27630	11975
70	12	2	12549	1994
Sum	328	344	177163	165020

The Effective Strain for Data Set 1 is $\sqrt[3]{177163}$ = 56.2; the Effective Strain for Data Set 2 is $\sqrt[3]{165020}$ = 54.9. The ESD for this example is then 56.2 – 54.9 = **1.3**.

4.3 Week-to-Week Comparisons

In order to determine if two data sets are similar or different based on the parameters, threshold values for the parameters need to be selected. If a parameter calculated for two data sets being compared falls below the given threshold then the data sets are deemed to be similar and if it falls above then the data sets are deemed to be dissimilar. These threshold values are based on "control" data sets which are assumed to be very similar: the transducer must be located in the exact same position, the temperatures must be similar, the bridge must be in the same condition and traffic patterns cannot be disparate. These conditions are met by comparing two single weeks of a two-week monitoring period which should reduce most variability. As long as at least fourteen days of data was collected during the monitoring period, this comparison could be made. The results of these week-to-week histogram comparisons are shown in Table 4.6.

Table 4.6: Comparison parameters for week-to-week histograms from 2009 to 2011 data sets

Bridge Number	Number of Events		AD	SRSSD	ESD
	Week 1	Week 2			
1-781 (1)	1,602	986	119.58	10.60	2.19
1-781 (2)	986	1,301	89.65	9.56	2.26
1-781 (3)*	1,602	1,301	205.63	19.00	0.07
1-728	605	202	98.54	9.32	11.89
1-704	667	176	28.43	3.01	18.9
1-262 S*	1,176	118	383.92	41.41	17.77
1-791	793	637	56.21	5.65	0.61
2-918 N	2,346	1,406	93.25	7.39	4.85
2-920 N	3,351	2,592	111.22	11.1	1.76
1-911 S (11/2010)	2,829	963	114.58	7.45	12.17
1-907 S	719	457	80.34	6.16	7.67
1-394 S	1,338	1,352	80.30	6.68	1.23
1-149	3,681	2,262	140.20	11.13	1.82

* Normalized histograms show qualitative difference

4.3.1 Threshold Values

The results of the week-to-week comparisons are used to extract threshold values for the Area Difference, Square Root Sum of the Squares of Differences and Effective Strain Difference parameters. The method for selecting these values is based on outlier determination (Mendenhall & Sincich, pp. 30-39). First, the upper quartile, Q_U, and lower quartile, Q_L, are determined based on the values for each parameter. The value at which 75% of values in a set are lower is the upper quartile and the value at which 25% of values are lower is the lower quartile. Next, the interquartile range, IQR, is calculated. This is the difference between the upper and lower quartiles ($Q_U - Q_L$). Then the upper "inner fence" is determined. This is the upper quartile plus 1.5·IQR. Only an upper fence needs to be determined for this research since outliers will only be values that are too high above a value of zero. Using the data in Table 4.6, the upper fence values for the three parameters are calculated in Table 4.7.

Table 4.7: Calculation of upper fence values for Table 4.6 data

	AD	SRSSD	ESD
Average	123.22	11.42	6.40
Q_U	140.20 ≈ 140	11.13 ≈ 11	12.17 ≈ 12
Q_L	80.30 ≈ 80	6.16 ≈ 6	1.23 ≈ 1
IQR	140 – 80 = 60	5	11
1.5·IQR	1.5·60 = 90	7.5	16.5
Upper Fence	60 + 90 = 230	18.5	28.5

Values greater than the upper fence are those suspected of being outliers. The following parameter threshold values were selected:

- 230 for Area Difference
- 18.5 for Square Root Sum of Squares of Differences
- 28.5 for Effective Strain Difference

While values of zero would represent a perfect match, parameter values that fall below these values should represent a relatively good match and values above should represent relatively poor matches in histogram comparisons.

4.3.2 Sample Week-to-Week Comparisons

Data was collected for fifteen days on Bridge 1-791 allowing for a two-week comparison (Figure 4.2). This week-to-week comparison is an example of very similar histogram data collected from one week to the next. Both histograms appear to follow an exponential decay distribution. The AD, SRSSD, and ESD parameters all fall well below their respective threshold values.

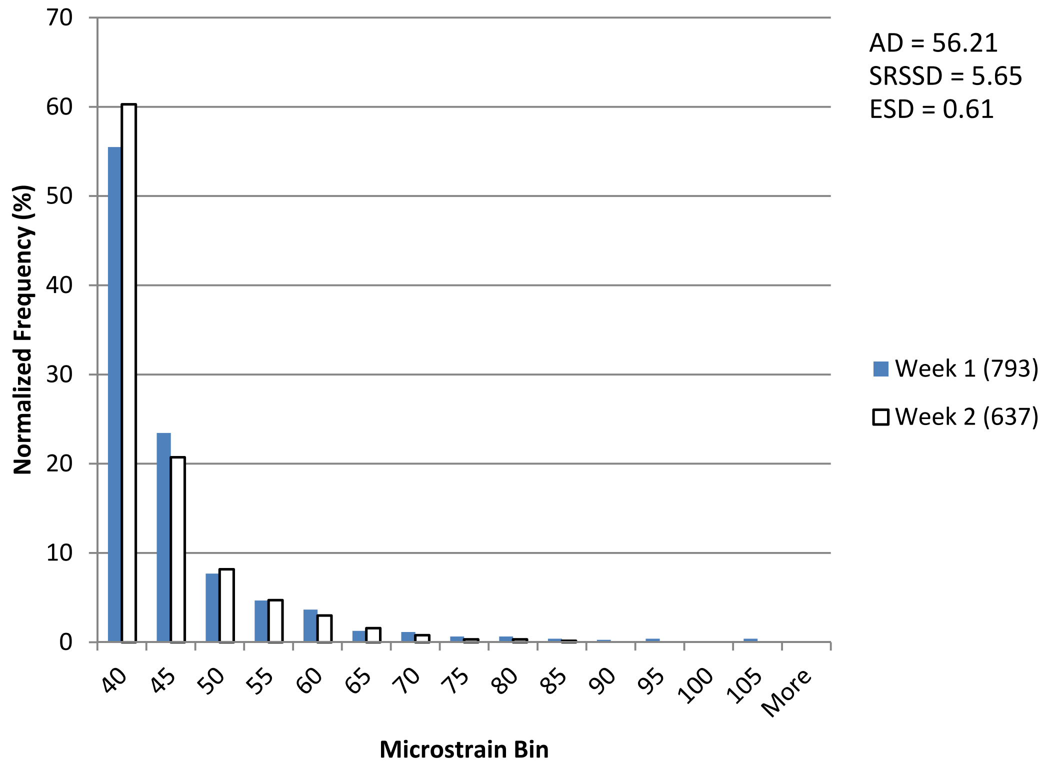

Figure 4.2: Bridge 1-791 week-to-week histogram comparison

Data was collected for fourteen days on Bridge 2-918 N allowing for a two-week comparison (Figure 4.3). This week-to-week comparison is another example of very similar histogram data collected from one week to the next. Both histograms appear to follow a similar distribution. The AD, SRSSD, and ESD parameters all fall well below their respective threshold values.

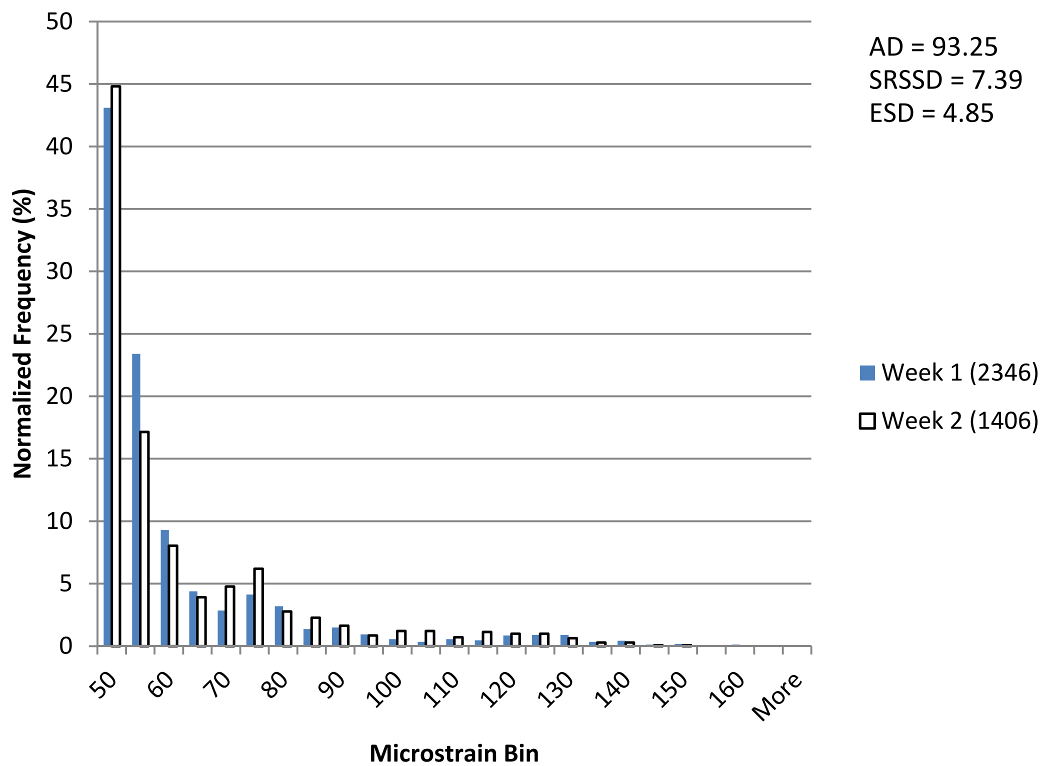

Figure 4.3: Bridge 2-918 N week-to-week histogram comparison

Data was collected for twenty-one days on Bridge 1-781 allowing for three week-to-week comparisons (Figure 4.4). All three plots appear to follow a similar distribution shape but have inconsistent values in each of the bins. The AD, SRSSD and ESD parameters fall within their thresholds for comparisons 1 and 2. Interestingly however, the SRSSD falls outside its threshold and the AD comes close to its threshold while the ESD remains inside for comparison 3 (Table 4.8). Note that Thanksgiving Day occurred during Week 2.

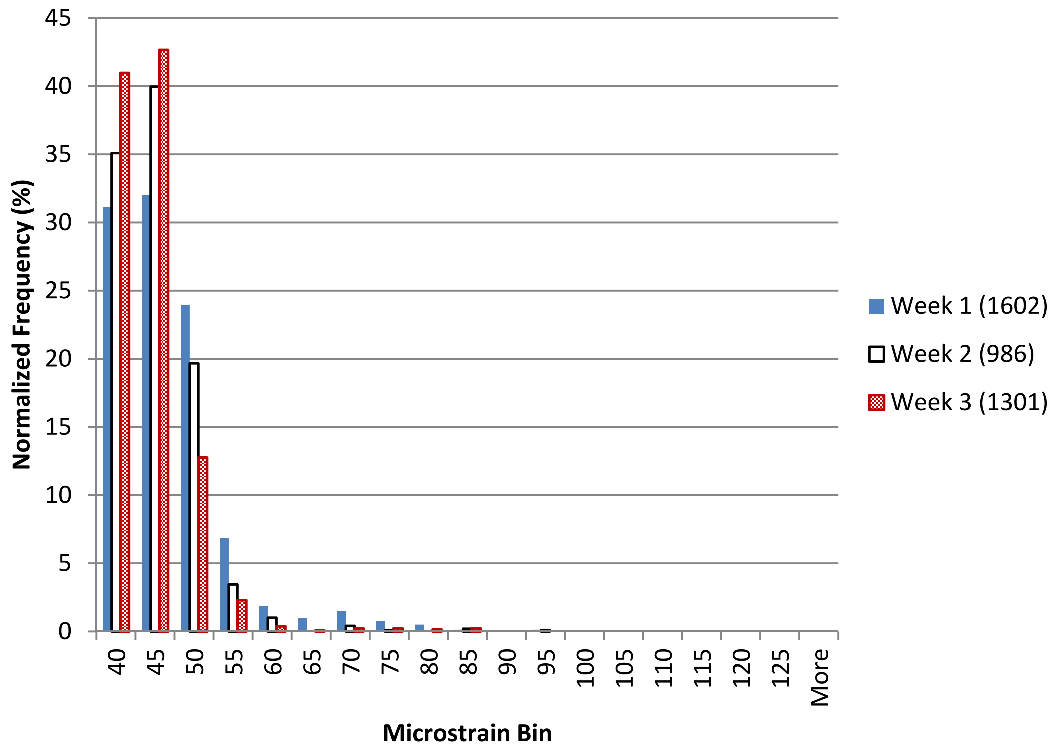

Figure 4.4: Bridge 1-781 week-to-week histogram comparison

Table 4.8: Bridge 1-781 three-week parameter values

Comparison	AD	SRSSD	ESD
Week 1 to Week 2 (1)	119.58	10.60	2.19
Week 2 to Week 3 (2)	89.65	9.56	2.26
Week 1 to Week 3 (3)	205.63	19.00	0.07

Data was collected for fourteen days on Bridge 1-262 S allowing for a two-week comparison (Figure 4.5). This week-to-week comparison is another example of differences in histogram data collected from one week to the next. The distributions are quite different in appearance. Week 2 has a large spike in the first bin and decays rapidly after that while Week 1 starts lower and decays over the bin range. The AD and SRSSD values fall well outside their thresholds while the ESD is within its threshold. There was a large difference between events collected during Week 1 compared with events collected during Week 2 (see timeline plot, Figure 3.9 in Section 3.2.5.) which, likely, could have skewed the histogram data.

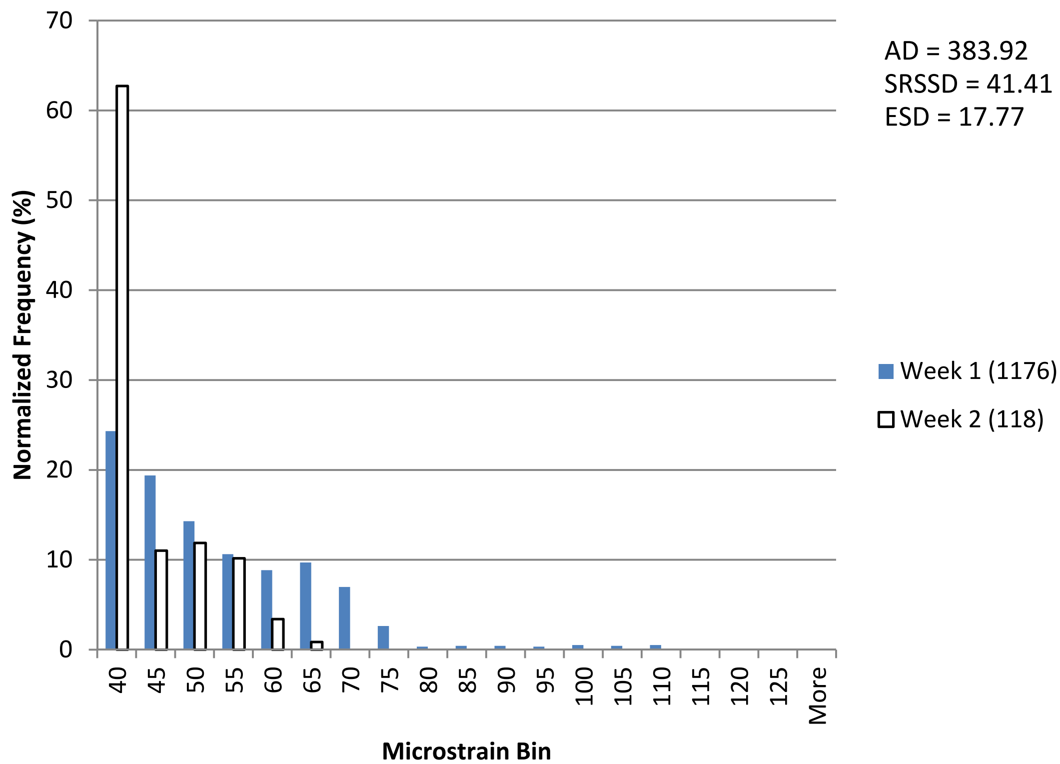

Figure 4.5: Bridge 1-262 S week-to-week histogram comparison

The selected parameter threshold values correlate with subjective comparisons for determining if data sets are similar or different. The AD and SRSSD thresholds seem to be more discerning and reliable than the ESD. None of the bridges' ESD values went over their thresholds even when obvious differences were present. As such, more weight should be given to the AD and SRSSD values, which seem to parallel one another in analysis.

4.4 Year-to-Year Comparisons

The parameter threshold values determined using week-to-week histogram data were implemented for year-to-year histogram comparisons. This section compares data collected during this project with data collected in previous years but during the same approximate time of year. This should remove the variation due to the effects of temperature differences for the most part. A summary of the in-service data is provided in Table 4.9 and the comparison parameters are reported in Table 4.10.

Table 4.9: In-service data being compared for year-to-year histograms

Bridge Number	Number of Days		Comparison Threshold	Events Collected		Events Compared	
	New	Previous		New	Previous	New	Previous
1-781	21	13	40	3,889	3,027	2,511	3,027
1-728	9	17	30	807	1,145	506	1,145
1-262 S	14	14	50	1,294	754	511	754
1-826 N	5	15	50	5,283	4,204	3,296	4,204
1-911 S	6	5	70	5,100	5,793	2,089	1,755
1-821 N	5	6	65	4,697	5,937	4,697	4,690
1-791	15	14	35	1,430	2,889	1,430	2,887
2-918 N	14	14	50	3,752	1,576	2,111	1,576
1-149	13	14	50	5,943	1,892	3,510	1,892

Table 4.10: Comparison parameters for year-to-year histograms

Bridge Number	Date Monitored		AD	SRSSD	ESD
	New	Prev.			
1-781*	11/2009	9/2007	215.93	23.98	0.91
1-728	12/2010	12/2007	135.14	10.44	0.58
1-262 S*	6/2010	6/2006	226.46	21.39	0.91
1-826 N*	6/2010	5/2006	250.38	24.47	0.67
1-911 S	7/2010	6/2007	101.2	6.32	1.52
1-821 N*	7/2010	8/2007	341.45	18.39	28.42
1-791*	10/2010	10/2006	273.42	30.42	2.07
2-918 N	10/2010	11/2007	95.06	6.93	4.08
1-149*	4/2011	3/2006	299.7	32.09	6.54

* Normalized histograms show qualitative difference

Table 4.11 shows the results of comparing the calculated parameters for each bridge with their threshold values. Check marks indicate a quantifiable difference.

Table 4.11: Quantifiably different histogram data for year-to-year comparisons

Bridge Number	AD	SRSSD	ESD
1-781		✓	
1-728			
1-262 S		✓	
1-826 N	✓	✓	
1-911 S			
1-821 N	✓		
1-791	✓	✓	
2-918 N			
1-149	✓	✓	

4.4.1 Bridge 1-781

The histogram comparison for this bridge shows some distinct changes in the normalized plots of the two sets of microstrain data collected (Figure 4.6). The 2007 data seems to be in the shape of a normal distribution while the 2009 data resembles an exponential decay. The SRSSD parameter falls above its threshold while the AD is slightly under. Differences could be due to traffic variation between the two monitoring periods: the bridge was originally monitored in September 2007 but was monitored for this project in late November and early December 2009 which included the Thanksgiving holiday traveling period.

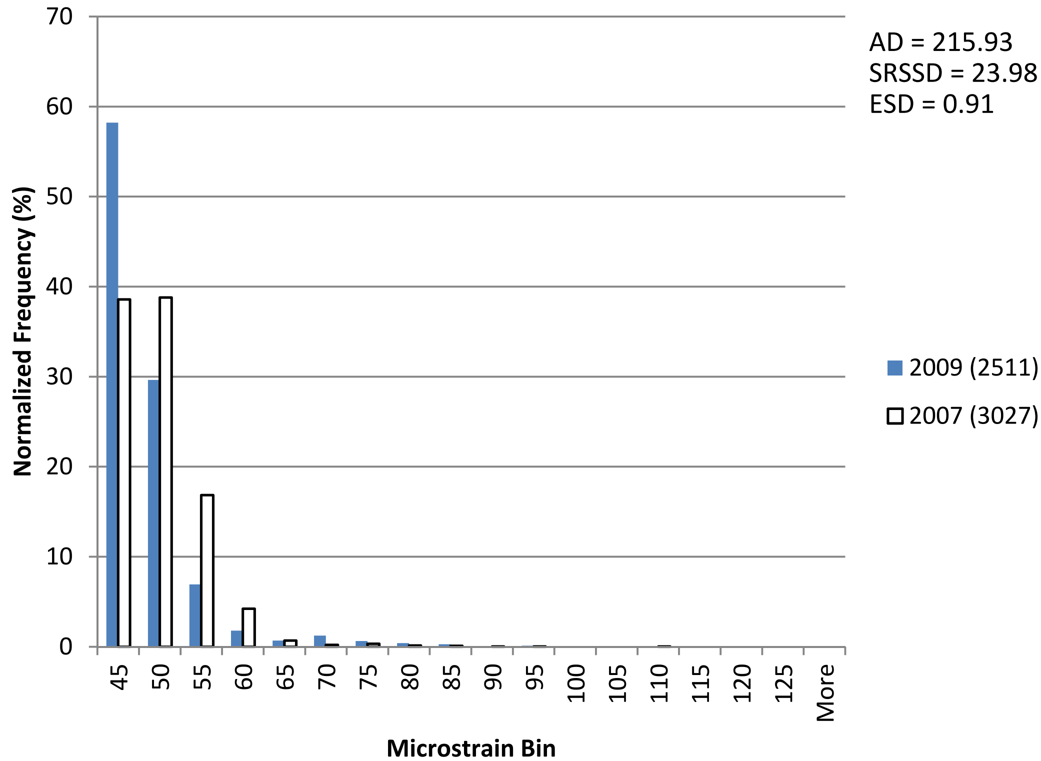

Figure 4.6: Bridge 1-781 normalized histogram comparison plot

4.4.2 Bridge 1-728

The histogram comparison for this bridge shows good correlation (Figure 4.7). Visually, the plots appear to follow a similar distribution and all parameters fall below their thresholds.

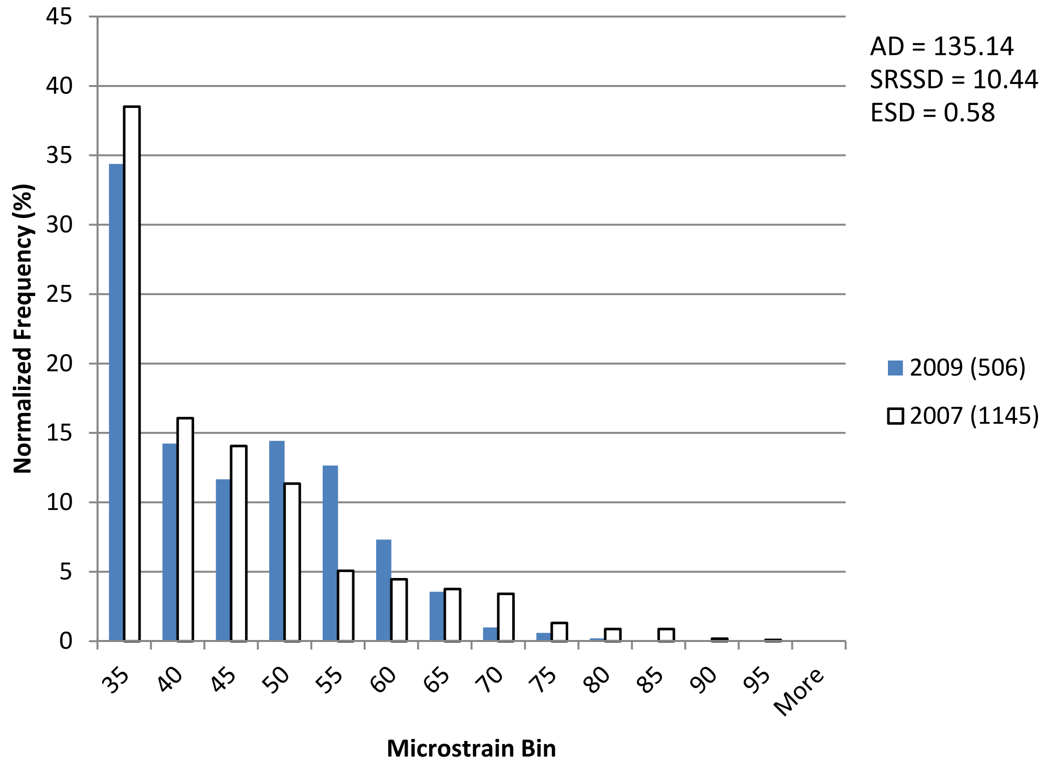

Figure 4.7: Bridge 1-728 normalized histogram comparison plot

4.4.3 Bridge 1-262 S

There are some distinct differences in the normalized histogram plots for this bridge (Figure 4.8). The SRSSD value falls above its threshold while the AD value comes very close. It should be noted that the week-to-week comparisons for the latest monitoring period for this bridge were also dissimilar as shown in Figure 4.5. The cause for such dissimilarities could not be identified.

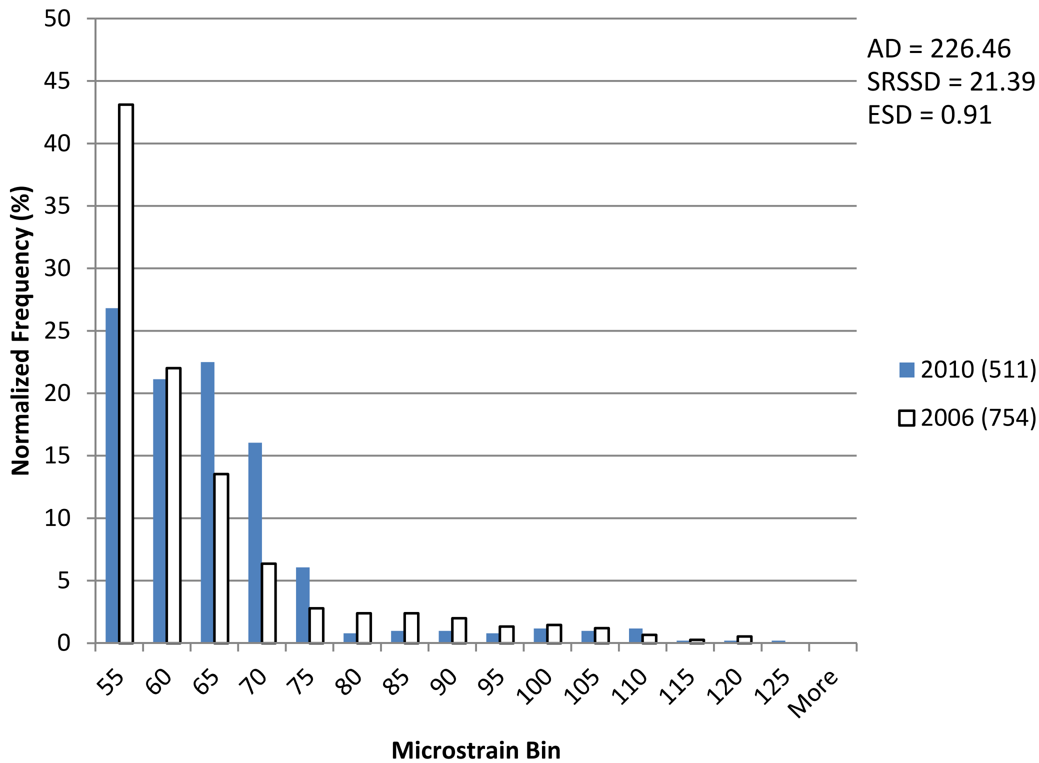

Figure 4.8: Bridge 1-262 S normalized histogram comparison plot

4.4.4 Bridge 1-826 N

There are some noticeable differences in the normalized histograms for this bridge (Figure 4.9). The 2006 plot seems to follow a normal distribution while the 2010 plot appears to be an exponential decay. The AD and SRSSD values fall above their thresholds. During the 2006 monitoring period the right lane of I-495 N was closed approximately one mile north of 1-826 N which may have led to fewer trucks going over the bridge in the right lane.

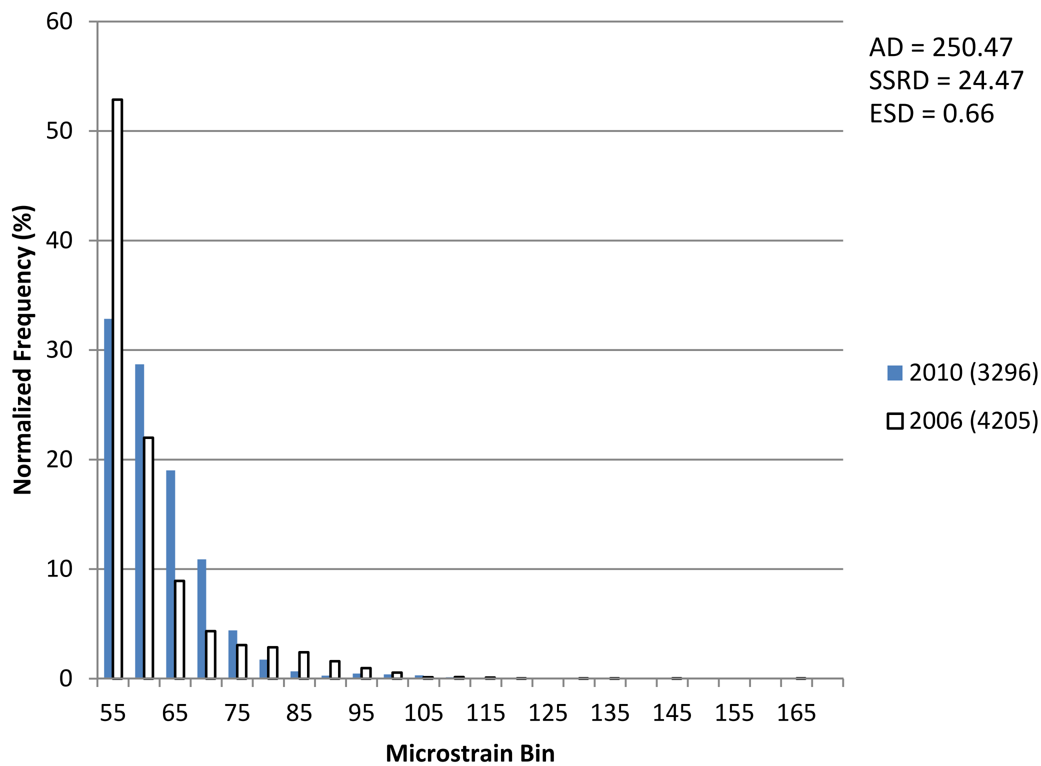

Figure 4.9: Bridge 1-826 N normalized histogram comparison plot

4.4.5 Bridge 1-911 S

The histogram comparison for this bridge shows good correlation (Figure 4.10). Visually, the plots appear to follow a similar distribution and all parameters fall below their thresholds.

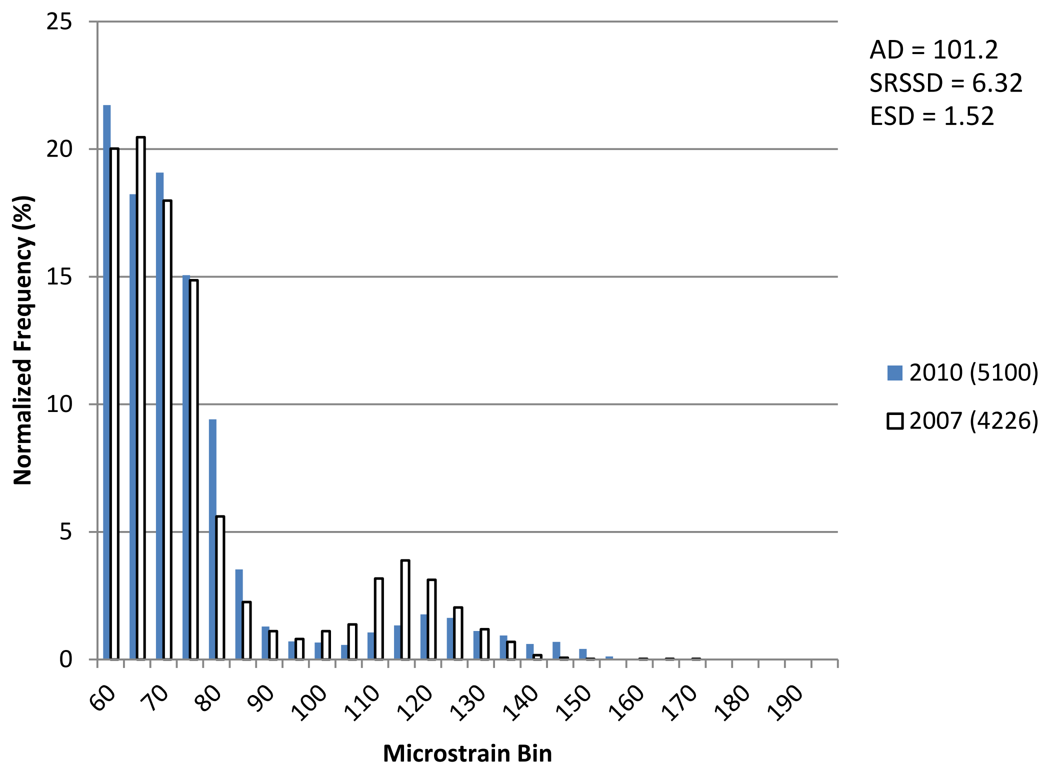

Figure 4.10: Bridge 1-911 S normalized histogram comparison plot

4.4.6 Bridge 1-821 N

There are major differences with the normalized histograms for this bridge (Figure 4.11). The distributions of the data sets look somewhat similar, however it appears that they are shifted on the x-axis and do not match up against each other. The AD value falls above its threshold. While the SRSSD and ESD parameters are below their thresholds, they are very close to their cutoff values. In between the two monitoring periods the bearings had been replaced on the bridge. This structural modification may be responsible for the distinct shift in the histograms.

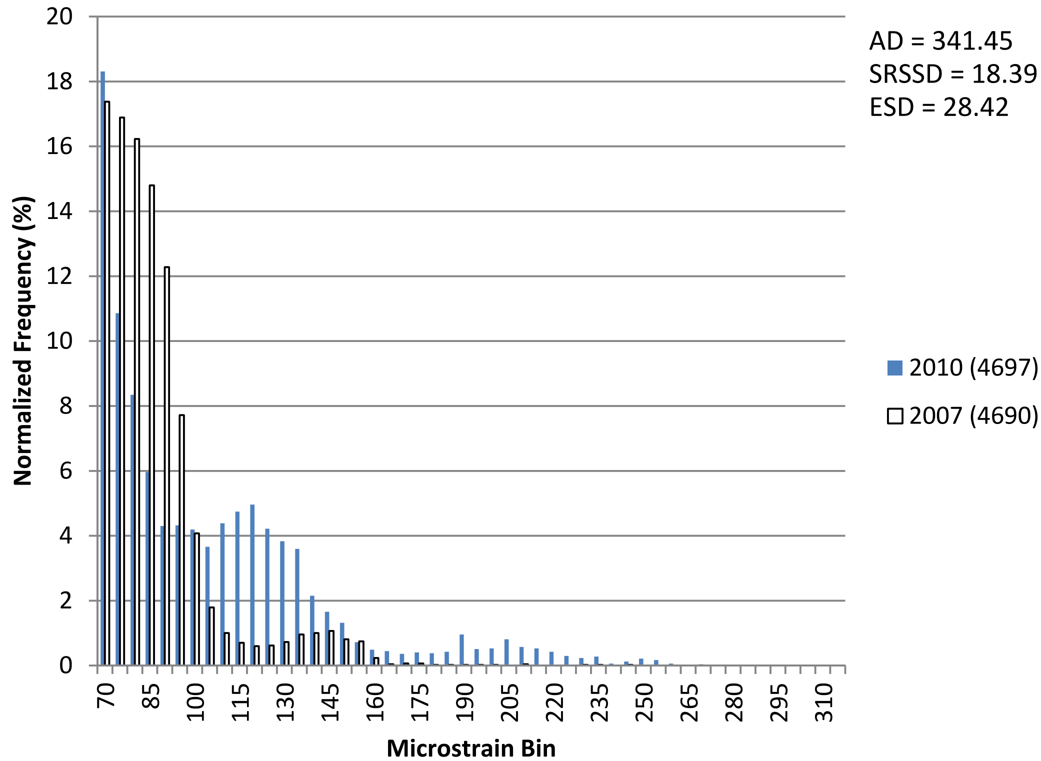

Figure 4.11: Bridge 1-821 N normalized histogram comparison plot

4.4.7 Bridge 1-791

The histogram comparison for this bridge shows some distinct changes in the normalized plots of the two sets of microstrain data collected (Figure 4.12). The 2006 data seems to be in the shape of a normal distribution while the 2010 data resembles an exponential decay. The AD and SRSSD values fall above their thresholds. The location of the gauges during the two monitoring periods may have been different due to inadequate notes. This could have resulted in differing data collection.

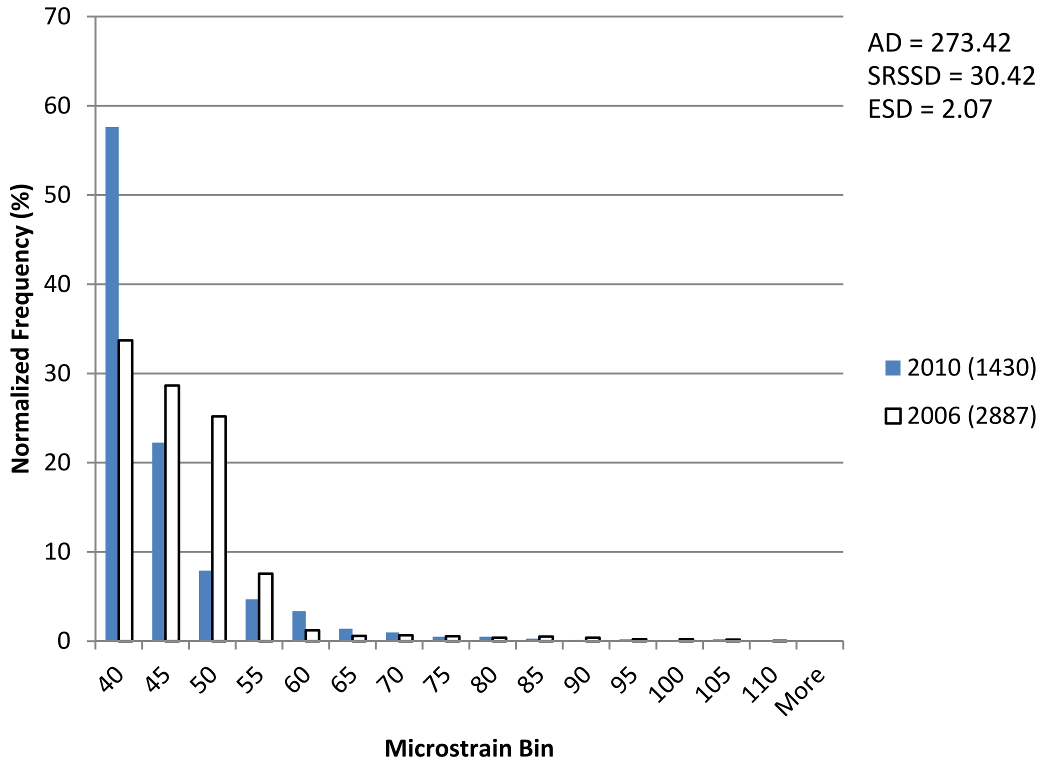

Figure 4.12: Bridge 1-791 normalized histogram comparison plot

4.4.8 Bridge 2-918 N

The histogram comparison for this bridge shows fairly good correlation (Figure 4.13). Visually, the plots appear to follow a similar distribution and all parameters fall below their thresholds.

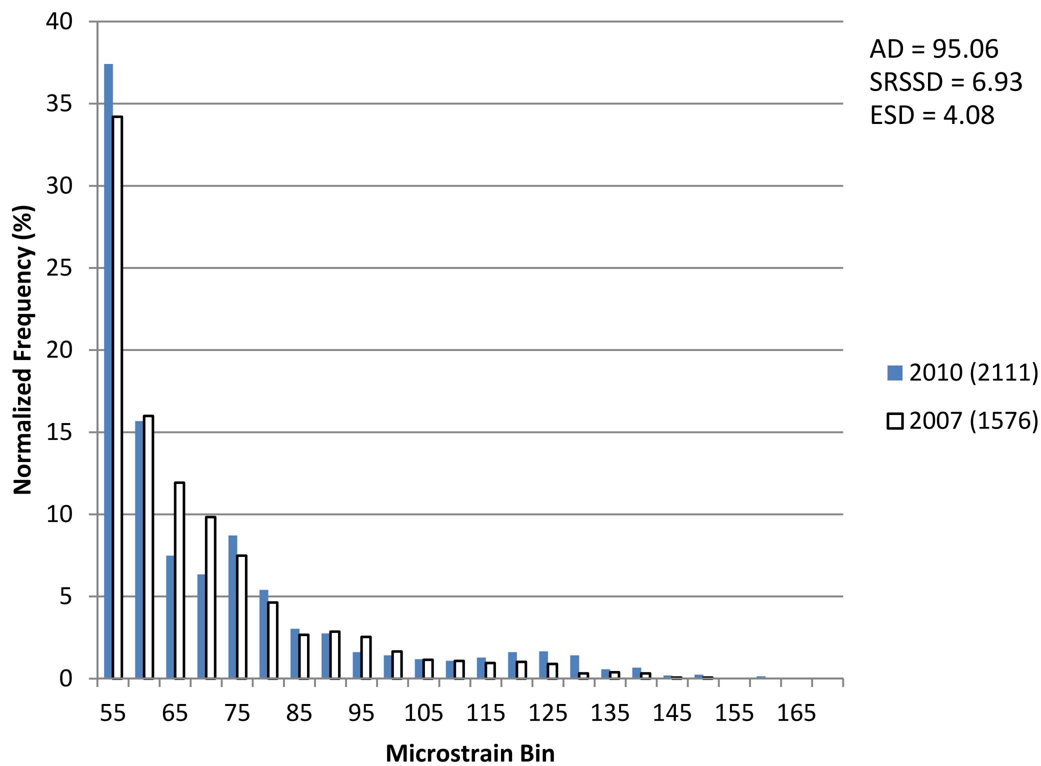

Figure 4.13: Bridge 2-918 N normalized histogram comparison plot

4.4.9 Bridge 1-149

The histogram comparison for this bridge shows some distinct changes in the normalized plots of the two sets of microstrain data collected (Figure 4.14). The 2006 data seems to be in the shape of an exponential decay while the 2011 data resembles a normal distribution. The AD and SRSSD values fall above their thresholds. The location of the gauges during the two monitoring periods may have been different due to inadequate notes. This could have resulted in differing data collection.

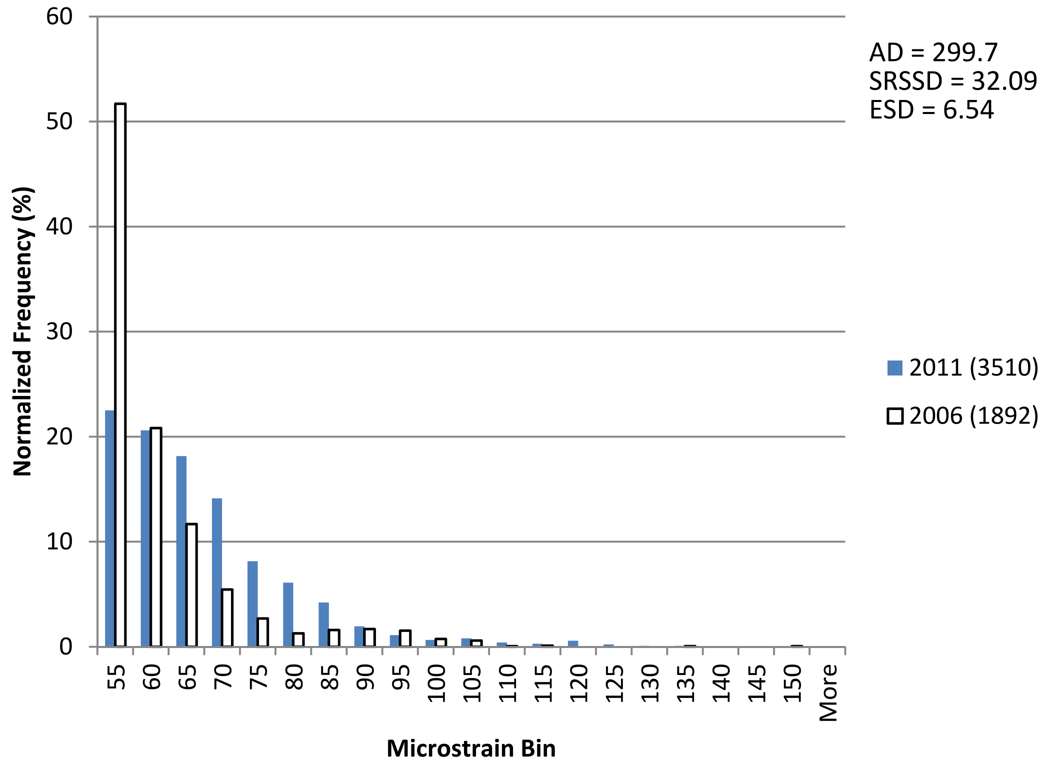

Figure 4.14: Bridge 1-149 normalized histogram comparison plot

4.5 Seasonal Comparisons

To see if there is any effect of temperature or seasonal variations on the measured data, data sets recorded on the same bridge during different times of the year were compared. Again, parameter threshold values defined in the week-to-week comparisons are implemented for comparisons. A summary of the in-service data is provided in Table 4.12 and comparison parameters are provided in Table 4.13.

Table 4.12: In-service data being compared for seasonal histograms

Bridge Number	Number of Days		Comparison Threshold	Events Collected		Events Compared	
	New	Previous		New	Previous	New	Previous
1-704	10	13	55	843	1,543	843	513
1-911 S (1)	15	5	70	3,836	5,793	3,836	1,755
1-911 S (2)		6			5,100		2,089
1-826 N (1)	8	15	50	5,943	5,283	5,943	4,205
1-826 N (2)		5			3,296		3,296
1-394 S	24	20	45	3,141	1,275	2,169	1,275

Table 4.13: Comparison parameters for seasonal histograms

Bridge Number	Date Monitored		AD	SRSSD	ESD
	New	Prev.			
1-704	3/2010	9/2006	92.19	10.04	1.4
1-911 S (1)	11/2010	6/2007	172.55	15.57	5.42
1-911 S (2)	11/2010	7/2010	153.73	60.68	2.79
1-826 N (1)	2/2011	5/2006	163.91	14.18	0.93
1-826 N (2)	2/2011	5/2010	119.82	11.66	0.43
1-394 S*	8/2007	3/2011	211.77	18.36	2.69

* Normalized histogram shows qualitative difference

Table 4.14 shows the results of comparing the calculated parameters for each bridge with their threshold values. Check marks indicate a quantifiable difference.

Table 4.14: Quantifiably different histogram data for seasonal comparisons

Bridge Number	AD	SRSSD	ESD
1-704			
1-911 S (1)			

1-911 S (2)		✓	
1-826 N (1)			
1-826 N (2)			
1-394 S			

4.5.1 Bridge 1-704

The histogram comparison for this bridge shows good correlation (Figure 4.15). Visually, the plots appear to follow exponential decay distribution and all parameters fall below their thresholds. The first monitoring period took place in September 2006 and the second during March 2010 – so this is also a year-to-year comparison.

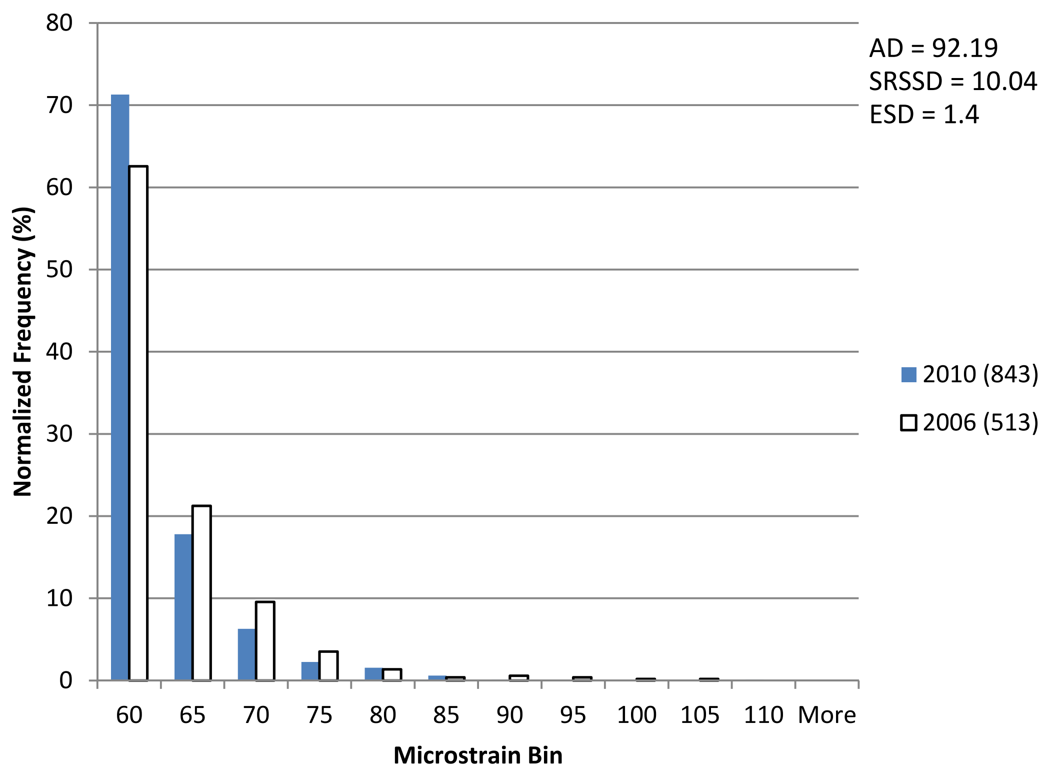

Figure 4.15: Bridge 1-704 normalized seasonal histogram comparison plot

4.5.2 Bridge 1-911 S

The 2010 November monitoring histogram is compared to the 2010 July monitoring and the original 2007 monitoring histograms for this bridge (Figure 4.16). Visually, all three plots appear to follow a similar distribution; however magnitudes of the normalized frequencies vary in some of the bins. The AD and ESD values fall below their thresholds for the comparison but the SRSSD value falls above its threshold for the November to July 2010 comparison (Table 4.15).

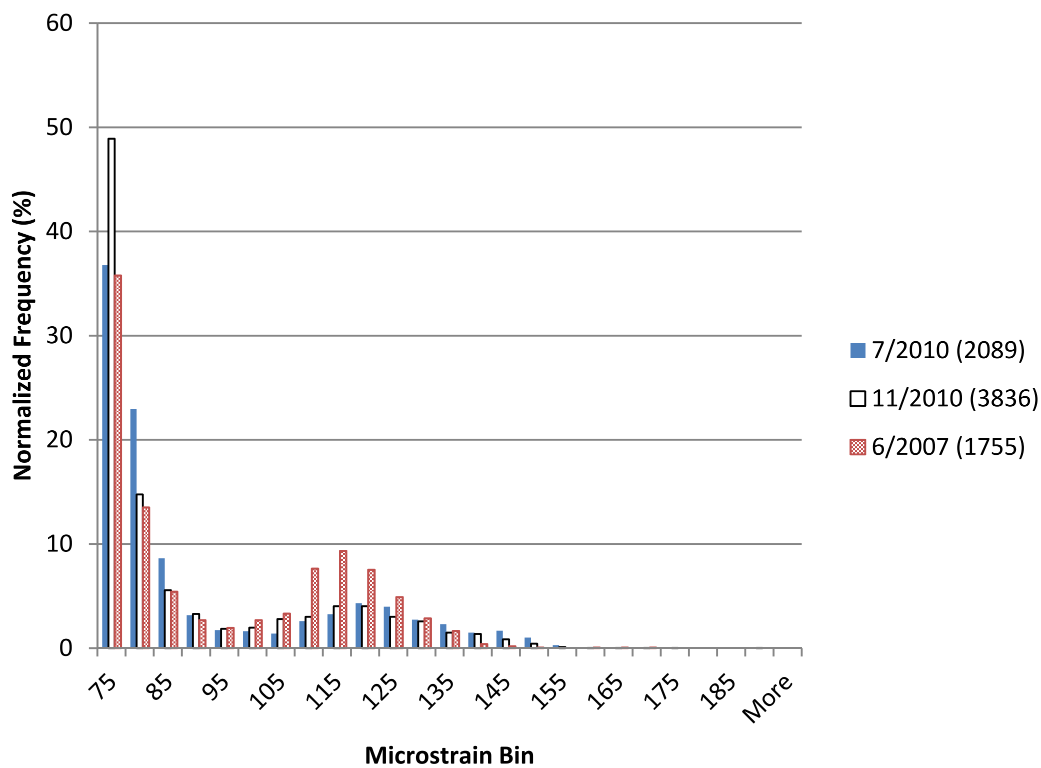

Figure 4.16: Bridge 1-911 S normalized seasonal histogram comparison plot

Table 4.15: Bridge 1-911 S seasonal comparison parameter values

Comparison	AD	SRSSD	ESD
11/2010 to 6/2007 (1)	172.55	15.57	5.42
11/2010 to 7/2010 (2)	153.73	60.68	2.79

4.5.3 Bridge 1-826 N

The 2011 February monitoring histogram is compared to the 2010 May monitoring and the original 2006 monitoring histograms for this bridge (Figure 4.17). Visually, the plots follow a similar distribution with the biggest variations occurring in the first microstrain bin. All parameter values fall below their thresholds (Table 4.16).

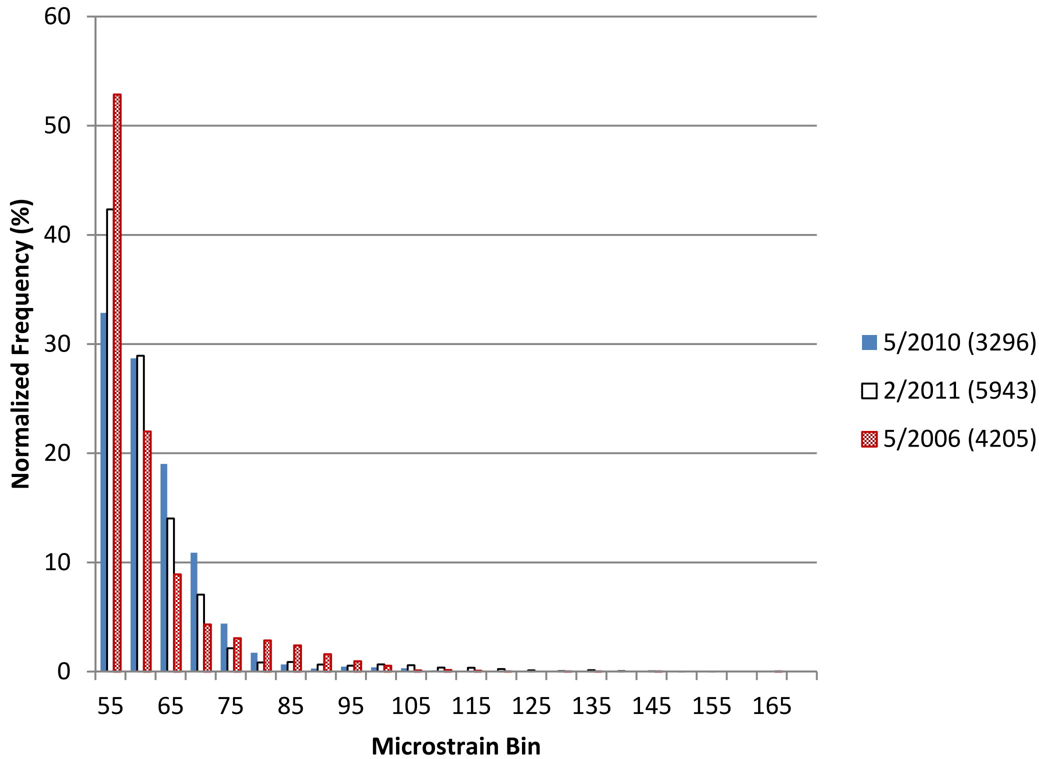

Figure 4.17: Bridge 1-826 N normalized seasonal histogram comparison plot

Table 4.16: Bridge 1-826 N seasonal comparison parameter values

Comparison	AD	SRSSD	ESD
2/2011 to 5/2006 (1)	163.91	14.18	0.93
2/2011 to 5/2010 (2)	119.82	11.66	0.43

4.5.4 Bridge 1-394 S

The histogram comparison for this bridge shows some variability (Figure 4.18). While the AD and SRSSD values fall below their thresholds, they are close to their cutoff values. The most prevalent variability between the two plots is the difference in magnitude of the frequencies in the first microstrain bin. Neglecting the first bin, the two plots match up fairly well. The first monitoring period took place in August 2007 and the second during March 2011 – so this is also a year-to-year comparison.

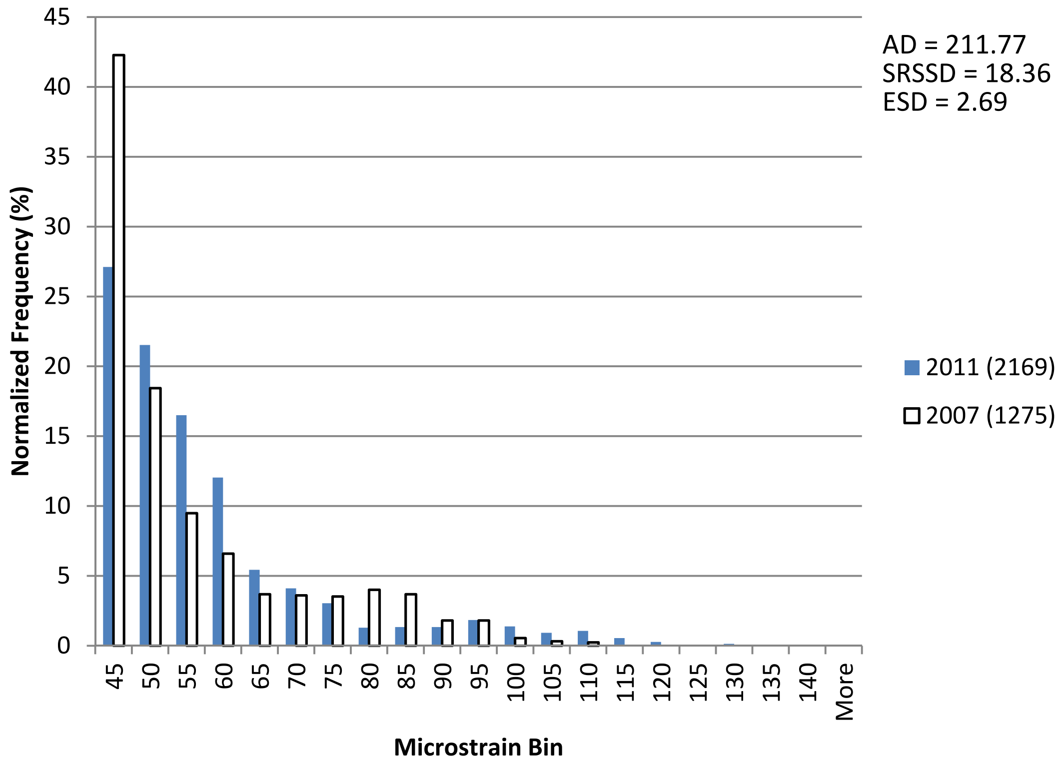

Figure 4.18: Bridge 1-394 S normalized seasonal histogram comparison plot

4.6 Summary

Three parameter values – AD, SRSSD and ESD – were implemented in the quantitative comparison of normalized histograms for fifteen monitoring periods that occurred during this research. Threshold values were determined using outlier analysis on week-to-week comparisons. These thresholds were used to recognize differences in data sets in year-to-year and seasonal comparisons.

Based on the results of this chapter, the AD and SRSSD values are fairly dependable in discerning similarities or differences between the normalized histograms of data sets. The two values were typically confirmed by qualitative analyses and tended to parallel one another. This is to be expected since the method of calculation of each is comparable to the other. There were a few instances where neither threshold was exceeded even when a noticeable difference in the plots was apparent. However, in these cases the AD and SRSSD values tended to be quite close to their threshold values indicating each method's reliability. While both the AD and SRSSD parameters were able to sufficiently recognize significant differences, the SRSSD seemed to be slightly more sensitive and accurate than the AD. The level of accuracy of the parameters, however, is a function of the input values used to designate thresholds using the outlier analysis. A larger sample of similar data sets (week-to-week for example) may yield more valid threshold values for both AD and SRSSD parameters.

As discussed at the end of Section 4.3, the AD and SRSSD values are more reliable than the ESD value at detecting differences in data sets. This was apparent in the week-to-week, year-to-year and seasonal comparison analyses. The ESD never exceeded its threshold determined using outlier analysis for any of the histogram comparisons. Should a different approach be used to determine the ESD threshold value? This does not seem to be the case based on the inconsistencies of the ESD values throughout the chapter. While a subjective analysis and the AD and SRSSD values indicate a major difference in data, the ESD expressed a quantitatively good match in some instances. On the other hand, in instances such as the week-to-week comparisons of bridges 1-728 and 1-704 the ESD values were relatively large even though the AD and SRSSD values pointed to similar distributions (see values in Table 4.6). The only times the ESD value was appropriately large was in its analysis of cases with extreme differences as seen in Figure 4.5 and Figure 4.11. Yet, even in these situations, the ESD was below its threshold.

In most cases a probable cause of disparateness could be determined when a significant difference was noted. Possible roots of variation were traffic changes, structural modifications or unintended, inconsistent ISBMS locations during the different monitoring periods. Based on the results of Section 4.5, there seems to be little seasonal variation on the bridges. This would imply that the effects of temperature fluctuation are negligible for ISBMS monitoring and that the loads due to truck traffic remain constant throughout the year.

Chapter 5

STRAIN PROJECTION AND LOAD RATINGS

5.1 Introduction

An objective of ISBMS data collection is to assess the current condition of the structure. The determination of load ratings, which represent the live load carrying capacity of a bridge, is desired for such an assessment. These ratings can indeed be based on strain data collected using the ISBMS. However, the ratings based on the actual in-service data collected would only be applicable for the amount of time over which the data was collected. Monitoring periods for this project are at most three weeks and this is not a very practical time period on which to base load ratings. Instead, projected strains are determined from extrapolation of data collected during a given monitoring period. It is these strains on which the load ratings will be based. DelDOT uses a computer program, Bridge Rating and Analysis of Structural Systems (BRASS), developed by the Wyoming Department of Transportation (WyDOT), to rate their bridges. BRASS uses finite element analysis along with AASHTO specifications for its evaluation.

An assumption of a normal distribution for all histograms of strain data must be made in order to allow for strain projection of in-service data. The top 20% of truck weights have been assumed to have a normal distribution (National Cooperative Highway Research Program (NCHRP), 2001). Due to limited memory, however, events resulting from the top 20% of trucks cannot be recorded entirely.

The histograms produced during this project are truncated at the point of the trigger level. The left side of the distribution is absent. In order to establish normalcy of ISBMS data, Rakowski presented a method to test the distribution (Rakowski, 2008). ISBM data was plotted and compared against an assumed normal distribution. For the most part, with a major exception being events near the trigger level, the histograms for each of Brookes' and Rakowski's bridges matched up well with the normal distributions (Rakowski, 2008).

5.2 Strain Projection Methodology

The same strain projection methodology used under Rakowski was implemented for this project and is summarized in this section. To predict future strains for a specific period of time, the events collected on a particular bridge (see Chapter 3) must be plotted versus their reliability index. The equation for the reliability index, β, is:

$$\beta = \Phi^{-1}(P) \qquad \text{Equation 5.1}$$

where,

- Φ^{-1} is the inverse of the standard normal distribution function
- $(P) = (1 - P_e)$ is the value from the cumulative distribution function (CDF) or 1 minus the probability of exceedance, P_e

The following steps must be followed to yield an equation that can be used to project strains for a particular period of time:

1. Sort the recorded events from least to greatest in magnitude.
2. Assign a rank to each value from greatest to least in magnitude.

3. Calculate P_e. This value, the probability of exceedance, is the probability that an event greater than the value in question will occur for a given population.
    - $P_e = \frac{rank\ of\ event}{\#\ of\ events+1}$
4. Calculate P. This value, the CDF value, is the probability that an event less than the value in question will occur for a given population.
    - $P = 1 - P_e$
5. Calculate β. This is determined using the Microsoft Excel NORMSINV() function with P as the input value.
6. Plot β on the ordinate axis with the microstrain on the abscissa.
7. Determine where the curve becomes linear and fit a line to those points. This is done at the right tail end where the curve tends to straighten out. Non-linear data is neglected.
8. Calculate the equation of the fitted line. The equation should be manipulated to return a microstrain value for a given β.
9. Calculate β values based on the number of events for a specified time period. The number of events for a time period is extrapolated from the number of events for the monitoring period.
10. Calculate microstrain values for the computed β values.

As an example of this procedure, the raw data collected during a one day monitoring period (shown in the first column of Table 5.1) is to be projected. First, the events are sorted from lowest to highest in the Ranked Event column. Next, the rank of each event is displayed; the event with the highest magnitude is of rank 1 and the event with the lowest magnitude is of rank *n* where *n* is the number of events. Then the probability of exceedance, P_e, is calculated. The CDF value, P, is calculated by subtracting P_e from 1. Finally, β is determined using the reliability index equation.

Table 5.1: Example calculation of reliability index for sample one-day data

Event (με)	Ranked Event (με)	Rank of Event	P_e	P	β
37	37	16	1/(16+1) = 0.9412	1 – 0.9412 = 0.0588	NORMSINV(0.0588) = -1.5647
48	38	15	0.8824	0.1176	-1.1868
70	39	14	0.8235	0.1765	-0.9289
63	41	13	0.7647	0.2353	-0.7215
74	42	12	0.7059	0.2941	-0.5414
78	43	11	0.6471	0.3529	-0.3774
39	46	10	0.5882	0.4118	-0.2230
42	48	9	0.5294	0.4706	-0.0738
41	51	8	0.4706	0.5294	0.0738
88	54	7	0.4118	0.5882	0.2230
54	58	6	0.3529	0.6471	0.3774
43	63	5	0.2941	0.7059	0.5414
46	70	4	0.2353	0.7647	0.7215
58	74	3	0.1765	0.8235	0.9289
38	78	2	0.1176	0.8824	1.1868
51	88	1	0.0588	0.9412	1.5647

The reliability index is then plotted on the y-axis versus microstrain on the x-axis for each event (Figure 5.1). A line representing the projection of future strain values is fit to the most linear region of the plot at the right tail end. There is inherent subjectivity in this process since the projection line will be dependent on which points are used to create it. The equation of the trend line, in terms of strain (ε in microstrain), is provided in the upper right-hand corner of the plot. This equation is manipulated and is used to calculate strain projections for 1-, 2-, 10-, 50- and 75-year periods in Table 5.2.

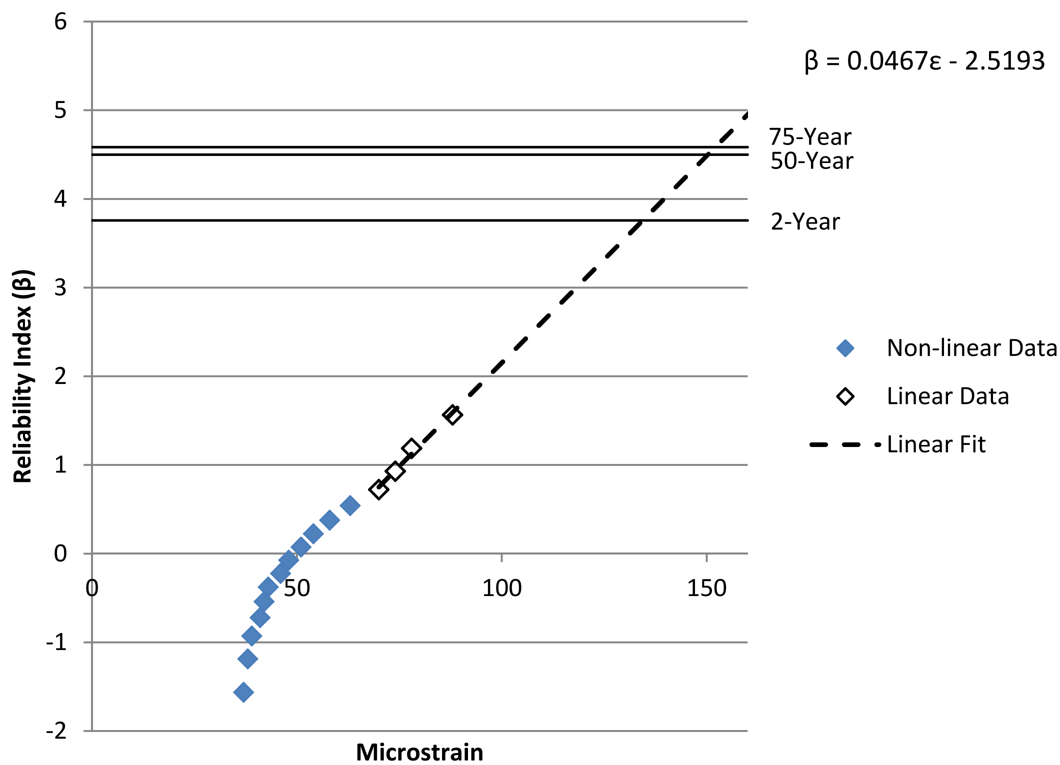

Figure 5.1: Strain projection plot for events in Table 5.1

Table 5.2: Strain projection for events in Table 5.1

Period (Yrs)	# of Events	P	β	Strain (με)
1/365 = 0.00274	16	0.937500	1.534	(1.534 + 2.5193)/0.0467 = 86.80
1	16/0.00274 = 5,840	0.999829	3.581	130.62
2	5840·2 = 11,680	0.999914	3.758	134.42
10	5840·10 = 58,400	0.999983	4.143	142.67
50	292,000	0.999997	4.498	150.27
75	438,000	0.999998	4.584	152.10

5.3 Strain Projections

Projected strains are determined for each of the bridges monitored. The strain projection is plotted and the strain predictions for 1-, 2-, 10-, 50- and 75-year events are computed for each bridge. If applicable, the strain projections for this work are plotted with Rakowski's projection plots, for comparison. A solid line is located where the projection plot intersects the reliability index for 2-, 50- and 75-year events for the most recent data collection. In addition, the projected strain values are compared.

5.3.1 Bridge 1-781

The strain projection curves for this bridge match up fairly well for the two data sets and the projection lines are almost identical (Figure 5.2). This may be coincidental as these data sets were found to be dissimilar in Section 4.4.1. Projected values are provided in Table 5.3.

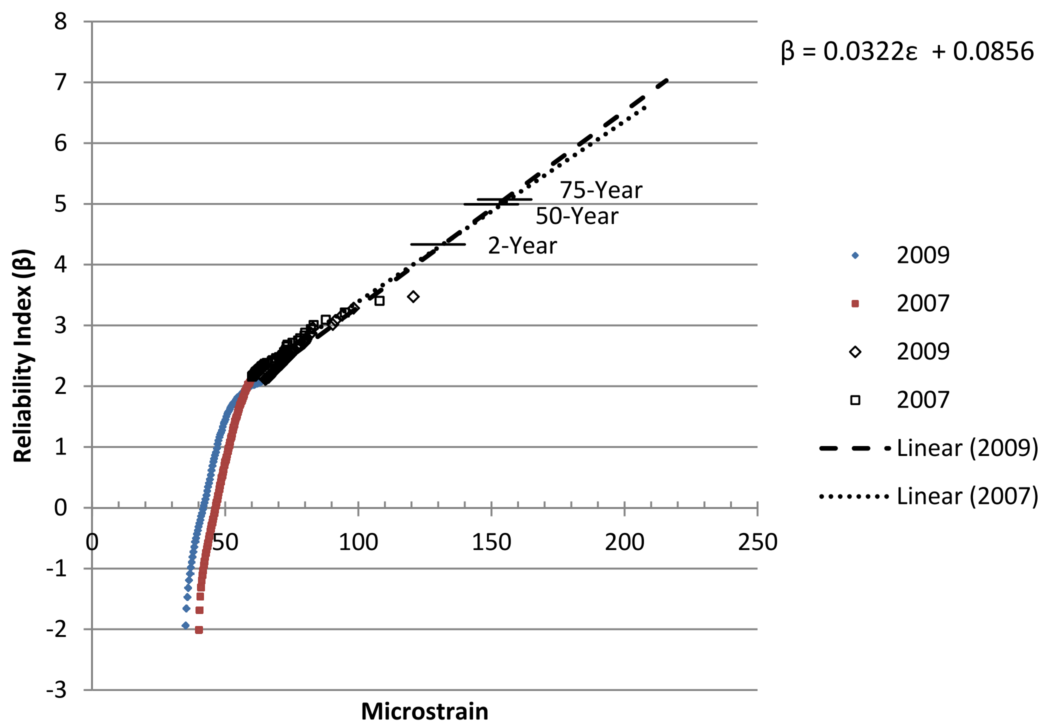

Figure 5.2: Bridge 1-781 strain projection plot

Table 5.3: Bridge 1-781 strain projection values

Period	# of Events	β	με (2009)	με (2007)
In-service	3,889	3.47	105.2	101.2
1 Year	67,808	4.18	127.1	127.5
2 Years	135,615	4.33	131.9	132.7
10 Years	678,075	4.67	142.5	144.1
50 Years	3,390,377	4.99	152.5	154.8
75 Years	5,085,566	5.07	154.9	157.4

5.3.2 Bridge 1-728

A shift in the two projection curves can be noted due to different microstrain thresholds for this bridge and projection values are offset (Figure 5.3).

While it seems that this offset causes a shift in strain projection, this is not the case. A lower trigger level will cause lower reliability indices and vice versa. The 2-, 50- and 75-year marks only correspond to the 2009 data projections. Lower strains are projected than in the past. These data sets were found to be similar in Section 4.4.2. Projected values are provided in Table 5.4.

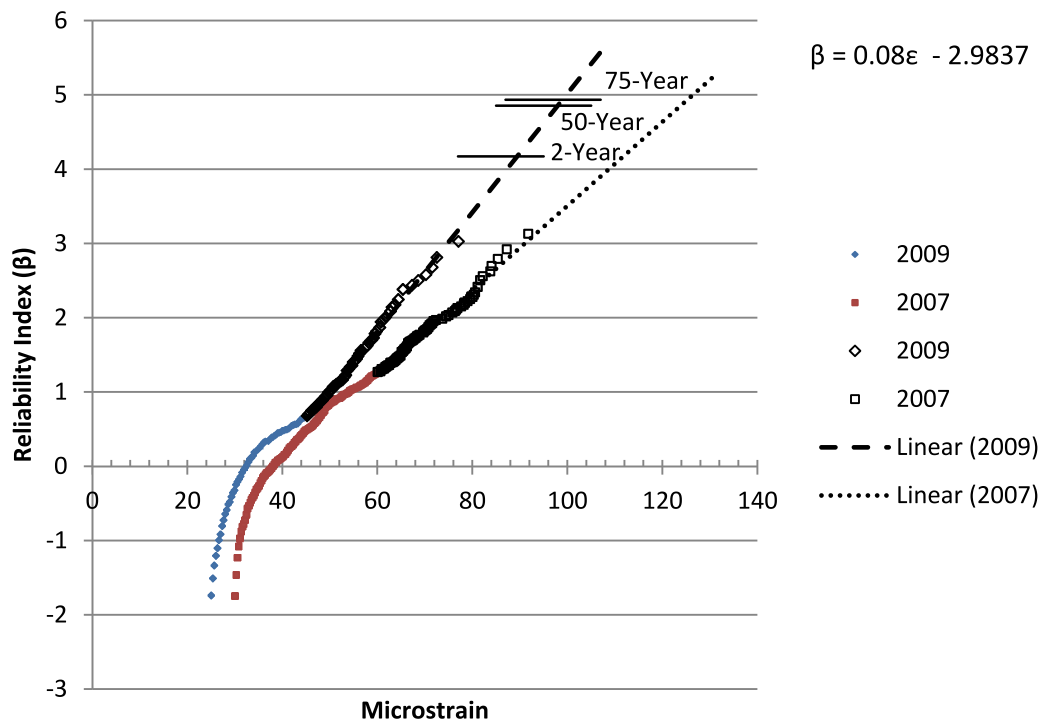

Figure 5.3: Bridge 1-728 strain projection plot

Table 5.4: Bridge 1-728 strain projection values

Period	# of Events	β	με (2009)	με (2007)
In-service	807	3.03	75.1	92.7
1 Year	33,002	4.01	87.4	107.5
2 Years	66,003	4.17	89.4	110.4
10 Years	330,016	4.52	93.8	116.7
50 Years	1,650,082	4.85	98.0	122.6
75 Years	2,475,124	4.93	99.0	124.0

5.3.3 Bridge 1-704

The curves for this bridge follow the same shape but then diverge for projections after an intersection (Figure 5.4). The linear portions of the curves result in differing projection line trajectories. Lower strains are projected than in the past. These data sets were found to be similar in Section 4.5.1. Projected values are provided in Table 5.5.

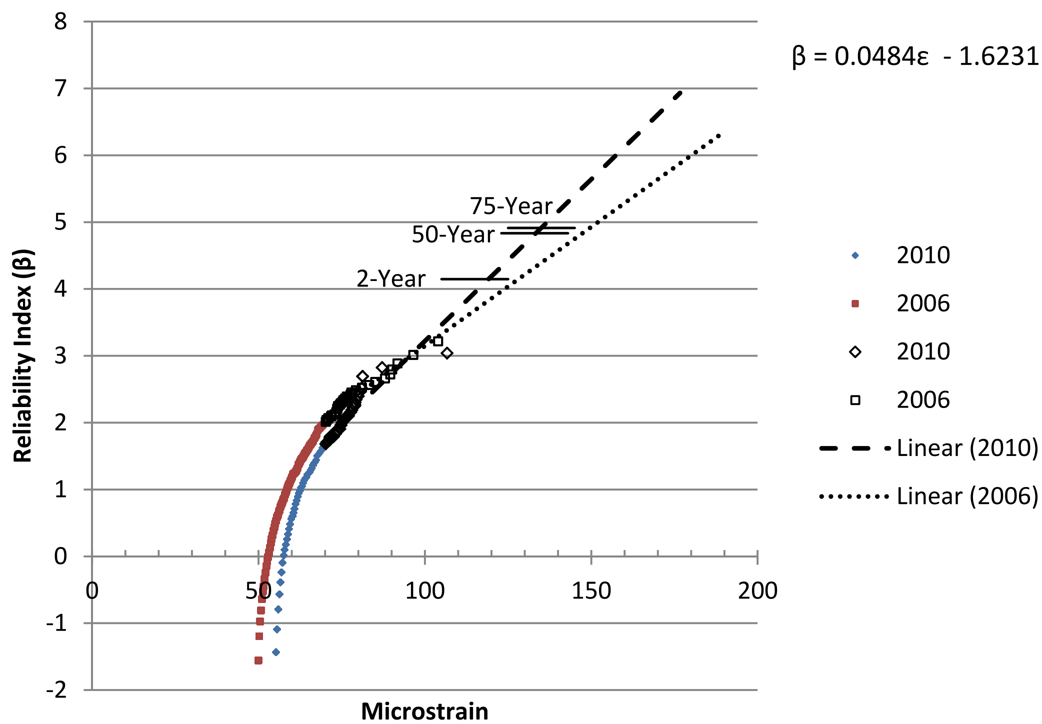

Figure 5.4: Bridge 1-704 strain projection plot

Table 5.5: Bridge 1-704 strain projection values

Period	# of Events	β	με (2010)	με (2006)
In-service	843	3.04	96.3	102.5
1 Year	29,809	3.99	115.9	125.6
2 Years	59,618	4.15	119.2	130.0
10 Years	298,092	4.50	126.6	139.6
50 Years	1,490,461	4.83	133.4	148.6
75 Years	2,235,692	4.91	135.1	150.8

5.3.4 Bridge 1-826 S

This is the first time this bridge has been monitored with the ISBMS so there is no curve to compare it to (Figure 5.5). Projected values are provided in Table 5.6.

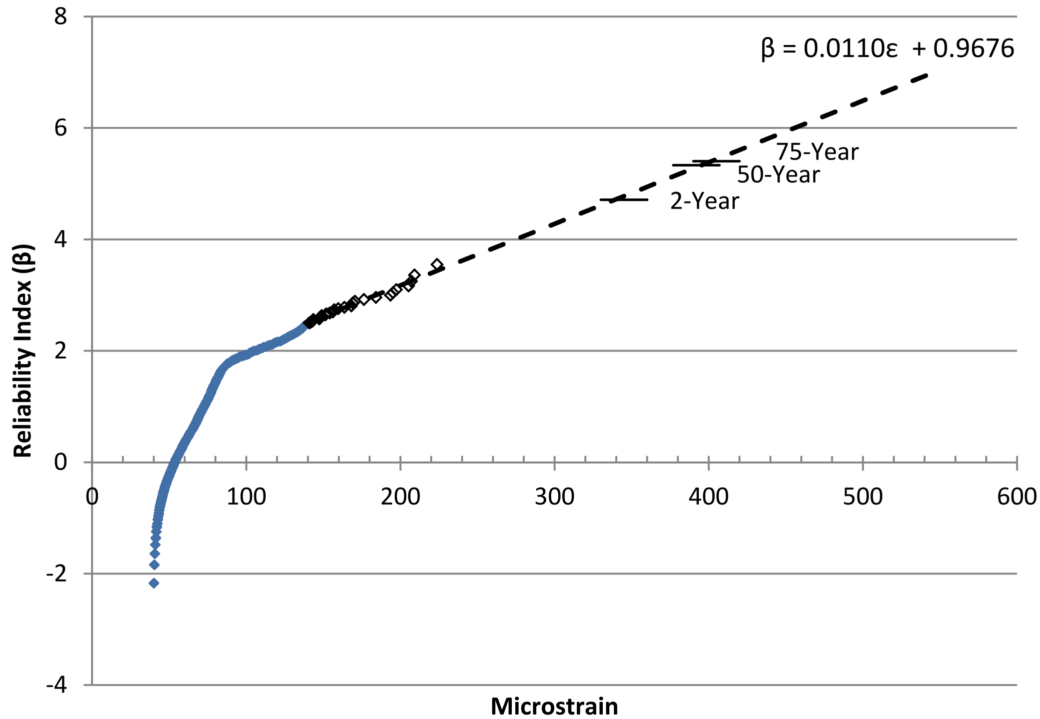

Figure 5.5: Bridge 1-826 S strain projection plot

Table 5.6: Bridge 1-826 S strain projection values

Period	# of Events	β	με (2010)
5 Days	5,163	3.55	234.6
1 Year	408,579	4.57	327.4
2 Years	817,158	4.71	340.4
10 Years	4,085,790	5.03	369.3
50 Years	20,428,950	5.33	396.6
75 Years	30,643,425	5.40	403.3

5.3.5 Bridge 1-262 S

The curves for this bridge have dissimilar shapes and their projection lines diverge after intersection (Figure 5.6). Higher strains are projected than in the past. These data sets were found to be dissimilar in Section 4.4.3. Projected values are provided in Table 5.7.

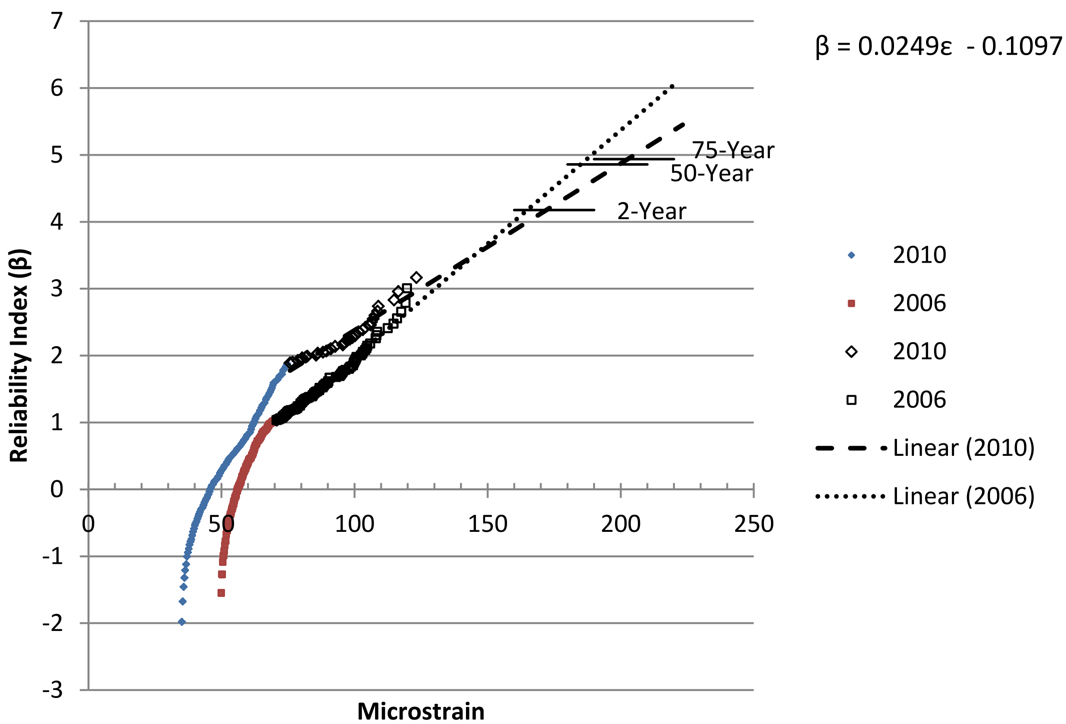

Figure 5.6: Bridge 1-262 S strain projection plot

Table 5.7: Bridge 1-262 S strain projection values

Period	# of Events	β	με (2010)	με (2006)
In-service	1,294	3.17	131.6	130.5
1 Year	33,728	4.02	165.7	156.3
2 Years	67,456	4.18	172.1	161.2
10 Years	337,280	4.53	186.3	171.8
50 Years	1,686,399	4.86	199.5	181.6
75 Years	2,529,598	4.94	202.7	184.0

5.3.6 Bridge 1-826 N

The projection curves for June 2010 and February 2011 are shown for this bridge in Figure 5.7 and Figure 5.8, respectively. The projection trend lines for this bridge's curves diverge from the 2006 projection after an intersection in both cases. Lower strains are projected than in the past. The June 2010 vs. 2006 data comparison found the data sets to be dissimilar in Section 4.4.4, but the February 2011 to 2006 data comparison found the data sets to be similar in Section 4.5.3. Projected values for June 2010 and February 2011 are provided in Table 5.8 and Table 5.9, respectively.

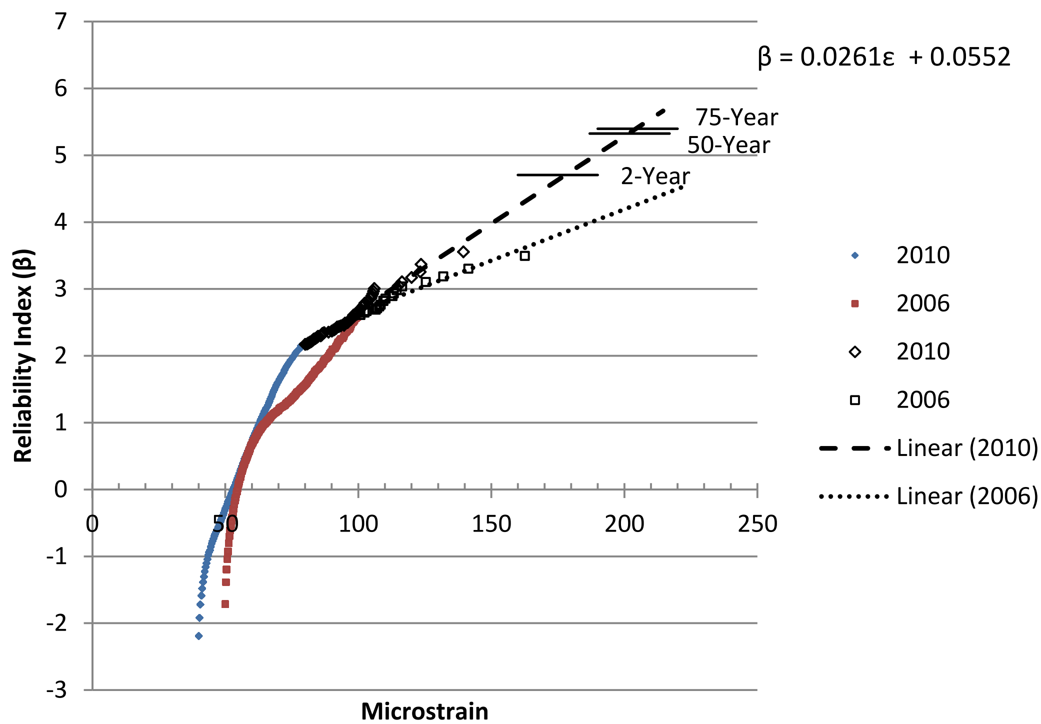

Figure 5.7: Bridge 1-826 N June 2010 strain projection plot

Table 5.8: Bridge 1-826 N June 2010 strain projection values

Period	# of Events	β	με (2010)	με (2006)
In-service	5,283	3.55	134.1	154.3
1 Year	394,477	4.56	172.7	203.9
2 Years	788,954	4.71	178.2	213.6
10 Years	3,944,772	5.02	190.4	235.2
50 Years	19,723,860	5.32	201.9	255.4
75 Years	29,585,791	5.40	204.7	260.3

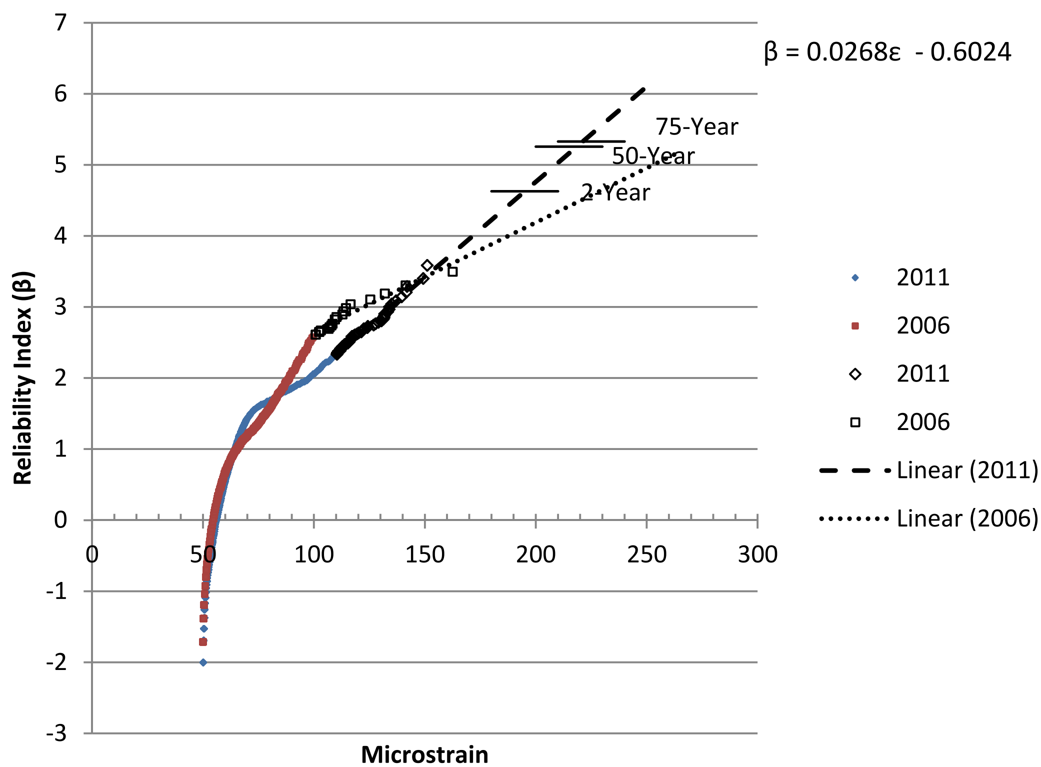

Figure 5.8: Bridge 1-826 N February 2011 strain projection plot

Table 5.9: Bridge 1-826 N February 2011 strain projection values

Period	# of Events	β	με (2011)	με (2006)
In-service	5,943	3.59	156.3	154.3
1 Year	271,986	4.48	189.8	203.9
2 Years	543,972	4.63	195.2	213.6
10 Years	2,719,860	4.95	207.2	235.2
50 Years	13,599,298	5.26	218.6	255.4
75 Years	20,398,946	5.33	221.4	260.3

5.3.7 Bridge 1-911 S

The projection curves for July and November 2010 are shown for this bridge in Figure 5.9 and Figure 5.10, respectively. The curves are both similar and result in projection lines that are parallel to each other. In both cases, the projected strain values are higher than in the past. These data sets were found to be similar in Section 4.4.5 and Section 4.5.2. Projected values for July and November are provided in Table 5.10 and Table 5.11, respectively.

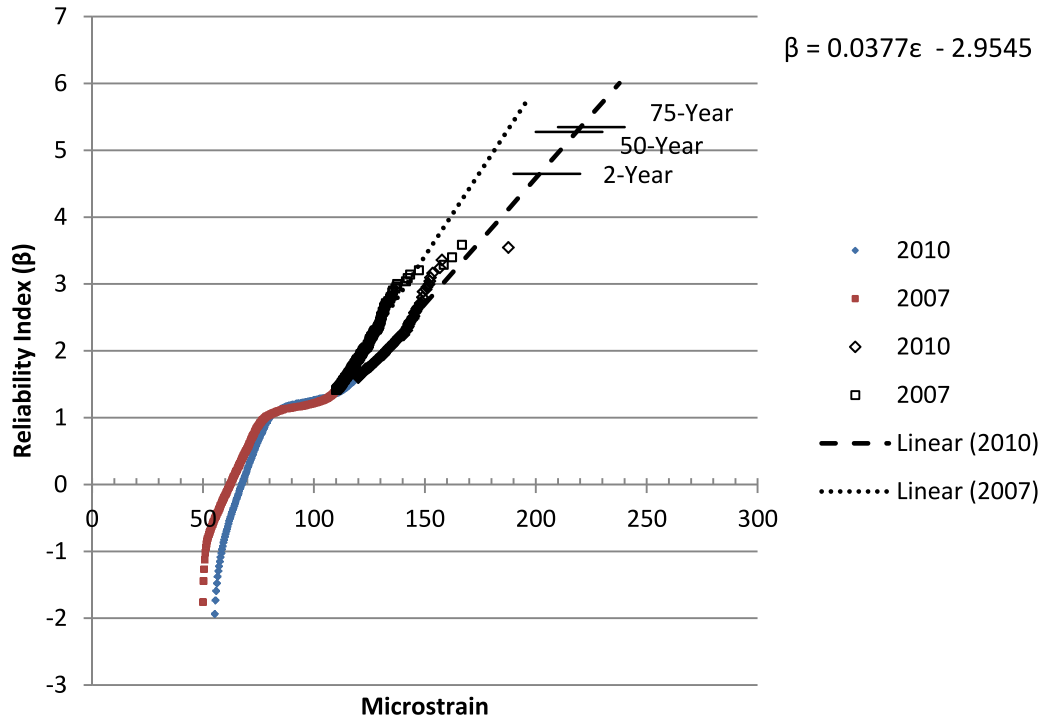

Figure 5.9: Bridge 1-911 S July strain projection plot

Table 5.10: Bridge 1-911 S July strain projection values

Period	# of Events	β	με (2010)	με (2007)
In-service	5,100	3.55	172.4	159.0
1 Year	298,963	4.50	197.8	173.7
2 Years	597,926	4.65	201.7	176.5
10 Years	2,989,628	4.97	210.2	182.8
50 Years	14,948,139	5.27	218.3	188.8
75 Years	22,422,208	5.35	220.2	190.2

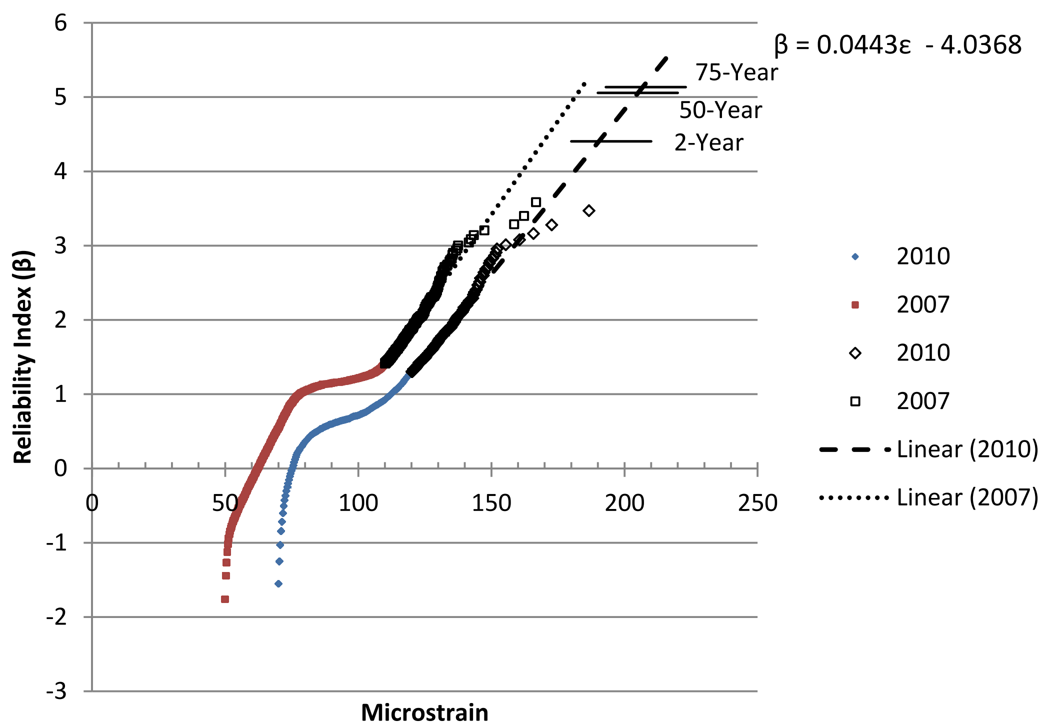

Figure 5.10: Bridge 1-911 S November strain projection plot

Table 5.11: Bridge 1-911 S November strain projection values

Period	# of Events	β	με (2010)	με (2007)
In-service	3,836	3.47	169.4	159.0
1 Year	93,759	4.25	187.1	173.7
2 Years	187,517	4.40	190.5	176.5
10 Years	937,586	4.74	198.1	182.8
50 Years	4,687,932	5.06	205.3	188.8
75 Years	7,031,899	5.13	207.0	190.2

5.3.8 Bridge 1-821 N

The curves for this bridge are dissimilar and diverge after intersecting near the two year projection (Figure 5.11). Trigger levels had a difference of 5 με. Higher strains are projected than in the past for all return periods 1-year and above. These data sets were found to be dissimilar in Section 4.4.6. Projected values are provided in Table 5.12.

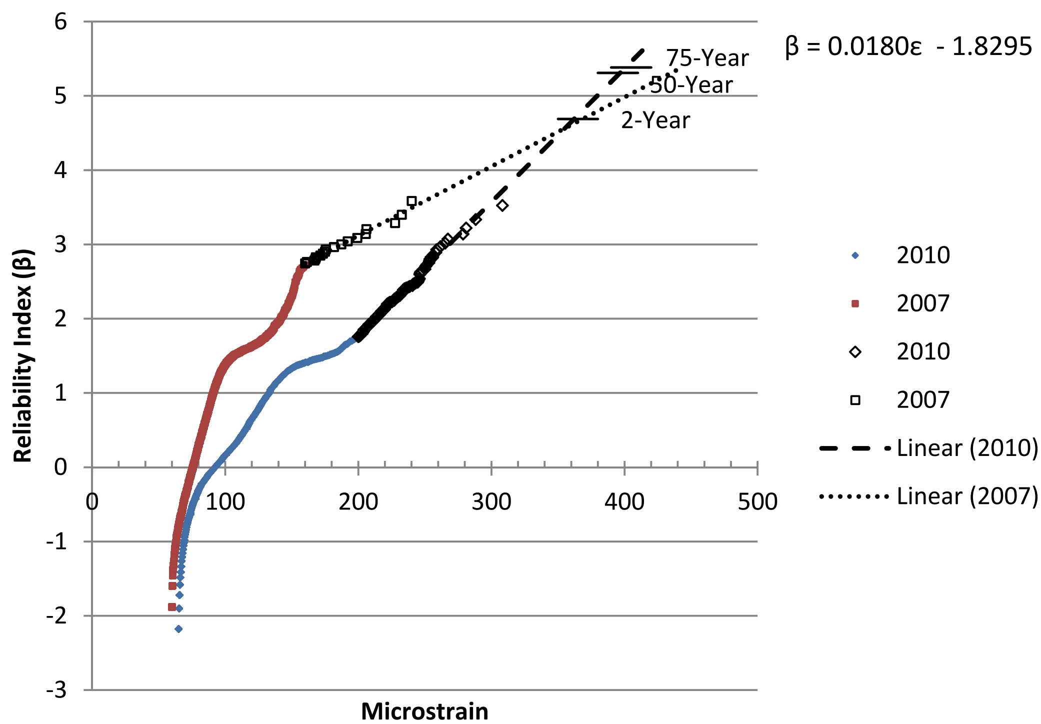

Figure 5.11: Bridge 1-821 N strain projection plot

Table 5.12: Bridge 1-821 N strain projection values

Period	# of Events	β	με (2010)	με (2007)
In-service	4,697	3.52	297.4	273.7
1 Year	362,864	4.54	354.1	353.5
2 Years	725,727	4.69	362.1	369.0
10 Years	3,628,637	5.01	379.8	403.3
50 Years	18,143,185	5.31	396.6	435.8
75 Years	27,214,778	5.38	400.7	443.7

5.3.9 Bridge 1-791

The curves for this bridge are shaped differently, but result in similar strain projection lines (Figure 5.12). Trigger levels were the same for both monitoring periods. Projected strains are higher than in the past for all return periods of 1-year and above. These data sets were found to be dissimilar in Section 4.4.7. Projected values are provided in Table 5.13.

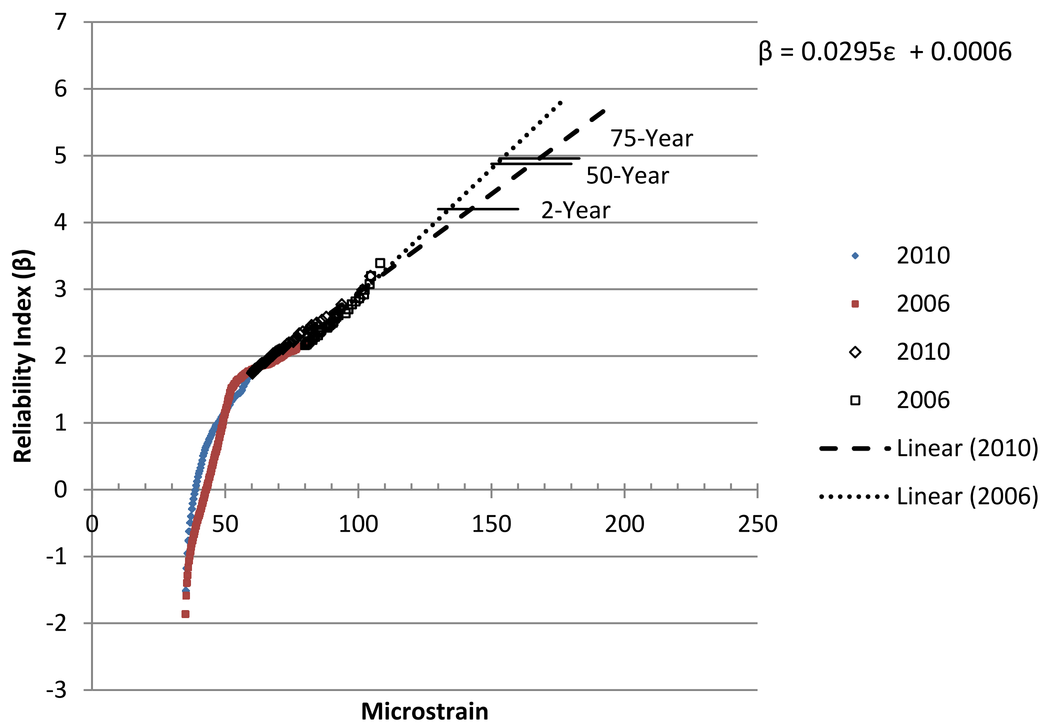

Figure 5.12: Bridge 1-791 strain projection plot

Table 5.13: Bridge 1-791 strain projection values

Period	# of Events	β	με (2010)	με (2006)
In-service	1,430	3.19	108.3	113.2
1 Year	37,396	4.04	136.9	134.4
2 Years	74,792	4.20	142.3	138.5
10 Years	373,960	4.55	154.2	147.4
50 Years	1,869,802	4.88	165.4	155.8
75 Years	2,804,703	4.96	168.0	157.8

5.3.10 Bridge 2-918 N

The curves for this bridge are similar in shape and the projection lines run parallel to each other (Figure 5.13). Trigger levels had a difference of 5 με. Projected strains are higher than in the past. These data sets were found to be similar in Section 4.4.8. Projected values are provided in Table 5.14.

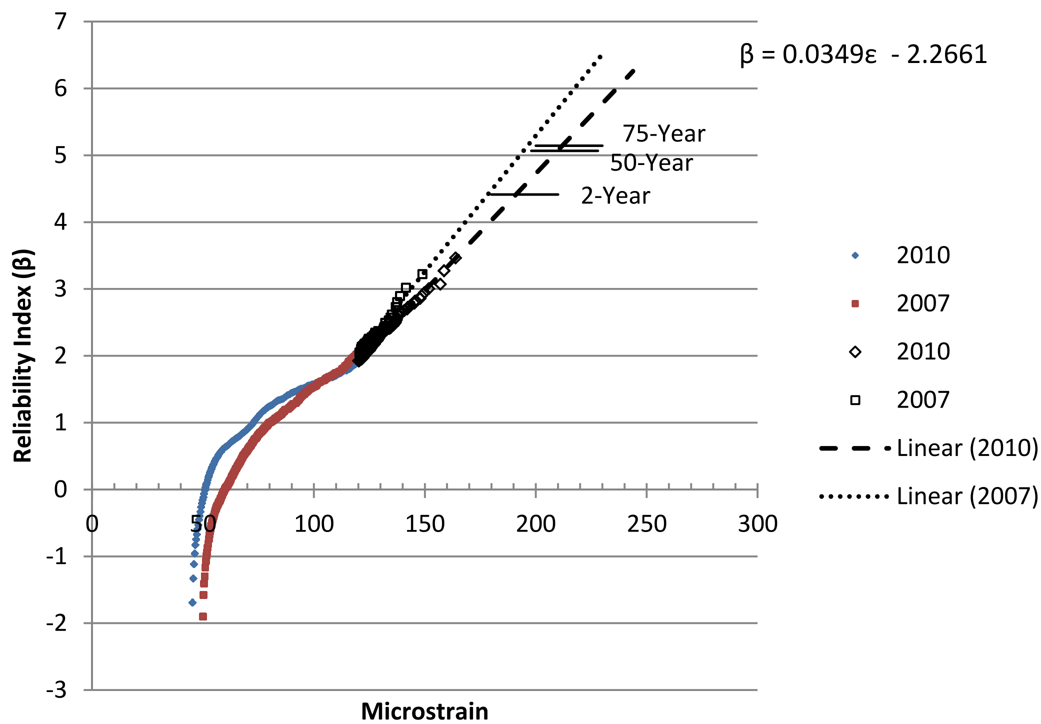

Figure 5.13: Bridge 2-918 N strain projection plot

Table 5.14: Bridge 2-918 N strain projection values

Period	# of Events	β	με (2010)	με (2007)
In-service	3,752	3.46	164.2	149.4
1 Year	98,366	4.26	187.0	169.7
2 Years	196,732	4.41	191.4	173.6
10 Years	983,662	4.75	201.0	182.3
50 Years	4,918,308	5.07	210.1	190.4
75 Years	7,377,462	5.14	212.3	192.3

5.3.11 Bridge 2-920 N

This is the first time this bridge has been monitored with the ISBMS so there is no curve to compare it to (Figure 5.14). Projected values are provided in Table 5.15.

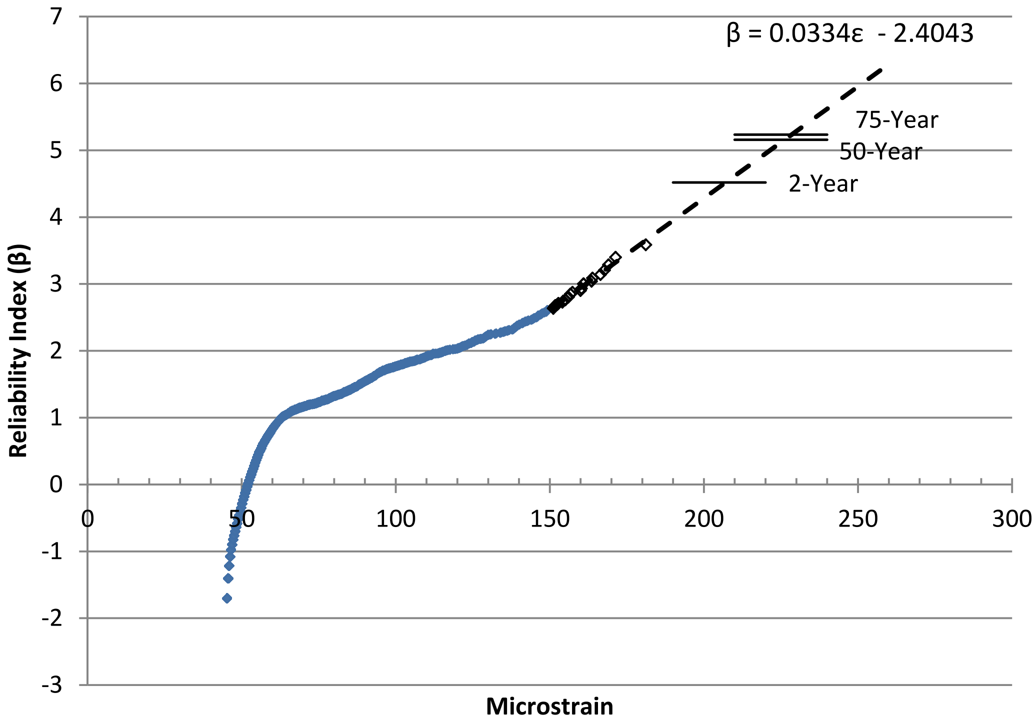

Figure 5.14: Bridge 2-920 N strain projection plot

Table 5.15: Bridge 2-920 N strain projection values

Period	# of Events	β	με (2010)
14 Days	5,943	3.59	179.3
1 Year	160,296	4.37	202.8
2 Years	320,591	4.52	207.3
10 Years	1,602,956	4.85	217.1
50 Years	8,014,781	5.16	226.4
75 Years	12,022,172	5.23	228.7

5.3.12 Bridge 1-907 S

This is the first time this bridge has been monitored with the ISBMS so there is no curve to compare it to (Figure 5.15). Projected values are provided in Table 5.16.

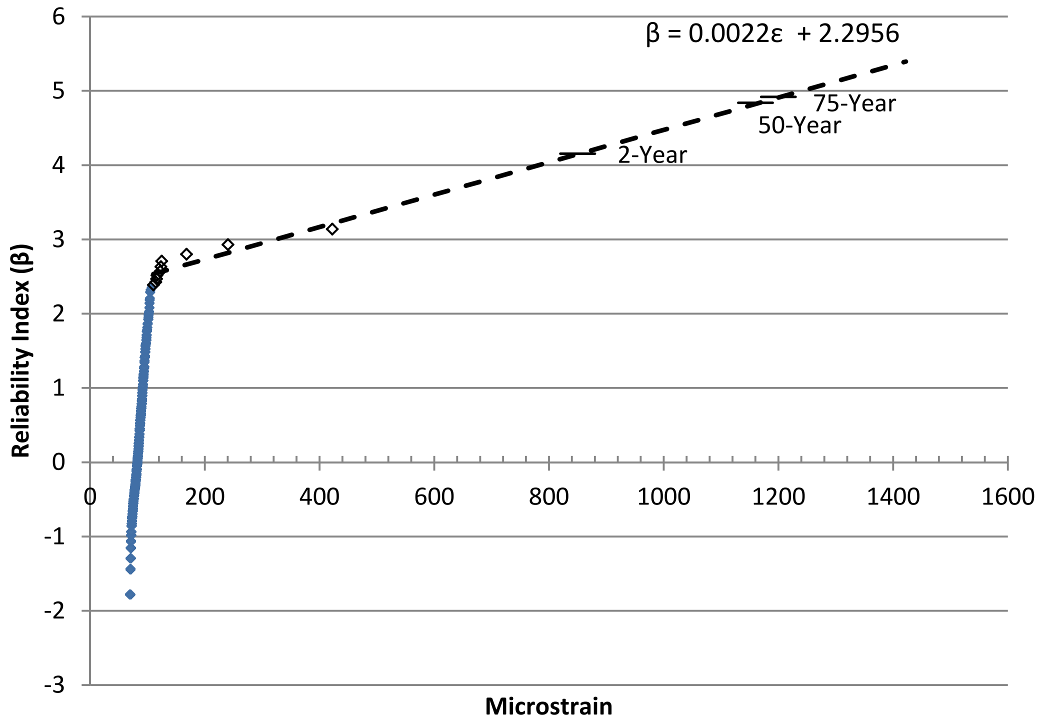

Figure 5.15: Bridge 1-907 S strain projection plot

Table 5.16: Bridge 1-907 S strain projection values

Period	# of Events	β	με (2010)
14 Days	1,176	3.14	382.9
1 Year	30,673	3.99	771.6
2 Years	61,345	4.15	844.9
10 Years	306,726	4.51	1006.0
50 Years	1,533,628	4.84	1156.2
75 Years	2,300,441	4.92	1192.5

Since a large, single event causes the projection line to have a very shallow slope and may exaggerate future strains, a second projection plot was created with the outlier removed (Figure 5.16). These revised strain projections are provided in Table 5.17. While these values give more reasonable strain predictions, the slope is still shallow and results in high projected strain values.

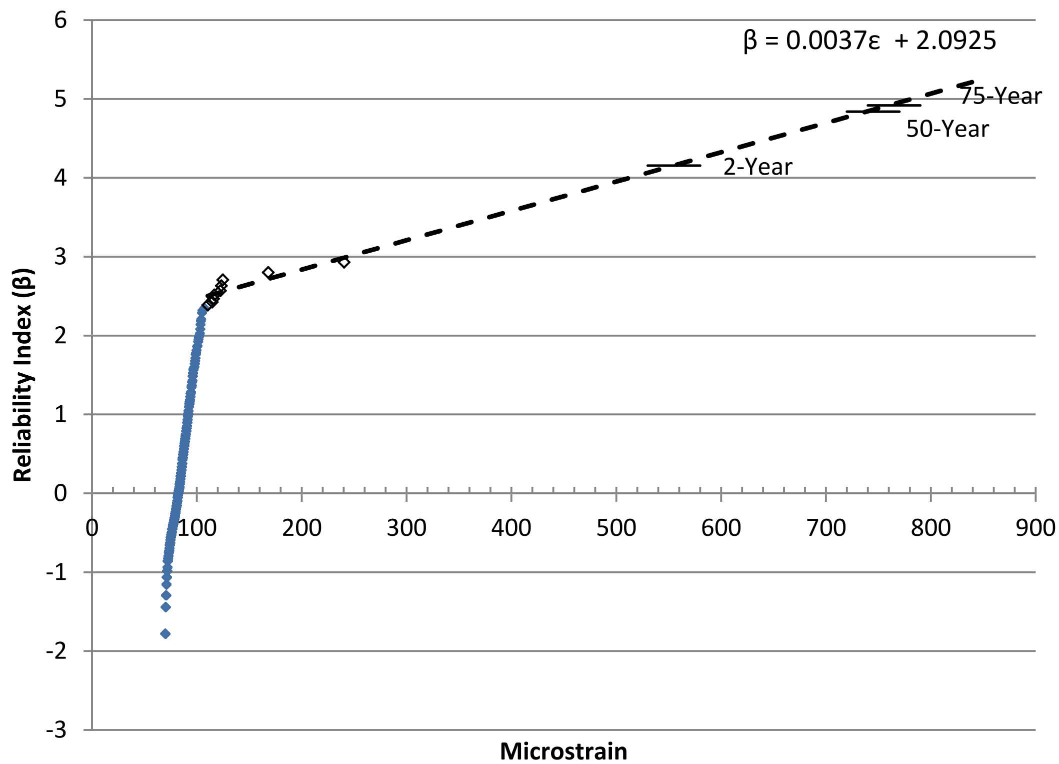

Figure 5.16: Bridge 1-907 S revised strain projection plot

Table 5.17: Bridge 1-907 S revised strain projection values

Period	# of Events	β	με (2010)
14 Days	1,176	3.14	282.6
1 Year	30,673	3.99	513.7
2 Years	61,345	4.15	557.3
10 Years	306,726	4.51	653.0
50 Years	1,533,628	4.84	742.3
75 Years	2,300,441	4.92	763.9

5.3.13 Bridge 1-394 S

The curves for this bridge are somewhat similar in shape but projection lines diverge (Figure 5.17). Trigger levels had a difference of 5 με. Projected strains are higher than in the past. These data sets were found to be somewhat similar in Section 4.5.4. Projected values are provided in Table 5.18.

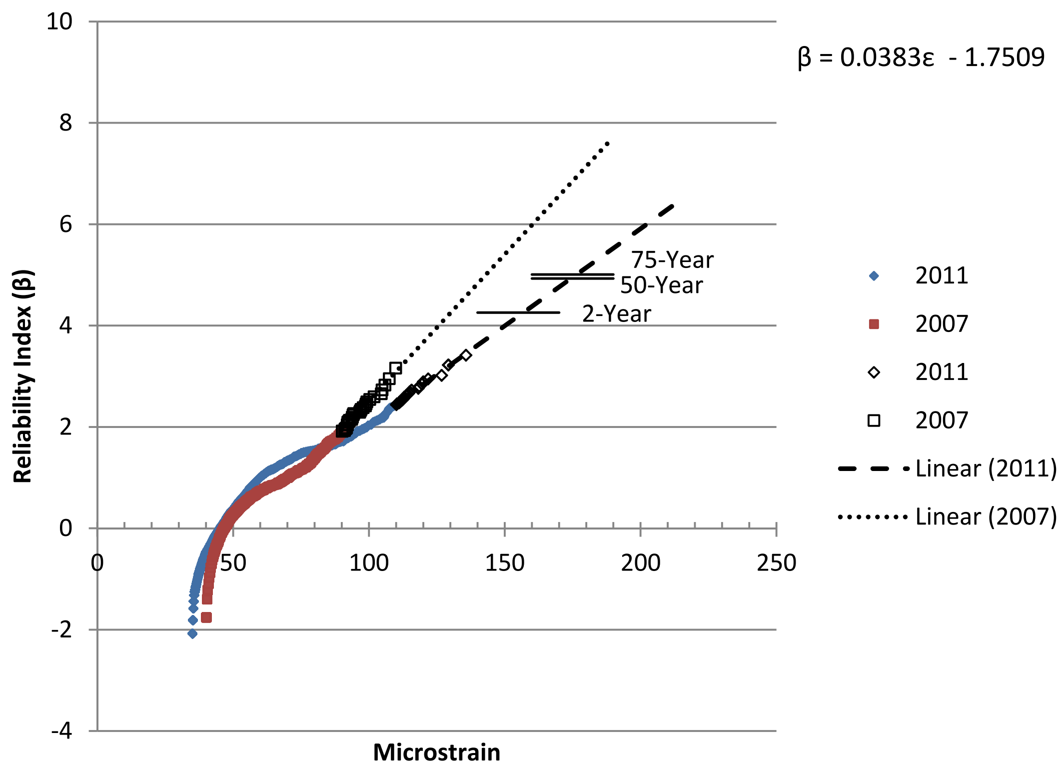

Figure 5.17: Bridge 1-394 S strain projection plot

Table 5.18: Bridge 1-394 S strain projection values

Period	# of Events	β	με (2011)	με (2007)
In-service	3,141	3.42	134.9	111.0
1 Year	48,204	4.10	152.7	125.0
2 Years	96,408	4.26	156.9	127.7
10 Years	482,040	4.60	165.9	133.7
50 Years	2,410,198	4.93	174.4	139.2
75 Years	3,615,298	5.01	176.4	140.5

5.3.14 Bridge 1-149

The curves for this bridge are dissimilar and diverge after intersecting near the two year projection (Figure 5.18). Lower strains are projected than in the past. These data sets were found to be dissimilar in Section 4.4.9. Projected values are provided in Table 5.19.

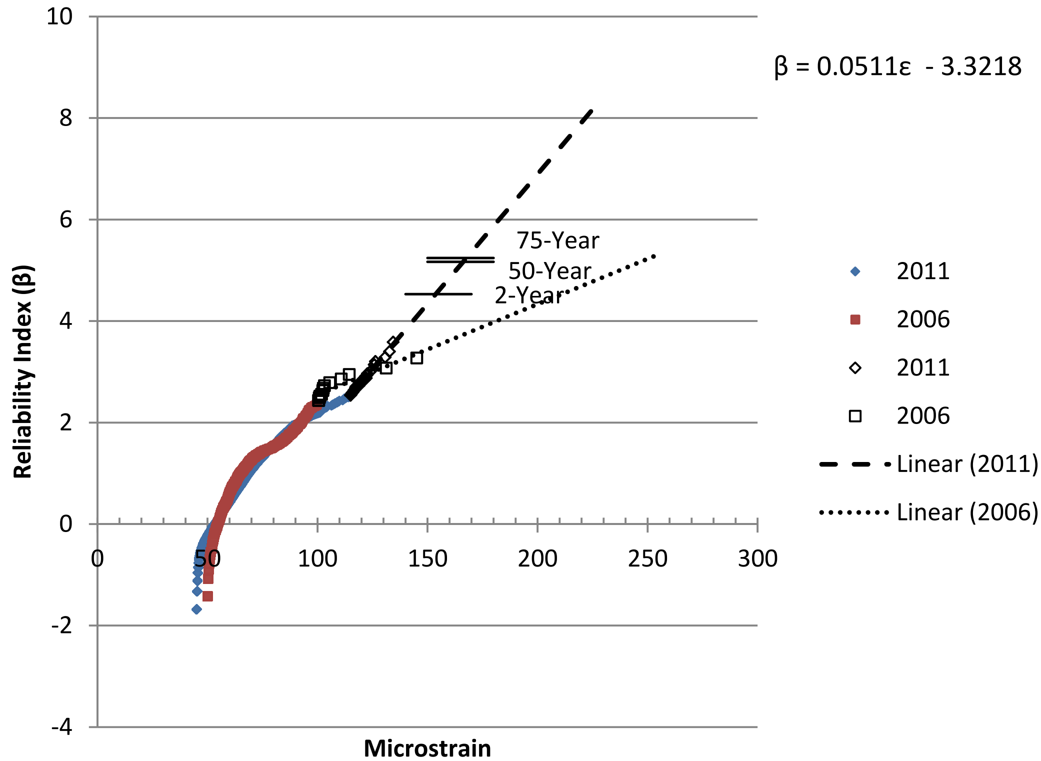

Figure 5.18: Bridge 1-149 strain projection plot

Table 5.19: Bridge 1-149 strain projection values

Period	# of Events	β	με (2011)	με (2006)
In-service	5,943	3.59	135.2	140.3
1 Year	168,955	4.38	150.7	184.8
2 Years	337,910	4.53	153.6	193.3
10 Years	1,689,550	4.86	160.1	211.9
50 Years	8,447,752	5.17	166.1	229.4
75 Years	12,671,628	5.24	167.6	233.6

5.4 Strain Projection Summary

A summary of the strain projections for all bridges is provided in Table 5.20. The projection plots may be useful for comparison. Data sets with similarly shaped curves tend to have similar data comparisons in Section 4.4 and Section 4.5. However, the strain projection lines are based on the tail-end of the plot so if there is much variability in these regions, the lines may diverge. Data sets that have similarly shaped curves but different tail-ends may result in very different projection values.

Table 5.20: Strain projection summary

Bridge Number	Max Strain Recorded (με)	2-Year Projection (με)	50-Year Projection (με)	75-Year Projection (με)
1-781	121	132	152	155
1-728	77	89	98	99
1-704	107	119	133	135
1-826 S	224	340	397	403
1-262 S	123	172	200	203
1-826 N (1)	140	178	202	205
1-826 N (2)	151	195	219	221
1-911 S (1)	188	202	218	220
1-911 S (2)	187	191	205	207
1-821 N	308	362	397	401
1-791	105	142	165	168
2-918 N	164	191	210	212
2-920 N	181	207	226	229
1-907 S	240	557	742	764
1-394 S	136	157	174	176
1-149	134	154	166	168

5.5 In-service Load Rating Factors Methodology

The projected strain values determined in Section 5.3 are used to compute load ratings for each of the bridges in the ISBMS inventory. Projected maximum strain values are used to calculate 1-, 2-, 10-, 50- and 75-year ratings. The actual recorded strain over the monitoring period is used to calculate the load rating for the in-service period. These ratings are compared to those previously calculated for this research and to the current American Association of State Highway and Transportation Officials (AASHTO) 50-year ratings.

A similar procedure used and described in detail by Rakowski for obtaining rating factors (Rakowski, 2008) is employed for this work, however load factors are based on the updated AASHTO Load and Resistance Factor Rating (LRFR) section 6.4 procedure (AASHTO).

Two load rating factors are reported in this report for each bridge – one for the HS20 truck loading and one for the governing rating factor. The governing factor may be due to a different loading scenario analyzed by BRASS that results in a rating lower than the rating due to the HS20 loading. The rating factor calculated from BRASS, LRFR, is defined in Equation 5.2 and the rating factors calculated using BRASS outputs in addition to ISBMS projected strain values, ISFR, are defined in Equation 5.3. Note that the factored load output in BRASS can either be in terms of moments or stresses.

$$LRFR = \frac{\varphi R_n - \gamma_D DL}{\gamma_L LL} \qquad \text{Equation 5.2}$$

$$ISRF = \frac{\varphi R_n - \gamma_D DL}{LL_M} \qquad \text{Equation 5.3}$$

where,

- φR_n ≡ factored resistance, BRASS output
- $\gamma_D DL$ ≡ factored dead load, BRASS output
- $\gamma_L LL$ ≡ factored live load, BRASS output
- LL_M ≡ measured live load, either:
  - = $M = \frac{\varepsilon EI}{y}$ ≡ Bernoulli Euler beam bending equation, moment
  - = $\sigma = \varepsilon E$ ≡ stress
- ε ≡ strain, projected from collected ISBMS data
- E ≡ steel modulus of elasticity, 29,000 ksi
- I ≡ moment of inertia, BRASS output
- y ≡ distance to neutral axis, BRASS output

The load resistance factors that are applied during BRASS calculations are presented in Table 6-1 of the LRFR manual (AASHTO). Each rating factor is governed by a particular limit state, either strength or service. The strength limit state may be governed by flexure or shear, but unless otherwise noted it is governed by flexure in this analysis. Strength I shall be checked for the strength limit state and Service II shall be checked for the service limit state for steel bridges as specified in Section 6.6.4.1 of the LRFR manual. They are displayed in Table 5.21.

Table 5.21: Load factors for inventory design load ratings, LRFR (AASHTO)

Limit State	γ_{DC}(structural components)	γ_{DW}(other DL)	γ_L
Strength I	1.25	1.50	1.75
Service II	1.00	1.00	1.30

BRASS applies the factors automatically in its output. The factors used for comparison are the inventory critical rating factors. These factors only apply to the critical location on the bridge for a given loading. In cases where the ISBMS was placed at a location different than the critical location, a multiplier must be used to apply the ISRF to the critical rating. This multiplier is the ratio of the BRASS rating factor at the critical location to the ISBMS rating factor at the location where the ISBMS was placed. The derivation of this ratio is provided in Appendix B.

As an example, a rating for a bridge with the BRASS output displayed in Table 5.22 is calculated. The ISBMS in this case was not placed in the critical location for the bridge. The HS20 and governing rating factors are calculated using Equation 5.2 for the critical location and the location where the ISBMS was placed.

Table 5.22: Example BRASS data

BRASS Variable	Critical Location Value	ISBMS Location Value
Gov. HS20 Limit State	Strength I	Strength I
I	5000 in^4	5000 in^4
y	15 in	15 in
φR_n	1200 k·ft	1200 k·ft
$\gamma_D DL$	187.5 k·ft	162.5 k·ft
HS20 $\gamma_L LL$	437.5 k·ft	393.75 k·ft
HS20 RF	2.31	2.63
Governing $\gamma_L LL$	612.5 k·ft	525 k·ft
Governing RF	1.65	1.98

Now, the rating factors for the bridge based on projected strains are used to calculate a stress or moment – moment in this example. A given strain of 88 με, would result in a moment of 70.9 k·ft. The moment is the live load input for Equation 5.3.

$$ISBMS\ RF = \frac{1200 - 162.5}{70.9} = 14.63$$

While this calculation yields an ISRF, it is only valid at the location the strains were recorded. Since the ISBMS was not placed at the critical location, ratios must be computed in order to apply the rating to the overall bridge. These ratios act as reduction factors. For the example they are:

$$HS20\ ratio = \frac{2.31}{2.63} = 0.878$$

$$Gov.ratio = \frac{1.65}{1.98} = 0.833$$

These values are multiplied by the ISBMS RF and result in the HS20 ISRF and Governing ISRF for the bridge as shown in Table 5.23 for a given range of projected strains.

Table 5.23: In-service rating factors for Table 5.22 data

Period	Strain (με)	Moment (k·ft)	HS20 ISRF	Gov. ISRF
In-service	88	70.9	12.85	12.24
1 Year	130.62	105.2	8.66	8.25
2 Years	134.42	108.3	8.42	8.01
10 Years	142.67	114.9	7.93	7.55
50 Years	150.27	121.1	7.53	7.17
75 Years	152.10	122.5	7.44	7.08

5.6 Load Ratings

Load ratings are calculated for each of the bridges monitored during this research. The critical location versus the ISBMS location is described for each bridge. BRASS output is provided and used to compute ratings for in-service, 1-, 2-, 10-, 50- and 75-year periods. BRASS files for the bridges monitored in this project were supplied by DelDOT.

5.6.1 Bridge 1-781

The critical location of this bridge for the HS20 and governing loadings is at the end bearing of Span 1 and the governing limit state is Strength I for shear. Shear analysis is not compatible with data garnered from the ISBMS so a comparison is made to the BRASS ratings at the ISBMS location. The ISBMS location is at mid-span of Span 1. BRASS output is summarized in Table 5.24 and ISRFs are provided in Table 5.25.

Table 5.24: Bridge 1-781 BRASS data

BRASS Variable	ISBMS Location Value
Governing Limit State	Service II
I	8316.1 in^4
y	24.27 in
ϕR_n	34.2 ksi
$\gamma_D D_n$	6.45 ksi
HS20 $\gamma_L L_n$	12.41 ksi
HS20 RF	2.24
Governing $\gamma_L L_n$	15 ksi
Governing RF	1.85

Table 5.25: Bridge 1-781 in-service rating factors

Period	Strain (με)	Stress (ksi)	HS20 ISRF	Gov. ISRF
In-service	120.66	3.50	7.93	7.93
1 Year	127.07	3.69	7.53	7.53
2 Years	131.89	3.82	7.26	7.26
10 Years	142.51	4.13	6.71	6.71
50 Years	152.45	4.42	6.28	6.28
75 Years	154.86	4.49	6.18	6.18

5.6.2 Bridge 1-728

The critical location of this bridge for the HS20 and governing loadings is at mid-span of Span 2 while the ISBMS location is mid-span of Span 1. Therefore, ratios are used to compute the ISRFs at the critical location. BRASS output is summarized in Table 5.26 and ISRFs are provided in Table 5.27.

Table 5.26: Bridge 1-728 BRASS data

BRASS Variable	Critical Location Value	ISBMS Location Value
Governing Limit State	Strength I	Service II
I	21567.3 in^4	13966.8 in^4
y	16.35 in	25.39 in
ϕR_n	-32 ksi	30.4 ksi
$\gamma_D D_n$	-12 ksi	4.74 ksi
HS20 $\gamma_L L_n$	-14.2 ksi	7.87 ksi
HS20 RF	1.41	3.26
Governing $\gamma_L L_n$	-18.9 ksi	9.53 ksi
Governing RF	1.06	2.69

Table 5.27: Bridge 1-728 in-service rating factors

Period	Strain (με)	Stress (ksi)	HS20 ISRF	Gov. ISRF
In-service	77.08	2.24	4.96	4.51
1 Year	87.43	2.54	4.37	3.98
2 Years	89.44	2.59	4.27	3.89
10 Years	93.85	2.72	4.07	3.71
50 Years	97.97	2.84	3.90	3.55
75 Years	98.96	2.87	3.86	3.51

5.6.3 Bridge 1-704

The critical location of this bridge for the HS20 loading is at the fourth tenth point and the governing loading at mid-span of Span 3. The ISBMS location is at mid-span of Span 3. Therefore, a ratio is used to compute the ISRF at the governing critical location. BRASS output is summarized in Table 5.28 and ISRFs are provided in Table 5.29.

Table 5.28: Bridge 1-704 BRASS data

BRASS Variable	Critical Location Value	ISBMS Location Value
Governing Limit State	Strength I	Strength I
I	2340.5 in^4	2340.5 in^4
y	12.05 in	12.05 in
ϕR_n	33 ksi	33 ksi
HS20 $\gamma_D D_n$	6.6 ksi	6.8 ksi
HS20 $\gamma_L L_n$	22 ksi	21.7 ksi
HS20 RF	1.20	1.21
Governing $\gamma_D D_n$	6.8 ksi	6.8 ksi
Governing $\gamma_L L_n$	32.8 ksi	32.8 ksi
Governing RF	0.80	0.80

Table 5.29: Bridge 1-704 in-service rating factors

Period	Strain (με)	Stress (ksi)	HS20 ISRF	Gov. ISRF
In-service	106.68	3.09	8.42	8.47
1 Year	115.9	3.36	7.75	7.80
2 Years	119.24	3.46	7.53	7.58
10 Years	126.57	3.67	7.09	7.14
50 Years	133.4	3.87	6.73	6.77
75 Years	135.05	3.92	6.65	6.69

5.6.4 Bridge 1-826 S

The critical location of this bridge for the HS20 and governing loadings is the first tenth point of Span 2 while the ISBMS location is mid-span of Span 3. Therefore, ratios are used to compute the ISRFs at the critical location. BRASS output is summarized in Table 5.30 and ISRFs are provided in Table 5.31.

Table 5.30: Bridge 1-826 S BRASS data

BRASS Variable	Critical Location Value	ISBMS Location Value
Governing Limit State	Strength I	Strength I
I	22578.9 in^4	29911.1 in^4
y	33.81 in	32.89 in
ϕR_n	-36 k·ft	3257.9 k·ft
$\gamma_D D_n$	-10.4 k·ft	541.6 k·ft
HS20 $\gamma_L L_n$	-13.3 k·ft	1186.1 k·ft
HS20 RF	1.92	2.29
Governing $\gamma_L L_n$	-18.9 k·ft	1556.2 k·ft
Governing RF	1.35	1.75

Table 5.31: Bridge 1-826 S in-service rating factors

Period	Strain (με)	Moment (k·ft)	HS20 ISRF	Gov. ISRF
In-service	223.76	491.78	4.64	4.29
1 Year	327.42	719.60	3.17	2.93
2 Years	340.44	748.21	3.05	2.82
10 Years	369.34	811.73	2.81	2.60
50 Years	396.63	871.71	2.62	2.42
75 Years	403.29	886.34	2.58	2.38

5.6.5 Bridge 1-262 S

The critical location of this bridge for the HS20 loading is at the end bearing of Span 4 and the governing loading is at the end bearing of Span 2. The ISBMS location is mid-span of Span 1. Therefore, ratios are used to compute the ISRFs at the critical location. BRASS output is summarized in Table 5.32 and ISRFs are provided in Table 5.33.

Table 5.32: Bridge 1-262 S BRASS data

BRASS Variable	Critical Location Value	ISBMS Location Value
Governing Limit State	Strength I	Service II
I	80962.6 in4	52904.1 in4
y	44.41 in	46.47 in
ϕR_n	-36 ksi	34.2 ksi
HS20 $\gamma_D D_n$	-18 ksi	8.08 ksi
HS20 $\gamma_L L_n$	-9.6 ksi	4.35 ksi
HS20 RF	1.88	6.00
Governing $\gamma_D D_n$	-18.1 ksi	8.08 ksi
Governing $\gamma_L L_n$	-24 ksi	11.9 ksi
Governing RF	0.75	2.19

Table 5.33: Bridge 1-262 S in-service rating factors

Period	Strain (με)	Stress (ksi)	HS20 ISRF	Gov. ISRF
In-service	123.26	3.57	2.28	2.48
1 Year	165.67	4.80	1.70	1.85
2 Years	172.12	4.99	1.63	1.78
10 Years	186.29	5.40	1.51	1.64
50 Years	199.50	5.79	1.41	1.53
75 Years	202.71	5.88	1.39	1.51

5.6.6 Bridge 1-826 N

The critical location of this bridge for the HS20 loading is at the first tenth point and the governing loading is at the end bearing of Span 2. The ISBMS location is mid-span of Span 3. Therefore, ratios are used to compute the ISRFs at the critical location. BRASS output is summarized in Table 5.34, ISRFs for the June monitoring period are provided in Table 5.35 and the ISRFSs for the February monitoring period in Table 5.36.

Table 5.34: Bridge 1-826 N BRASS data

BRASS Variable	Critical Location Value	ISBMS Location Value
Governing Limit State	Strength I	Service II
I	22578.9 in^4	29911.1 in^4
y	33.81 in	32.89 in
ϕR_n	-36 ksi	34.2 ksi
HS20 $\gamma_D D_n$	-10.4 ksi	8.2 ksi
HS20 $\gamma_L L_n$	-13.3 ksi	11.5 ksi
HS20 RF	1.92	2.26
Governing $\gamma_D D_n$	-22.8 ksi	15.15 ksi
Governing $\gamma_L L_n$	1.04	1.72
Governing RF	Strength I	Service II

Table 5.35: Bridge 1-826 N June 2010 in-service rating factors

Period	Strain (με)	Stress (ksi)	HS20 ISRF	Gov. ISRF
In-service	139.53	4.05	5.47	3.89
1 Year	172.67	5.01	4.42	3.14
2 Years	178.16	5.17	4.28	3.05
10 Years	190.36	5.52	4.01	2.85
50 Years	201.88	5.85	3.78	2.69
75 Years	204.68	5.94	3.73	2.65

Table 5.36: Bridge 1-826 N February 2011 in-service rating factors

Period	Strain (με)	Stress (ksi)	HS20 ISRF	Gov. ISRF
In-service	151.07	4.38	5.05	3.59
1 Year	189.76	5.50	4.02	2.86
2 Years	195.2	5.66	3.91	2.78
10 Years	207.25	6.01	3.68	2.62
50 Years	218.6	6.34	3.49	2.48
75 Years	221.37	6.42	3.45	2.45

5.6.7 Bridge 1-911 S

The critical location of this bridge for the HS20 and governing loadings is at mid-span of its span which is also the ISBMS location. BRASS output is summarized in Table 5.37 and ISRFs are provided in Table 5.38 for the July monitoring period and Table 5.39 for the November monitoring period.

Table 5.37: Bridge 1-911 S BRASS data

BRASS Variable	Critical Location Value
Governing Limit State	Service II
I	34947.6 in^4
y	33.24 in
ϕR_n	47.5 ksi
$\gamma_D D_n$	12.67 ksi
HS20 $\gamma_L L_n$	12.64 ksi
HS20 RF	2.76
Governing $\gamma_L L_n$	16.26 ksi
Governing RF	2.14

Table 5.38: Bridge 1-911 S July in-service rating factors

Period	Strain (με)	Stress (ksi)	HS20 ISRF	Gov. ISRF
In-service	187.66	5.44	6.40	6.40
1 Year	197.82	5.74	6.07	6.07
2 Years	201.67	5.85	5.96	5.96
10 Years	210.2	6.10	5.71	5.71
50 Years	218.25	6.33	5.50	5.50
75 Years	220.21	6.39	5.45	5.45

Table 5.39: Bridge 1-911 S November in-service rating factors

Period	Strain (με)	Stress (ksi)	HS20 ISRF	Gov. ISRF
In-service	186.64	5.41	6.44	6.44
1 Year	187.07	5.43	6.42	6.42
2 Years	190.52	5.53	6.30	6.30
10 Years	198.13	5.75	6.06	6.06
50 Years	205.27	5.95	5.85	5.85
75 Years	207	6.00	5.80	5.80

5.6.8 Bridge 1-821 N

The critical location of this bridge for the HS20 loading is at the sixth tenth point in Span 4 and the governing loading is at the end bearing of Span 2. The ISBMS location is mid-span of Span 3. Therefore, ratios are used to compute the ISRFs at the critical location. BRASS output is summarized in Table 5.40 and ISRFs are provided in Table 5.41.

Table 5.40: Bridge 1-821 N BRASS data

BRASS Variable	Critical Location Value		ISBMS Location Value	
Loading Case	HS20	Governing	HS20	Governing
Governing Limit State	Service II	Strength I	Service II	Service II
I	22578.9 in^4	14028.1 in^4	22578.9 in^4	22578.9 in^4
y	33.81 in	17.81 in	33.81 in	33.81 in
ϕR_n	34.2 ksi	36 ksi	34.2 ksi	34.2 ksi
$\gamma_D D_n$	7.65 ksi	12.4 ksi	6.56 ksi	6.56 ksi
$\gamma_L L_n$	13.96 ksi	19.2 ksi	13.9 ksi	3.71 ksi
RF	1.9	1.23	1.99	7.45

Table 5.41: Bridge 1-821 N in-service rating factors

Period	Strain (με)	Stress (ksi)	HS20 ISRF	Gov. ISRF
In-service	308.32	8.94	2.96	0.51
1 Year	354.1	10.27	2.57	0.44
2 Years	362.1	10.50	2.52	0.43
10 Years	379.84	11.02	2.40	0.41
50 Years	396.58	11.50	2.30	0.40
75 Years	400.66	11.62	2.28	0.39

5.6.9 Bridge 1-791

The critical location of this bridge for the HS20 loading is at the fourth tenth point in Span 1 and the governing loading is at the sixth point in Span 3 but analysis for these two locations is identical in BRASS. The ISBMS location is mid-span of Span 1. Therefore, ratios are used to compute the ISRFs at the critical location. BRASS output is summarized in Table 5.42 and ISRFs are provided in Table 5.43.

Table 5.42: Bridge 1-791 BRASS data

BRASS Variable	Critical Location Value	ISBMS Location Value
Governing Limit State	Strength I	Strength I
I	3923.8 in4	3923.8 in4
y	14.82 in	14.82 in
ϕR_n	36 ksi	36 ksi
$\gamma_D D_n$	3.2 ksi	2 ksi
HS20 $\gamma_L L_n$	19.8 ksi	19 ksi
HS20 RF	1.66	1.79
Governing $\gamma_L L_n$	25.8 ksi	25.3 ksi
Governing RF	1.27	1.34

Table 5.43: Bridge 1-791 in-service rating factors

Period	Strain (με)	Stress (ksi)	HS20 ISRF	Gov. ISRF
In-service	104.56	3.03	10.38	10.61
1 Year	136.92	3.97	7.93	8.10
2 Years	142.34	4.13	7.62	7.79
10 Years	154.24	4.47	7.04	7.19
50 Years	165.35	4.80	6.56	6.71
75 Years	168.04	4.87	6.46	6.60

5.6.10 Bridge 2-918 N

The critical location of this bridge for the HS20 and governing loadings is at mid-span of its span which is also the ISBMS location. BRASS output is summarized in Table 5.44 and ISRFs are provided in Table 5.45.

Table 5.44: Bridge 2-918 N BRASS data

BRASS Variable	Critical Location Value
Governing Limit State	Service II
I	36150.2 in4
y	33.82 in
ϕR_n	47.5 ksi
$\gamma_D D_n$	13.14 ksi
HS20 $\gamma_L L_n$	12.39 ksi
HS20 RF	2.77
Governing $\gamma_L L_n$	15.95 ksi
Governing RF	2.15

Table 5.45: Bridge 2-918 N in-service rating factors

Period	Strain (με)	Stress (ksi)	HS20 ISRF	Gov. ISRF
In-service	163.84	4.75	7.23	7.23
1 Year	187.03	5.42	6.33	6.33
2 Years	191.40	5.55	6.19	6.19
10 Years	201.04	5.83	5.89	5.89
50 Years	210.08	6.09	5.64	5.64
75 Years	212.28	6.16	5.58	5.58

5.6.11 Bridge 2-920 N

The critical location of this bridge for the HS20 and governing loadings is at mid-span of its span which is also the ISBMS location. BRASS output is summarized in Table 5.46 and ISRFs are provided in Table 5.47.

Table 5.46: Bridge 2-920 N BRASS data

BRASS Variable	Critical Location Value
Governing Limit State	Service II
I	36150.2 in4
y	33.82 in
ϕR_n	47.5 ksi
$\gamma_D D_n$	13.14 ksi
HS20 $\gamma_L L_n$	12.4 ksi
HS20 RF	2.77
Governing $\gamma_L L_n$	15.95 ksi
Governing RF	2.15

Table 5.47: Bridge 2-920 N in-service rating factors

Period	Strain (με)	Stress (ksi)	HS20 ISRF	Gov. ISRF
In-service	181.11	5.25	6.54	6.54
1 Year	202.80	5.88	5.84	5.84
2 Years	207.26	6.01	5.72	5.72
10 Years	217.13	6.30	5.46	5.46
50 Years	226.42	6.57	5.23	5.23
75 Years	228.68	6.63	5.18	5.18

5.6.12 Bridge 1-907 S

The critical location of this bridge for the HS20 and governing loadings is at the end bearing of the span and the governing limit state is Strength I for shear. Shear analysis is not compatible with data garnered from the ISBMS so a comparison is made to the BRASS ratings at the ISBMS location. The ISBMS location is at mid-span. BRASS output is summarized in Table 5.48 and ISRFs are provided in Table 5.49.

Table 5.48: Bridge 1-907 S BRASS data

BRASS Variable	ISBMS Location Value
Governing Limit State	Service II
I	60187.6 in4
y	40.02 in
ϕR_n	47.5 ksi
$\gamma_D D_n$	13.79 ksi
HS20 $\gamma_L L_n$	11.96 ksi
HS20 RF	2.82
Governing $\gamma_L L_n$	15.98 ksi
Governing RF	2.11

Table 5.49: Bridge 1-907 S in-service rating factors

Period	Strain (με)	Stress (ksi)	HS20 ISRF	Gov. ISRF
In-service	240.39	6.97	4.84	4.84
1 Year	513.69	14.90	2.26	2.26
2 Years	557.29	16.16	2.09	2.09
10 Years	653.05	18.94	1.78	1.78
50 Years	742.33	21.53	1.57	1.57
75 Years	763.95	22.15	1.52	1.52

5.6.13 Bridge 1-394 S

The critical location of this bridge for the HS20 and governing loadings is at end bearing of Span 2 while the ISBMS location is mid-span of Span 2. Therefore, ratios are used to compute the ISRFs at the critical location. BRASS output is summarized in Table 5.50 and ISRFs are provided in Table 5.51.

Table 5.50: Bridge 1-394 S BRASS data

BRASS Variable	Critical Location Value	ISBMS Location Value
Governing Limit State	Strength I	Service II
I	21635.1 in4	15866.6 in4
y	24.17 in	25.98 in
ϕR_n	32 ksi	30.4 ksi
$\gamma_D D_n$	12.4 ksi	5.2 ksi
HS20 $\gamma_L L_n$	10.3 ksi	9.56 ksi
HS20 RF	1.90	2.64
Governing $\gamma_L L_n$	15.2 ksi	11.99 ksi
Governing RF	1.29	2.10

Table 5.51: Bridge 1-394 S in-service rating factors

Period	Strain (με)	Stress (ksi)	HS20 ISRF	Gov. ISRF
In-service	135.7	3.94	4.62	3.93
1 Year	152.74	4.43	4.11	3.49
2 Years	156.86	4.55	4.00	3.40
10 Years	165.92	4.81	3.78	3.21
50 Years	174.39	5.06	3.60	3.06
75 Years	176.44	5.12	3.56	3.02

5.6.14 Bridge 1-149

The critical location of this bridge for the HS20 and governing loadings is at mid-span of its span which is also the ISBMS location. BRASS output is summarized in Table 5.52 and ISRFs are provided in Table 5.53.

Table 5.52: Bridge 1-149 BRASS data

BRASS Variable	Critical Location Value
Governing Limit State	Service II
I	36616.1 in4
y	31.28 in
ϕR_n	47.5 ksi
$\gamma_D D_n$	15.81 ksi
HS20 $\gamma_L L_n$	11.86 ksi
HS20 RF	2.67
Governing $\gamma_L L_n$	15.8 ksi
Governing RF	2.01

Table 5.53: Bridge 1-149 in-service rating factors

Period	Strain (με)	Stress (ksi)	HS20 ISRF	Gov. ISRF
In-service	134.38	3.90	8.13	8.13
1 Year	150.73	4.37	7.25	7.25
2 Years	153.64	4.46	7.11	7.11
10 Years	160.08	4.64	6.83	6.83
50 Years	166.14	4.82	6.58	6.58
75 Years	167.61	4.86	6.52	6.52

5.7 Load Rating Summary

Almost all of the 50-year in-service rating factors calculated in Section 5.6 are greater than those 50-year ratings calculated by BRASS. These comparisons point out the conservative nature of conventional ratings. For the HS20 loading, only Bridge 1-907 S had a higher BRASS rating (see Table 5.54 and Figure 5.19). For the governing loading, 1-262 S, 1-821 N and 1-907 S had higher BRASS ratings (see Table 5.55 and Figure 5.20). Bridge 1-821 N and Bridge 1-907 S had high maximum strain values which may have skewed the projected strains to yield relatively low rating factors. With the possible exception of Bridge 1-149, all of the previous 50-year rating factors calculated under Rakowski match up reasonably well to those calculated for this research.

Table 5.54: HS20 rating factor summary

Bridge Number	50-Year BRASS RF	2-Year ISRF	50-Year ISRF	Previous 50-Year ISRF (Rakowski, 2008)	75-Year ISRF
1-781	2.24	7.26	6.28	6.20	6.18
1-728	1.41	4.27	3.90	3.12	3.86
1-704	1.20	7.53	6.73	6.04	6.65
1-826 S	1.92	3.05	2.62	N/A	2.58
1-262 S	1.88	4.47	4.24	4.24	3.86
1-826 N (1)	1.92	4.28	3.78	2.99	3.73
1-826 N (2)	1.92	3.91	3.49	2.99	3.45
1-911 S (1)	2.76	5.96	5.50	6.36	5.45
1-911 S (2)	2.76	6.30	5.85	6.36	5.80
1-821 N	1.90	2.52	2.30	2.09	2.28
1-791	1.66	7.62	6.56	6.97	6.46
2-918 N	2.77	6.19	5.64	6.22	5.58
2-920 N	2.77	5.72	5.23	N/A	5.18
1-907 S	2.82	2.09	1.57	N/A	1.52
1-394 S	1.90	4.00	3.60	4.51	3.56

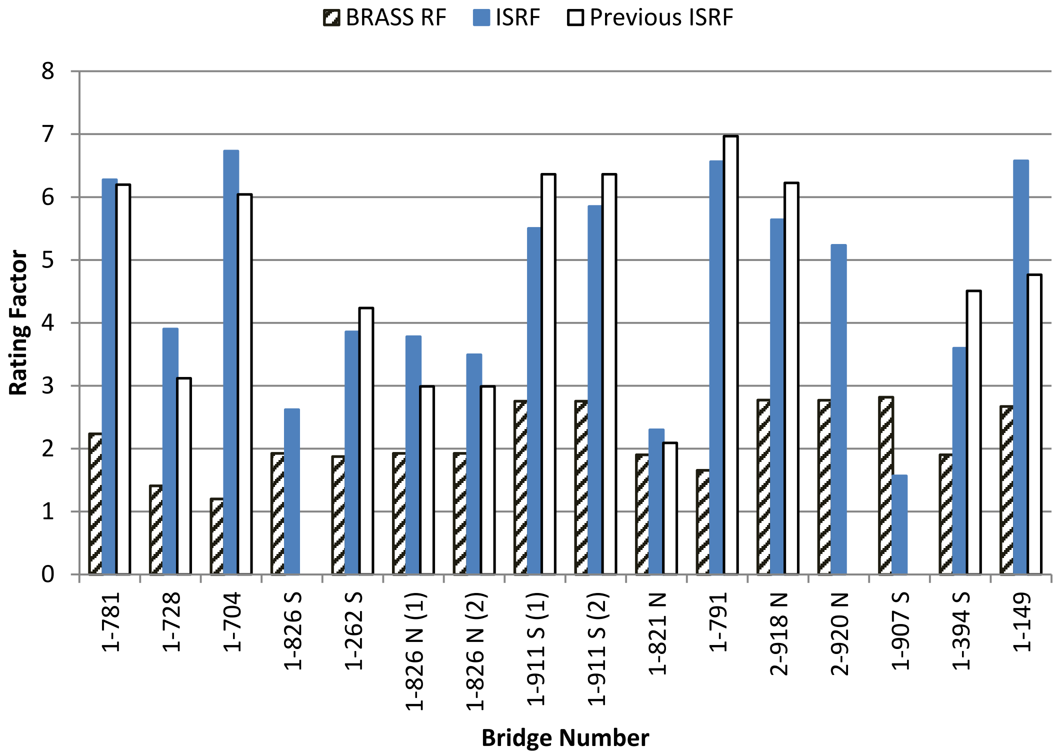

Figure 5.19: 50-Year HS20 rating factor comparison plot (Rakowski, 2008)

Table 5.55: Governing rating factor summary

Bridge Number	BRASS RF	2-Year ISRF	50-Year ISRF	Previous 50-Year ISRF (Rakowski, 2008)	75-Year ISRF
1-781	1.85	7.26	6.28	6.20	6.18
1-728	1.06	3.89	3.55	2.84	3.51
1-704	0.80	7.58	6.77	6.08	6.69
1-826 S	1.35	2.82	2.42	N/A	2.38
1-262 S	0.75	0.65	0.56	0.62	0.55
1-826 N (1)	1.04	0.65	0.56	2.13	2.65
1-826 N (2)	1.04	2.78	2.48	2.13	2.45
1-911 S (1)	2.14	5.96	5.50	6.36	5.45
1-911 S (2)	2.14	6.30	5.85	6.36	5.80
1-821 N	1.23	0.43	0.40	0.36	0.39
1-791	1.27	7.79	6.71	7.12	6.60
2-918 N	2.15	6.19	5.64	6.22	5.58
2-920 N	2.15	5.72	5.23	N/A	5.18
1-907 S	2.11	2.09	1.57	N/A	1.52
1-394 S	1.29	3.40	3.06	3.83	3.02

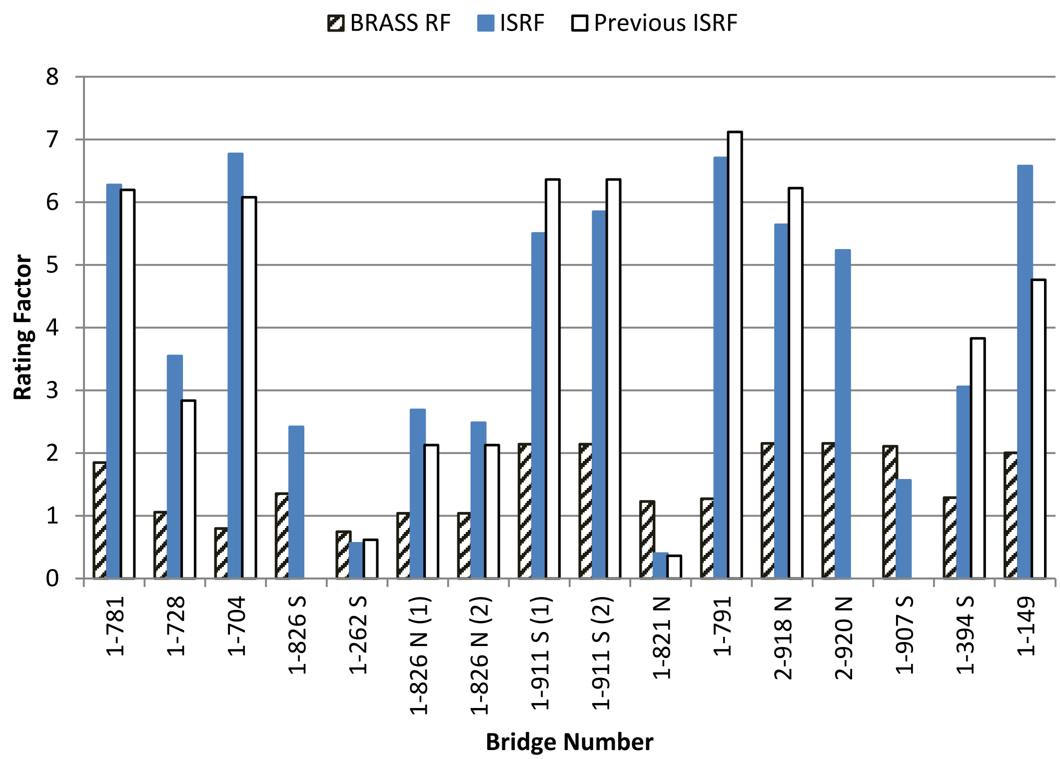

Figure 5.20: 50-Year governing rating factor comparison plot (Rakowski, 2008)

Chapter 6

CONCLUSIONS AND RECOMMENDATIONS

6.1 Conclusions

In this research fourteen bridges were monitored throughout New Castle County and Kent County, Delaware using the In-Service Bridge Monitoring System. The majority of these bridges had been previously monitored allowing for comparison of data sets. Methods were developed to make quantitative comparisons and to determine whether data sets collected were similar or different from past data sets. Load ratings were calculated based on strain projections. These were compared to ratings determined from previous ISBMS strain projections and DelDOT ratings.

All bridges monitored for this research were slab-on-steel girder highway bridges. While the basic design of all bridges monitored is the same, they vary in member size, span length, routes they carry and the number of trucks that pass over it per day. Some are composed of simple spans while others are continuous. Four of the bridges were monitored during different seasons so that the effects of temperature and traffic variations at different times of the year could be analyzed.

Data recorded for each bridge was organized into timeline and histogram plots. These plots express the distribution of events according to when they occurred and their frequency. The effectiveness of selected trigger levels was also analyzed. In some cases the trigger was well suited to collect an appropriate number of events for a particular monitoring period. In other cases the trigger needed to be raised to prevent the ISBMS from filling its memory with events too quickly. Alternatively, the trigger needed to be lowered to collect more events during the monitoring period on other occasions.

Three parameters – Area Difference (AD), Square Root Sum of the Squares of Differences (SRSSD) and Effective Strain Difference (ESD) – were used to compare different data sets on a bridge. Histograms of the in-service data were normalized and plotted together. Threshold values were designated for each parameter using outlier analysis of week-to-week histogram comparisons; 230 for AD, 18.5 for SRSSD and 28.5 for ESD. The effectiveness of the parameters was evaluated during year-to-year and seasonal histogram comparisons. The SRSSD parameter was determined to be the most accurate and reliable, but the AD was found to be fundamentally equivalent. The ESD parameter was inconsistent for the presented comparisons and was concluded to be a poor evaluator of histogram comparisons. Comparisons using the parameters indicated that there was no major variation on bridges during different seasons.

As done in past work on this project, maximum strain events were forecast from 1- up to 75-year return periods. These projections were based on the events collected during monitoring periods. These periods ranged in length from less than one week up to more than three weeks. Rating factors were calculated for several return periods using the extrapolated maximum strain values. These were then compared to the 50-year rating factor calculated by DelDOT using the BRASS program as well as rating factors based on data collected under Rakowski (Rakowski, 2008). The latest rating factors show fairly good agreement with Rakowski's. The contrast between the ISBMS and BRASS ratings points out the overly conservative nature of current bridge ratings.

While the ISBMS had previously been operated on several bridges, the promise of such a system lies in the ability to compare newly collected data sets with those of the past. Comparison of data collected using the ISBMS over time has the potential to be an effective method of bridge evaluation. Loss of capacity or an increase in load that can be imperceptible through visual or physical inspection may be apparent in ISBMS comparisons.

6.2 Recommendations

In-service data collected on the same bridge at two different times can only be compared if the ISBMS is placed in the same exact location. Inadequate notes can make consistent placement difficult. In order to ensure congruous locations between different monitoring periods, it is imperative that field notes are recorded. It was partially with this in mind that the ISBM forms were developed. Sketches of the bridge layout and gauge location as well as photos taken at the bridge site are good methods of documenting the ISBMS.

While the methods of comparison developed seem capable of detecting changes in bridge data, a structure with a known change should be monitored as an example of a true variation. For instance, a bridge that is undergoing structural rehabilitation could be monitored before and after completion of construction. Obvious differences should be prevalent in analysis and the root cause would be known – a structural change in the bridge. As a simpler example, the ISBMS could be deployed on a bridge near roadwork on the route. It could be expected that the truck traffic distribution would change during the construction. In-service data collected during and after the work should show event variations due to a fluctuation in traffic.

Alternatively, Weigh-in-Motion (WIM) data could be used to analyze changes “after the fact.” If data from a bridge does not match up well with a previous set and no known difference can be identified, WIM data could be used to explore effects related to traffic. Of course, the bridge would need to be located close enough to a WIM station. Fortunately, some of the bridges in the ISBMS inventory are in such locations (Rakowski, 2008).

There are a seemingly infinite number of ways to perceive the data collected by the ISBMS. Additional comparison methods could be used to substantiate the findings of this research. Perhaps different approaches would provide more reliable comparisons than those evaluated in this report.

The use of another ISBMS could be beneficial in collecting more data sets. As a supplement to the SSPM4 used in this project, the ISBMS developed under Howell could be used (Howell, 2003).

Appendix A

IN-SERVICE BRIDGE MONITORING SYSTEM

A.1 ISBMS and Communication

The ISBMS used during this research has two main components; a modified Snap Shock Plus M4 (SSPM4) unit manufactured by Instrumented Sensor Technology (IST), Inc. and a full-bridge Bridge Diagnostics Incorporated (BDI) strain transducer. The SSPM4 is powered by a 9-volt battery and the transducer is powered by a rechargeable 6-volt battery. Communication with the system is required to synchronize the time, input a trigger level and cutoff window. After being deployed, the ISBMS records peak strain data for the monitoring period until the battery life runs out or the memory gets filled up with events at which point it will deactivate. After retrieval, recorded data can be downloaded. Images of the ISBMS are provided in a previous thesis (Brookes, pp. 22, 23).

The SSPM4 has four modes:

- "Standby" (OFF): Indicated by a green and red light, is a low power mode in which the unit powers down with the exception of its clock. This is the mode the unit cycles to when it deactivates.
- "Comm1" (RS232 COM): Indicated by the first single red light when cycling, enables the system to communicate with a PC by activating the serial communication interface.
- "Comm2" (IRDA COM): Indicated by the second single red light when cycling, enables the infrared transmission interface. This mode is not used during this project.
- "Active" (ACT): Indicated by a single green light, is the mode in which the ISBMS records data.

The following components are required for communication between a PC or laptop and the ISBMS:

- IST ShockView 32 (sv32) software for Windows (XP)
- Belkin USB/Serial Adapter Cable (with software disc installation)

- Available USB COMM Port on computer

Transducer Number 346 was used for all monitoring during this project. A detailed description of how the system records, stores and converts events is detailed in a previous thesis (Holloway, pp. 9-14).

A.2 Calibration Settings

Three values need to be input into the SSPM4 calibration settings before using the unit. Note that the sv32 software only allows factors of three digits to be programmed into the system. The constants that must be input into the Z boxes are:

- Acceleration Calibration Constant
- Drive
- Offset

Steps to input the calibration settings in the SSPM4 are as follows:

- Connect ISBM system to computer with serial cable
- Cycle system to "Comm1" mode on Snap Shock Plus
- Open sv32 program
- Select "Calibration" tab → "Set Cal"
- Input factors in the Z-axis boxes for:
    - "Offset"
    - "Drive"
    - "Accel Calibration Constants"
- Click "OK"

A.2.1 Offset

The offset value recommended by Holloway is 128 counts (Holloway, p. 16).

A.2.2 Drive

The output of the BDI transducer, i.e., a tensile or compressive strain, is a voltage. The drive number sets the full-scale range (in mV), and therefore resolution (in mV), of the Snap Shock Plus data acquisition unit (Holloway, p. 12). The smaller the drive number the larger the full-scale and the larger the resolution. “It is recommended to use a full-scale that will be as close to the anticipated maximum strain reading as possible, in order to have the greatest resolution” (Holloway, p. 16). A drive number of 220 was used between 11/2009 and 12/2010 and a drive number of 238 was used between 2/2011 and 4/2011. The resolutions corresponding to drive numbers are provided in Appendix A of Holloway’s thesis.

A.2.3 Acceleration Calibration Constant (ACC)

The SSPM4 was designed to record acceleration events so all inputs and units are in terms of acceleration. The ACC factor converts events into units of microstrain for the purposed of this project. Events read by the BDI transducer are recorded as a certain number of analog-to-digital “counts.” The voltage is converted into counts using the Transducer Calibration Factor (TCF) which is specified for each transducer by the manufacturer in units of με/mV (Holloway, p. 13). The value in counts is then converted into a strain (in microstrain, με) using the ACC determined prior to system activation. The ACC was originally calculated in Holloway’s thesis by dividing the Calibration Constant, which is a ratio of the full scale in counts (1280 cts.) to the full scale in mV, by the TCF. During Brookes’ research the ACC was determined using a shunt calibration procedure. The determination of the ACC for this research is described in the sections that follow.

A.2.3.1 Shunt Calibration Method

The ACC was initially determined for this research using the shunt calibration process described by Brookes (Brookes, p. 29). This value was calculated as 2.371 cts/με and was used during the monitoring of several bridges between 10/2009 and 7/2010. The following method uses a simulated strain reading (shunt) to calibrate the system:

1. Connect ISBM system to computer with serial cable
2. Cycle system to "Comm1" mode on Snap Shock Plus
3. Open sv32 program
4. "Calibration" tab → "Get Z Counts", record as z_o. This number should be within 768 cts of 2048 cts.
5. Flip Shunt switch on
6. "Calibration" tab → "Get Z Counts", record as z_s. This is the simulated recording of a 125 με event in counts.
7. Calculate the ACC in cts/με:

$$\mathrm{ACC} = \frac{(z_s - z_o)}{125\ \mu\varepsilon}$$

A.2.3.1.1 Calibration Factor Determined (11/12/2009)

Before the system was deployed for the first time during this research a shunt calibration was completed to determine the ACC. The result was factored in order to get recorded strains to be consistent with BDI readings. The following steps were using to determine the factor:

1. Weight applied to transducer
2. 104.4 με recorded from BDI unit
3. Shunt calibration:
   - z_o = 1938 cts
   - z_s = 2320 cts
   - $\frac{(2320-1938)}{125}$ = 3.056 cts/με

4. 3.05 input as ACC
5. ISBMS records a strain of 81 με
6. Shunt calibration value factored:
   - $\frac{81\mu\varepsilon}{104.4\mu\varepsilon} * 3.056$ cts/με = 2.371 cts/με
7. 2.37 input as ACC
8. ISBMS records a strain of 105 με

While using the calculated ACC during monitoring, the system filled up with events quickly (usually in less than one week.) In addition, a distinct shift of the histogram plots could be observed when comparing the new data to data collected in the past. Since the ISBMS seemed to be recording events at a higher strain level than actual strains should have been, the ACC was revisited.

A.2.3.2 BDI Calibration Method

Since the shunt calibration method did not produce an accurate ACC factor an alternative calibration method was used (Figure A.1). Using this approach, a known weight was hung from the BDI transducer and the induced strain was recorded using a BDI Structural Testing System (STS). The strain was then recorded using the SSPM4. From this data the ACC was determined.

A known weight was hung from the transducer by clamping a rod to a table and sliding the transducer onto the rod using the circular hole closest to the wire connection (Figure A.2). Copper wire was used to hang the weight on the transducer through the other hole. The steps for calculating the ACC are as follows:

1. With the transducer connected to the STS, record BDI unit strain reading, ε_0, of transducer without weight
2. Apply weight to transducer and record strain, ε_1, using the BDI STS unit
3. Take difference of strain readings (ε_1 - ε_0) to determine true strain reading, ε

4. Remove weight
5. Connect transducer to ISBMS
6. “Calibration” tab → “Get Z Counts”, this is the value for z_o
7. Place weight on transducer again
8. “Calibration” tab → “Get Z Counts”, this is the value for z_1
9. Calculate the ACC in cts/με:
   - $\mathrm{ACC} = \frac{(z_1 - z_o)}{\varepsilon}$

Figure A.1: Set-up for calibration

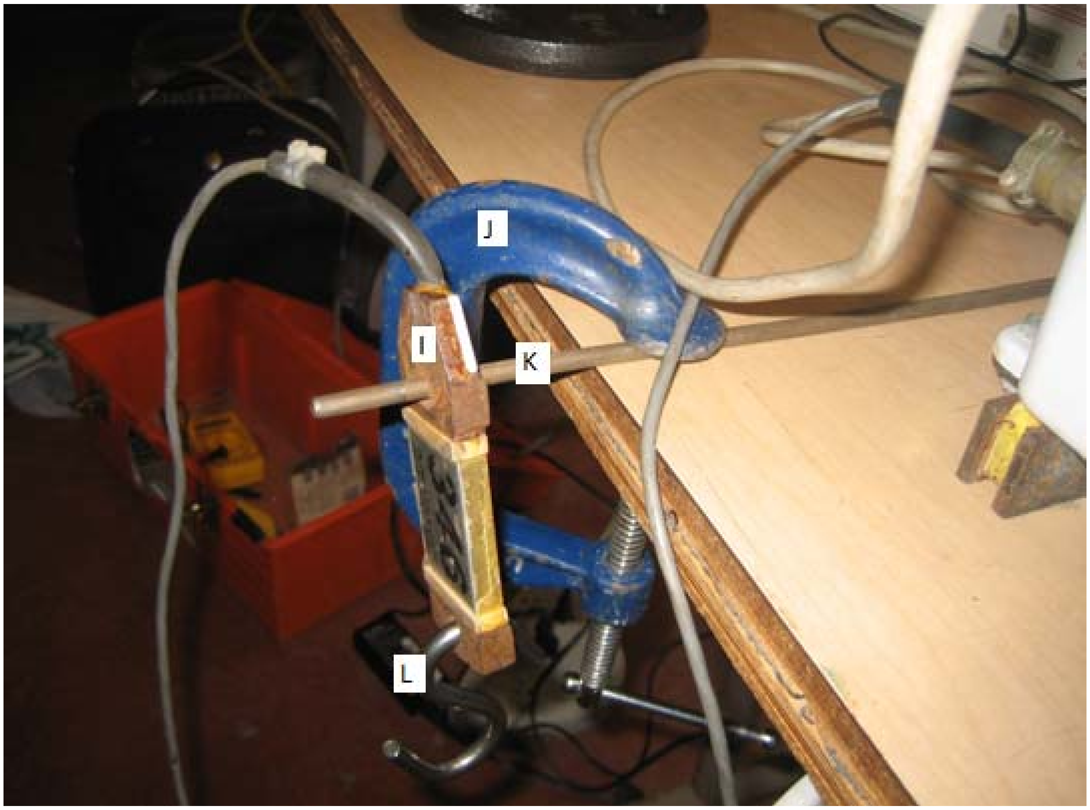

Figure A.2: Transducer set-up for calibration

Items of interest in Figure and Figure:

A. BDI Structural Testing Unit
B. BDI Transducer Connector
C. Three transducers
D. ISBMS
E. USB to Serial Port Cable
F. Computer
G. Trigger
H. Known weight with copper wire
I. Transducer being used with ISBMS
J. Clamp
K. Steel Rod
L. Hook

A.2.3.2.1 Calibration Factor Determined (8/26/2010)

The following steps produced the initial revised ACC:

1. A known weight was hung from four transducers and the strains were recorded using a BDI unit
2. The average strain for the four transducers was calculated. The "standard" strain:
   - ε = 138.8 $\mu\varepsilon$.
3. For gauge 346:
   - z_o = 1995 cts
   - z_1 = 2422 cts
   - ACC = 3.076 cts/$\mu\varepsilon$
4. 3.07 input for calibration factor
5. ISBMS records an average strain of 141.8 $\mu\varepsilon$ for the weight

Strain data already collected using the initial ACC was multiplied by the quotient of the initial factor (2.371) and the revised factor (3.076), 0.77, to correct the offset. This calibration factor was used between 10/2010 and 12/2010.

A.2.3.2.2 Calibration Factor Determined (2/2/2011)

After an electronic failure, the system was sent to the manufacturer for repairs. After it came back recalibration was necessary. The following steps were used to recalibrate:

1. A five pound weight was hung from BDI strain transducer 346
2. Strain for weight was recorded using BDI unit:
   - ε = 155 $\mu\varepsilon$
3. For gauge 346:
   - z_o = 2097 cts
   - z_1 = 3034 cts
   - ACC = 6.046 cts/$\mu\varepsilon$
4. 6.05 input for calibration factor

5. ISBMS records strains between 151 με and 156 με for the five pound weight

It should be expected that the same ACC would be produced during the 2/2/2011 calibration as the 8/26/2010 calibration since the same procedure is being employed and the same BDI transducer is being used. The large increase in the value of the ACC is due to the modified drive value after repair of the SSPM4. The full-scale was almost halved; consequently the ACC is almost doubled. This ACC (6.05) was used for the remainder of the project.

A.3 Programming

As explained earlier the ISBMS must be programmed prior to deployment in order to collect data. ISBMS programming details have been previously provided (Brookes, pp. 24-27). Steps to program the system for deployment for this research are as follows:

1. Connect ISBMS to computer with serial cable
2. Cycle ISBMS to “Comm1”
3. Open sv32 program
4. “Actions” tab → “Set RCPs”
5. “Trigger” tab
6. “Acceleration Z” box → input trigger threshold in microstrain
7. “Velocity Change Z” box → input 0
8. “Filter” tab
9. Cutoff → slide to 10Hz (min)
10. Click “OK”
11. “Actions” tab → “Set Time”
12. “Actions” tab → “Send RCPs”
13. Cycle system to “Standby”

Note: Programming selections will reset if the 9-volt battery is removed

A.4 Deployment

The system was only deployed on steel bridges. The following items are needed for installation on a bridge:

- ISBMS (SSPM4, BDI strain transducer and batteries)
- Two c-clamps
- Voltmeter

Before deployment the voltage of the batteries is checked with the voltmeter and recorded. Field installation details have been previously provided (Brookes, pp. 27, 28). Steps to install the system for this research are as follows:

1. Attach ISBMS to beam web using magnets on back of box
2. Connect BDI gauge to ISBMS
3. Attach strain transducer to flange of beam using one c-clamp at each end
4. Zero the system:
    - Insert voltmeter prongs between S+ and S- terminals in ISBMS to measure voltage
    - Unlock Null Pot (turn lock switch counterclockwise)
    - Adjust Null Pot until voltage reading is 0.000
    - Lock Null Pot (turn lock switch clockwise)
5. Cycle ISBMS to "Active"
6. Check that ISBMS is in "Active" mode
7. Fill initial information into the ISBM form

A.5 Retrieval and Data Acquisition

Details regarding retrieving data from the field have been previously provided (Brookes, pp. 29-32). Steps to retrieve the data for this research are as follows:

1. Check ISBMS mode – "Active" or "Standby"
2. Cycle ISBMS to "Standby" if still in "Active" mode
3. Disconnect ISBMS from beam

4. Connect ISBMS to computer
5. Cycle to “Comm1”
6. Open sv32 program
7. “Actions” tab → “Get Data”
8. Name and save data file

The voltage of the batteries used during monitoring is checked and timeline and histogram plots are generated. Note that data can be copied and pasted into Excel from the sv32 program At this point the ISBM form may be completed.

A.6 ISBMS Issues

As previously mentioned, at one point during the course of this project the ISBMS was unable to communicate which made it impossible to program or collect data. When the unit is unable to communicate with a computer the following message pops up: “The unit is not responding! Check connection, com mode, and battery life. You may need to cycle the unit.” After extensive examination, it was determined that this issue was related to a hardware malfunction and the SSPM4 unit was sent to IST for repairs. The problem was related to a defective chip in the RS232 connector which allows the unit to communicate with a serial cable. The chip was replaced and the ISBMS communicated without issue for the remainder of this project.

Another issue related to unit deactivation. During five monitoring periods the ISBMS deactivated even though the memory had not been filled and sufficient battery life remained in both the 6- and 9-volt batteries. The number of events was too low on four of the monitoring periods to be usable for this research. One possible explanation may be a communication device on trucks that causes the

ISBMS to cycle to the “Standby” mode. This issue was not resolved at the conclusion of this research.

Appendix B

LOAD RATING RATIO DERIVATION AND PROOF

A ratio is calculated and used in Section 5.5 and Section 5.6 to determine the load rating at the critical location based on the in-service data. This appendix derives and proves the ratio. Subscript “M” denotes values corresponding to the location where the ISBMS recorded data and subscript “C” denotes values corresponding to the critical location on the bridge as shown in Figure B.1. The different variables used for the derivation are displayed in Table B.1.

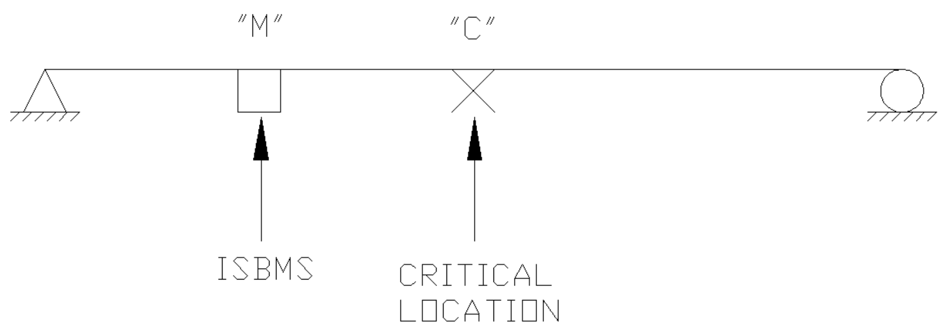

Figure B.1: Placement of ISBMS at a non-critical location on a bridge

Table B.1: Load rating ratio derivation variables

	Measured Location	Critical Location
Measured Live Load (HS20 or Governing)	LL_{MM}	LL_{MC}
Theoretical Live Load	LL_{TM}	LL_{TC}
Factored Resistance – Factored Dead Load	$(\varphi R_n - \gamma_D DL)_M$	$(\varphi R_n - \gamma_D DL)_C$
Rating Factor (RF)	$RF_M = \frac{(\varphi R_n - \gamma_D DL)_M}{\gamma_L LL_{TM}}$	$RF_C = \frac{(\varphi R_n - \gamma_D DL)_C}{\gamma_L LL_{TC}}$
In-Service Rating Factor (ISRF)	$ISRF_M = \frac{(\varphi R_n - \gamma_D DL)_M}{LL_{MM}}$	$ISRF_C = \frac{(\varphi R_n - \gamma_D DL)_C}{LL_{MC}}$

where,

- LL_{MM} is the maximum applied live load, in terms of moment or stress, projected from the strains recorded at the location of the ISBMS
- LL_{MC} is the maximum applied live load, in terms of moment or stress, projected from the strains recorded at the critical location
- LL_{TM} is the theoretical live load at the measured location
- LL_{TC} is the theoretical live load at the critical location
- γ_L is the live load factor
- φR_n is the factored resistance at the given location, calculated by BRASS
- $\gamma_D DL$ is the factored dead load at the given location, calculated by BRASS

Assume: $\frac{LL_{MC}}{LL_{MM}} = \frac{LL_{TC}}{LL_{TM}} \rightarrow LL_{MC} = \frac{LL_{TC}}{LL_{TM}} \cdot LL_{MM}$

$$\frac{RF_M}{RF_C} = \frac{\frac{(\varphi R_n - \gamma_D DL)_M}{\gamma_L LL_{TM}}}{\frac{(\varphi R_n - \gamma_D DL)_C}{\gamma_L LL_{TC}}} = \frac{LL_{TC}}{LL_{TM}} \cdot \frac{(\varphi R_n - \gamma_D DL)_M}{(\varphi R_n - \gamma_D DL)_C}$$

let $\frac{(\varphi R_n - \gamma_D DL)_M}{(\varphi R_n - \gamma_D DL)_C} = \alpha$

$$\frac{RF_M}{RF_C} = \frac{LL_{TC}}{LL_{TM}} \cdot \alpha \rightarrow \frac{LL_{TC}}{LL_{TM}} = \frac{1}{\alpha} \cdot \frac{RF_M}{RF_C}$$

$$\therefore\ LL_{MC} = \frac{1}{\alpha} \cdot \frac{RF_M}{RF_C} \cdot \mathrm{LL_{MM}}$$

$$\therefore ISRF_C = \frac{(\varphi R_n - \gamma_D DL)_C}{\frac{1}{\alpha} \cdot \frac{RF_M}{RF_C} \cdot \mathrm{LL_{MM}}} = \alpha \cdot \frac{RF_C}{RF_M} \cdot \frac{(\varphi R_n - \gamma_D DL)_C}{\mathrm{LL_{MM}}}$$

and $ISRF_C = \alpha \cdot \frac{RF_C}{RF_M} \cdot \frac{(\varphi R_n - \gamma_D DL)_M}{\alpha \cdot LL_{MM}} = \frac{RF_C}{RF_M} \cdot \frac{(\varphi R_n - \gamma_D DL)_M}{LL_{MM}}$

$$\boxed{ISRF_C = \frac{RF_C}{RF_M} \cdot ISRF_M}$$

Appendix C

ISBM FORMS

An ISBM Form template was created during the course of this project to facilitate the recording of a monitored bridge's characteristics and the in-service data collected on it. The form includes spaces to fill in general information about the bridge, general information relating to monitoring, the location of the strain transducer, and a summary of the in-service data collected on it. A plan of the bridge along with a cross-section of the span being monitored and a detail of the instrumented girder are provided for transducer location clarity. Finally, the timeline and histogram plots based on the in-service data are displayed on a second sheet.

Descriptions of items on the form:

Bridge Number: the identifying number designated to the bridge

Facility Carried: the roadway that the bridge supports

Facility Crossed: the roadway or waterway that the bridge crosses over

Span Monitored: the number of the span (if there are more than one) being monitored

Span Length: the length of the span being monitored

Gauge Location: the number of the girder where the transducer is located and where on the girder it is located, i.e. bottom flange (BF)

Flange Location: the girder centerlines that the transducer is located between

Date Activated: the date that the ISBMS began collecting data

Temp. at Act. (°F): the temperature of the area around the bridge at activation

Last Monitored: the month and year that the ISBMS was last used on the bridge (if applicable)

Date Retrieved: the date that the ISBMS was removed

Log. Stat. at Ret.: the status of the ISBMS data logger at retrieval – Active or Standby

Date Deactivated: the date that the ISBMS stopped collecting data

Days Monitored: the number of days that the ISBMS collected data

Trigger Level (με): the trigger level that is input into the ISBMS prior to deployment

Num. Events: the number of events that the ISBMS recorded during the monitoring period

Max Event (με): the maximum event that the ISBMS recorded during the monitoring period

Avg. Event (με): the average event that the ISBMS recorded during the monitoring period

Battery Voltage: the voltage of the 9V and 6V batteries before and after deployment

Access: equipment and support needed to access the bridge

Notes: general notes specific to the particular bridge

Sensor #: the identifying number designated to the strain transducer used during monitoring period

Drive #: the drive number set for the ISBMS relating to the ISBMS's resolution availability

Cal. Factor: the calibration factor set for the ISBMS during monitoring period

IN-SERVICE BRIDGE MONITORING RECORD

Bridge Number	1-781	**Date Retrieved**	12/08/09
Facility Carried	I-95 N	**Log. Stat. at Ret.**	Active
Facility Crossed	Silverside Rd	**Date Deactivated**	12/08/09
Span Monitored	1	**Days Monitored**	20.9
Span Length	32'-0"	**Trigger (με)**	35
Gauge Location	G10, BF	**Num. Events**	3,889
Flange Location	G10/G11	**Max Event (με)**	120.66
Date Activated	11/17/09	**Avg. Event (με)**	42.77
Temp. at Act. (°F)	N/A		
Last Monitored	9/2007		

Battery Voltage:	Deployed	Retrieved
6V	N/A	N/A
9V	N/A	N/A

Bridge Sketch

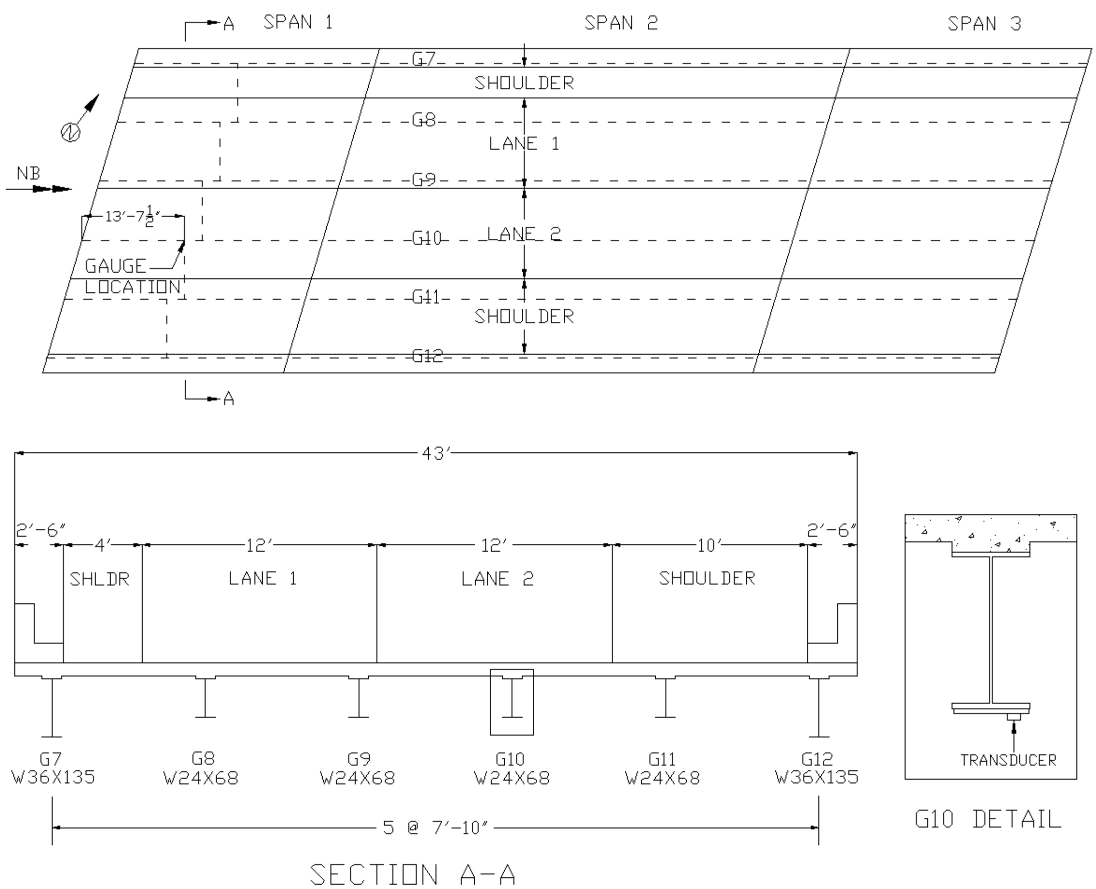

16’ ladder from slope to diaphragm.

Acces s					
Notes	Gauge placed on bottom of flange cover plate located on bottom of BF.				
Sensor #	346	**Drive #**	220	**Cal. Factor**	2.37

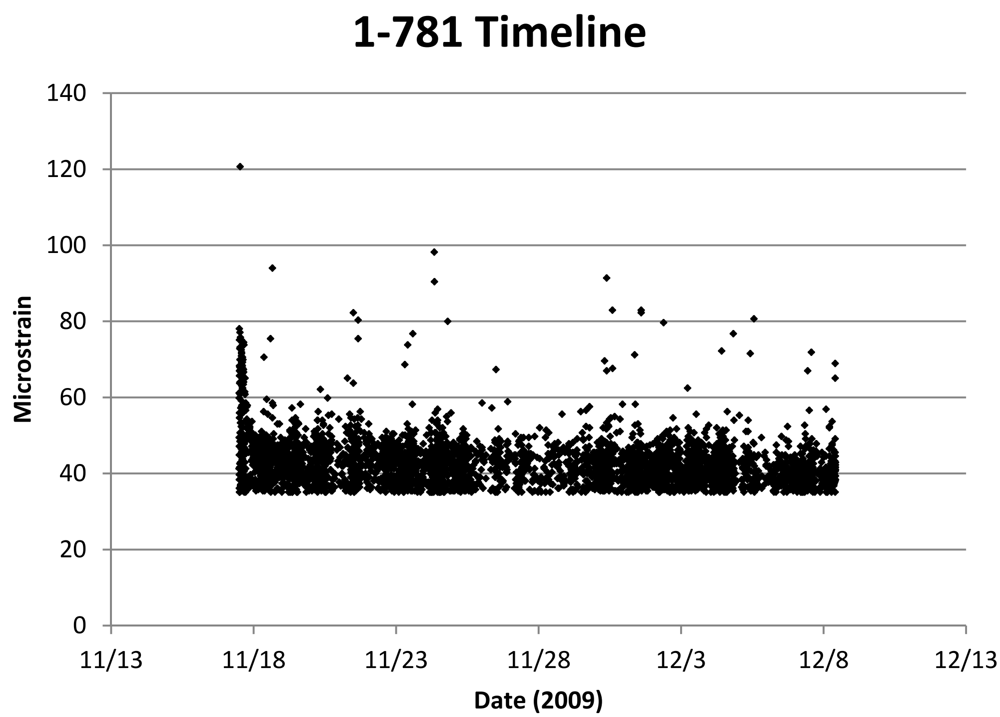
1-781 Timeline
Microstrain
140
120
100
80
60
40
20
0
11/13
11/18
11/23
11/28
12/3
12/8
12/13
Date (2009)

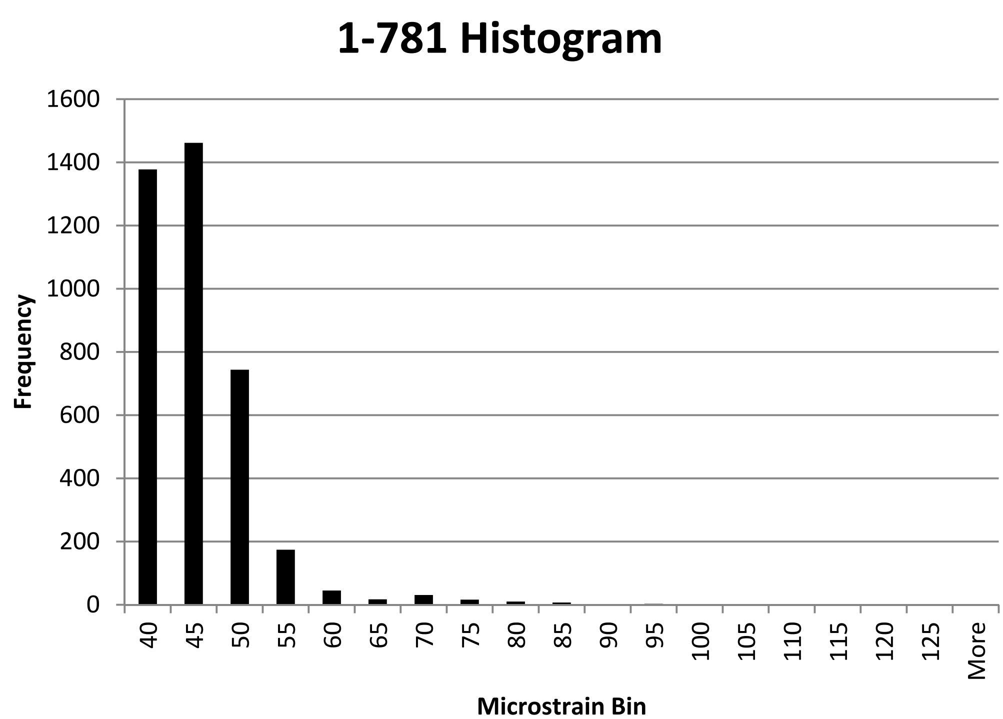
1-781 Histogram
Frequency
1600
1400
1200
1000
800
600
400
200
0
40
45
50
55
60
65
70
75
80
85
90
95
100
105
110
115
120
125
More
Microstrain Bin

IN-SERVICE BRIDGE MONITORING RECORD

Bridge Number	1-728	**Date Retrieved**	12/22/09
Facility Carried	I-295 N	**Log. Stat. at Ret.**	Standby
Facility Crossed	US-13 S	**Date Deactivated**	12/19/09
Span Monitored	1	**Days Monitored**	8.9
Span Length	35'-3"	**Trigger (με)**	25
Gauge Location	G3, BF	**Num. Events**	807
Flange Location	G3/G4	**Max Event (με)**	77.08
Date Activated	12/10/09	**Avg. Event (με)**	36.79
Temp. at Act. (°F)	N/A		
Last Monitored	12/2007		

Battery Voltage:	Deployed	Retrieved
6V	N/A	2.7
9V	N/A	7.7

Bridge Sketch

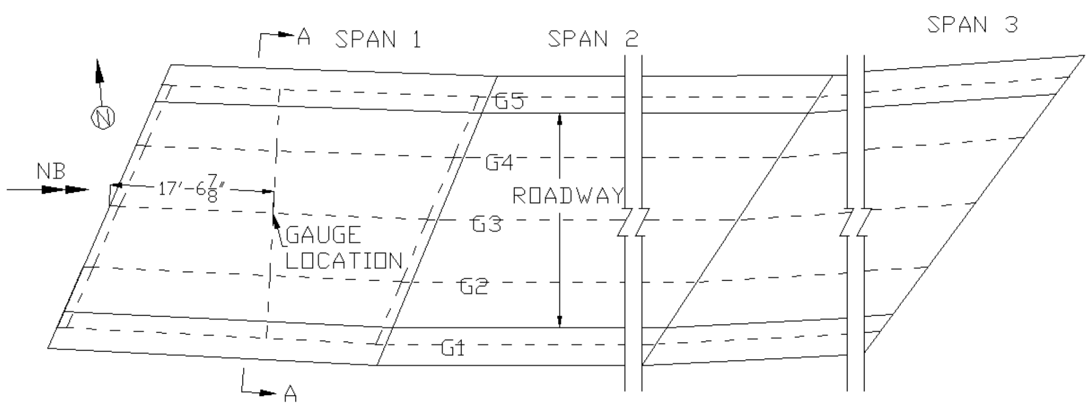

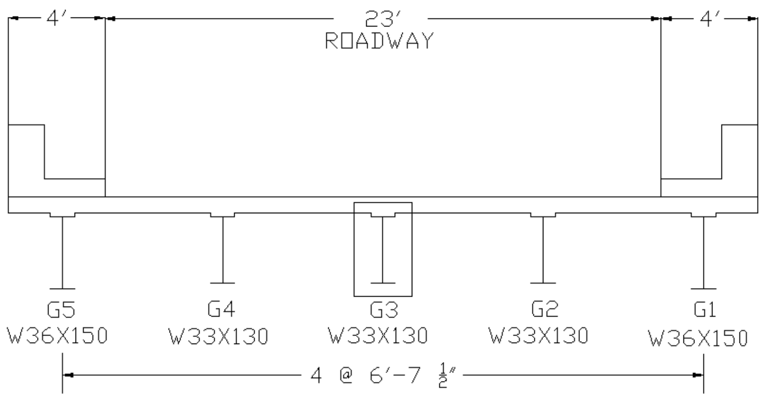

SECTION A-A

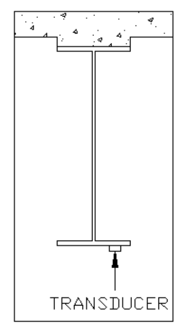

G3 DETAIL

Access	24' ladder from sidewalk to mid-span diaphragm.				
Notes	Located under an off-ramp to US-13N. Gauge deactivated during snowstorm.				
Sensor #	346	**Drive #**	220	**Cal. Factor**	2.37

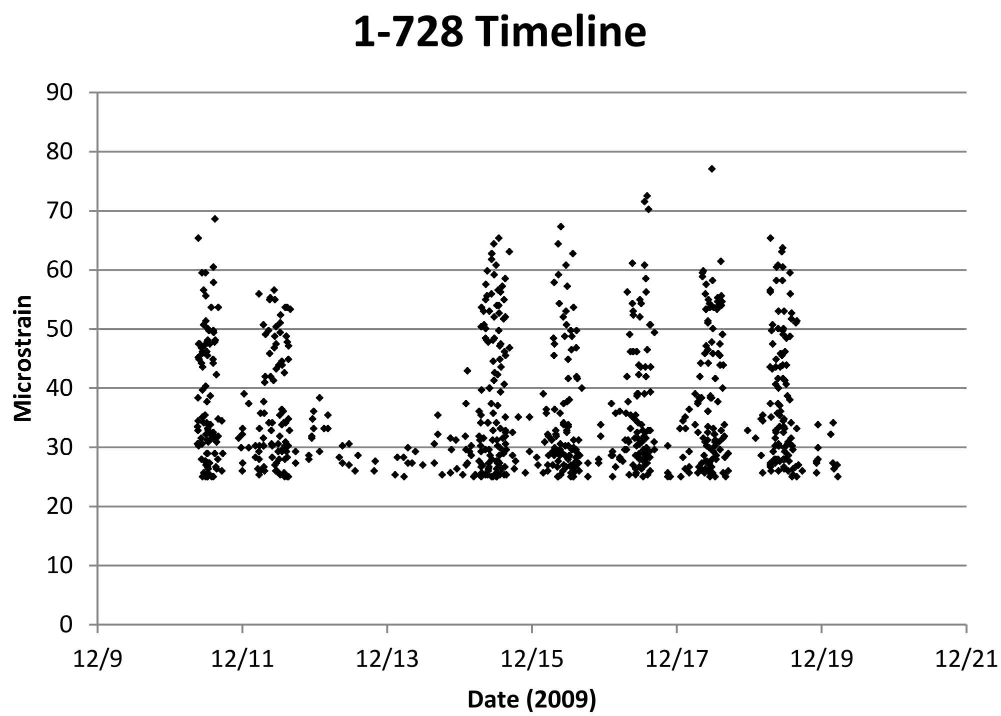
1-728 Timeline
90
80
70
60
50
40
30
20
10
0
Microstrain
12/9
12/11
12/13
12/15
12/17
12/19
12/21
Date (2009)

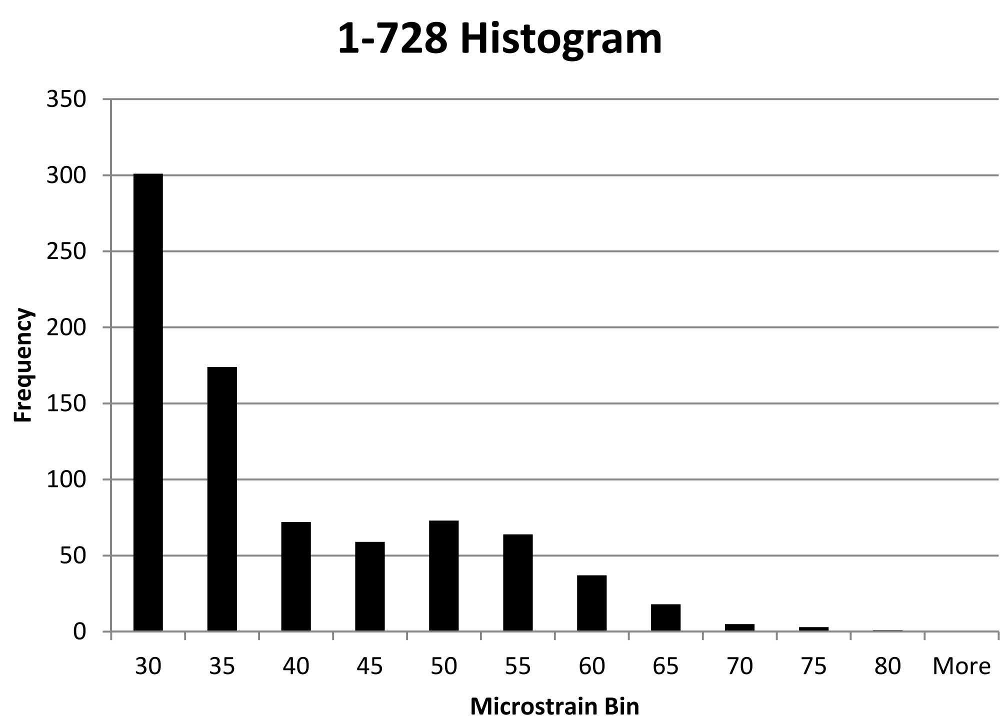
1-728 Histogram
350
300
250
200
150
100
50
0
Frequency
30
35
40
45
50
55
60
65
70
75
80
More
Microstrain Bin

IN-SERVICE BRIDGE MONITORING RECORD

Bridge Number	1-704	**Date Retrieved**	03/23/10
Facility Carried	I-95 S	**Log. Stat. at Ret.**	Active
Facility Crossed	Christina Creek	**Date Deactivated**	03/23/10
Span Monitored	3	**Days Monitored**	13.9
Span Length	25'-1 3/4"	**Trigger (με)**	55
Gauge Location	G6, BF	**Num. Events**	843
Flange Location	G5/G6	**Max Event (με)**	106.68
Date Activated	03/09/10	**Avg. Event (με)**	59.46
Temp. at Act. (°F)	50		
Last Monitored	6/2006		

Battery Voltage:	Deployed	Retrieved
6V	6.27	2.55
9V	9.31	8.23

Bridge Sketch

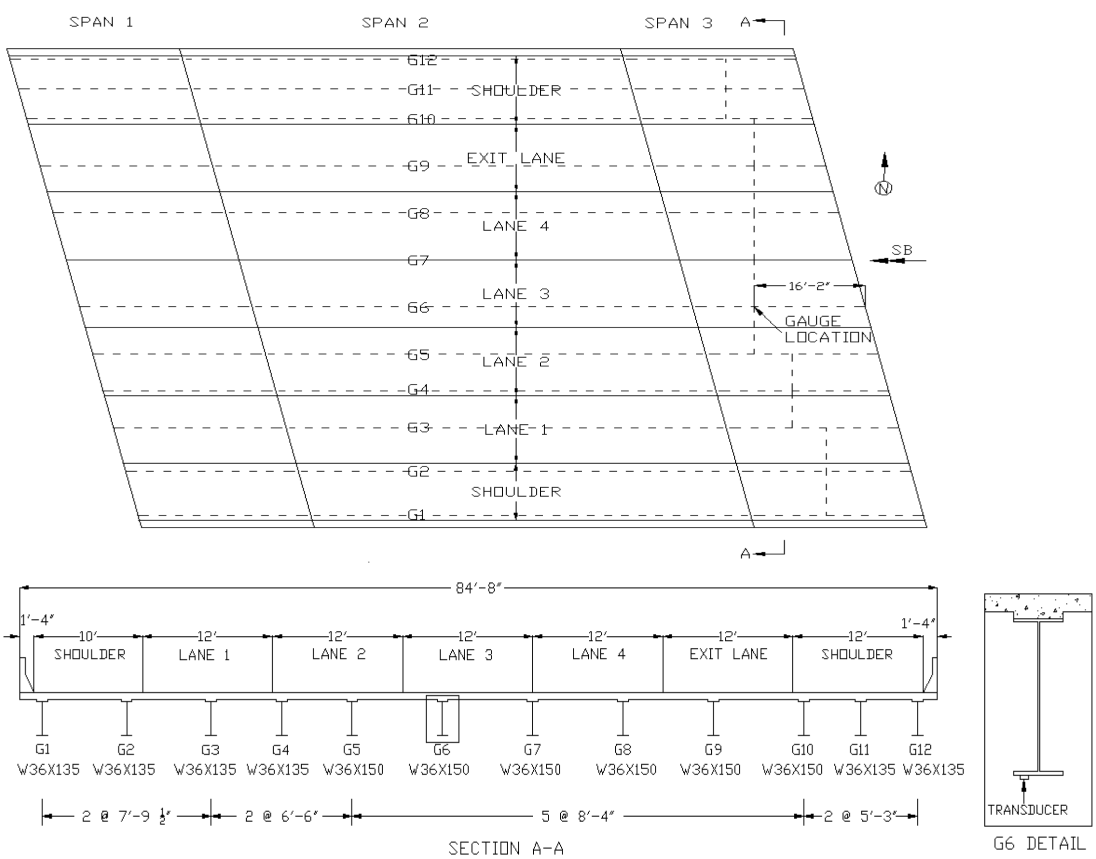

Access	16’ ladder from bank of creek to diaphragm.				
Notes	No events recorded after 3/19/2010.				
Sensor #	346	**Drive #**	220	**Cal. Factor**	2.37

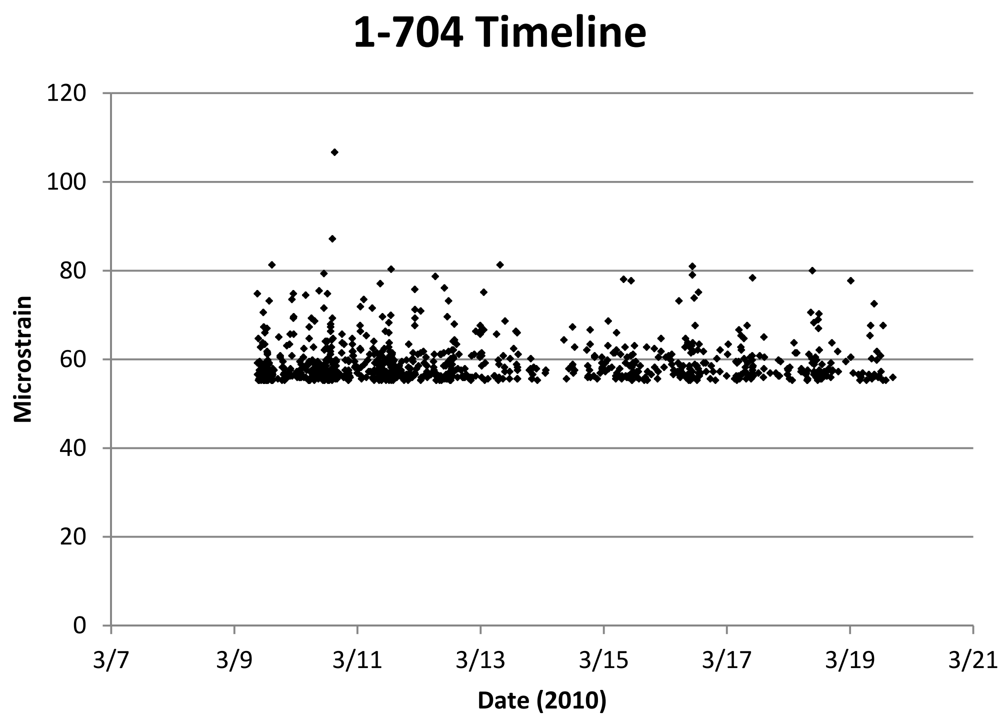
1-704 Timeline
Microstrain
120
100
80
60
40
20
0
3/7
3/9
3/11
3/13
3/15
3/17
3/19
3/21
Date (2010)

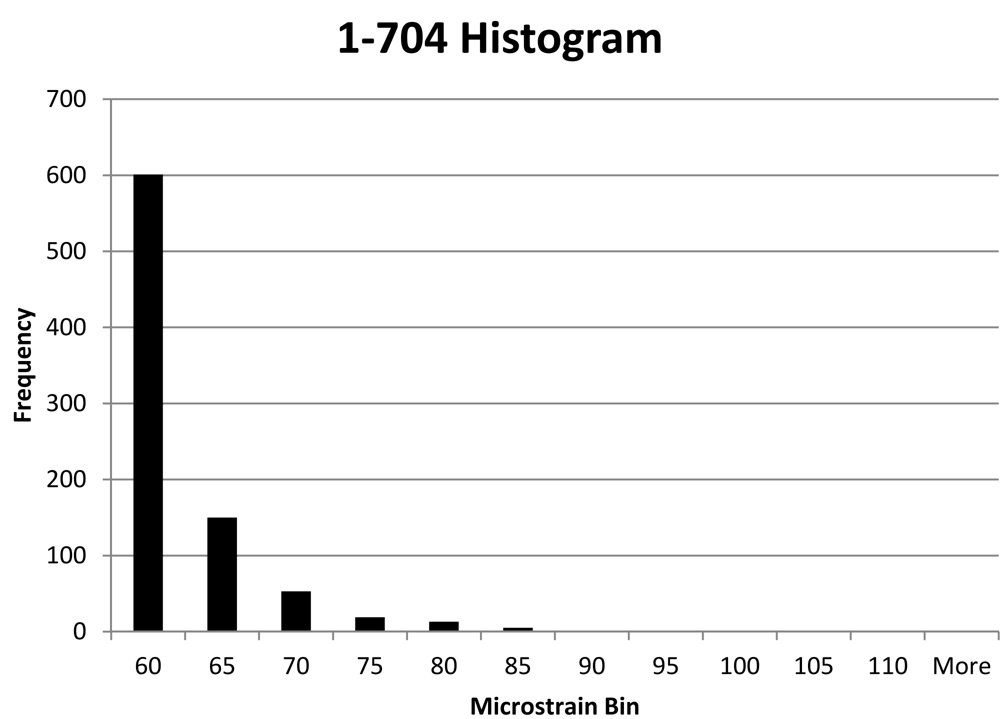
1-704 Histogram
Frequency
700
600
500
400
300
200
100
0
60
65
70
75
80
85
90
95
100
105
110
More
Microstrain Bin

IN-SERVICE BRIDGE MONITORING RECORD

Bridge Number	1-826 S	**Date Retrieved**	06/04/10	
Facility Carried	I-495 S	**Log. Stat. at Ret.**	Standby	
Facility Crossed	Stoney Creek	**Date Deactivated**	05/26/10	
Span Monitored	3	**Days Monitored**	4.6	
Span Length	70'-0"	**Trigger (με)**	40	
Gauge Location	G4, BF	**Num. Events**	5163	
Flange Location	G4/G5	**Max Event (με)**	223.76	
Date Activated	05/21/10	**Avg. Event (με)**	58.15	
Temp. at Act. (°F)	82	**Battery Voltage:**	Deployed	Retrieved
Last Monitored	N/A	**6V**	6.39	3.53
		9V	9.85	8.92

Bridge Sketch

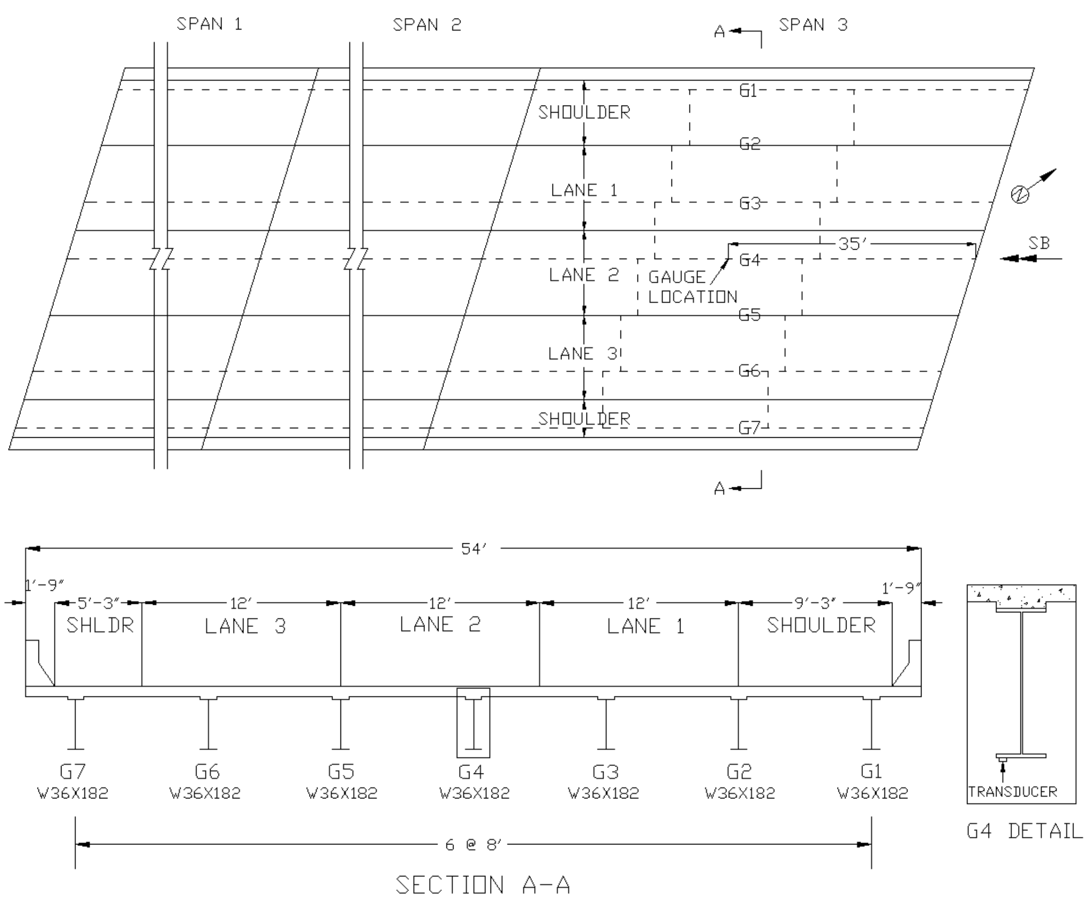

Acces No ladder required.

s

Notes	Low trigger level.				
Sensor #	346	**Drive #**	220	**Cal. Factor**	2.37

1-826 S Timeline

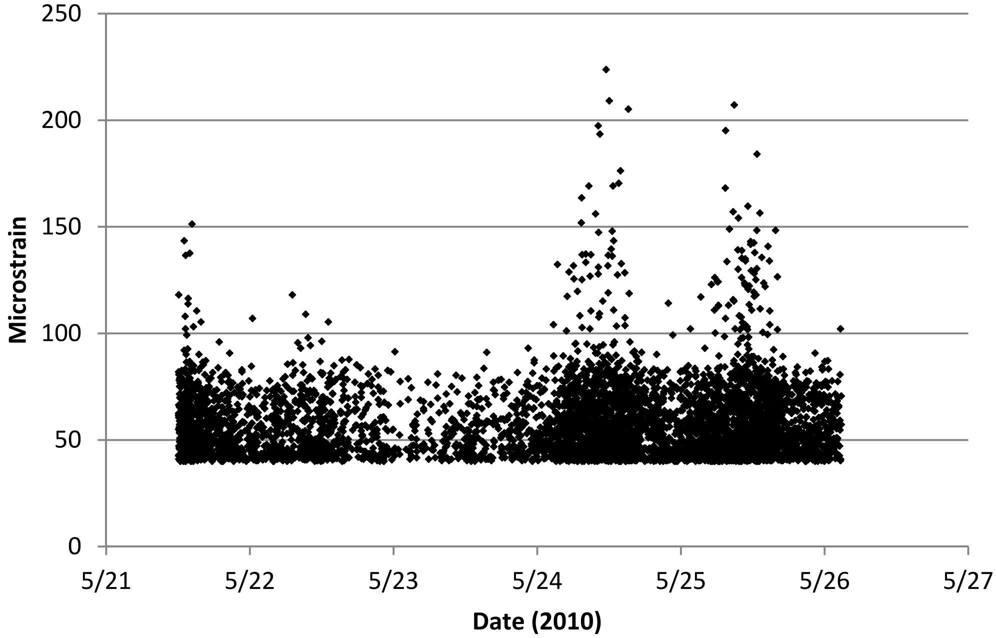

1-826 S Histogram

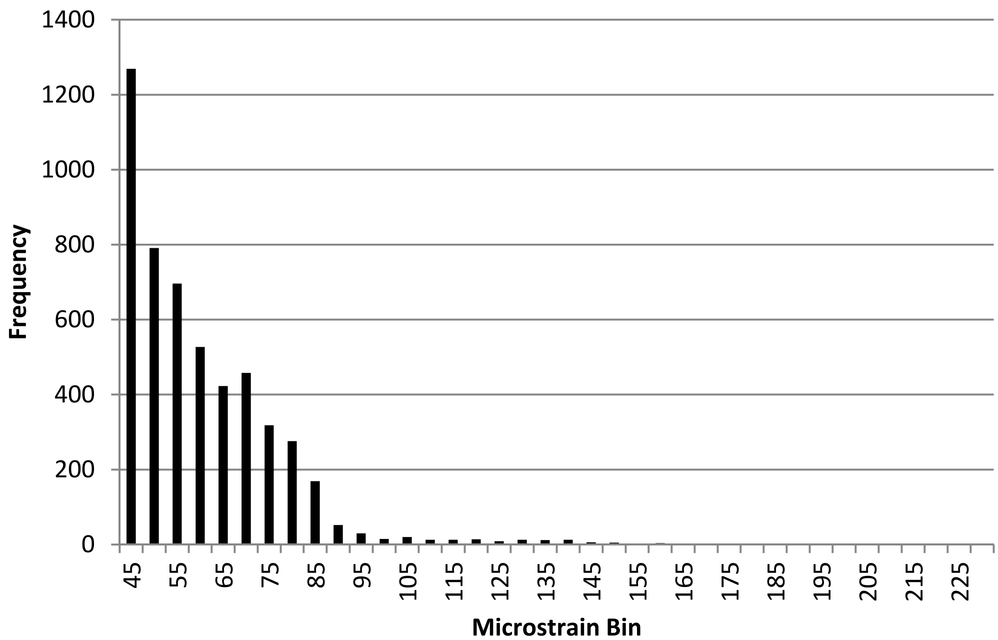

IN-SERVICE BRIDGE MONITORING RECORD

Bridge Number	1-262 S	**Date Retrieved**	06/24/10
Facility Carried	SR-4/SR-7 S	**Log. Stat. at Ret.**	Active
Facility Crossed	White Clay Creek	**Date Deactivated**	06/24/10
Span Monitored	1	**Days Monitored**	14.0
Span Length	90'-0"	**Trigger (με)**	35
Gauge Location	G3, BF	**Num. Events**	1294
Flange Location	G3/G4	**Max Event (με)**	123.26
Date Activated	06/10/10	**Avg. Event (με)**	49.56
Temp. at Act. (°F)	75		
Last Monitored	6/2006		

Battery Voltage:	Deployed	Retrieved
6V	6.45	3.52
9V	9.17	8.45

Bridge Sketch

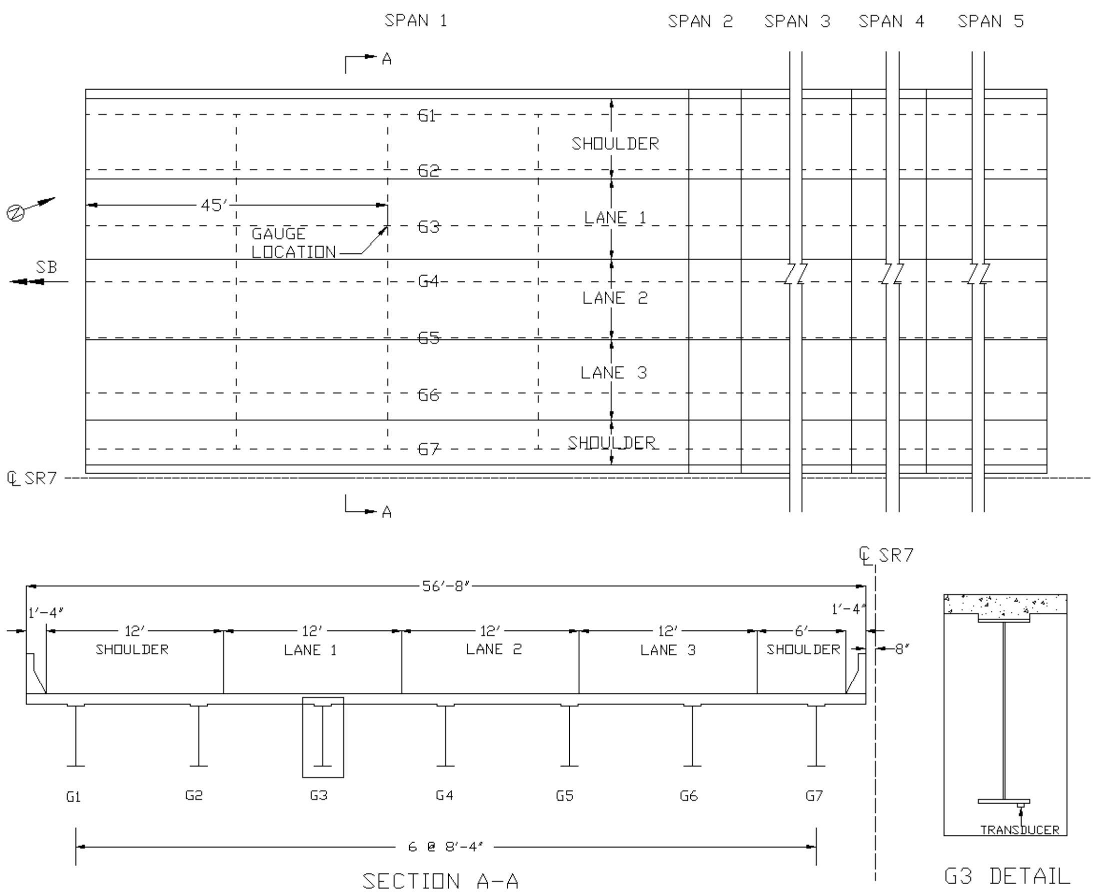

Acces 24' ladder used.

s

Notes	High trigger level.				
Sensor #	346	**Drive #**	220	**Cal. Factor**	2.37

1-262 S Timeline

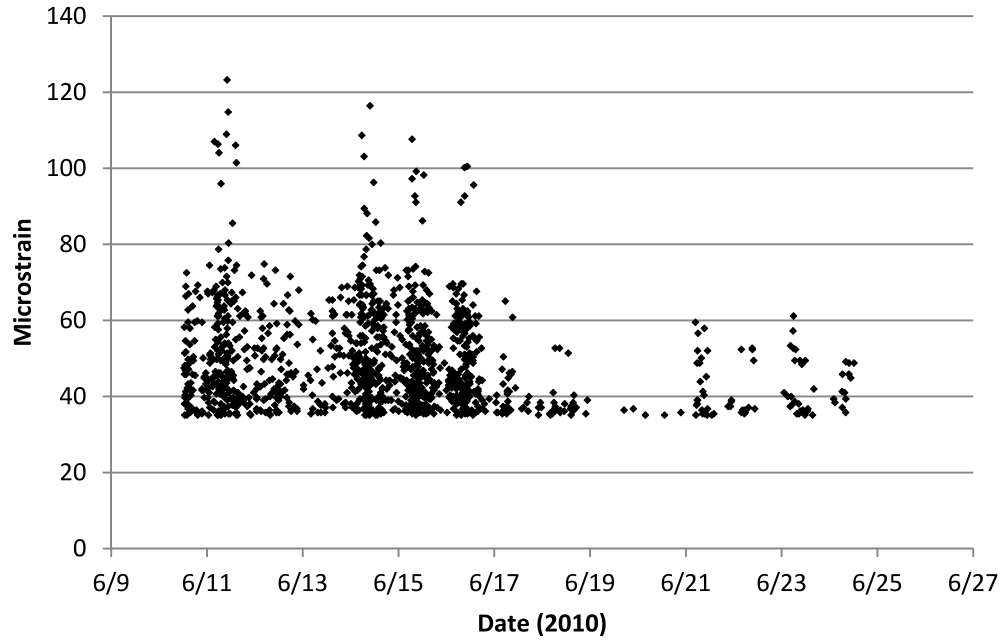

1-262 S Histogram

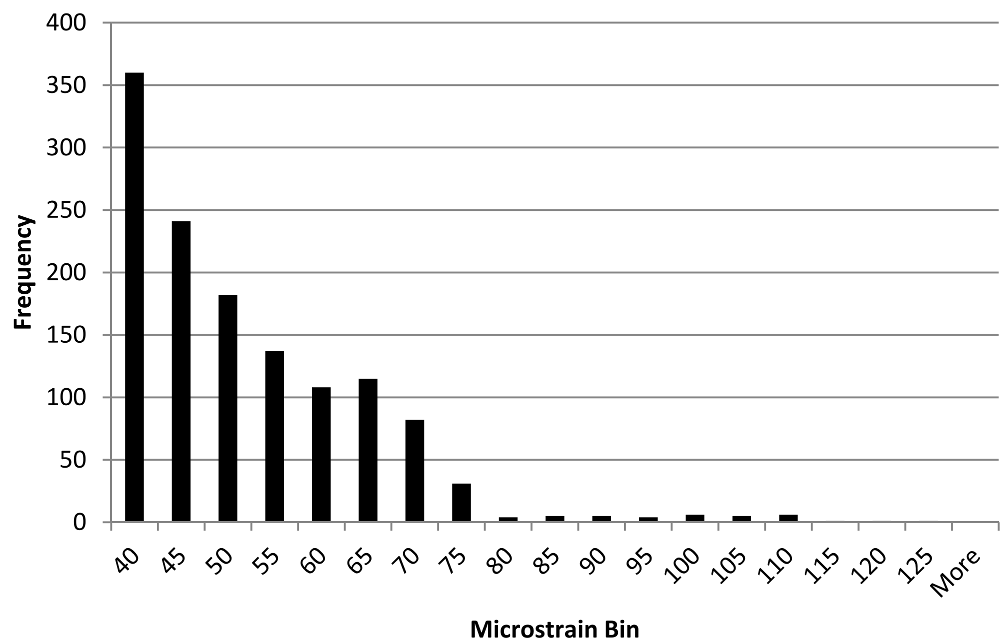

IN-SERVICE BRIDGE MONITORING RECORD

Bridge Number	1-826 N	**Date Retrieved**	07/08/10
Facility Carried	I-495 N	**Log. Stat. at Ret.**	Standby
Facility Crossed	Stoney Creek	**Date Deactivated**	06/29/10
Span Monitored	3	**Days Monitored**	4.9
Span Length	70'-0"	**Trigger (με)**	40
Gauge Location	G4, BF	**Num. Events**	5283
Flange Location	G4/G5	**Max Event (με)**	139.53
Date Activated	06/24/10	**Avg. Event (με)**	54.02
Temp. at Act. (°F)	94		
Last Monitored	5/2006		

Battery Voltage:	Deployed	Retrieved
6V	6.34	3.47
9V	8.59	6.75

Bridge Sketch

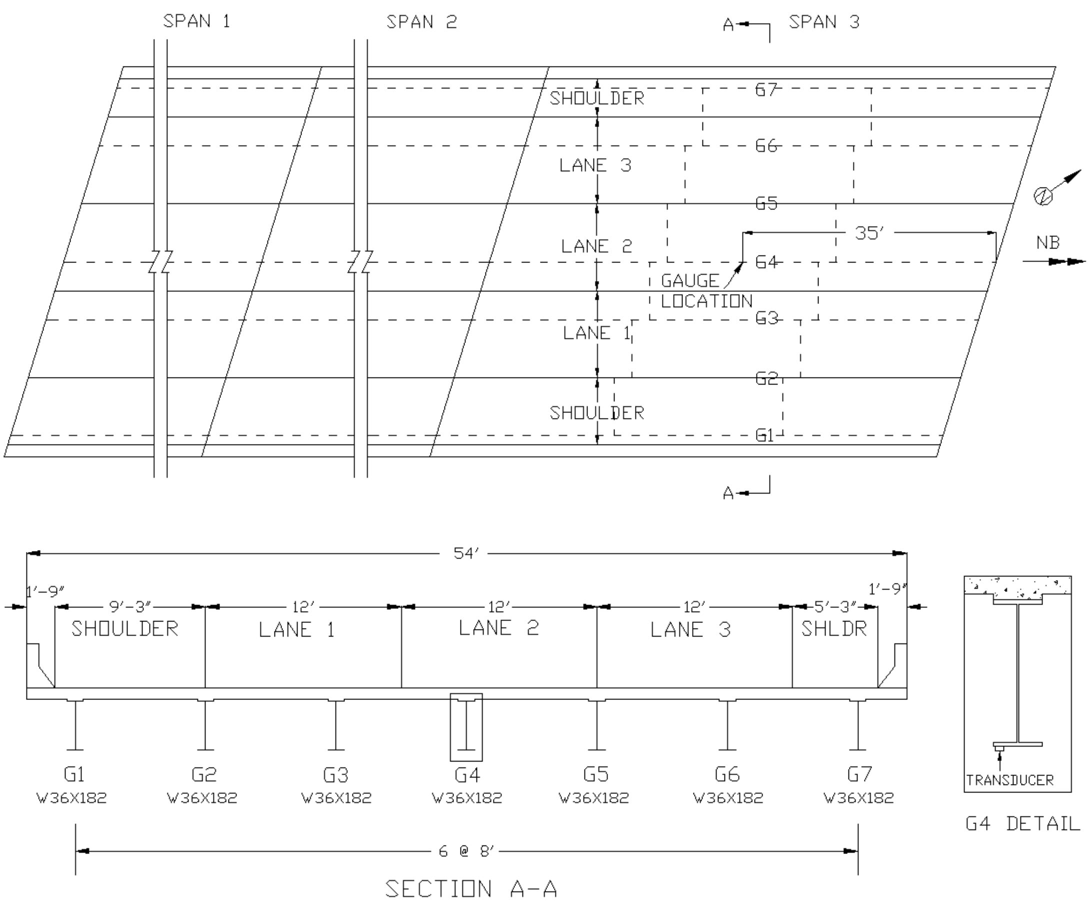

No ladder required.

Acces s					
Notes					
Sensor #	346	**Drive #**	220	**Cal. Factor**	

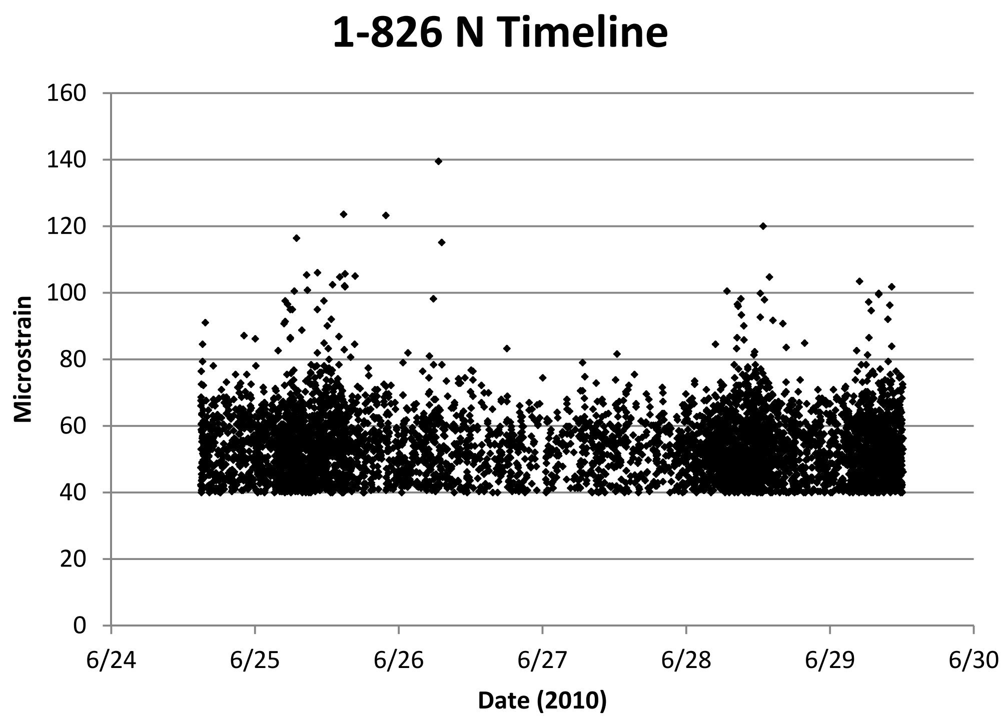
1-826 N Timeline
Microstrain
160
140
120
100
80
60
40
20
0
6/24
6/25
6/26
6/27
6/28
6/29
6/30
Date (2010)

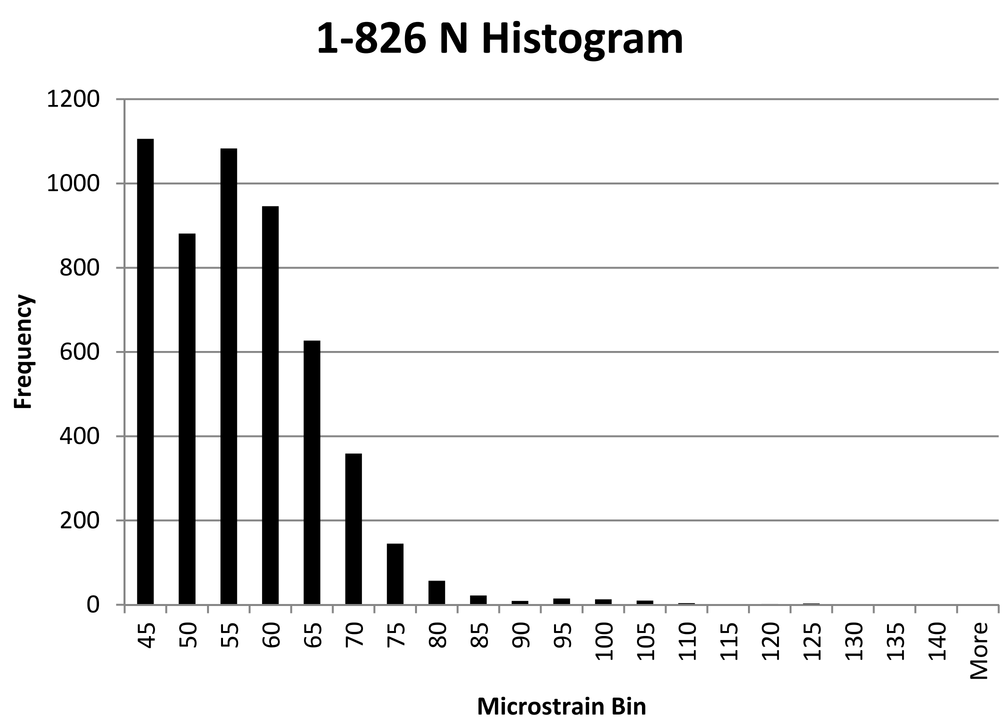
1-826 N Histogram
Frequency
1200
1000
800
600
400
200
0
45
50
55
60
65
70
75
80
85
90
95
100
105
110
115
120
125
130
135
140
More
Microstrain Bin

IN-SERVICE BRIDGE MONITORING RECORD

Bridge Number	1-911 S	**Date Retrieved**	07/22/10
Facility Carried	SR-1 S	**Log. Stat. at Ret.**	Standby
Facility Crossed	Black Diamond Rd	**Date Deactivated**	07/15/10
Span Monitored	1	**Days Monitored**	6.2
Span Length	65'-0"	**Trigger (με)**	55
Gauge Location	G3, BF	**Num. Events**	5100
Flange Location	G3/G4	**Max Event (με)**	187.66
Date Activated	07/09/10	**Avg. Event (με)**	72.86
Temp. at Act. (°F)	83		
Last Monitored	6/2007		

Battery Voltage:	Deployed	Retrieved
6V	6.3	3.66
9V	9.42	9.01

Bridge Sketch

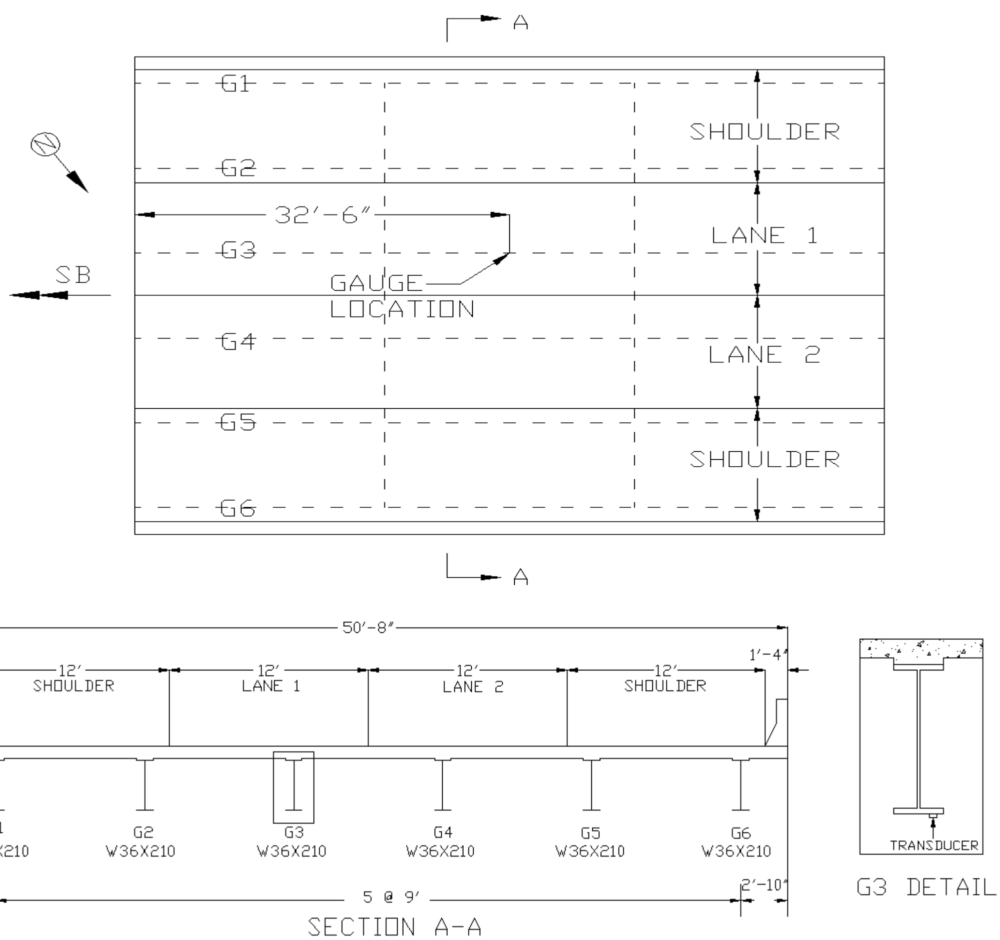

DelDOT provided bucket truck and traffic control.

Access Notes					
Sensor #	346	**Drive #**	220	**Cal. Factor**	2.37

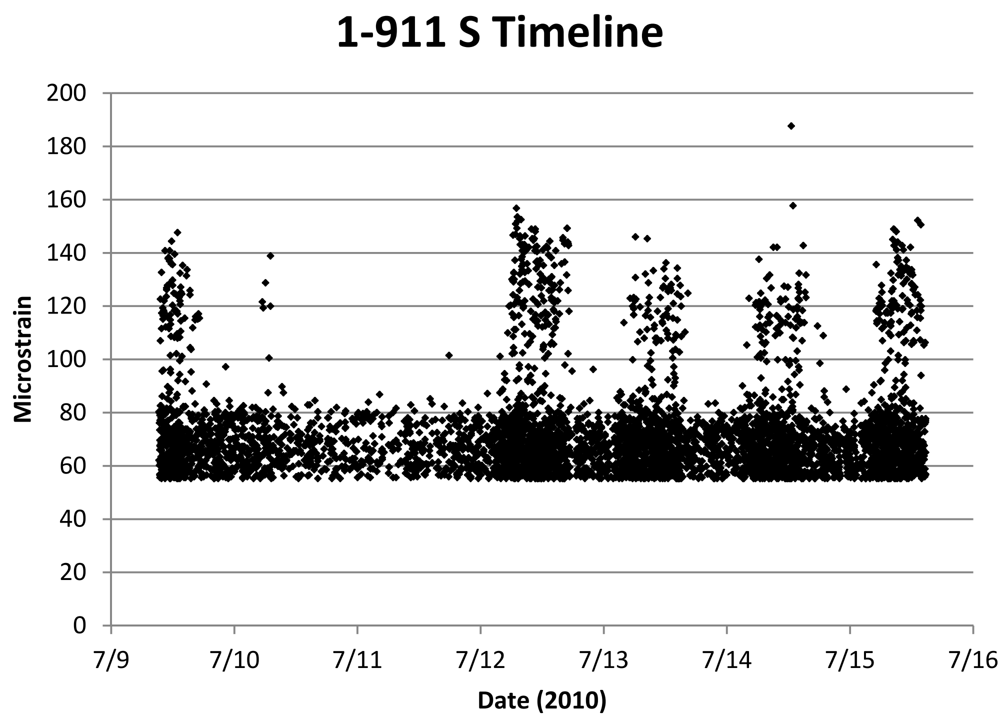
1-911 S Timeline
200
180
160
140
120
100
80
60
40
20
0
Microstrain
7/9
7/10
7/11
7/12
7/13
7/14
7/15
7/16
Date (2010)

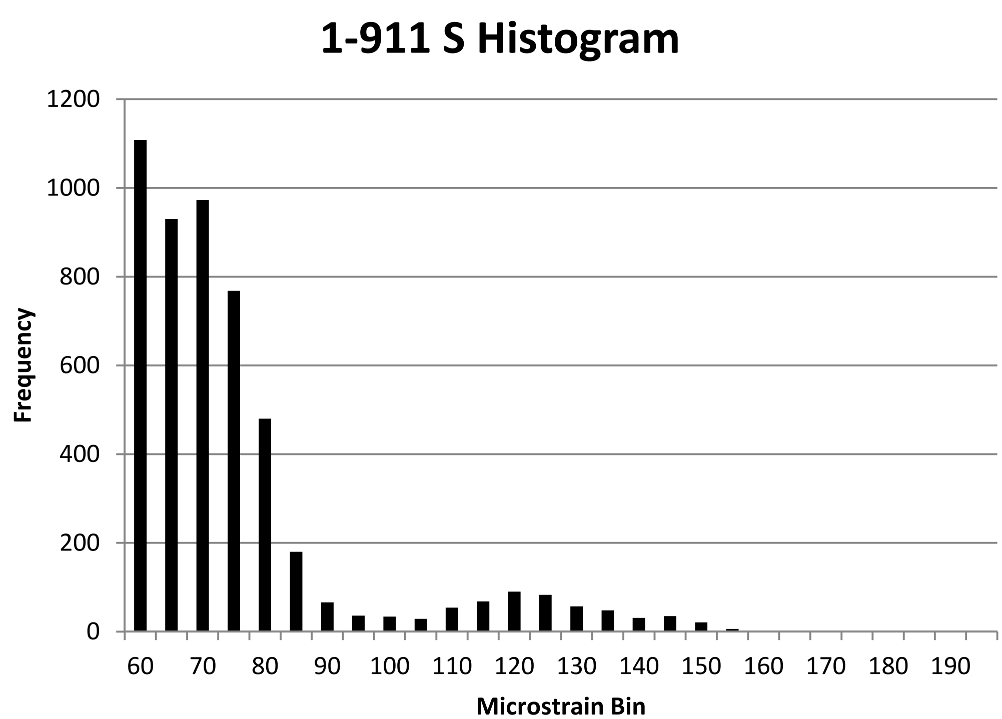
1-911 S Histogram
1200
1000
800
600
400
200
0
Frequency
60
70
80
90
100
110
120
130
140
150
160
170
180
190
Microstrain Bin

IN-SERVICE BRIDGE MONITORING RECORD

Bridge Number	1-821 N	**Date Retrieved**	08/10/10
Facility Carried	I-495 N	**Log. Stat. at Ret.**	Standby
Facility Crossed	Edgemoor Rd	**Date Deactivated**	07/27/10
Span Monitored	3	**Days Monitored**	4.7
Span Length	76'-7 5/8"	**Trigger (με)**	65
Gauge Location	G5, BF	**Num. Events**	4697
Flange Location	G4/G5	**Max Event (με)**	308.32
Date Activated	07/22/10	**Avg. Event (με)**	103.03
Temp. at Act. (°F)	90		
Last Monitored	8/2007		

Battery Voltage:	Deployed	Retrieved
6V	6.55	2.75
9V	9.84	8.9

Bridge Sketch

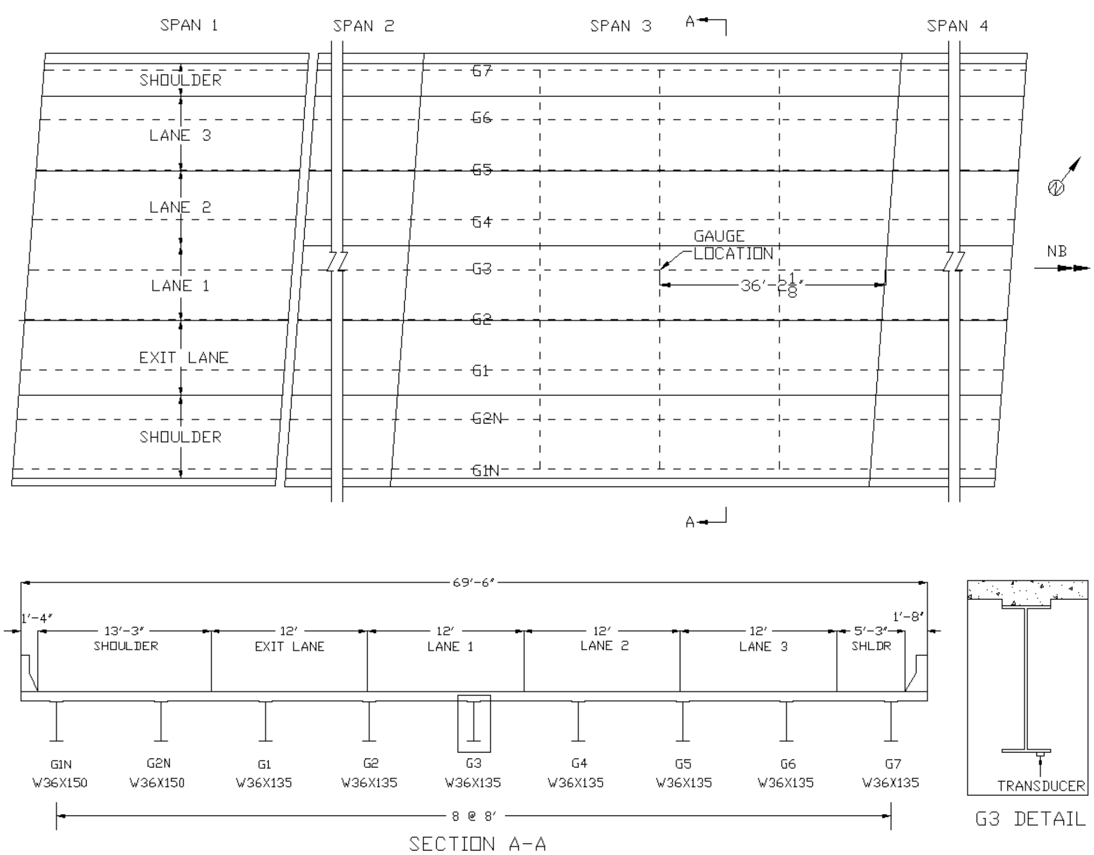

Acces DelDOT provided bucket truck.

s

Notes	Bearings had been replaced since previous monitoring period.				
Sensor #	346	**Drive #**	220	**Cal. Factor**	2.37

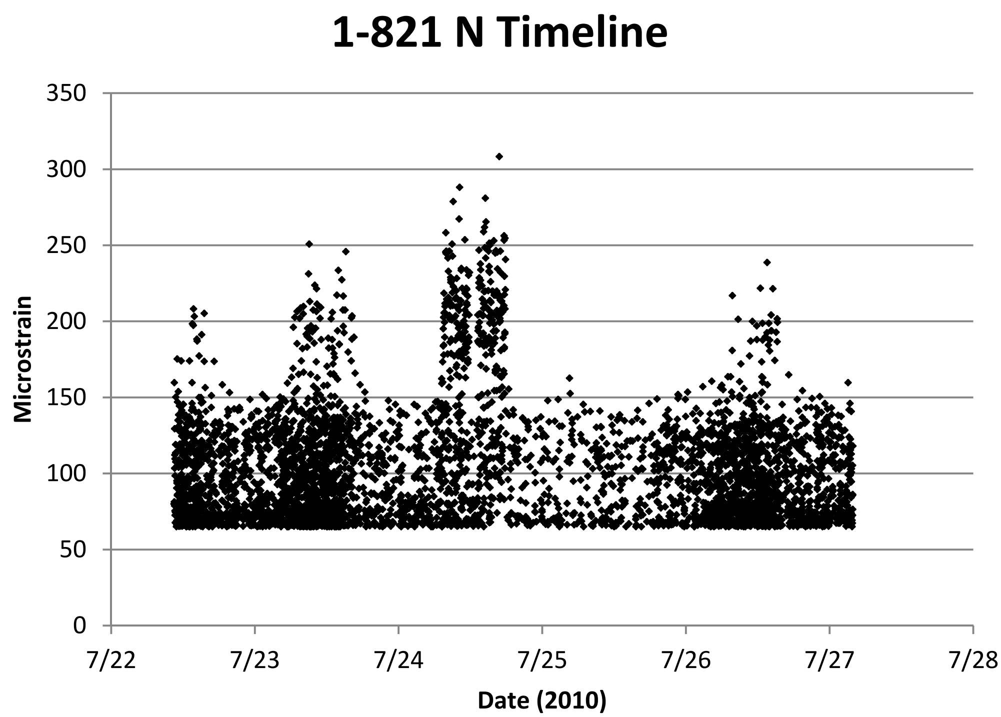
1-821 N Timeline
350
300
250
200
150
100
50
0
Microstrain
7/22
7/23
7/24
7/25
7/26
7/27
7/28
Date (2010)

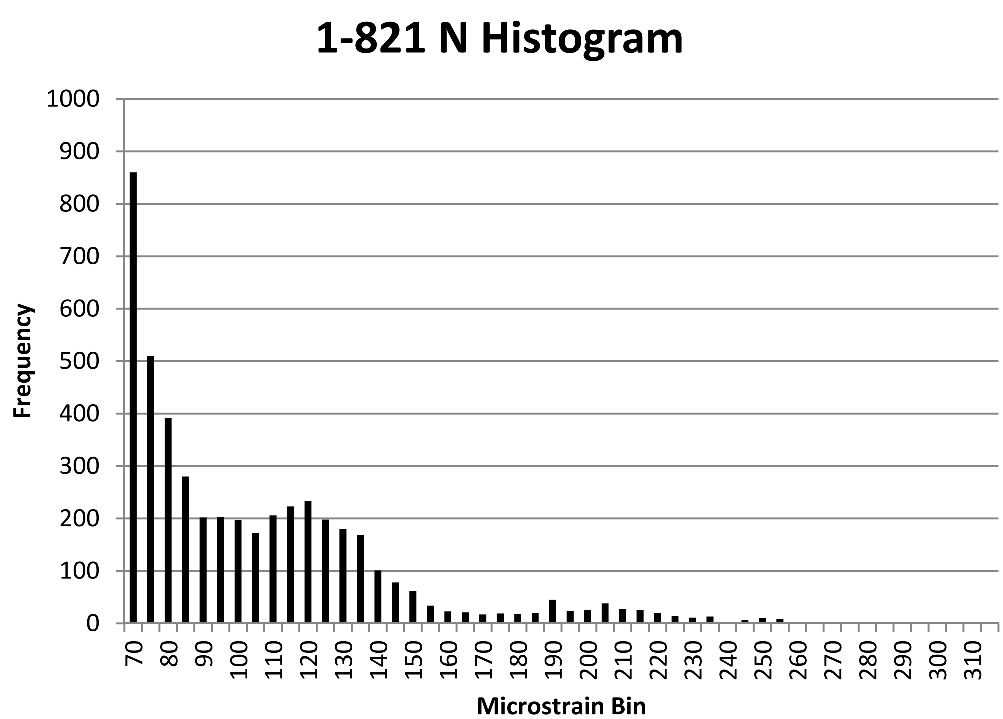
1-821 N Histogram
1000
900
800
700
600
500
400
300
200
100
0
Frequency
70
80
90
100
110
120
130
140
150
160
170
180
190
200
210
220
230
240
250
260
270
280
290
300
310
Microstrain Bin

IN-SERVICE BRIDGE MONITORING RECORD

Bridge Number	1-791	**Date Retrieved**	10/15/10
Facility Carried	I-95 N	**Log. Stat. at Ret.**	Active
Facility Crossed	Darley Rd	**Date Deactivated**	10/15/10
Span Monitored	1	**Days Monitored**	14.5
Span Length	35'-0"	**Trigger (με)**	35
Gauge Location	G3, BF	**Num. Events**	1430
Flange Location	G3/G4	**Max Event (με)**	104.56
Date Activated	10/01/10	**Avg. Event (με)**	41.81
Temp. at Act. (°F)	70		
Last Monitored	9/2006		

Battery Voltage:	Deployed	Retrieved
6V	6.47	5.54
9V	9.84	8.69

Bridge Sketch

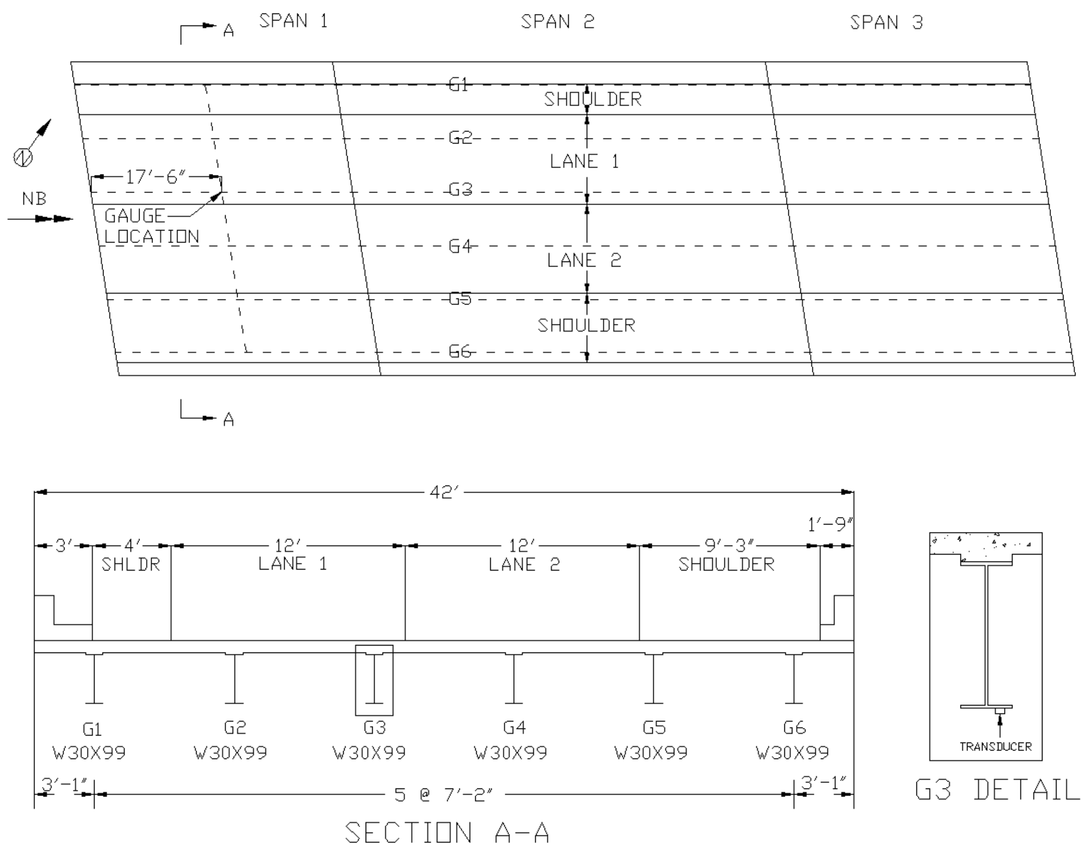

Acces 16' used for access. 7' fence must be scaled.

s

Notes	Girder location may be different from 2006 monitoring period.				
Sensor #	346	**Drive #**	220	**Cal. Factor**	3.07

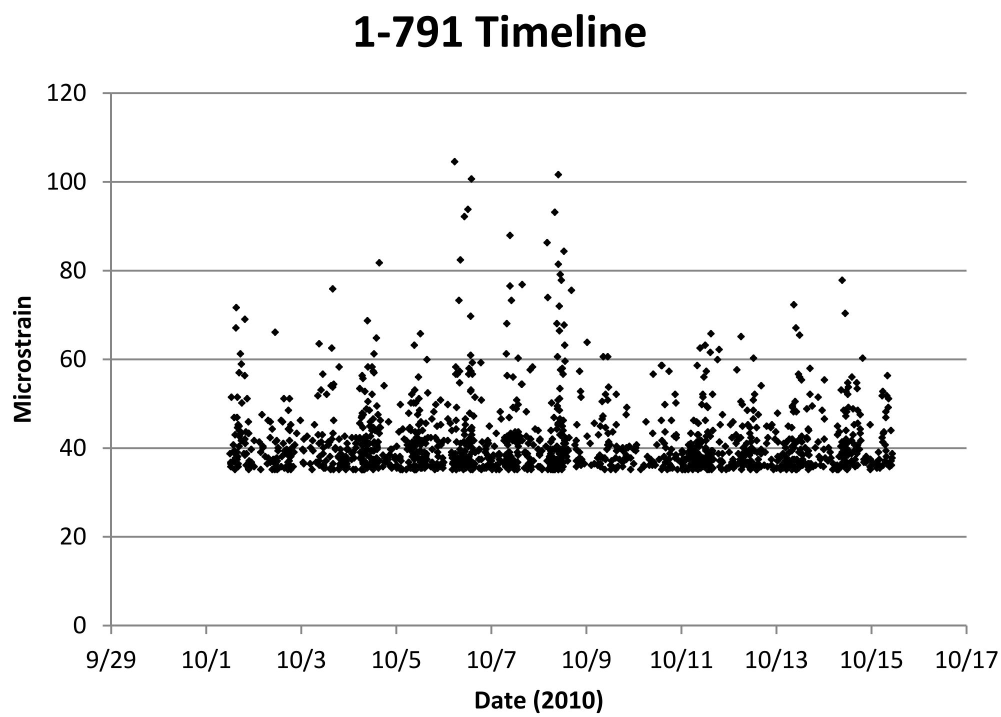
1-791 Timeline
120
100
80
60
40
20
0
Microstrain
9/29
10/1
10/3
10/5
10/7
10/9
10/11
10/13
10/15
10/17
Date (2010)

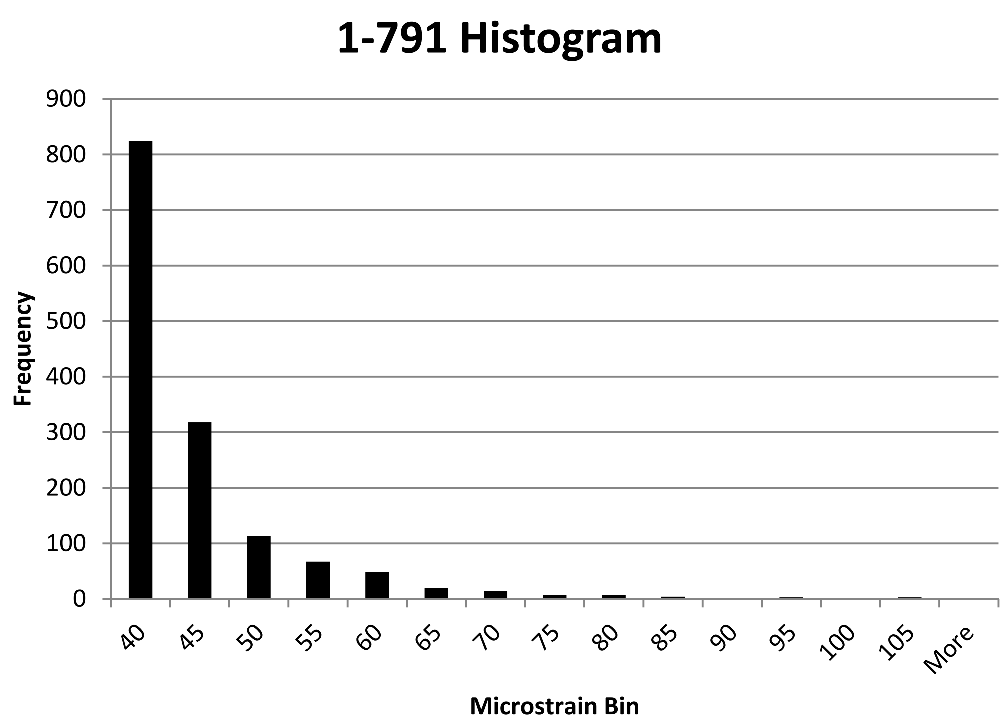
1-791 Histogram
900
800
700
600
500
400
300
200
100
0
Frequency
40
45
50
55
60
65
70
75
80
85
90
95
100
105
More
Microstrain Bin

IN-SERVICE BRIDGE MONITORING RECORD

Bridge Number	2-918 N	**Date Retrieved**	11/03/10
Facility Carried	SR-1 N	**Log. Stat. at Ret.**	Active
Facility Crossed	Big Oak Rd	**Date Deactivated**	11/03/10
Span Monitored	1	**Days Monitored**	13.9
Span Length	65'-0"	**Trigger (με)**	45
Gauge Location	G10, BF	**Num. Events**	3752
Flange Location	G10/G11	**Max Event (με)**	163.84
Date Activated	10/20/10	**Avg. Event (με)**	58.83
Temp. at Act. (°F)	50		
Last Monitored	10/2007		

Battery Voltage:	Deployed	Retrieved
6V	6.45	3.93
9V	9.22	8.32

Bridge Sketch

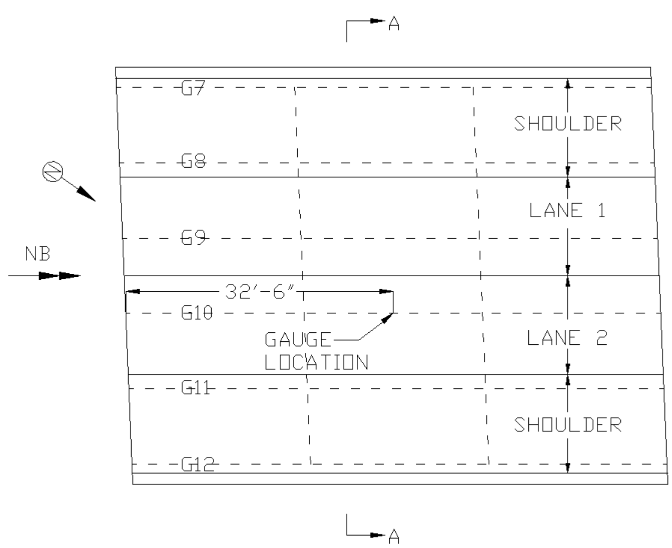

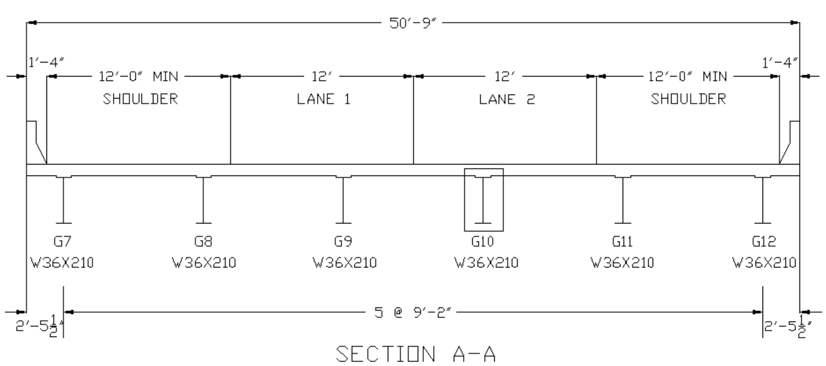

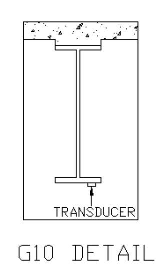

DelDOT provided bucket truck.

Acces s Notes					
Sensor #	346	**Drive #**	220	**Cal. Factor**	3.07

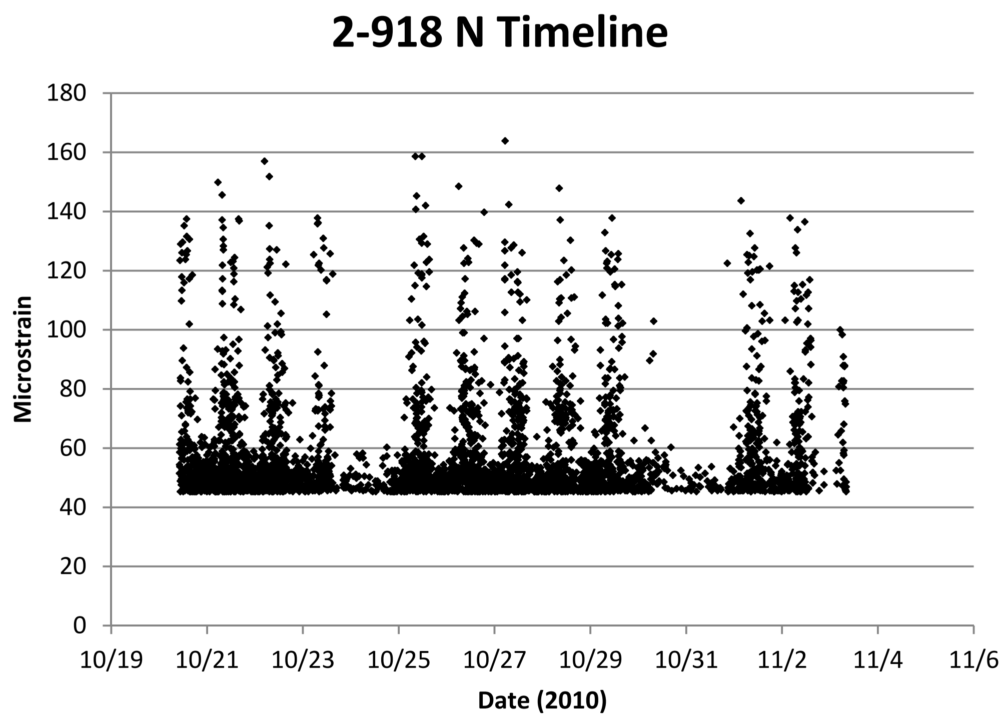
2-918 N Timeline
Microstrain
180
160
140
120
100
80
60
40
20
0
10/19
10/21
10/23
10/25
10/27
10/29
10/31
11/2
11/4
11/6
Date (2010)

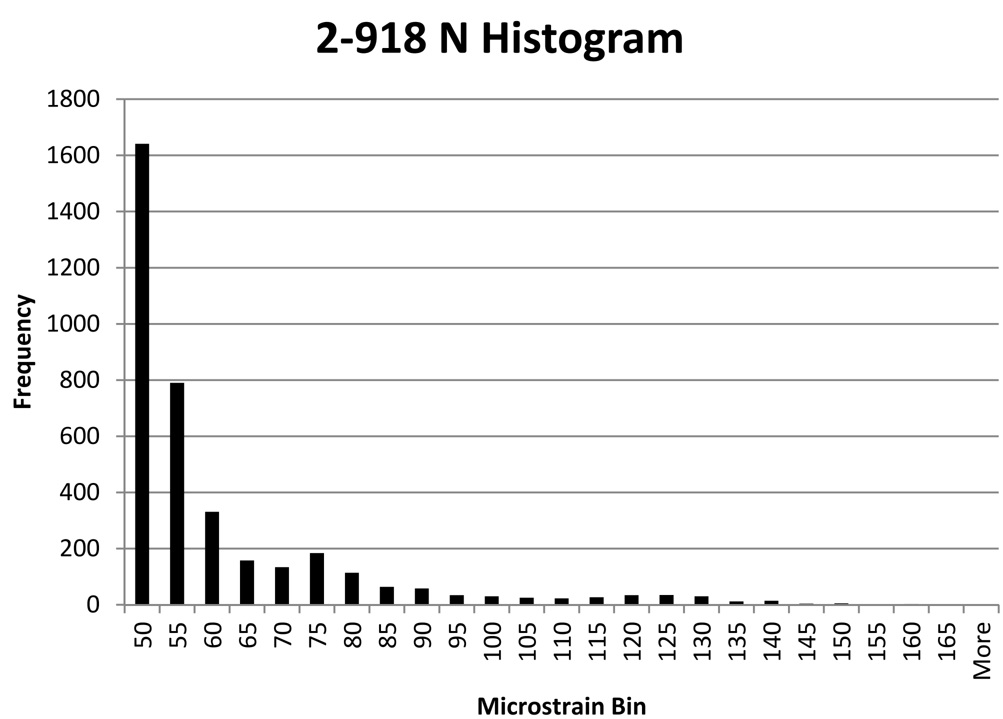
2-918 N Histogram
Frequency
1800
1600
1400
1200
1000
800
600
400
200
0
50
55
60
65
70
75
80
85
90
95
100
105
110
115
120
125
130
135
140
145
150
155
160
165
More
Microstrain Bin

IN-SERVICE BRIDGE MONITORING RECORD

Bridge Number	2-920 N	**Date Retrieved**	11/17/10
Facility Carried	SR-1 N	**Log. Stat. at Ret.**	Standby
Facility Crossed	Dyke Branch Rd	**Date Deactivated**	11/16/10
Span Monitored	1	**Days Monitored**	13.5
Span Length	65'-0"	**Trigger (με)**	45
Gauge Location	G11, BF	**Num. Events**	5943
Flange Location	G10/G11	**Max Event (με)**	181.11
Date Activated	11/03/10	**Avg. Event (με)**	57.58
Temp. at Act. (°F)	40		
Last Monitored	N/A		

Battery Voltage:	Deployed	Retrieved
6V	6.49	5.62
9V	9.14	7.98

Bridge Sketch

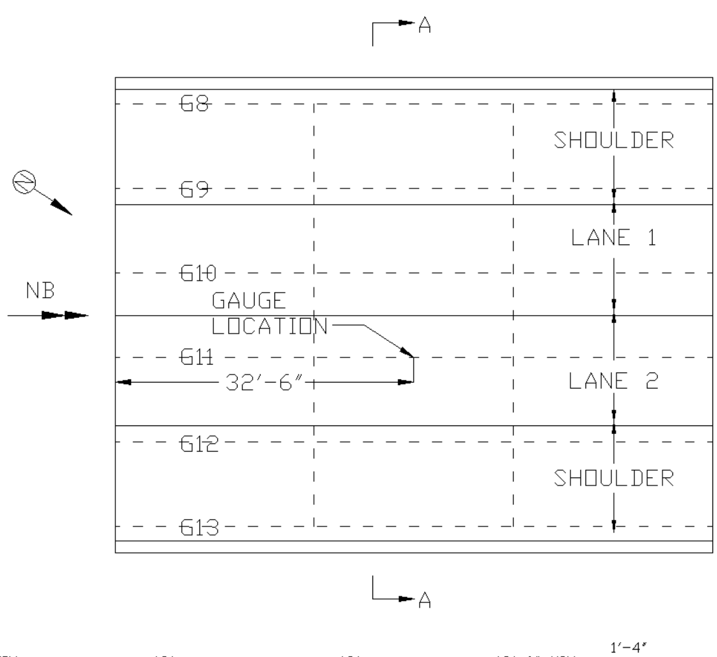

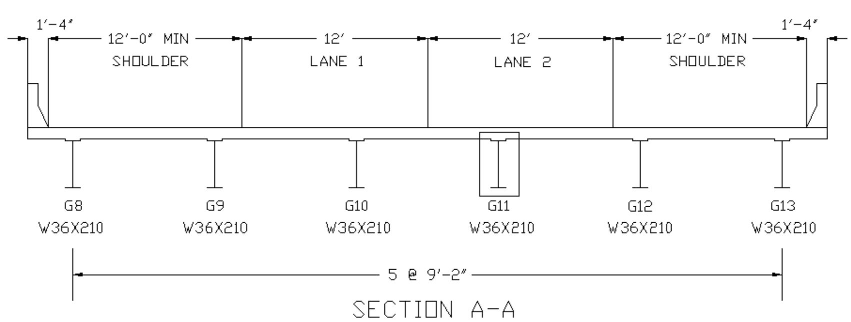

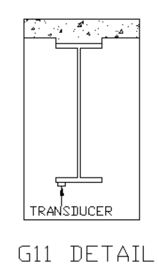

Access	DelDOT provided bucket truck.				
Notes					
Sensor #	346	**Drive #**	220	**Cal. Factor**	3.07

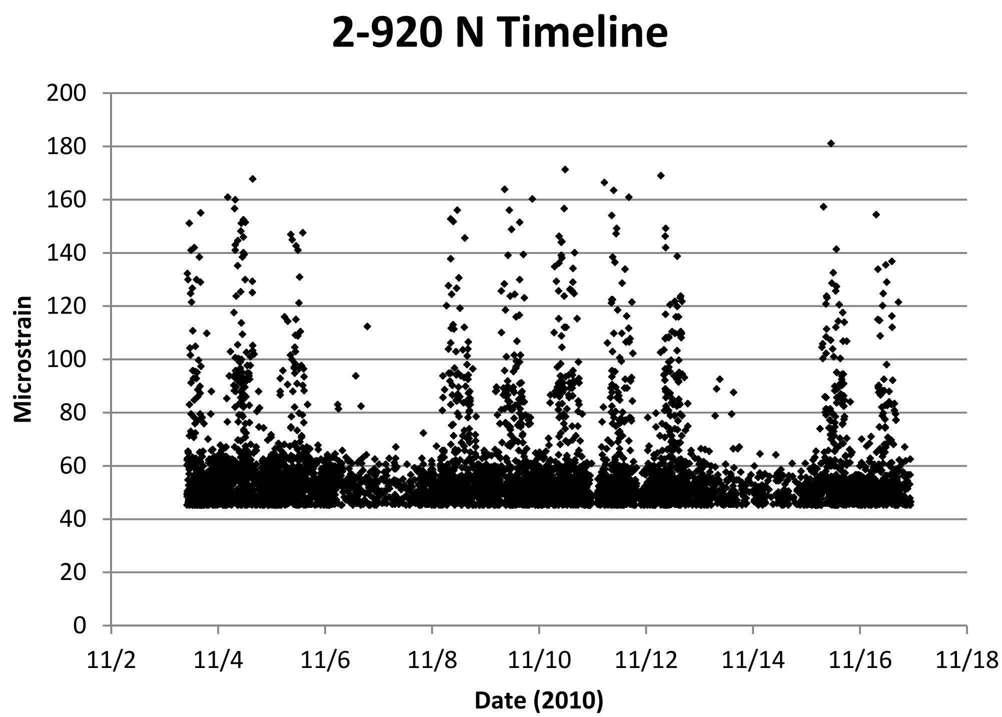

2-920 N Timeline
Microstrain
200
180
160
140
120
100
80
60
40
20
0
11/2
11/4
11/6
11/8
11/10
11/12
11/14
11/16
11/18
Date (2010)

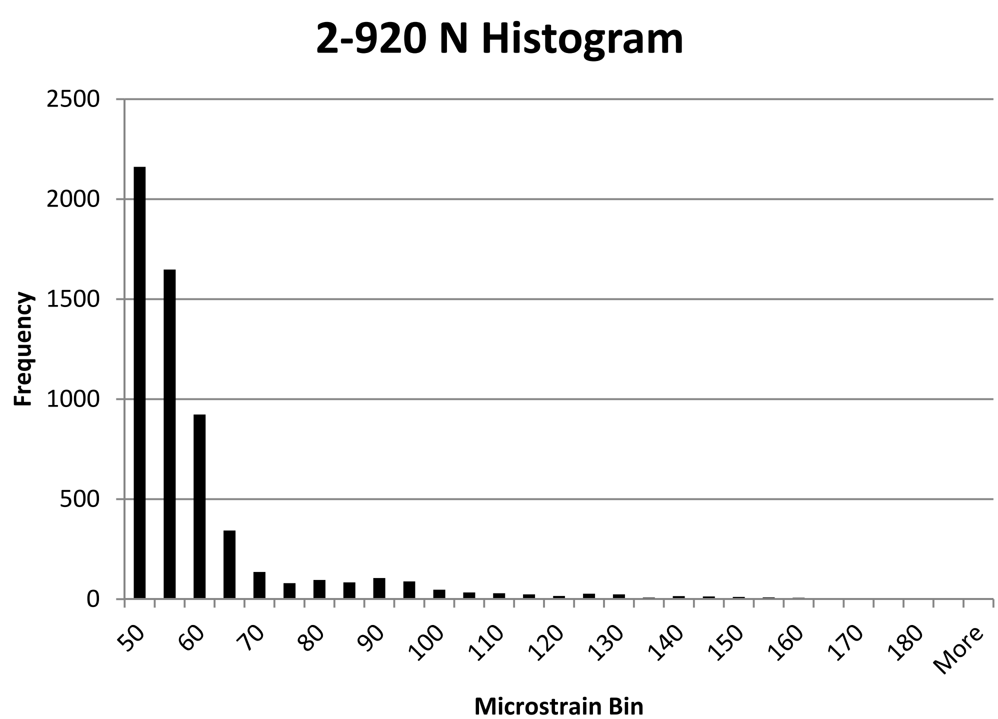

2-920 N Histogram
Frequency
2500
2000
1500
1000
500
0
50
60
70
80
90
100
110
120
130
140
150
160
170
180
More
Microstrain Bin

IN-SERVICE BRIDGE MONITORING RECORD

Bridge Number	1-911 S	**Date Retrieved**	12/02/10
Facility Carried	SR-1 S	**Log. Stat. at Ret.**	Active
Facility Crossed	Black Diamond Rd	**Date Deactivated**	12/02/10
Span Monitored	1	**Days Monitored**	14.9
Span Length	65'-0"	**Trigger (με)**	70
Gauge Location	G3, BF	**Num. Events**	3836
Flange Location	G3/G4	**Max Event (με)**	186.65
Date Activated	11/17/10	**Avg. Event (με)**	85.79
Temp. at Act. (°F)	55		
Last Monitored	7/2010		

Battery Voltage:	Deployed	Retrieved
6V	6.45	3.61
9V	9.58	8.61

Bridge Sketch

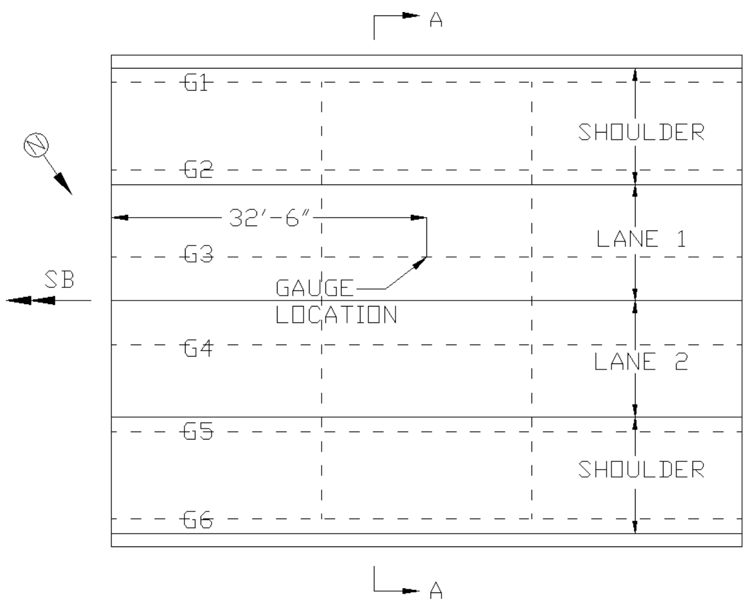

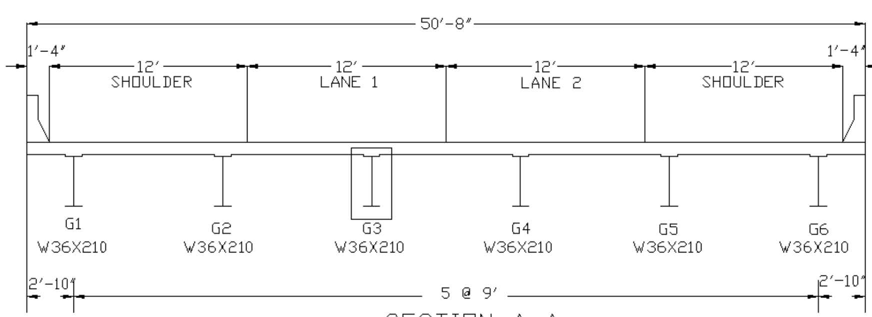

SECTION A-A

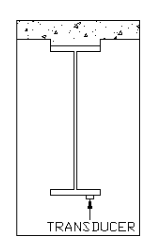

G3 DETAIL

Access Notes	DelDOT provided bucket truck and traffic control.				
Sensor #	346	**Drive #**	220	**Cal. Factor**	3.07

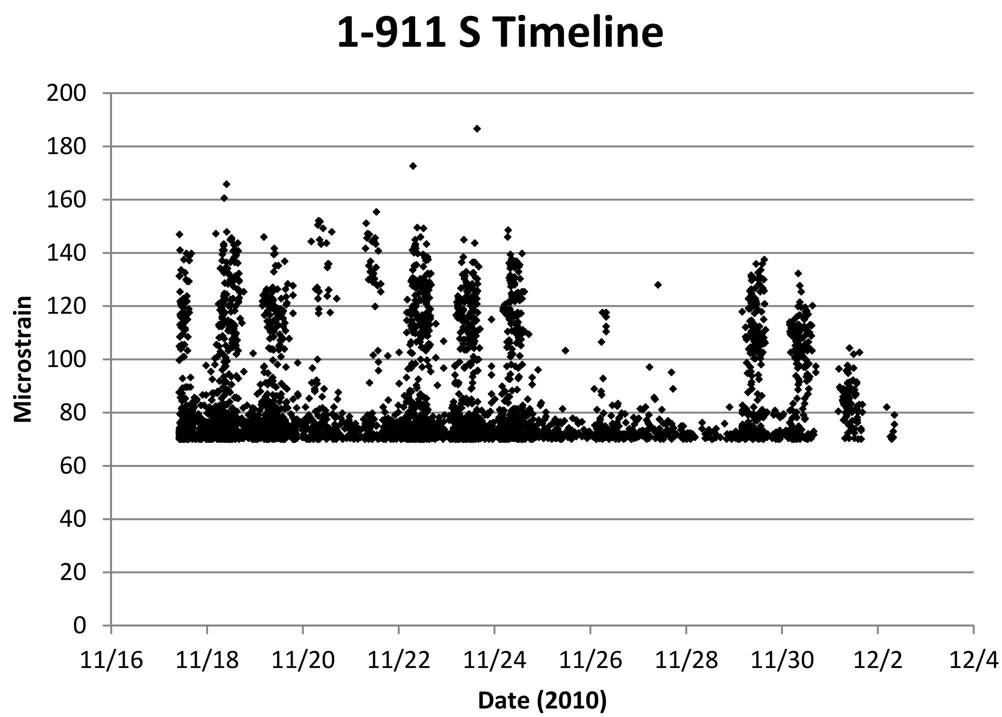
1-911 S Timeline
Microstrain
200
180
160
140
120
100
80
60
40
20
0
11/16
11/18
11/20
11/22
11/24
11/26
11/28
11/30
12/2
12/4
Date (2010)

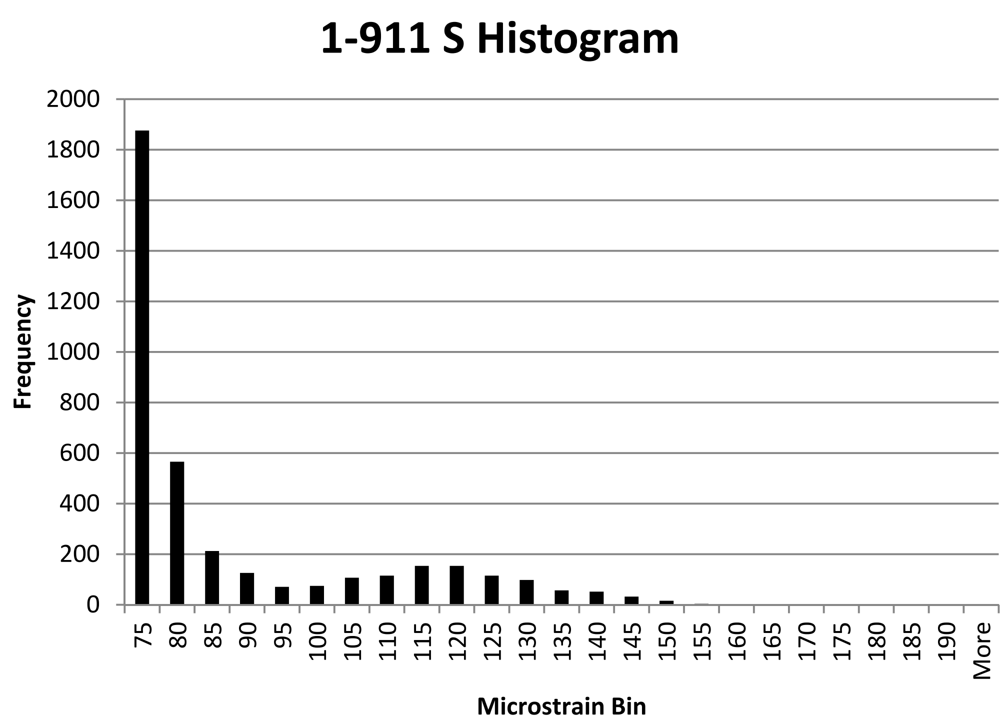
1-911 S Histogram
Frequency
2000
1800
1600
1400
1200
1000
800
600
400
200
0
75
80
85
90
95
100
105
110
115
120
125
130
135
140
145
150
155
160
165
170
175
180
185
190
More
Microstrain Bin

IN-SERVICE BRIDGE MONITORING RECORD

Bridge Number	1-907 S	**Date Retrieved**	12/16/10
Facility Carried	SR-1	**Log. Stat. at Ret.**	Active
Facility Crossed	Pine Tree Rd	**Date Deactivated**	12/16/10
Span Monitored	1	**Days Monitored**	14.0
Span Length	81'-0"	**Trigger (με)**	70
Gauge Location	G3, BF	**Num. Events**	1176
Flange Location	G3/G4	**Max Event (με)**	422.15
Date Activated	12/02/10	**Avg. Event (με)**	82.53
Temp. at Act. (°F)	35		
Last Monitored	N/A		

Battery Voltage:	Deployed	Retrieved
6V	6.48	5.5
9V	9.69	9.09

Bridge Sketch

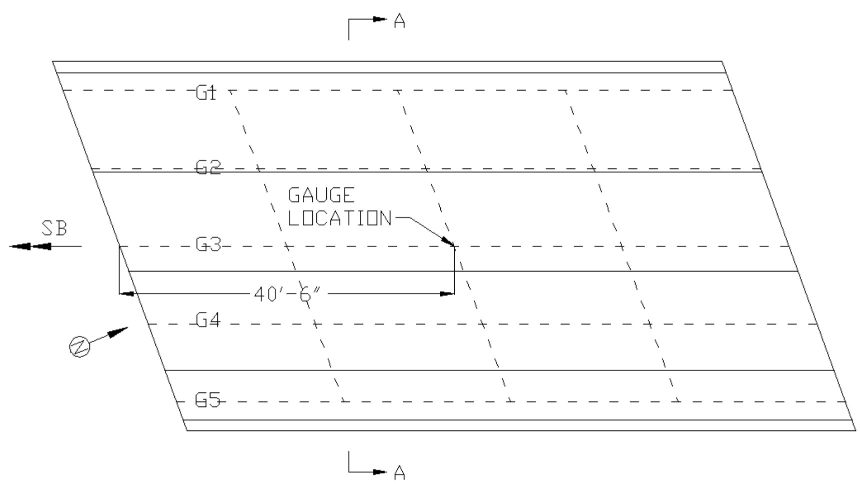

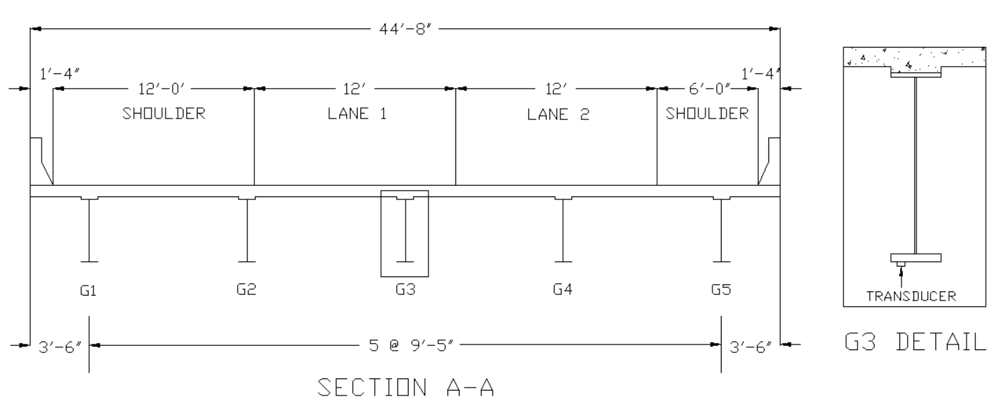

DelDOT provided bucket truck and traffic control.

Access Notes					
Sensor #	346	**Drive #**	220	**Cal. Factor**	3.07

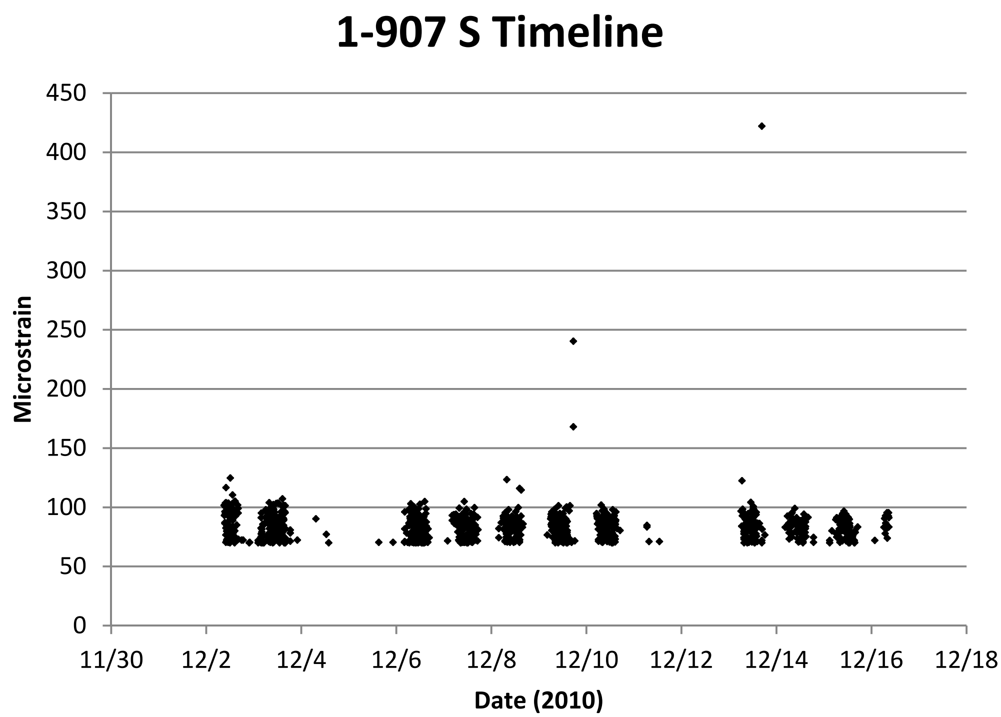
1-907 S Timeline
Microstrain
450
400
350
300
250
200
150
100
50
0
11/30
12/2
12/4
12/6
12/8
12/10
12/12
12/14
12/16
12/18
Date (2010)

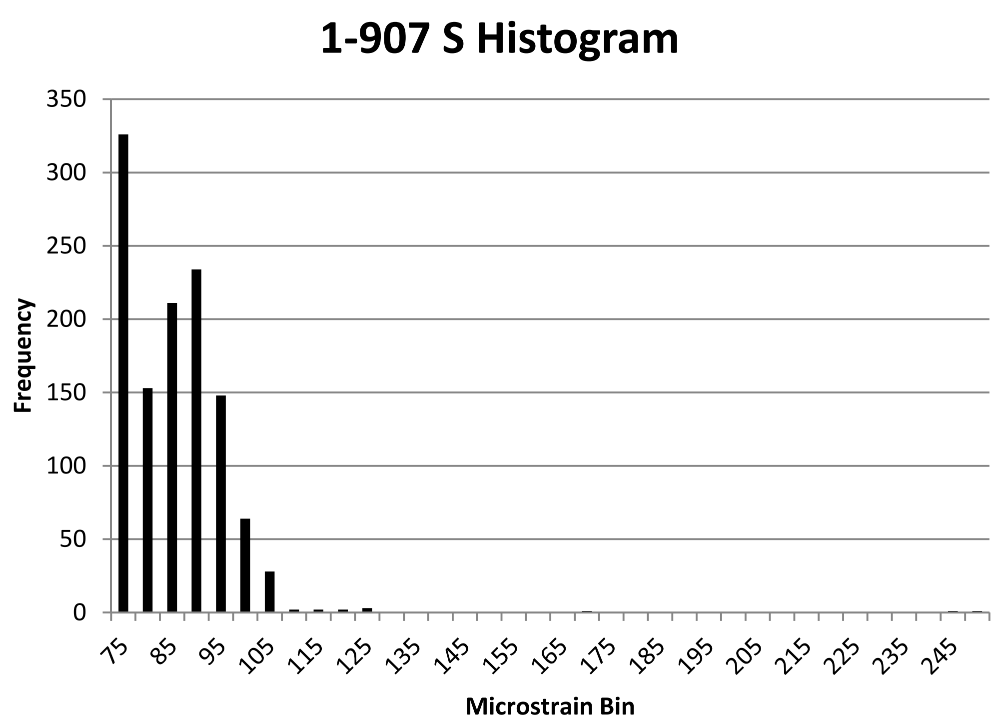
1-907 S Histogram
Frequency
350
300
250
200
150
100
50
0
75
85
95
105
115
125
135
145
155
165
175
185
195
205
215
225
235
245
Microstrain Bin

IN-SERVICE BRIDGE MONITORING RECORD

Bridge Number	1-826 N	**Date Retrieved**	02/16/11
Facility Carried	I-495 N	**Log. Stat. at Ret.**	Standby
Facility Crossed	Stoney Creek	**Date Deactivated**	02/10/11
Span Monitored	3	**Days Monitored**	8.0
Span Length	70'-0"	**Trigger (με)**	50
Gauge Location	G4, BF	**Num. Events**	5,943
Flange Location	G4/G5	**Max Event (με)**	151.07
Date Activated	02/02/11	**Avg. Event (με)**	58.97
Temp. at Act. (°F)	40		
Last Monitored	7/2010		

Battery Voltage:	Deployed	Retrieved
6V	6.4	4.6
9V	9.77	8.91

Bridge Sketch

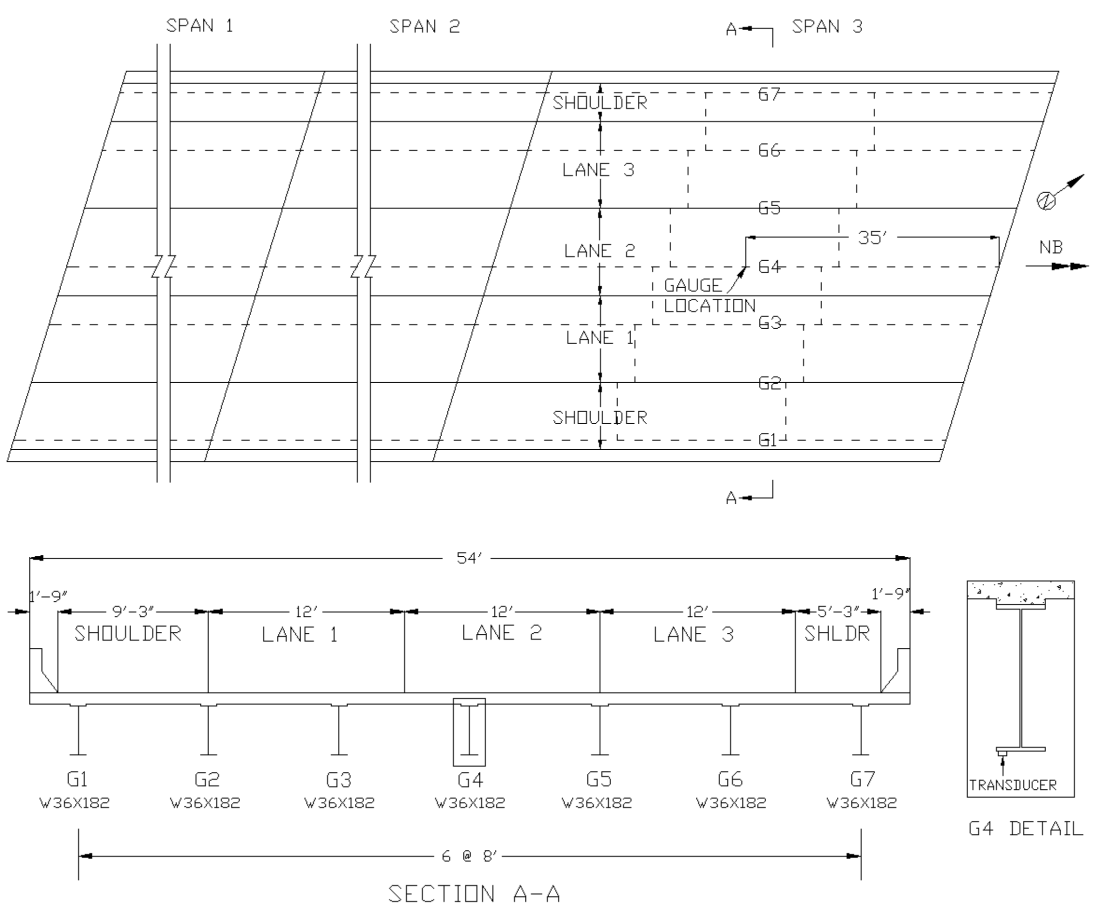

No equipment needed for ISBMS placement.

Acces s Notes

Sensor #	346	**Drive #**	238	**Cal. Factor**	6.05

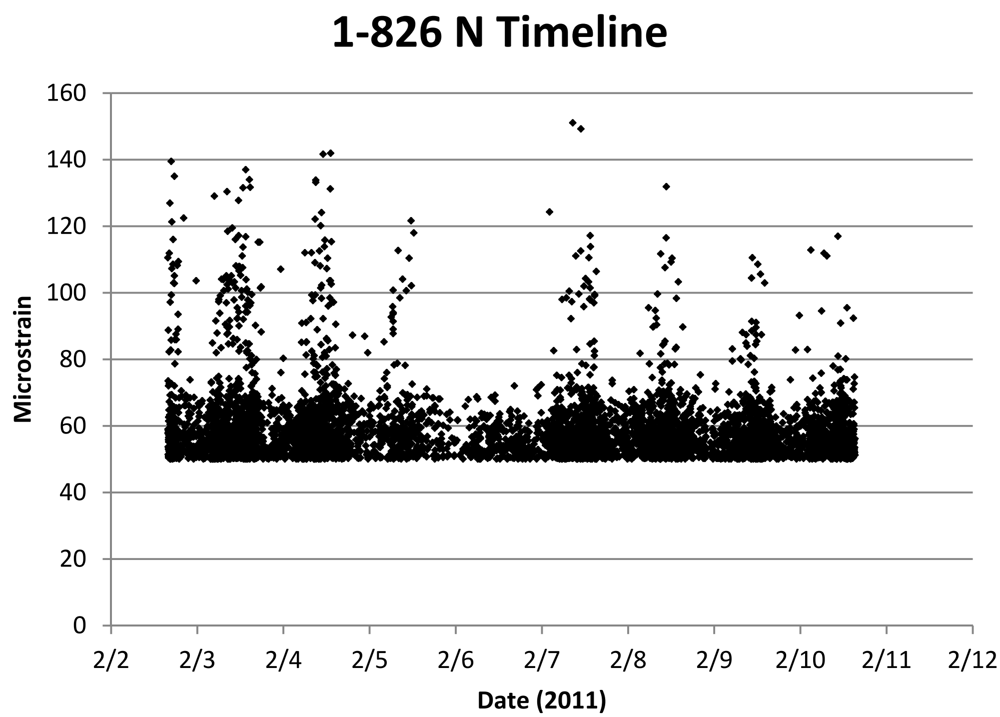
1-826 N Timeline
Microstrain
160
140
120
100
80
60
40
20
0
2/2
2/3
2/4
2/5
2/6
2/7
2/8
2/9
2/10
2/11
2/12
Date (2011)

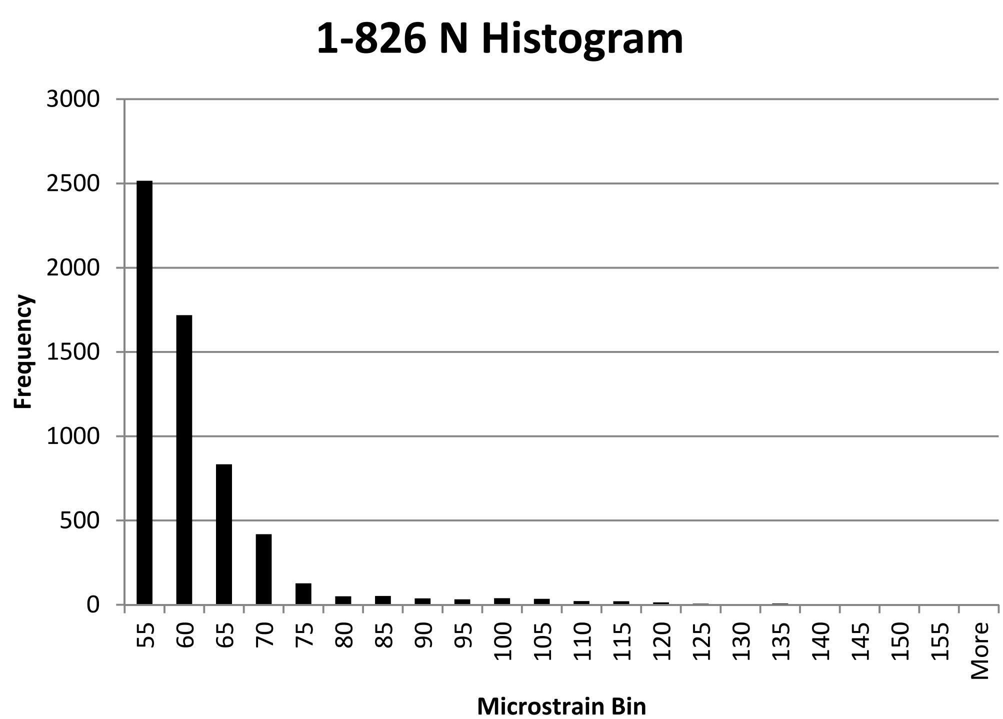
1-826 N Histogram
Frequency
3000
2500
2000
1500
1000
500
0
55
60
65
70
75
80
85
90
95
100
105
110
115
120
125
130
135
140
145
150
155
More
Microstrain Bin

IN-SERVICE BRIDGE MONITORING RECORD

Bridge Number	1-394 S	**Date Retrieved**	03/31/11
Facility Carried	US-13 S	**Log. Stat. at Ret.**	Active
Facility Crossed	Drawyers Creek	**Date Deactivated**	03/31/11
Span Monitored	2	**Days Monitored**	23.8
Span Length	62'-0"	**Trigger (με)**	35
Gauge Location	G2, BF	**Num. Events**	3141
Flange Location	G1/G2	**Max Event (με)**	135.70
Date Activated	03/07/11	**Avg. Event (με)**	49.59
Temp. at Act. (°F)	45		
Last Monitored	8/2007		

Battery Voltage:	Deployed	Retrieved
6V	6.45	2.53
9V	9.47	8.13

Bridge Sketch

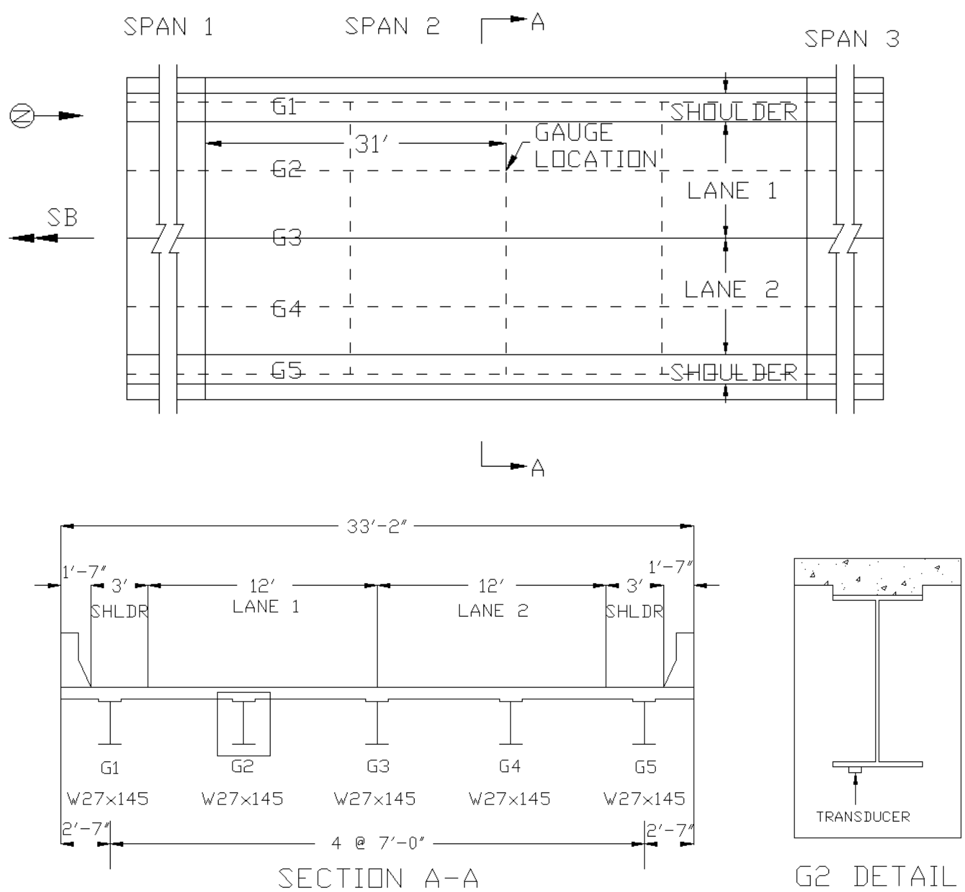

Rowboat required – provided by DelDOT

Access					
Notes					
Sensor #	346	**Drive #**	238	**Cal. Factor**	6.05

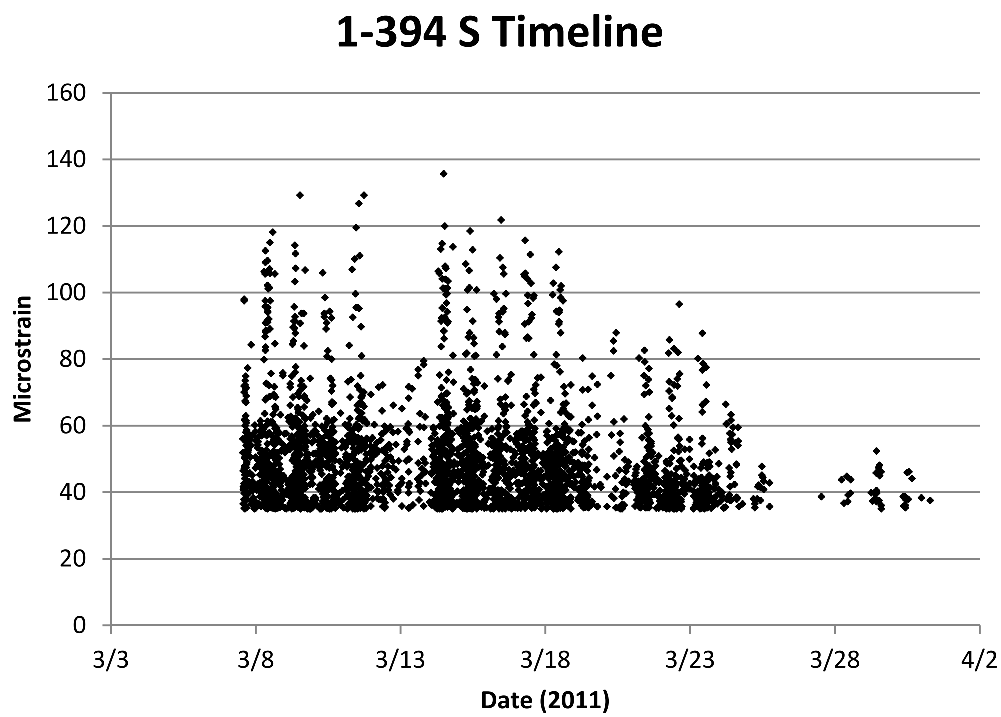

1-394 S Timeline
Microstrain
160
140
120
100
80
60
40
20
0
3/3
3/8
3/13
3/18
3/23
3/28
4/2
Date (2011)

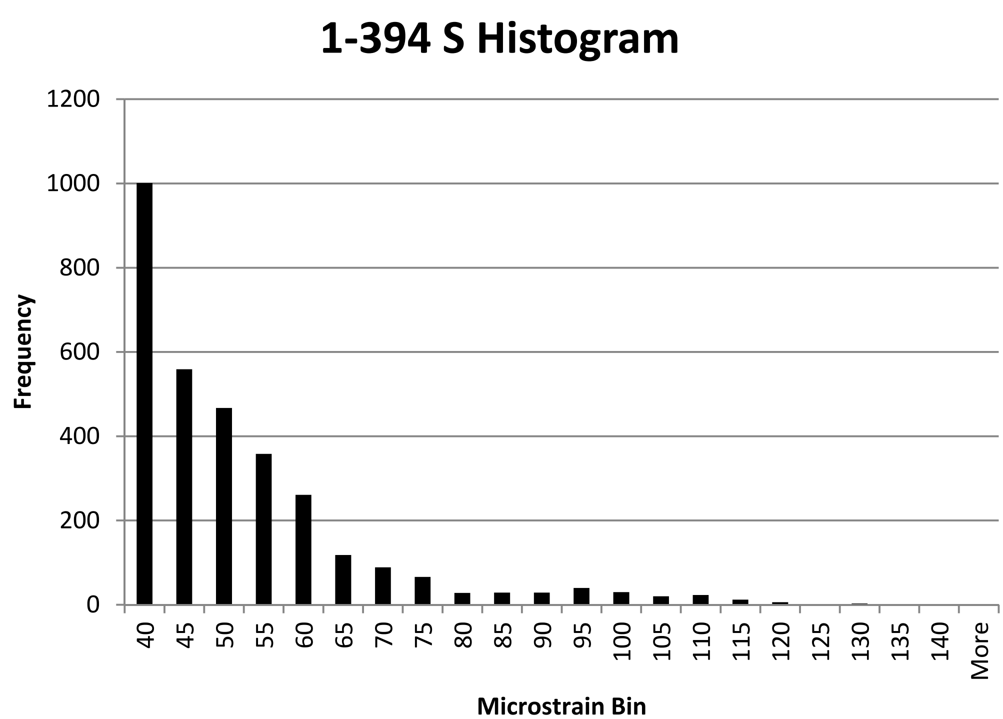

1-394 S Histogram
Frequency
1200
1000
800
600
400
200
0
40
45
50
55
60
65
70
75
80
85
90
95
100
105
110
115
120
125
130
135
140
More
Microstrain Bin

IN-SERVICE BRIDGE MONITORING RECORD

Bridge Number	1-149	**Date Retrieved**	04/15/11
Facility Carried	Newport Gap Pike	**Log. Stat. at Ret.**	Standby
Facility Crossed	Red Clay Creek	**Date Deactivated**	04/13/11
Span Monitored	1	**Days Monitored**	12.8
Span Length	80'-0"	**Trigger (με)**	45
Gauge Location	G8	**Num. Events**	5943
Flange Location	G8/G9	**Max Event (με)**	134.38
Date Activated	03/31/11	**Avg. Event (με)**	57.20
Temp. at Act. (°F)	39		
Last Monitored	3/2006		

Battery Voltage:	Deployed	Retrieved
6V	6.35	4.53
9V	9.85	8.8

Bridge Sketch

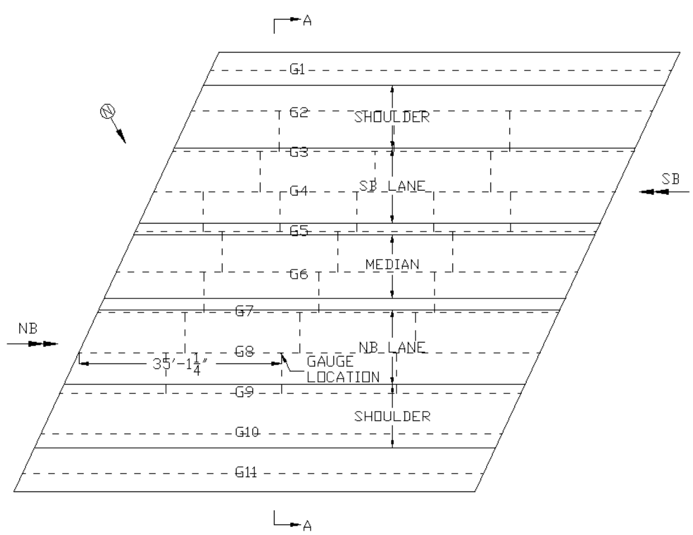

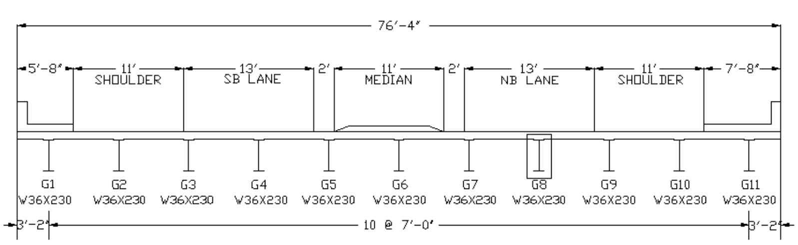

SECTION A-A

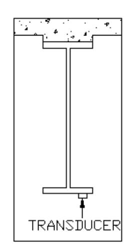

G8 DETAIL

Waders and 16 foot articulating ladder required.

Access Notes					
Sensor #	346	**Drive #**	238	**Cal. Factor**	6.05

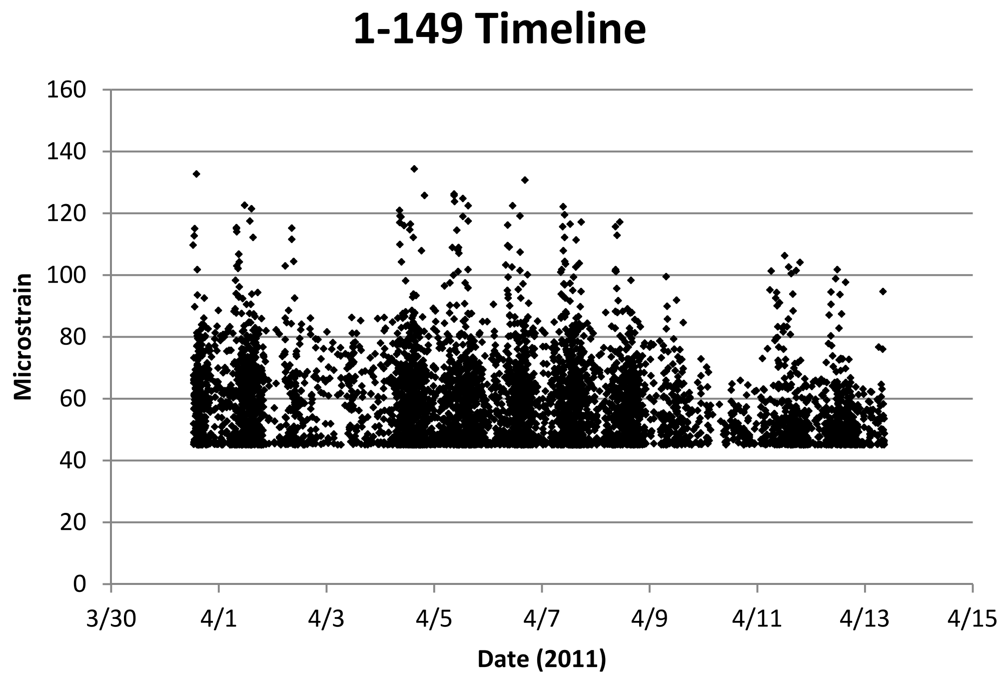

1-149 Timeline
Microstrain
160
140
120
100
80
60
40
20
0
3/30
4/1
4/3
4/5
4/7
4/9
4/11
4/13
4/15
Date (2011)

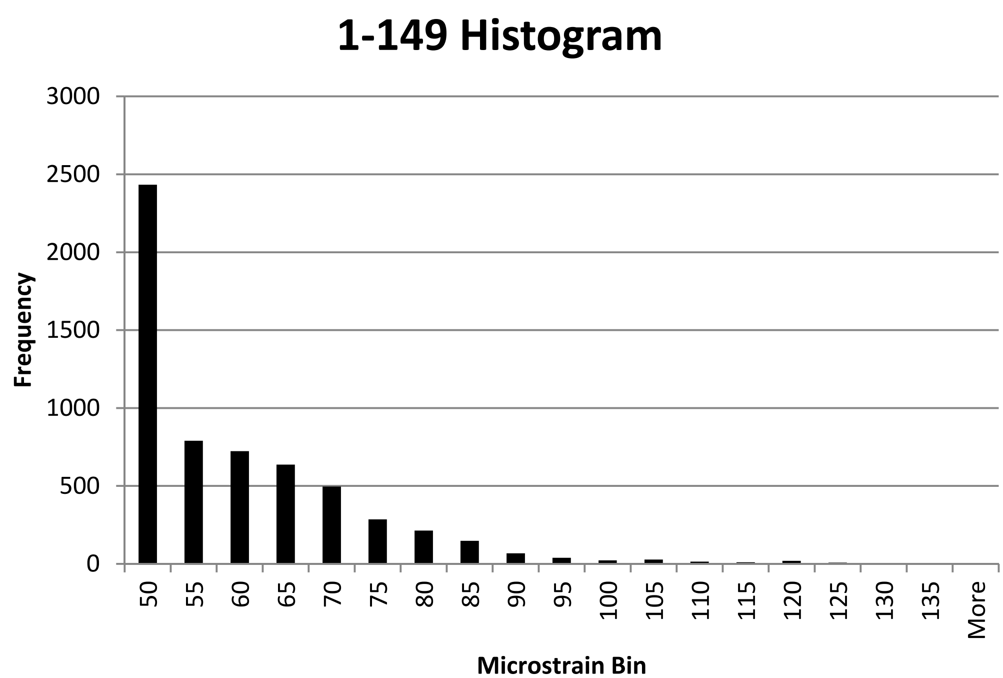

1-149 Histogram
Frequency
3000
2500
2000
1500
1000
500
0
50
55
60
65
70
75
80
85
90
95
100
105
110
115
120
125
130
135
More
Microstrain Bin

REFERENCES

AASHTO. Manual for Condition Evaluation and LRFR of Highway Bridges. In *Section 6: Load and Resistance Factor Rating.*

Brookes, B. (2007). Load Rating Using an In-Service Bridge Monitoring System. Newark, DE: University of Delaware.

Connor, K. S. (2011). Comparison of Historical In-Service Monitoring Data for Improved Maintenance and Management of Bridges. Newark, DE: University of Delaware

DelDOT. (2008, January). Pontis Element Data Collection Manual.

FHWA. (2009). *NBI ASCII Files*. Retrieved November 15, 2010, from http://www.fhwa.dot.gov/bridge/nbi/disclaim.cfm?nbiYear=2009&nbiState=DE09

Google Earth. (2010, July 10). *"Middle Delaware" 39°18'18.93" N and 75°35'16.75" W*. Retrieved April 10, 2011

Google Earth. (2010, April 12). *"Northern Delaware" 39°42'41.61" N and 75°35'16.59" W*. Retrieved April 10, 2011

Holloway, E. (1999). A Long-term Monitoring System for Highway Bridges. Newark, DE: University of Delaware.

Howell, D. (2003). Development of a Wireless In-Service Bridge Monitoring System. Newark, DE: University of Delaware.

Mendenhall, W., & Sincich, T. (1992). *Statistics for Engineering and the Sciences.* Dellen Publishing Company: San Francisco.

National Cooperative Highway Research Program (NCHRP). (2001). *Calibration of Load Factors for LRFR Bridge Evaluation: NCHRP Report 454.* Washington, D.C.

Rakowski, M. (2008). Bridge Evaluation Using In-Service and Weigh-In-Motion Data. Newark, DE: University of Delaware.

Schumacher, T., Higgins, C. C., & Lovejoy, S. C. (2011). *Estimating Operating Load Conditions on Reinforced Concrete Highway Bridges with b-Value Analysis from Acoustic Emission Monitoring.*

Shenton III, H. W., Connor, K., Chajes, M. J., Rakowski, M., & Brookes, B. (2009). Analysis of In-Service Data Collected During Bienniel Inspections on Typical Bridges.

Sincich, W. M. (1992). *Statistics for Engineering and the Sciences.* Dellen Publishing Company: San Francisco.